

MILENE SORAIA COSTA DA SILVA

HEME AND IRON SHAPE MACROPHAGE PLASTICITY: A ROLE IN HEMOLYTIC DISORDERS AND CANCER?

Tese de Candidatura ao grau de Doutor em Biologia
Básica e Aplicada submetida ao Instituto de Ciências
Biomédicas Abel Salazar da Universidade do Porto.

Orientador – Martina U. Muckenthaler

Categoria – Professor

Afiliação – Heidelberg University

Co-orientador – Adelheid Cerwenka

Categoria – PD Dr. rer. nat.

Afiliação – German Cancer Research Center (DKFZ)

Co-orientador – Maria de Sousa

Categoria – Professora Catedrática Emérita

Afiliação – Instituto de Ciências Biomédicas Abel
Salazar da Universidade do Porto.

Publications list

Publications discussed in this thesis

Vinchi, F.*, **Costa da Silva, M.***, Ingoglia, G., Petrillo, S., Brinkman, N., Zuercher, A., Cerwenka, A., Tolosano, E., and Muckenthaler, M.U. (2016). Hemopexin therapy reverts heme-induced proinflammatory phenotypic switching of macrophages in a mouse model of sickle cell disease. *Blood* 127, 473-486. *equal first contribution.

Milene Costa da Silva, Margareta P. Correia, Ana Stojanovic, Michael Meister, Thomas Muley, Adelheid Cerwenka, Martina U. Muckenthaler. A role for heme and iron in the tumor microenvironment. *Manuscript in preparation.*

This work was supported by Fundação para a Ciências e Tecnologia (FCT) by means of a PhD fellowship SFRH/BD/51290/2010 awarded to Milene Soraia Costa da Silva through the Graduate Program in Areas of Basic and Applied Biology (GABBA), Universidade do Porto, Portugal. The work was also supported by The University of Heidelberg, Faculty of Medicine with a prize in the value of 10.000€ awarded to Milene Soraia Costa da Silva under the program „Stiftungen und Preise 2012” and also supported with funding from Deutsches Zentrum für Lungenforschung (DZL) with the reference TP CF-1.1.



Aos meus pais e irmão

ACKNOWLEDGMENTS

The journey of a PhD student is not a lonely path. All the people I met during these years were as important as my scientific achievements.

I would like to, first of all, show my appreciation and gratitude to the GABBA program, for giving me the opportunity to be a part of this scientific family and for the opportunity to do my PhD. I would like to thank all the Professors, but especially Professor Maria de Sousa who became my supervisor and shared her knowledge with me. Among all the things she taught me, what I will remember the most is the importance of having courage. I will never forget that.

I want to thank my GABBA colleagues from the 14th edition (who rapidly became my friends) who shared this journey with me: Filipa Ferreira, Ricardo Pinto, Daniel Bandarra, Inês Tenente, Bruno Moraes, Mariana Fontes, Pedro Miranda, Filipa Neto, André Lindo, Catarina Oliveira and André Martins. This PhD wouldn't have been the same without your companionship, friendship and support.

This work wouldn't have been possible without Martina Muckenthaler, my supervisor. Thank you, Martina, for accepting me in your lab. Most of all, thank you for believing in me. I learned innumerable things from you and I have you as an example of success, both inside and outside the lab. I am immensely grateful to you and I am certain that the years spent in your lab will influence me in a positive way, no matter what career path I will choose next.

A big “thank you” to my co-supervisor, Adelheid Cerwenka. Dear Heidi, thank you so much for embarking in this risky journey with me and for sharing the expertise of your lab. Your good humor and positive thinking always made me look to the bright side. As I said to Martina, I feel very lucky to have had successful women as supervisors.

I feel very honored to have worked side by side with all the amazing members of the Muckenthaler's Lab and Cerwenka's Lab. Each one of them taught me something new, but also supported me during the challenging moments of my PhD.

To the Muckenthaler's Lab members: thank you so much Claudia, Flavia, Debbie, Nico, Maja, Christoph, Kasia, Regina, Julia, Andreas and Richard. Thank you Sylvia, for helping me during my PhD, you are one of the sweetest persons I know. A special thanks to Joana and Ana Rita, for all the support, friendship and laughter, I am sure this PhD wouldn't have been the same without you. Thank you Sandro, for always being there for me, for the friendship and for all the cups of coffee. Thank you so much Francesca, for

teaching me almost everything and for sharing my ideas and scientific discoveries. It was a pleasure to work with you.

To Cerwenka's Lab members: thank you all for your support and for making me feel part of the group. An enormous "thank you" to Ana, who I admire and follow as an example. At last, but not the least, thank you so much Margareta. Thank you for all the help with my work, but most of all, thank you for all the laughter, the nights shared in the DKFZ office and FACS, the dinners between experiments, the adventures, friendship, everything.

Outside the lab, I was extremely lucky to be the singer of "The Wild Types". Thank you for sharing my passion for music and for keeping me sane. I dedicate my thesis to all my friends outside the lab, who made this city feel like home. Thank you Babitha and Yamuna, Asrar, Reinhard, Iliona and Bebiana.

Thank you Pedro and Manuela for being my family here.

Thank you Phivos for keeping everything in tune.

I dedicate this thesis to my parents and brother, and words are not enough to say and to appreciate how much you have done for me.

Table of Contents

ABSTRACT / RESUMO	1
<i>ABSTRACT</i>	3
<i>RESUMO</i>	5
<i>ABBREVIATIONS</i>	7
I – GENERAL INTRODUCTION	9
1. <i>Iron Homeostasis: keeping the balance</i>	11
1.1 Why is iron an essential element?	11
1.2 Systemic iron regulation	11
1.3 The hepcidin/ferroportin axis	12
1.4 Cellular iron regulation	15
1.5 Macrophages: the iron-recycling machinery	17
2. <i>Heme: essential and toxic</i>	18
2.1 The essential role of heme	18
2.2 The toxic side of heme	18
2.3 The inflammatory side of heme	19
2.4 Free heme and hemolytic disorders: sickle cell anemia	21
3. <i>Macrophages in immune response and iron regulation</i>	22
3.1 Macrophages: origin and function	22
3.2 Macrophage polarization	25
3.3 Macrophage polarization and iron	28
4. <i>Iron and the tumor microenvironment</i>	30
4.1 The tumor microenvironment	30
4.2 Tumor-associated macrophages (TAMs)	32
4.3 Iron and cancer	35
4.4 Lung cancer: the contribution of iron and macrophages	36
4.5 The Lewis Lung Carcinoma model	38
4.6 Inflammation and iron: from infection to cancer	39
5. <i>Question and Aims</i>	42

II – RESEARCH WORK.....	43
CHAPTER I: HEMOPEXIN THERAPY REVERTS HEME-INDUCED PRO-INFLAMMATORY PHENOTYPIC SWITCHING OF MACROPHAGES IN A MOUSE MODEL OF SICKLE CELL DISEASE	45
CHAPTER II: A ROLE FOR HEME AND IRON IN THE TUMOR MICROENVIRONMENT	91
III – GENERAL DISCUSSION.....	133
1. <i>Main findings</i>	135
2. <i>Discussion</i>	136
3. <i>Future Perspectives</i>	148
IV – REFERENCES.....	149

ABSTRACT / RESUMO

ABSTRACT

Macrophages are cells of the innate immune system that have many different functions such as iron recycling, fighting infections, repair lesions and immune response against cancer. A simple dichotomous nomenclature defines macrophages as classically activated M1 “pro-inflammatory” or alternatively activated M2 “immune-regulatory”. Heme was shown to activate innate immunity by recruiting and activating neutrophils and macrophages. Here we hypothesized if heme and iron loading in macrophages could affect macrophage plasticity and polarization in two different contexts: in an experimental model of hemolytic disease and an experimental model of lung cancer.

Hemolytic diseases, such as sickle cell anemia and thalassemia, are characterized by enhanced release of hemoglobin and heme into the circulation, heme-iron loading of reticuloendothelial system macrophages as well as chronic inflammation. In “Research work - Chapter I” of this thesis it is shown that heme excess directs macrophages towards an M1-like pro-inflammatory phenotype. We demonstrate that exposure of cultured macrophages to hemolytic aged red blood cells; heme or iron causes their functional phenotypic change towards a pro-inflammatory state. In addition, hemolysis and macrophage heme/iron accumulation in a mouse model of sickle disease triggers similar pro-inflammatory phenotypic alterations in hepatic macrophages. On the mechanistic level, this critically depends on reactive oxygen species production and activation of the Toll-like receptor 4 signaling pathway. We further demonstrate that the heme scavenger hemopexin protects reticuloendothelial macrophages from heme overload and reduces production of cytokines and reactive oxygen species. Importantly, in sickle mice the administration of human exogenous hemopexin attenuates the inflammatory phenotype of macrophages. Our data suggest that therapeutical administration of hemopexin is beneficial to counteract heme-driven macrophage-mediated inflammation and its pathophysiological consequences in sickle cell disease.

In the context of cancer we investigate in “Research work - Chapter II” whether leakage of red blood cells from the vasculature, or heme and/or iron generated by hemolysis, can affect the inflammatory profile of tumor-associated macrophages (TAMs), the composition of the tumor microenvironment and/or influence tumor growth. Iron staining of samples from non-small cell lung carcinoma and experimental murine lung tumors revealed that iron accumulates preferentially in TAMs whereas cancer cells are relatively iron spared. We detected two populations of TAMs regarding iron content. Iron loaded macrophages are located close to red blood cell extravasation sites in the tumor microenvironment and are enriched at the invasive front of the tumor. Hemorrhagic areas in tumors do not only show increased numbers of iron loaded TAMs but also enhanced infiltration of myeloid

cells. We monitor an enhanced inflammatory response, with increased expression of cytokines and chemokines responsible for macrophage and neutrophil recruitment, and macrophage differentiation, namely Cxcl1, Cxcl2, Csf1 and Csf2. We show that macrophages in the presence of tumor cells or conditioned media from tumor cells polarize towards an M2-like phenotype which can be shifted to a M1-like inflammatory phenotype by applying different sources of iron. We have identified a novel subpopulation of TAMs, whose phenotype is characterized by iron loading. The results point to a role of red blood cell derived iron and heme in modulating the immune response, macrophage plasticity and cytokine production in the tumor microenvironment.

In conclusion, the present thesis offers an additional basis for the growing evidence that heme and iron contribute to inflammation, not only in the context of hemolytic disorders but also as a contributing factor to inflammation in the tumor microenvironment.

RESUMO

Macrófagos são células do sistema imune inato que desempenham diversas funções, tais como reciclagem do ferro, combate de infecções, reparação de lesões e resposta imune contra o cancro. Os macrófagos podem ser classificados, através de uma nomenclatura simples e dicotómica, em dois grupos de polarização: activação clássica M1 “pro-inflamatória” e activação alternativa M2 “anti-inflamatória”. Foi previamente demonstrado que o grupo heme consegue activar o sistema imune inato, através do recrutamento e activação de neutrófilos e macrófagos. Nesta tese levantámos a hipótese de que o excesso de heme e ferro pode afectar a plasticidade e polarização dos macrófagos em dois contextos diferentes: num modelo experimental para doenças hemolíticas e num modelo experimental para cancro do pulmão.

Doenças hemolíticas, tais como a anemia falciforme e talassemia, são caracterizadas por um aumento de libertação de hemoglobina e heme para a circulação; sobrecarga de ferro e heme nos macrófagos do sistema reticuloendotelial; assim como inflamação crónica. No capítulo I do trabalho de investigação desta tese é demonstrado que o excesso de heme direcciona os macrófagos para um fenótipo pro-inflamatório semelhante a M1. Demonstrámos que a exposição de macrófagos em cultura celular a góbulos vermelhos hemolíticos e envelhecidos, heme ou ferro causa uma mudança no fenótipo dos macrófagos em direcção a um estado pro-inflamatório. Além disso, hemólise e acumulação de heme/ferro em macrófagos residentes no fígado num modelo de anemia falciforme despoleta um fenótipo pro-inflamatório semelhante. A nível mecanístico, esta alteração é dependente da produção de espécies reactivas de oxigénio e activação de vias de sinalização relacionadas com o “Toll-like receptor 4”. Também demonstrámos que a hemopexina, uma proteína que sequestra o grupo heme, protege os macrófagos reticuloendoteliais da sobrecarga de heme, resultando na redução da produção de citocinas e espécies reactivas de oxigénio, atenuando desta forma, o fenótipo inflamatório dos macrófagos. Os nossos resultados sugerem que a administração de hemopexina como terapia é benéfica para contrariar a inflamação resultante da acção de heme sobre os macrófagos, assim como as consequências patofisiológicas, em anemia falciforme.

No capítulo II deste trabalho de investigação, questionámos se o derrame de glóbulos vermelhos presentes na vasculatura; o grupo heme e/ou ferro gerados por hemólise, podem afectar o perfil inflamatório dos macrófagos associados a tumores; assim como a composição do microambiente tumoral e/ou influenciar o crescimento tumoral. A coloração de ferro em amostras histológicas de pacientes com carcinoma de células não pequenas do pulmão e amostras histológicas de um modelo murino experimental para tumores do pulmão, revelou que o ferro está preferencialmente acumulado nos

macrófagos associados a tumores. Por sua vez, as células tumorais são negativas para esta coloração. Detectámos duas populações de macrófagos relativamente à composição em ferro. Macrófagos com ferro estão preferencialmente localizados em áreas onde se verifica a extravasão de glóbulos vermelhos no microambiente tumoral e em áreas de invasão tumoral. Áreas hemorrágicas no tumor, não só demonstram um aumento em macrófagos com ferro mas também um aumento na infiltração de células mielóides. Verificámos que nestas áreas há uma resposta inflamatória ampliada, com uma expressão aumentada de citocinas e quemoquinas responsáveis pelo recrutamento de macrófagos e neutrófilos, nomeadamente Cxcl1, Cxcl2, Csf1 e Csf2. Para além disso, demonstrámos que quando os macrófagos estão na presença de células tumorais ou meio de cultura condicionado, estes são polarizados em direcção ao fenótipo M2. Após tratamento com diferentes fontes de ferro, este fenótipo M2 é deslocado para um fenótipo mais semelhante a M1. Identificámos com este trabalho, uma nova subpopulação de macrófagos associados a tumores, cujo fenótipo é caracterizado por acumulação de ferro. Os resultados apontam para uma capacidade dos glóbulos vermelhos, em particular do grupo heme e ferro que fazem parte da sua composição, em modular a resposta imune, a plasticidade dos macrófagos e a produção de citocinas no microambiente tumoral.

Em conclusão, a presente tese de doutoramento completa e aumenta o conhecimento de que heme e ferro contribuem para um conceito de inflamação estéril, não só no contexto de doenças hemolíticas mas também como um factor relevante para a inflamação em ambiente tumoral.

ABBREVIATIONS

Bach1	Btb And Cnc Homology 1
BMDM	Bone Marrow-Derived Macrophages
BMP	Bone Morphogenetic Protein
CCL2	Chemokine (C-C motif) ligand 2 (or MCP-1)
CD	Cluster of Differentiation
cDNA	Complementary DNA
CxCL	chemokine (C-X-C motif) ligand
DFO	Desferrioxamine
DMT1	Divalent Metal Transporter 1
DNA	Deoxyribonucleic Acid
EP	Erythrophagocytosis
ERK	Extracellular-Signal-Regulated Kinases
FeNTA	Ferric Nitrilotriacetate
GM-CSF (or CSF2)	Granulocyte-Macrophage Colony-Stimulating Factor
Hb	Hemoglobin
HFE	Hemochromatosis gene
HLA	Human leukocyte antigen
HO-1 (Hmox1)	Heme Oxygenase 1
Hp	Haptoglobin
Hx	Hemopexin
IFNγ	Interferon gamma
IL	Interleukin
iNOS	inducible Nitric Oxide Synthase
IRE	Iron Responsive Element
IRFs	Interferon Regulatory Factors
IRP	Iron Regulatory Protein
JAK	Janus Kinase
KC (or CxCL1)	Keratinocyte Chemoattractant
KO	Knock-out
LLC	Lewis Lung Carcinoma
LPS	Lipopolysaccharide
Ly6C	Lymphocyte antigen 6 complex, locus C
Ly6G	Lymphocyte antigen 6 complex, locus G
MAPK	Mitogen-Activated Protein Kinases

MDSCs	Myeloid Derived Suppressor Cells
M-CSF (or CSF1)	Macrophage Colony-Stimulating Factor
MHC	Major Histocompatibility Complex
MMP	Matrix Metalloproteinase
mRNA	Messenger RNA
MyD88	Myeloid differentiation primary response gene 88
NAC	N-acetyl-cysteine
NF-κB	Nuclear factor kappa-light-chain-enhancer of activated B cells
Nrf2	Nuclear factor erythroid 2-related factor-2
NO	Nitric Oxide
RBC	Red Blood Cells
RES	Reticuloendothelial System
RNA	Ribonucleic Acid
ROS	Reactive Oxygen Species
RPM	Red Pulp Macrophages
SCA	Sickle Cell Anemia
SCD	Sickle Cell Disease
SMAD	Mothers against decapentaplegic homolog
STAT	Signal Transducer and Activator of Transcription
TAMs	Tumor-associated Macrophages
TANs	Tumor-associated Neutrophils
Tf	Transferrin
TfR1	Transferrin Receptor 1
TGFβ	Transforming Growth Factor- β
TLR	Toll-like Receptor
TNFα	Tumor necrosis factor alpha
VEGF	Vascular Endothelial Growth Factor
WT	Wild Type
Ym1	chitinase-like 3

I – GENERAL INTRODUCTION

1. Iron Homeostasis: keeping the balance

1.1 Why is iron an essential element?

Iron is an essential micronutrient in nearly all organisms where it is required for numerous cellular and metabolic functions. All mammalian cells need iron for basic processes such as DNA synthesis, cell cycle progression and mitochondrial activity. More than 60% of total body iron is present in erythrocytes, where it is incorporated in heme. Heme, a porphyrin ring with the ferrous ion in the center, is the major component of hemoglobin (Hb), the iron-containing oxygen-transport metalloprotein in the red blood cells (RBC). Iron also contributes to the catalysis of redox reactions in the iron-sulfur cluster containing enzymes, such as nitrogenases and hydrogenases. We can think about iron as a double-edged sword. Thus, on the one hand iron is an essential micronutrient, its deficiency can limit erythropoiesis and cause anemia. On the other hand iron overload leads to oxidative stress due to the production of reactive oxygen species (ROS) through the Fenton Reaction (Papanikolaou and Pantopoulos, 2005). ROS can promote damage of DNA, lipids and proteins, leading in severe cases to organ malfunction. To avoid these extreme situations, it is important to keep iron levels in balance.

To prevent the toxic effect caused by iron accumulation and to assure a correct distribution of iron throughout the body, systemic and cellular iron regulation are required (reviewed by (Hentze et al., 2010)).

Since iron cannot be excreted in a regulated manner (except for epithelial skin losses and small bleedings) the key to iron homeostasis is controlling iron absorption. Organs such as the small intestine; liver and spleen play a critical role in iron homeostasis and express molecules that allow controlled iron uptake, storage and recycling both at a systemic level as well as at a cellular level.

1.2 Systemic iron regulation

Dietary iron is absorbed in the duodenum. In the diet, iron is mainly found in its oxidized state, ferric iron Fe(III). Ferric iron needs to be reduced by Duodenal cytochrome B (DcytB) to ferrous iron Fe(II) to be imported via Divalent Metal Transporter 1 (DMT1) which is expressed in the duodenal enterocytes at the brush border (Gunshin et al., 1997). Also heme iron can be imported by duodenal enterocytes but the mechanism is still unknown. Once inside the enterocyte, heme iron is released by the activity of heme oxygenase-1 (HO-1, *Hmox*) (Ferris et al., 1999). Iron export into the circulation is

dependent on ferroportin (Donovan et al., 2005; McKie et al., 2000), the only known iron exporter. Ferroportin is expressed at the basolateral membrane of enterocytes. Hephaestin, a multicopper oxidase homolog of liver ceruloplasmin, oxidases Fe(II) to Fe(III) allowing iron to be loaded onto transferrin (Tf). Transferrin is an iron transporter that contains two specific high-affinity Fe(III) binding sites. Once bound to transferrin, iron is transported in the blood stream and can be delivered to all cell types. Diferric transferrin binds to transferrin receptor 1 (TfR1), expressed at the cell membrane, and triggers the endocytosis of the complex (Cheng et al., 2004). Iron can be stored in the liver as well as other organs, such as spleen, bone marrow and muscle. Iron stores will be mobilized in accordance to cellular demand.

Iron is required for erythropoiesis. For erythropoiesis, not only dietary iron is utilized but also iron that is recycled from aged red blood cells. Iron recycling takes place in reticuloendothelial macrophages. These cells take up aged and damaged RBC and catabolize heme via the enzyme HO-1. Iron is then exported from the macrophages via ferroportin. In macrophages, ferroportin needs ceruloplasmin to oxidize iron so iron can be loaded onto transferrin and be made available for erythropoiesis and other cellular processes (Figure 1A).

1.3 The hepcidin/ferroportin axis

The maintenance of iron homeostasis critically depends on the interaction between hepcidin and the iron exporter ferroportin. The control of iron uptake and availability is dependent on the expression of ferroportin. Ferroportin is regulated by the small hormone hepcidin (Nemeth et al., 2004b). Hepcidin is a 25 amino acid peptide secreted by the liver and it was shown to be the major systemic regulator of ferroportin (Altamura et al., 2014; Nemeth et al., 2004b).

The regulation of ferroportin can occur at transcriptional, posttranscriptional and posttranslational levels.

Transcriptional regulation of ferroportin was first shown in macrophages. In iron-recycling macrophages, after erythropoiesis, heme and iron increase ferroportin expression (Marro et al., 2010). Ferroportin promoter can be bound either by Btb And Cnc Homology 1 (Bach1) (gene repression) or Nuclear factor erythroid 2-related factor-2 (Nrf2) (gene activation). Heme causes Bach1 degradation, allowing Nrf2 to facilitate ferroportin transcription. During infections with *Salmonella typhimurium*, Nitric oxide (NO) was shown

to activate Nrf2 in macrophages, resulting in increased ferroportin transcription. Lack of NO formation resulted in impaired Nrf2 expression, resulting in reduced ferroportin transcription (Nairz et al., 2013). Inflammation decreases the expression of ferroportin although part of the mechanism is still unknown. LPS injection in mice decreased ferroportin mRNA in the liver and spleen (Liu et al., 2005; Yang et al., 2002). LPS is a Gram negative bacterial membrane component that activates Toll-like receptor 4 (TLR4). Recently it was shown that the ligation of FSL1 to TLR2/6 can induce ferroportin mRNA and protein downregulation in the liver and in the spleen, while ferroportin expression in the duodenum is unchanged (Guida et al., 2015). In duodenal enterocytes, HIF2 α stabilization due to hypoxia increases ferroportin mRNA. The promoter of the ferroportin gene contains HIF response elements (HREs) that are targets for HIF2 α binding. Mice lacking HIF2 α , fail to upregulate duodenal ferroportin mRNA in response to iron deficiency (Taylor et al., 2011).

At the **posttranscriptional** level, ferroportin is regulated via iron regulatory proteins (IRPs) and their interaction with iron responsive elements (IREs): the IRE/IRP system. Iron regulates ferroportin translationally by modulating the interaction of IRPs with IREs in its 5' untranslated region (UTR). This mechanism will be further explored in this thesis (see 1.4 Cellular Iron regulation).

Post translational regulation of ferroportin is mediated through the liver peptide hormone hepcidin. Hepcidin binds to ferroportin at the enterocyte brush border, hepatocytes' membrane and macrophages' membrane and induces endocytosis and proteolysis of ferroportin. Iron is then retained inside these cells and its availability is reduced (Figure 1B). When hepcidin expression is decreased, ferroportin is active and capable of exporting iron (Figure 1C).

The **regulation of hepcidin** expression in hepatocytes is a key process in iron homeostasis. The expression of hepcidin can be regulated by iron levels, erythropoiesis, hypoxia and inflammation.

Hepcidin is **regulated by iron** stores and iron plasma concentration. In case of high iron availability, hepcidin production is increased to limit dietary iron absorption and to promote cellular iron retention. When iron is required, a decrease in hepcidin production allows iron to enter the bloodstream. In cases of high concentrations of (Tf-Fe₂), Hemochromatosis gene (HFE) is displaced from TfR1 to promote HFE interaction with transferrin receptor 2 (TfR2). The HFE-TfR2 complex then activates hepcidin transcription via extracellular-signal-regulated kinases (ERK)/mitogen-activated protein kinases (MAPK) and bone morphogenetic protein (BMP)/ Mothers against decapentaplegic homolog (SMAD)

signaling (Goswami and Andrews, 2006). Activation of BMP signaling requires hemojuvelin (HJV). The BMP co-receptor hemojuvelin (HJV) interacts with type I and type II BMP receptors (BMPR) at the plasma membrane and induces phosphorylation of SMAD1/5/8 (Kautz et al., 2008). This phosphorylation allows the formation of a complex with SMAD4, that translocate to the nucleus and binds to the hepcidin promoter, increasing hepcidin expression.

Since one of the major requests for iron is the formation of new RBC, **erythropoiesis** also regulates hepcidin expression. Hepcidin suppression allows iron stores to be mobilized to the bone marrow for the production of erythrocytes. Factors such as Growth Differentiation Factor 15 (GDF15) and Twisted Gastrulation Protein Homolog 1 (TWSG1) (Tanno et al., 2007; Tanno et al., 2009), were implicated in hepcidin suppression by inhibiting BMP/SMAD pathway. These factors were associated with β -thalassemia patients and thalassemic mice respectively. Recently, erythroferrone (ERFE), a peptide hormone produced by erythropoietin-stimulated erythroblasts, was identified as the factor responsible for the inhibition of hepcidin expression in response to erythropoiesis demands (Kautz et al., 2014). **Hypoxia** induces erythropoietin (EPO) synthesis, which in turn stimulates erythropoiesis. By inducing erythropoiesis, hypoxia also plays a role in influencing hepcidin levels.

Inflammation also regulates hepcidin expression. Several pathogens require iron to proliferate and survive. In order to limit the access of microorganisms to iron, circulating iron levels are reduced during infection leading to hypoferrremia. Hypoferrremia is commonly associated to infections and inflammatory conditions. Hepcidin is known as a liver derived antimicrobial peptide, and is a clear example of the interface between immunity and iron (Kemna et al., 2005; Nemeth et al., 2003).

LPS, activates TLR4, a receptor mainly expressed in macrophages and dendritic cells, and initiates an inflammatory response. The subsequent production of Interleukin (IL)-6 and IL-1 by macrophages triggers the expression of hepatic hepcidin (Lee et al., 2005; Nemeth et al., 2004a). Hepcidin binds and degrades ferroportin in macrophages, causing intracellular iron sequestration and decreased plasma iron levels. Hepcidin upregulation was demonstrated also in macrophages and neutrophils exposed to LPS, Gram negative and Gram positive bacteria suggesting that hepcidin release from macrophages and neutrophils contributes to restrict iron access to pathogens during infections (Liu et al., 2005; Peyssonnaud et al., 2006). IL-6 activates Janus Kinase (JAK)/ Signal Transducer and Activator of Transcription (STAT) signaling pathway that promotes hepatic hepcidin transcription. Injection of LPS in wild type mice has revealed a role for Activin B (a

member of Transforming Growth Factor- β (TGF- β) superfamily) as a mediator of hepcidin expression. Activin B induces hepcidin expression through SMAD1/5/8 signaling pathway (Besson-Fournier et al., 2012).

Not only during infections but also in other diseases characterized by inflammation (for example, cancer, rheumatoid arthritis and chronic kidney disease), immune cell activation and massive inflammatory cytokine production lead to a subtype of chronic anemia called anemia of inflammation. Anemia of inflammation is a normocytic anemia with blunted erythropoiesis (review by (Weiss and Goodnough, 2005)). Due to the excess of hepcidin levels, ferroportin is consistently targeted for degradation and macrophages retain and accumulate iron impairing mobilization of iron from stores. Iron retention decreases serum iron and impairs erythropoiesis (Theurl et al., 2009).

1.4 Cellular iron regulation

Iron is required for the survival of mammalian cells. The main source of cellular iron is transferrin bound iron (Tf-Fe₂). The uptake of Tf-Fe₂ occurs via transferrin receptor 1 (TfR1). Once inside cells, iron can be stored in ferritin or can be used for metabolic processes. Similar to systemic regulation, cells have a system that allows for the regulation of iron uptake, storage and release. It relies on the trans-acting iron regulatory proteins (IRPs) and their interaction with iron responsive elements (IREs) that are conserved motifs in mRNAs of iron-related genes (reviewed by (Muckenthaler et al., 2008)). In the case of ferroportin and ferritin, a single IRE is located in the 5' untranslated regions (UTRs). Upon IRP binding, the translation of ferroportin and ferritin is inhibited. In the case of TfR1, several IREs placed in the 3' UTR serve to stabilize the mRNA upon IRP binding. IRPs exist in two isoforms, IRP1 and IRP2 which bind to IREs in response to the cellular labile iron pool. When iron levels are high IRP1 switches from its active RNA binding form to a cytosolic aconitase, at the same time IRP2 is targeted for proteasome degradation. When iron levels are low, iron deficiency must be counteracted: IRP1 is activated as RNA binding protein and IRP2 is stabilized, both becoming fully active. The inhibition of ferroportin and ferritin translation reduces iron export and storage, respectively. The stabilization of TfR1 mRNA increases iron uptake.

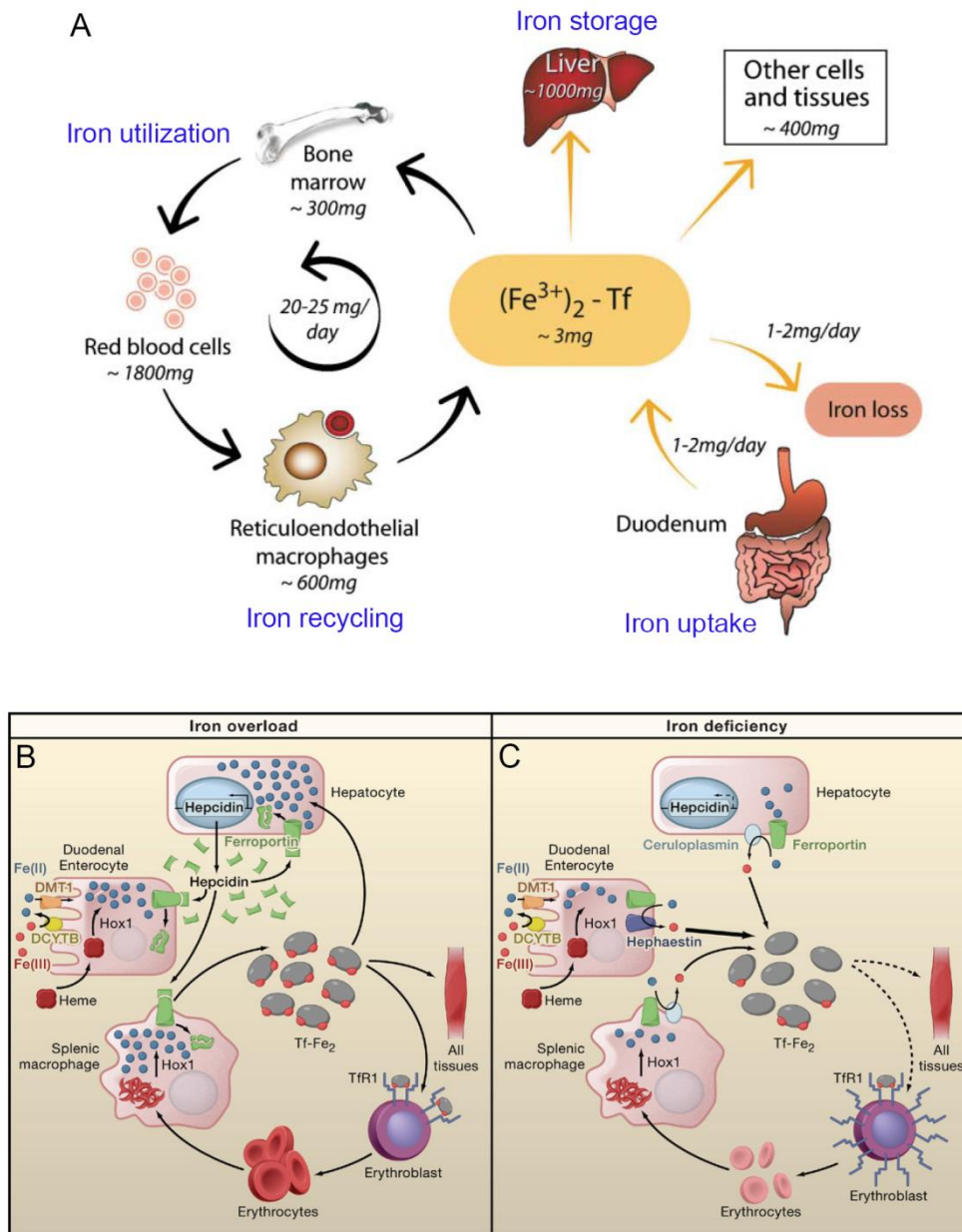


Figure 1 – Systemic iron regulation. (A) Iron uptake (1-2mg/day) occurs in the duodenum. Iron circulates in the plasma bound to transferrin (Tf-Fe_2). It is used for erythropoiesis and cellular processes or stored in the liver. Macrophages recycle 20-25mg from senescent or damaged erythrocytes. (B) In iron overload conditions, hepcidin is produced by the liver and leads to ferroportin degradation in the duodenal enterocytes, macrophages and hepatocytes, promoting cellular iron retention and a decrease of circulating iron levels. (C) In iron deficiency, hepcidin expression is reduced and ferroportin is fully active to export iron. Figure adapted from (Hentze et al., 2004; Hentze et al., 2010).

1.5 Macrophages: the iron-recycling machinery

RBC have a lifespan of approximately 120 days, after which they become senescent. Macrophages of the reticuloendothelial system (RES) in the spleen, liver and bone marrow are responsible for the recycling of aged RBC, a process known as erythrophagocytosis (EP). Macrophages can recycle 20-25mg of iron per day, which is a considerable amount if we take into account that only 1-2mg are absorbed from the diet in the duodenal brush border (review by (Ganz, 2012)). The RBC-containing phagosome merges with lysosomal vesicles (forming the erythrophagolysosome) where red blood cells are degraded. The content is subsequently imported into the macrophage cytosol. The enzyme heme oxygenase 1 (*HMOX-1*, HO-1), catabolizes heme (Poss and Tonegawa, 1997). HO-1 releases iron from the heme protoporphyrin ring and makes it available for storage in ferritin or for export. Knock-out mice for *HMOX-1* are not able to recycle heme iron and as a consequence they suffer from anemia, reduced serum iron levels and accumulation of iron in the liver and the spleen (Poss and Tonegawa, 1997). Due to heme toxicity, *HMOX-1* knock-out mice lack liver and splenic macrophages.

The mammalian homolog heme responsive gene 1 (HRG-1) is a transmembrane heme permease mainly expressed in macrophages. It transports heme from the phagolysosome to the cytoplasm during erythrophagocytosis (White et al., 2013). NRAMP1 (natural resistance-associated macrophages protein 1), a divalent metal transporter homologous to DMT1, is expressed within phagolysosomal membranes and participates in iron export from phagocytic vesicles (Soe-Lin et al., 2009). Ceruloplasmin oxidizes iron to allow for iron export via ferroportin. Iron can then be reused for erythropoiesis. Transcriptional induction of markers such as heme oxygenase 1, ferritin, and ferroportin is indicative of increased cellular heme and iron levels in macrophages during EP.

2. Heme: essential and toxic

2.1 The essential role of heme

Heme acts as prosthetic group in a range of hemoproteins that plays important roles in essential biological processes, such as, gas transport and storage, signal transduction, in the mitochondrial electron transport chain, drug metabolism and regulation of gene expression. The majority of iron that is recycled by macrophages is necessary for heme synthesis. Besides being the prosthetic group of many proteins (reviewed by (Tsiftoglou et al., 2006)), heme is mainly known for being a component of hemoglobin and myoglobin, that are used for oxygen transport and storage, respectively. Thanks to its iron moiety, heme can control redox reactions that are essential for the function of hemoproteins.

2.2 The toxic side of heme

Free heme, on the other hand, can be toxic. Its iron component, when not protected, will trigger the production of ROS that causes cell damage (Balla et al., 1991). In hemolytic disorders, such as sickle cell anemia, thalassemia and malaria, RBC breakage leads to the release of their components, hemoglobin and heme. Tissues are then exposed to large amounts of free heme that is associated with tissue damage.

To prevent heme-derived toxicity, hemoglobin is bound to haptoglobin (Hp), and the hemoglobin-haptoglobin complex is internalized through cluster of differentiation (CD)163 present in the surface of macrophages of the reticuloendothelial system and hepatocytes. When haptoglobin is not sufficient, hemoglobin is degraded to heme. Heme is then bound to albumin and subsequently bound to hemopexin (Hx), the heme scavenger (Figure 2). Heme-hemopexin complexes are taken up via Low density lipoprotein receptor-related protein 1 (LRP/CD91) (Hvidberg et al., 2005). After heme binding, Hx delivers heme to the liver (Smith and Morgan, 1978). Nevertheless, in pathological conditions, free heme might be abundant since haptoglobin and hemopexin are saturated and their scavenger capacity is exceeded, leading to non-desirable effects of heme.

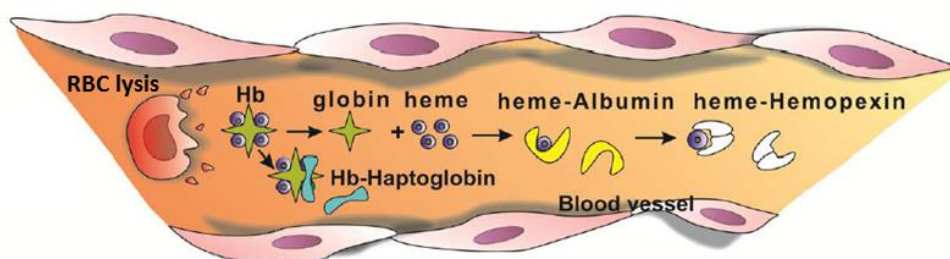


Figure 2 – Products of RBC lysis. RBC breakage leads to the release of their components, hemoglobin and heme. Hemoglobin is bound by Haptoglobin. When the buffering capacity of Haptoglobin is exceeded, hemoglobin liberates heme, which binds to albumin and is subsequently transferred to Hemopexin. (Courtesy of Francesca Vinchi).

The toxic effect of heme and its iron component includes:

- Generation of ROS through the Fenton reaction that can cause damage of lipids, proteins and nucleic acids (Balla et al., 1991; Jeney et al., 2002; Vercellotti et al., 1994);
- Iron present in heme catalyzes the oxidation of cell membrane and promotes the formation of cytotoxic lipid peroxide, which enhances membrane permeability, thus promoting cell lysis and death (Balla et al., 1991; Kumar and Bandyopadhyay, 2005; Ryter and Tyrrell, 2000);
- Heme potentiates hemolysis, since it can damage the membrane of erythrocytes (Chiu and Lubin, 1989)
- Heme impairs vascular function and activates cells of the vascular endothelium and induces the recruitment of leukocytes, potentiating inflammation (Wagener et al., 2001) (to be discussed in this thesis).

2.3 The inflammatory side of heme

One of the potential toxic effects of heme is connected with inflammation. Heme was shown to activate innate immune cells and non-hematopoietic cells thus, promoting inflammation (Wagener et al., 2001).

Heme injection in mice causes vascular permeability, recruitment and activation of neutrophils and macrophages, and an increased expression of acute-phase proteins (Lyoumi et al., 1999; Wagener et al., 2001).

Neutrophil activation induced by heme is dependent on ROS generation and protein kinase C (PKC) activation (Graca-Souza et al., 2002; Porto et al., 2007). Neutrophils attach firmly to the endothelium through adhesion molecules and migrate to parenchymal tissues. Heme injection was also shown to activate endothelial cells, inducing the expression of the adhesion molecules intercellular adhesion molecule 1 (ICAM-1), vascular cell adhesion molecule 1 (VCAM-1), E-selectin, P-selectin, and VWF (von Willebrand factor) (Belcher et al., 2014; Wagener et al., 1997). These adhesion molecules facilitate the adhesion of leucocytes and neutrophil migration. Neutrophils are important for controlling infections, nevertheless, prolonged activity of these cells is detrimental for tissue homeostasis since neutrophils can promote vascular and tissue injury by generating ROS and secreting proteases (reviewed by (Mocsai, 2013)).

Heme also activates macrophages and induces the production of Leukotriene B₄ (LTB₄), IL-1 β , Tumor necrosis factor alpha (TNF α), and Keratinocyte Chemoattractant (KC or CxCL1). LTB₄ (Monteiro et al., 2011) has an important function in heme-induced neutrophil migration and KC (Figueiredo et al., 2007) has neutrophil chemoattractant activity which contributes to the recruitment of neutrophils. IL-1 β and TNF α (Figueiredo et al., 2007) are pro-inflammatory cytokines. TNF α secretion induced by heme is important for necroptosis (necrotic cell death) (Fortes et al., 2012). The heme-mediated macrophage activation was shown to be dependent on the activation of TLR4 (Figueiredo et al., 2007). In macrophages, heme induces Myeloid differentiation primary response gene 88 (MyD88) activation and the secretion of the pro-inflammatory cytokines TNF α and KC. TLR4 activation leads to MAPK and Nuclear factor kappa-light-chain-enhancer of activated B cells (NF- κ B) activation, which are necessary for TNF α secretion. The activation of these pathways also leads to the formation of ROS. ROS generation can be induced by heme independently of TLR4. The presence of ROS potentiates the activation of NF- κ B, contributing to an enhanced production of TNF α .

Altogether, these findings classify heme as a damage-associated molecular pattern (DAMP), capable of causing sterile inflammation and tissue damage. Plasma scavengers of heme and hemoglobin play an important role in preventing the toxic and inflammatory effect of heme. For example, hemolysis or heme injection in hemopexin-null mice (*Hx*^{-/-}) cause increased inflammation and renal damage when compared to wild type (WT) mice (Vinchi et al., 2008).

2.4 Free heme and hemolytic disorders: sickle cell anemia

In hemolytic disorders such as sickle cell anemia, thalassemia and malaria, RBC breakage is enhanced and results in the release of their components: hemoglobin (Hb) and heme. Tissues are subsequently exposed to large quantities of free heme, since scavenging systems, haptoglobin (Hp) and hemopexin (Hx) are not sufficient to cope with the excess of free heme and hemoglobin. In the research work presented in this thesis, a mouse model for sickle cell disease was used to study the effects of free heme in macrophage plasticity.

Sickle-cell disease (SCD), also known as sickle-cell anemia (SCA), is a hereditary blood disorder (Pauling et al., 1949). A single point mutation in the β chain of Hb ($\beta 6\text{Glu}>\text{Val}$), leads to the synthesis of a modified Hb variant generally referred to as HbS. RBC assume an abnormal, rigid, sickle-like shape with shortened half-life and propensity to hemolysis.

Sickle-cell disease is associated with a number of acute and chronic health problems, such as severe infections, attacks of severe pain ("sickle-cell crisis"), vascular occlusion/dysfunction and development of stroke and renal failure. Sickle cell anemia is also associated with tissue iron overload, probably caused by chronic accumulation of free heme in the circulation (Hebbel et al., 1988; Reiter et al., 2002). Cell-free Hb might contribute to the pathogenesis of sickle cell anemia, by scavenging nitric oxide (NO) (Reiter et al., 2002), thereby promoting vasoconstriction, platelet aggregation and expression of adhesion molecules associated with endothelial cell activation (Belcher et al., 2003; Belcher et al., 2014). Interaction of NO with cell-free Hb also catalyzes the production of free radicals, promoting Hb oxidation and heme release. As mentioned before, free heme has inflammatory properties that can be intrinsically connected with inflammation in sickle cell disease. In this case, targeting cell-free Hb or free heme in plasma using Hp or Hx should ameliorate the pathological outcome of sickle cell disease and reduce inflammation.

3. Macrophages in immune response and iron regulation

3.1 Macrophages: origin and function

Macrophages (from Greek: big eaters, from makros "large" + phagein "eat") were first discovered at the end of the 19th century by Ilya Metchnikoff. These myeloid immune cells are central players in innate defense reactions and are strategically positioned throughout tissues. Macrophages have many different functions such as iron recycling, fighting infections, repair lesions and immune response against cancer. These cells are characterized by avid phagocytosis; they ingest and degrade dead cells, debris, and foreign material. Besides orchestrating inflammatory processes, macrophages also play a role in tissue remodeling and tissue clearance.

Macrophages are fascinating cells since their strategic distribution is correlated with the development of functional specificity (reviewed by (Epelman et al., 2014)). When we speak about macrophages, we are considering a large pleiotropic group of cells (Figure 3). In fact, the definition of macrophage comprises cells such as microglia, Kupffer cells, alveolar macrophages, among many other types of macrophages that differ not only in tissue localization, but also in the expression of surface markers, gene expression profiles (Gautier et al., 2012), function and even shape. It is this variety and plasticity that makes macrophages such an interesting subject for study. The origin and development of macrophages have been largely discussed. Macrophages can be subdivided in two groups: macrophages that have an embryonic/prenatal origin and macrophages that derive from the differentiation of tissue-infiltrating monocytes.

Most tissue-resident macrophages are established prenatally and are maintained through adulthood by longevity and self-renewal. Certain embryonic macrophage populations are established even before the emergence of circulating monocytes. In addition, monocytopenic animals display seemingly normal tissue macrophage compartments, and the number of tissue-resident macrophages is also largely unaffected in human patients suffering from monocytopenia.

The "second origin" of macrophages is monocyte-derived macrophages. Generally these macrophages display a limited life span and are associated with homeostatic but mainly

pathological inflammation, such as cancer and infections. Ly6C^{hi} monocytes in mice, and CD14⁺ monocytes in humans, represent classical monocytes, which are recruited to sites of pathological changes, such as tumor, and infection sites and can act as precursors of monocyte-derived tissue macrophages. Tumors are abundantly populated by macrophages, derived from infiltrating monocytes, as a consequence of an anti-tumoral response. Many of these tumor-associated macrophages (TAMs) are now known to promote tumor initiation, progression, and metastasis.

In this thesis, I will focus mainly on the following specific types of macrophages: macrophages of the RES, namely splenic macrophages and Kupffer cells, and later on, tumor-associated macrophages.

Splenic macrophages also known as red pulp macrophages (RPM) are specialized in iron recycling from senescent RBC (as previously described). RPMs have a prenatal origin and this population is maintained without necessary repopulation through monocytic input (Hashimoto et al., 2013). Murine RPMs are characterized by the expression of F4/80⁺ CD11b^{low/-} CD206⁺ and require the transcription factor SPI-C. As expected SPI-C deficient mice display an impaired clearance of erythrocytes (Kohyama et al., 2009). In case of toxic iron overload and impairment of RPMs, heme can trigger the differentiation of monocytes that contribute to establish new population of RPMs (Hashimoto et al., 2013). Also monocytes stored in the red pulp can be recruited under inflammatory conditions (Swirski et al., 2009).

Kupffer cells are the resident macrophage population of the liver and locate most abundantly in the periportal regions. Kupffer cells also play a role in immune surveillance, since they form a protective barrier preventing circulation of systemic pathogens. In the healthy liver, Kupffer cells display a tolerogenic phenotype, however under pathological conditions they can switch to an activated state and contribute to liver injury (Dixon et al., 2013). Under hemolytic conditions, the liver is one of the major sites for iron recycling of damaged erythrocytes. The expression of CD163 in the surface of Kupffer cells allows endocytosis of hemoglobin-haptoglobin complexes. The iron recycling function of Kupffer cells is a mechanism to protect the tissues against heme and hemoglobin mediated injury (Willekens et al., 2005).

Both splenic macrophages and Kupffer cells are necessary for homeostasis, but nevertheless, in pathological conditions, their role as homeostatic cells can be challenged and these cells can also contribute to the local immune/inflammatory response (Tacke and Zimmermann, 2014).



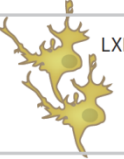








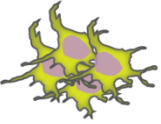

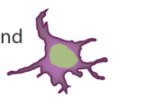

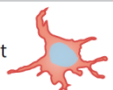
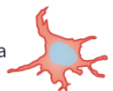
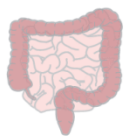
Precursor	Cell type	Organs and factors that shape macrophage tissue specificity	Function
Embryonic origin	Kupffer cell	 	Immunosurveillance Detoxification Iron and cholesterol recycling
	Marginal zone macrophage	 LXR	Immunosurveillance Detoxification
	Red pulp macrophage	 Heme ↓ Spi-C 	Iron recycling Antigen delivery to DCs
	Microglia	 CD200 CX ₃ CL1 TGF-β 	Immunosurveillance Clearing of cellular debris Synaptic pruning during development and adulthood
	Peritoneal macrophage	 Retinoic acid ↓ Gata-6 	Immunosurveillance Support of IgA production by peritoneal B1 cells
	Alveolar macrophage	 Surfactant CSF-2 CD200 	Immunosurveillance Phagocytosis of excessive surfactants and surfactant-opsonized particles
Adult Ly6C ^{hi} monocyte	Osteoclast	 CSF-1 RANKL 	Bone and joint remodeling through resorption
	Mammary gland macrophages	 CSF-1 TGF-β 	Immunosurveillance Support of branching morphogenesis
	Muscularis gut macrophage		Regulation of smooth muscle contractions
	Intestinal lamina propria macrophage	 IL-10 	Immunosurveillance Maintenance of gut homeostasis Cytokine production to establish mucosal immunity Luminal antigen uptake

Figure 3 – Macrophage origin and function. Macrophages of either embryonic origin or adult Ly6C^{hi} monocytic origin are exposed to tissue specific factors that shape macrophage differentiation, function and polarization. Figure adapted from (Varol et al., 2015).

3.2 Macrophage polarization

Under non-inflammatory conditions, tissue resident macrophages, promote homeostasis and tissue repair. What happens in pathological, inflammatory conditions? Not only tissue resident macrophages, but also monocyte-derived macrophages that infiltrate tissues in response to inflammation, are exposed to cytokines and chemokines that shape their function and inflammatory response. The observation that different subtypes of macrophages in inflammatory conditions exist, triggered a need for macrophage classification.

A simple dichotomous nomenclature defines macrophages as classically activated M1 “pro-inflammatory” or alternatively activated M2 “immune-regulatory” (Gordon, 2003; Mantovani et al., 2013; Sica and Mantovani, 2012). This nomenclature mimics the Th1/Th2 nomenclature that describes two activation states of helper T cells.

The two subsets of helper T cells (Th1 and Th2) are distinguished by the cytokines secreted after T lymphocyte activation. The Th1-type response is characterized by the production of Interferon gamma (IFN γ), thus promoting a cytotoxic response and polarization of macrophages towards a M1 phenotype. The term macrophage activation (classical activation) was first introduced by Mackaness who observed an enhanced and antigen-dependent microbicidal secondary response of macrophages against *Bacillus Calmette-Guérin* (BCG) and *Listeria* (Mackaness, 1962). Later this enhanced response was associated with IFN γ production, as a result of a Th1 response (Nathan et al., 1983).

Some years later, Th2-type response (characterized by the production of IL-4, and IL-13) was associated with an alternative activation of macrophages. This was connected to an anti-inflammatory response (Doyle et al., 1994), later called M2 macrophages.

The origin of M1/M2 nomenclature was established by Mills when he was studying arginine metabolism in macrophages (reviewed by (Mills, 2015)). Mills and colleagues observed that macrophages which have been activated in mouse strains with preferential Th1 or Th2- type response, responded differently to IFN γ or LPS stimuli (Mills et al., 2000). This difference relied simply on arginine metabolism. Macrophages have both inducible Nitric Oxide Synthase (iNOS) and Arginase enzymes that can convert arginine to NO or Ornithine. M1 macrophages express iNOS that converts arginine into NO and as consequence inhibits cell proliferation. M2 macrophages express Arginase that converts arginine into ornithine and promotes cell proliferation and repair (Mills, 2001). Later on, Mills also discovered that macrophage polarization could occur independent of T cells or

B cells, demonstrating the importance of innate immunity and how it is linked to adaptive immunity in a counterbalanced system (Mills et al., 2000). The concept of M1/kill and M2/repair was born.

M1 activity inhibits cell proliferation and causes tissue damage while M2 activity promotes cell proliferation and tissue repair.

In the last decade, macrophage polarization has been the center of many studies that tried to better characterize these two different subtypes. The polarization concept was linked to many diseases. The M1/M2 macrophages are no longer only associated with infections, but they also play an important role also in pathologies with “sterile inflammation”, such as atherosclerosis and cancer (Sica et al., 2015).

M1 macrophages, the classically activated macrophages, are characterized by a strong pro-inflammatory activity. The best understood stimuli that drive macrophages into M1 polarization are pathogen-associated molecular patterns (PAMPs) such as lipopolysaccharide (LPS) and inflammatory cytokines such as IFN γ . LPS is a TLR agonist, recognized by TLR4 and signals through MyD88, activating the transcription factors NF- κ B, STAT5 and interferon regulatory factors (IRFs). IFN γ binds to the IFN γ receptor (IFNGR1 and IFNGR2) and recruits JAK1 and JAK2 adaptors that activate STAT1 and IRFs (reviewed by (Martinez and Gordon, 2014)). These stimuli frequently occur together to polarize macrophages towards the M1 phenotype. Nevertheless, the gene expression profile of macrophages polarized independently with LPS or IFN γ is different from the combination of the two stimuli, although a significant overlap is observed (Martinez et al., 2006; Nau et al., 2002). Recently, Granulocyte-Macrophage Colony-Stimulating Factor (GM-CSF) was added to the category of M1 stimuli (Sierra-Filardi et al., 2010). GM-CSF signaling triggers the recruitment of JAK2 and activation of STAT5, NF- κ B and IRFs, a common feature with LPS and IFN γ activation. Although GM-CSF by itself doesn't show a strong polarization capacity (when compared to LPS or IFN γ) it is able to prime macrophages towards an M1 phenotype and to potentiate the effect of LPS and IFN γ . In general, M1 macrophages are characterized by the strong production of cytotoxic oxygen, nitrogen radicals and inflammatory cytokines such as IL-1 α/β , IL-6, TNF α , IL-12, IL-23 and also high expression of iNOS, CD86, Major Histocompatibility Complex (MHC) II and CD14. M1 macrophages have been associated with different pathologies. An obvious association is the role of M1 macrophages in infectious disease. M1 macrophages have bactericidal and bacteriostatic activity, as well as immune stimulatory activity. This subtype of macrophages is also associated with atherosclerosis, diabetes (M1

macrophages contribute to disease progression) and cancer. In association with cancer M1 macrophages are characterized by tumoricidal activity (Figure 4).

M2 macrophages, or alternative activated macrophages, are polarized after stimulation with anti-inflammatory cytokines. This macrophage subtype and its activation stimuli are more diverse than the M1 subgroup. M2 macrophages can be generated in the presence of cytokines such as IL-4, IL-13, IL-10, but also in the presence of TGF β , glucocorticoids and immune complexes (IgGs) (reviewed by (Martinez and Gordon, 2014)). Similar to what happens with M1 macrophages, also M2 macrophages can result from the combination of more than one stimulus. IL-4 and IL-13 are the best described cytokines that polarize macrophages towards M2. The binding of IL-4 to its receptors induces the activation of JAK1 and JAK3 and the subsequent activation of STAT6 (Martinez et al., 2009). IL-10 binding induces activation of the transcription factor STAT3. Although exposure of macrophages to IL-4 and IL-10 induces a different subtype of macrophages (M2a and M2c respectively), in terms of functionality they share common features. As mentioned before, macrophages can be exposed to more than one cytokine and the combination of stimuli is expected to occur in complex diseases such as cancer. In parallel to GM-CSF that primes macrophages towards M1, Macrophage Colony-Stimulating Factor (M-CSF) was described to prime and potentiate macrophages towards M2 polarization (Sierra-Filardi et al., 2010). Upon exposure to LPS, GM-CSF polarized (M1) macrophages produced TNF α and pro-inflammatory cytokines; while M-CSF polarized (M2) macrophages produced IL-10. M2 macrophages are characterized by the expression of Arginase-1, Ym1, IL-10, TGF β , Resistin like alpha (FIZZ1) (mouse), CD206 (mannose receptor) and scavenger receptors such as CD163. Functionally, M2 macrophages are key effectors for the resistance to parasites and for Th2 responses. M2 macrophages are also associated with diseases such as atherosclerosis and cancer. This subtype is involved in tissue remodeling, angiogenesis, immunoregulation which promotes tumor invasion and metastasis (Figure 4).

Although the concept M1/M2 is well established, it seems that the picture is far more complex. *In vivo*, macrophages can be exposed to several and diverse stimuli. This complexity of stimuli can drive macrophages in equally diverse subtypes that are not yet described or well characterized. Some authors have introduced macrophage nomenclature according to functional and homeostatic aspects (Mosser and Edwards, 2008). Recent guidelines, mainly *in vitro* systems, classify macrophages according to the expression of activation markers, the definition of the activators and the source of macrophages used (Murray et al., 2014). Also, network modeling analysis of human macrophage transcriptomes revealed at least 9 different macrophage activation programs

(Xue et al., 2014) extending the concept of M1/M2 binary classification. Since M1/M2 is the most well established nomenclature, in this thesis the markers associated with M1 and M2 were used as a mean to compare the macrophages analyzed and studied.

3.3 Macrophage polarization and iron

Since macrophages, especially RES macrophages are important for iron homeostasis, and play an important role in iron recycling, there is a strong hypothesis that iron handling by macrophages might be affected by macrophage polarization, or affect macrophage polarization.

When compared with M2 macrophages, M1 macrophages are associated with low iron turn-over. They show low expression of CD163, HO-1 and ferroportin and high expression of ferritin, suggesting that M1 macrophages show a phenotype compatible with iron retention. In contrast, M2 macrophages have a phenotype that is associated with high iron uptake, recycling and export (Recalcati et al., 2010). Furthermore, it is reported that treatment of polarized M1 and M2 macrophages with different sources of iron does not affect the expression of iron related genes such as ferroportin. These data suggest that, when compared to iron, cytokines involved in macrophage polarization (M1 – IFN γ and LPS; M2 – IL-4) have a dominant effect in the expression of the iron related genes, and determine iron handling in this two macrophages subtypes (Corna et al., 2010). In M-CSF (M2) differentiated macrophages, the expression of CD163, HO-1 and Ferroportin was higher when compared to GM-CSF (M1) polarized macrophages (Sierra-Filardi et al., 2010). In chronic venous leg ulcers, wound healing models and spinal cord injury, macrophage iron overload induces an unrestrained pro-inflammatory M1 phenotype, via enhanced production of TNF α , suggesting that iron accumulation in macrophages might contribute to a pro-inflammatory phenotype (Kroner et al., 2014; Sindrilaru et al., 2011). Also in atherosclerosis, several subsets of macrophages were described (M1, M2, M4, Mox and Mhem (reviewed by (Vinchi et al., 2014)). Mhem macrophages are associated with hemorrhagic areas, confirming that hemorrhage-derived hemoglobin is a source of iron for atherosclerosis-associated macrophages and directs their polarization into a phenotype that is dependent on Hemoglobin/iron uptake (Boyle et al., 2009). Macrophages associated with hemorrhage areas were characterized as CD163 high and human leukocyte antigen (HLA)-DR low (Boyle et al., 2011). Moreover, as a consequence of enhanced Hb clearance, Mhem macrophages show increased HO-1 and FPN expression, which might facilitate heme catabolism and reduced intracellular free iron.

GENERAL INTRODUCTION

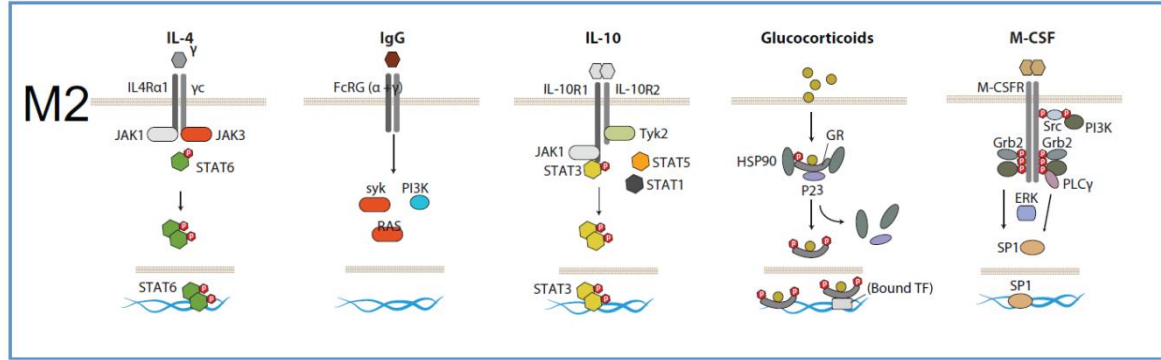
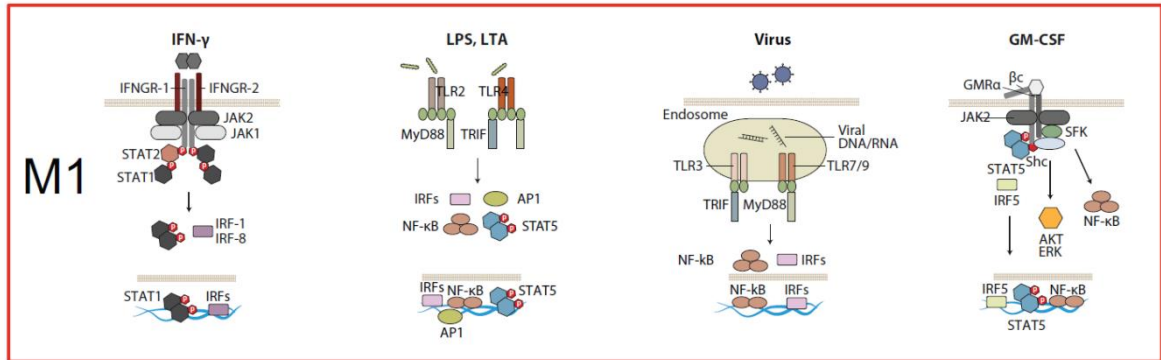
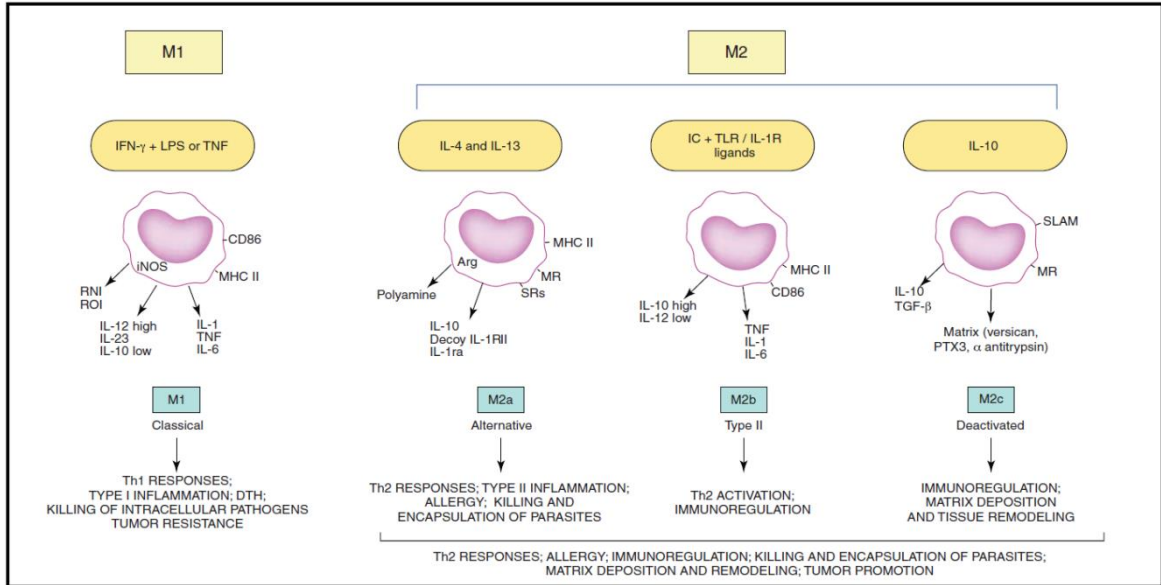


Figure 4 – Macrophage polarization subsets. Macrophages can be polarized to a M1 or M2 phenotype by different stimuli. M1 and M2 macrophage markers are represented as well as their function. Different stimuli that can give origin to M1 or M2 macrophage polarization are described with the respective signaling pathways (as described in the text). Figure adapted from (Martinez and Gordon, 2014).

4. Iron and the tumor microenvironment

4.1 The tumor microenvironment

Cancer is a complex disease that comprises many different stages and features. The metastasizing process, the most important and problematic feature of cancer, allows cancer cells to reach circulation and invade organs, leading to organ failure and death. The “hallmarks of cancer”, a concept developed by Hanahan and Weinberg (Hanahan and Weinberg, 2000, 2011) include sustaining proliferative signaling, evading growth suppressors, resisting cell death, enabling replicative immortality, inducing angiogenesis, activating invasion and metastasis, genome instability, inflammation, reprogramming of energy metabolism and evading immune destruction. Besides all these features that characterize cancer cells, another dimension of complexity can be added to this scenario: a complex tumor microenvironment that contributes to tumor progression and affects anti-tumor therapy. The tumor microenvironment includes fibroblasts, stroma, blood vessels and infiltrates of immune cells. It is a complex ecology of cells that changes with and provides support to tumor cells during transition to malignancy. Manipulation of the tumor microenvironment is seen as a current therapeutic strategy to improve cancer treatment. A better understanding of the functions of cellular constituents of tumors and the mechanisms involved in immune evasion is extremely important to develop the next generation of innovative cancer immunotherapies (Hanahan and Weinberg, 2011; van Kempen et al., 2003). On the one hand, cytotoxicity against tumor cells, mainly through IFN γ -mediated inflammatory response, is able to potentiate and mediate tumor elimination. On the other hand, tumor cells develop strategies to evade immune surveillance and also to modulate the immune system in order to suppress anti-tumoral immune responses.

Immune cells both from the innate immune system and from the adaptive immune system can be found in the tumor microenvironment and display specific roles and functions.

CD8+ T cytotoxic cells are effector cells of the adaptive immune system. These cells have been associated with good prognosis since they can exert anti-tumor effects by recognizing tumor-specific antigens presented on MHC I molecules (Vesely et al., 2011). They specifically recognize cancer cells and destroy them through perforin and granzyme mediated apoptosis (Trapani and Smyth, 2002). In order to escape from CD8 T cell mediated attack, cancer cells can downregulate MHC I molecules (Chen et al., 1996).

CD4+ T helper cells can be subdivided in Th1 cells and Th2 cells. Th1 cells are associated with early stages of tumor development and are associated with good prognosis while the presence of Th2 cells in tumors is associated with bad prognosis. The Th1 response is pro-inflammatory and anti-tumorigenic, while the Th2 response is anti-inflammatory and pro-tumorigenic. As mentioned in a previous chapter of this thesis, Th1 cells produce IFN γ , IL-2 and TNF β , which activate macrophages towards an M1 subtype. By contrast, Th2 cells produce IL-4, IL-5, IL-10, and IL-13. These cytokines activate eosinophils, and promote M2 macrophage polarization, thus contributing to tumor progression (Knutson and Disis, 2005). The identification of a third subset of Th cells expanded the Th1/Th2 paradigm. Th17 cells express ROR γ t and produce IL-17. T helper 17 cells' contributions to inflammation and autoimmunity have been established, but their role in tumor immunity remains unclear. Some reports show that Th17 cells eradicate tumors, while other reports reveal that they promote tumor progression (Zhang et al., 2014).

CD4+ T regulatory cells (Tregs) are associated with immunosuppression and cancer evasiveness. Tregs are CD25+ and depend on the transcription factor Foxp3 for their development (Fontenot et al., 2003). The most important mechanism by which Tregs mediate tumor evasion is the secretion of TGF- β and IL-10 that impair anti-tumor responses by CD4+, CD8+ and NK cells.

Gamma/delta T-cells are lymphoid cells that are in between innate and adaptive immunity. **$\gamma\delta$ T-cells** are potent producers of numerous cytokines, including IFN γ , TNF α , growth factors such as G-CSF and GM-CSF, and chemokines (Vivier et al., 2011) that can contribute to the lysis of tumor cells.

Natural Killer (NK) cells are cytotoxic lymphocytes that potently kill tumor cells, being a very important component in surveillance against cancer (Stojanovic and Cerwenka, 2011). These cells can respond against tumor cells via NK-like receptors such as NKG2D. Ligands for NKG2D are rarely detectable on the surface of healthy cells and tissues, but are frequently expressed by tumor cell lines and in tumor tissues (Nausch and Cerwenka, 2008). The potent anti-tumor response of these cells is mediated by the production of cytotoxic molecules such as perforins, granzymes and FasL and also cytokines such as IFN γ , TNF α and GM-CSF (Kaplan et al., 1998; Stojanovic et al., 2013).

Myeloid derived suppressor cells (MDSCs) are immature myeloid cells. MDSCs are defined as a population of CD11b+ Gr-1+ cells in tumor-bearing mice with demonstrated abilities to suppress CD8+ T-cell antitumor immunity (Bronte et al., 1998). It is now well accepted that MDSCs express high levels of inducible nitric oxide synthase (iNOS) and

arginase-1 which depletes essential aminoacids such as arginine from the microenvironment. Depletion of aminoacids impairs T cell growth and differentiation. MDSCs produce suppressive cytokines such as IL-10 and TGF- β and also induce Treg cell expansion (Huang et al., 2006; Srivastava et al., 2010).

Neutrophils (Tumor-associated neutrophils, TANs) are also characterized by the expression of CD11b and Gr1, which makes it difficult to distinguish from MDSC. The plasticity of neutrophils can be classified as N1 (tumor cytotoxicity and immune stimulation) versus N2 (tumor supporting mechanisms). The presence of (TGF β) in the tumor microenvironment prevents the generation of N1 neutrophils and favors N2 neutrophils. The blockade of TGF β results in the recruitment and activation of TANs with anti-tumor phenotype (N1) (Fridlender et al., 2009).

Dendritic cells (DCs), the professional antigen-presenting cells, are also compromised in the context of cancer. DCs are not able to do an efficient presentation of antigens to T cells due to the downregulation of MHC I and MHC II. Several tumor-derived mediators, such as Vascular Endothelial Growth Factor (VEGF), M-CSF, GM-CSF, IL-6, IL-10, and gangliosides, have been reported to contribute to the altered differentiation of DCs (Dhodapkar et al., 2001; Gabrilovich, 2004). These immature DCs often express no or low levels of costimulatory molecules, such as CD40, CD80, and CD86, and have been described to express indoleamine 2,3-dioxygenase, an enzyme that degrades the essential amino acid tryptophan that leads to the suppression of T-cell immunity (Munn et al., 2002).

4.2 Tumor-associated macrophages (TAMs)

Macrophages are among the most abundant immune cells in the tumor microenvironment. In some cases they can represent 50% of the infiltrated cell population. These stromal cells, which are marked by the expression of CD11b and F4/80 in mice and CD11b, CD14, CD33, and CD68 in humans, are frequently polarized towards an M2-like alternative activated macrophage phenotype (see “Macrophage polarization” chapter) (Biswas and Mantovani, 2010). Substantial evidence indicates that macrophages, rather than being tumoricidal as suggested after their activation *in vitro* (Fidler, 1988) adopt a pro-tumoral phenotype *in vivo* both in primary and metastatic sites (Biswas et al., 2013). This in part results from the production of anti-inflammatory cytokines that benefit tumor initiation, tumor promotion and immune suppression. TAMs also critically contribute to the

remodeling of the tumor microenvironment through the production of matrix metalloproteinases (MMP9 and MMP12), synthesis of growth and angiogenesis factors, and their engulfment of apoptotic cells (Condeelis and Pollard, 2006; Lewis and Pollard, 2006). TAMs that are recruited under hypoxic conditions and/or via growth factors orchestrate the angiogenic switch, which results in an increase in vascular density, facilitating invasion and metastasis and marking the transition to the malignant state (Lin and Pollard, 2007).

The **origin** of tumor-associated macrophages is not entirely understood. The most probable source of macrophages are recruited bone marrow (BM) monocytes (Wynn et al., 2013), circulating Ly6C⁺ monocytes (Movahedi et al., 2010) or monocytes that result from extramedullary hematopoiesis in the spleen that can be rapidly mobilized to the tumor (Cortez-Retamozo et al., 2012). In the case of Lewis Lung Carcinoma (LLC) it was shown that BM is the primary source of monocytes that generate TAMs and that the spleen has only a minor contribution (Shand et al., 2014). M-CSF is a major contributing factor for recruitment, differentiation and survival of TAMs (Qian and Pollard, 2010). Ablation of M-CSF resulted in a decrease in TAMs recruitment and delayed tumor initiation (Chitu and Stanley, 2006; Qian and Pollard, 2010). Besides M-CSF, also VEGFA, chemokine (C-C motif) ligand 2 (CCL2) and GM-CSF are important factors that contribute to macrophage recruitment and differentiation that might act independently from M-CSF (Lin and Pollard, 2007; Linde et al., 2012; Qian and Pollard, 2010). M-CSF -exposed macrophages orchestrate the “**angiogenic switch**” (Hanahan and Weinberg, 2011; Lin and Pollard, 2007). In part macrophages can produce VEGF and promote angiogenesis, an essential feature for invasion (Lin and Pollard, 2007). A specific population of TAMs that is characterized by the expression of TIE2 (TIE2+ macrophages) is mostly aligned near blood vessels, due to the expression of ANG2, the ligand for TIE2 expressed in endothelial cells (De Palma et al., 2005; Mazziere et al., 2011). Ablation of TIE2+ macrophages or ANG2 inhibits macrophage-vessel association and inhibits angiogenesis (Mazziere et al., 2011).

Macrophages are not only an important contributor to angiogenesis; they also help tumor cells to gain motility and reach circulation. The production of M-CSF by cancer cells stimulates macrophages to express Epidermal growth factor (EGF), which triggers the accumulation of cancer cells around blood vessels (Condeelis and Pollard, 2006). Macrophages also produce several other molecules that help tumor cell invasion and migration, namely Secreted Protein Acidic and Rich in Cysteine (SPARC) (increases tumor-cell-extracellular matrix interaction) (Sangaletti et al., 2008), cathepsin proteases

(matrix remodeling) (Laoui et al., 2011), and TGF- β (promotes epithelial-mesenchymal transition (EMT)) (Bonde et al., 2012).

Regarding **immune suppression**, TAMs are able to express HLA-E and HLA-G that can inhibit NK cells and a subset of T cells after the ligation to NKG2 (Borrego et al., 1998). HLA-E and HLA-G inhibit the migration of NK cells to the lymph node and consequential IFN γ production and CD8⁺T cell activation (Kelly et al., 2002). TAMs also produce enzymes, chemokines and cytokines that can directly suppress CD4⁺ and CD8⁺ T cells or indirectly, through the recruitment of natural Tregs to the tumor microenvironment or induction of CD4⁺ regulatory fraction. The production of TGF β and IL-10 by TAMs in different pathological scenarios was shown to upregulate Foxp3 in CD4⁺ cells, to suppress NK and CD8 T cells, further contributing to immunosuppression and Treg activation (Adeegbe and Nishikawa, 2013). Another mechanism for T cell suppression is the depletion of L-arginine in the tumor microenvironment. M1 macrophages (pro-inflammatory) express nitric-oxide synthase (iNOS) while M2 macrophages (anti-inflammatory) are hallmarked for the expression of Arginase-1 (Biswas and Mantovani, 2010; Sica and Mantovani, 2012). Arginase-1 produced by TAMs metabolizes L-arginine to urea and L-ornithine, depleting L-arginine from the tumor microenvironment. L-arginine is required for T cell function and CD3 re-expression, so its depletion by TAMs results in the suppression of T cell function (Rodriguez et al., 2003).

As addressed before, macrophages can be diverse in their function and they usually reflect upon the environment where they are localized. M1/M2 macrophage nomenclature, based on macrophage function is well established and characterized both *in vitro* and *in vivo*. In the tumor microenvironment TAMs were suggested to be either M1 (tumor killing) or M2 (tumor helper) (Martinez et al., 2009; Martinez et al., 2008; Sica et al., 2008). Although this dichotomy is well established, *in vivo* the situation is far more complex. In fact macrophages in the tumor microenvironment might be exposed to many different stimuli and play many different roles, leaving the possibility open for the existence of several subtypes of macrophages. Actually, macrophages in the tumor microenvironment are able to express both M1 and M2 markers (Qian and Pollard, 2010). These findings leave the door open to characterize and discover new subpopulations of macrophages within the tumor microenvironment.

4.3 Iron and cancer

Iron, being both toxic and essential, can be implicated in the onset of cancer and can also contribute to tumor proliferation and sustainability. Excessive iron can lead to the formation of ROS. ROS not only damages lipids and proteins, but also causes oxidative damage to DNA, which can be mutagenic (Dizdaroglu and Jaruga, 2012). Iron is a nutrient required for cell proliferation and for cell viability and cancer cells are not an exception. Iron homeostasis is altered in most cancer patients. As a result of cancer-related inflammation, cancer patients show impairment in iron homeostasis and develop anemia of cancer. The prevalence of anemia of cancer is around 40%, (when using a cutoff value of Hb of 12 g/dL for both men and women), as observed in the European Survey on Cancer Anemia (ECAS) in almost 15,000 cancer patients with different stages of disease and treatment (Ludwig et al., 2004). As seen in anemia of inflammation, the production of inflammatory cytokines such as IL-6 might have an impact in hepcidin production and macrophage iron retention, which leads to insufficient iron stores to be used in erythropoiesis (Rivera et al., 2005). Other factors that might contribute to anemia of cancer include: a blunted response to erythropoietin (EPO); bone marrow infiltration by the tumor or bone marrow suppression resulting from anticancer treatment (such as surgery, chemotherapy, or radiotherapy); and increased loss of RBC caused by blood loss from the tumor, surgery, or hemolysis (Schrijvers, 2011).

Iron was shown to be important for tumor cell proliferation; in fact, clinical and population-based studies collectively support a model in which increased levels of iron in the body are associated with increased cancer risk and increased tumor growth (Torti and Torti, 2013). The involvement of iron in processes related to DNA replication, maintaining genomic integrity (including DNA repair) and epigenetic regulation contribute both to the tumor-initiating and to the tumor-promoting propensities of iron. Iron is a co-factor for ribonucleotide reductase, an enzyme essential for cell viability and proliferation, that catalyses the rate-limiting step in DNA synthesis, the reductive conversion of ribonucleotides to deoxyribonucleotides. Iron was also implicated in the activation of several signaling pathways that are important for tumor growth and metastasis, namely p53, Wnt, NF- κ B, Hypoxia-inducible factor (HIF), cyclins and cell cycle regulation, AKT, and epidermal (EGF) and vascular endothelial growth factor (VEGF) (Torti and Torti, 2013; Zhang and Zhang, 2015).

The expression of iron related genes and proteins, has been also associated to cancer. Ferroportin, the only known iron exporter, was associated with prognosis of breast cancer.

Ferroportin expression analysis revealed that invasive subtypes of breast cancer express low levels of ferroportin, when compared to low grade tumors and benign tissue (Pinnix et al., 2010). Abnormal expression of TfR1 and Ferritin-H were observed in lung cancer and breast cancer, as well as increased levels of circulating hepcidin (Kukulj et al., 2010; Orlandi et al., 2014; Xiong et al., 2014). All these proteins are potential clinical predictors for the prognosis of a variety of cancers (Orlandi et al., 2014; Wu et al., 2004; Zhang and Zhang, 2015).

The fact that iron is essential, led to research of iron chelation therapies for cancer. Several **iron chelators**, such as desferrioxamine (DFO), deferiprone and deferasirox are used clinically for the treatment of patients with iron overload disorders. The avidity of cancer cells for iron has led to the question of whether iron chelators could be used in cancer therapy. Two broad strategies have been explored. The first has been to use iron chelators to deplete cancer cells of iron. A second, more recent strategy has been to use chelators that facilitate the redox cycling of iron to generate cytotoxic ROS within tumors. Both approaches are currently being pursued (Torti and Torti, 2013).

4.4 Lung cancer: the role of iron and macrophages

Cancer is a leading cause of death worldwide, accounting for 8.2 million deaths in 2012 (according to the World Cancer Report 2014 by the World Health Organization). **Lung cancer** is the most common cause of cancer death with 1.59 million deaths in 2012. To date, no effective treatment is available and the five-year survival rate remains less than 15%, despite advances in diagnosis and treatment. Numerous patients suffer from recurrence and metastasis following surgery, chemotherapy and radiotherapy (Goldstraw et al., 2011).

In terms of histological classification, lung cancer can be subdivided in two major categories: non-small-cell lung carcinoma (NSCLC) and small-cell lung carcinoma (SCLC). The three main subtypes of NSCLC are adenocarcinoma, squamous-cell carcinoma and large-cell carcinoma (although several subtypes are described and characterized inside each NSCLC subtype). The classification of the stage of lung cancer uses the Tumor Node Metastasis (TMN) classification. This is based on the size of the primary tumor, lymph node involvement, and distant metastasis (Mirsadraee et al., 2012).

The role of tumor associated macrophages in the progression of NSCLC is not clear. Most of the studies support the idea that M1 macrophages are associated with good prognosis.

In a study where NSCLC patients with prolonged survival were compared to those with poor survival, it was demonstrated that the presence of M1 macrophages (defined as CD68⁺ and by either HLA-DR⁺, iNOS⁺ or TNF α ⁺) was significantly increased in the extended survival group compared to those with poor survival (Ohri et al., 2009). In the extended survival group, M1 islet density was significantly increased compared with M2 density, 70% of islet macrophages were positive for M1 markers versus 38% for M2 markers (Ohri et al., 2009). These findings were confirmed in another study where NSCLC patients with extended survival had significantly higher tumor islet densities of M1 macrophages (defined as CD68⁺HLA-DR⁺) (Ma et al., 2010).

About 75% of lung cancers occur in smokers while 25% of lung cancer cases worldwide are not attributable to tobacco smoking (Sun et al., 2007). Iron accumulation in alveolar macrophages due to smoking is a common observation (Corhay et al., 1992). A study performed using the Broncho-alveolar lavage (BAL) of smokers showed that compared with the lower lobes, upper lobes of the lungs of smokers contain higher extracellular concentrations of ferritin-bound iron and decreased concentrations of transferrin. Also, compared with nonsmokers, lobes of smokers contained higher concentrations of iron and ferritin. This distribution of lung iron and iron-binding proteins may promote oxidative injury in the upper lobes of smokers (Nelson et al., 1996). It is not known if iron accumulation in alveolar macrophages or iron in the BAL contributes for the onset of lung cancer.

Some studies connected **lung cancer and iron**. Iron oxide was shown to increase the incidence of primary lung tumors in mice (Campbell, 1940). Also, subjects with high body iron stores, in particular a transferrin saturation level exceeding 60%, were shown to have an increased 1.5 relative risk to develop lung cancer when compared with subjects with lower levels (Knekt et al., 1994). Studies with human H1299 lung cancer cells revealed that the overexpression of the IRP1 impaired the capacity of the cells to form solid tumor xenografts in nude mice. IRP1 overexpression increased the expression of TfR1, but did not affect ferritin and ferroportin expression (Chen et al., 2007). In a similar setting, the induction of IRP2 stimulated the growth of tumor xenografts, while the depletion of IRP2 impaired tumor growth when compared to control mice (Maffettone et al., 2010). These data demonstrate an apparent tumor suppressor activity of IRP1 and pro-oncogenic activity of IRP2 and provide a direct regulatory link between the IRE/IRP system and human lung cancer.

A different study analyzed the expression of transferrin receptor 1 (TfR1) and ferritin in tumor tissue, tumor stroma, and normal lung tissue of NSCLC patients. The expression of TfR1 and ferritin in tumor cells was observed in 88% or 62% of patients, respectively while

tumor stroma was TfR1 negative and sporadically ferritin positive. A correlation between TfR1/ferritin expression in tumor tissue and survival was not observed. At the time of diagnosis more than 50% of the patients had anemia and significantly elevated serum ferritin. Iron content of serum ferritin (ICF) was below the reference values in 90% of patients. (Kukulj et al., 2010). The authors concluded that elevated serum ferritin in sera of NSCLC patients may be the result of inflammation and oxidative stress, rather than body iron overload. Higher expression of ferritin in tumor tissue may be the consequence of local toxicity induced by environmental factors (Kukulj et al., 2010).

A recent study showed that miR-20a regulates ferroportin expression post-transcriptionally in NSCLC human cells lines and that low ferroportin expression stimulated proliferation and colony formation. (Babu and Muckenthaler, 2016). Another interesting study revealed that subtoxic concentrations of iron, which specifically induce cellular hydroxyl radicals, affected cancer stem cell-like subpopulation of human non-small cell lung carcinoma (NSCLC). Iron-exposed NSCLC human cell lines (H460 and H292) exhibited an increase ability to form cancer stem cell spheroids and to proliferate, migrate and invade (Chanvorachote and Luanpitpong, 2016).

All these studies target the cancer cell itself, and the impact of iron in cancer cell proliferation or survival. So far, the role of iron in the tumor microenvironment of lung cancer, namely in the polarization and function of tumor-associated macrophages, was not addressed.

4.5 The Lewis Lung Carcinoma model

In order to study the impact of iron on tumor growth and cancer related inflammation, we used the Lewis Lung Carcinoma (LLC) model. The Lewis Lung Carcinoma cell line was initially described by Dr. Margaret R. Lewis in 1951. This cell line originated spontaneously as a carcinoma of the lung of a C57BL/6 mouse. The LLC cell line is a well-established mouse cancer model that is commonly used as a transplantable malignancy model in syngeneic C57BL/6 mice. LLC has been widely used as a model of metastasis and to study the mechanisms of cancer chemotherapeutic agents.

The use of this model has several advantages. So far, LLC is the only widely used syngeneic model of NSCLC (Kellar et al., 2015). The major advantage is that LLC cells can be injected in an immunocompetent murine background, such as C57BL, and immune responses can be evaluated as well as the monitoring of tumor growth. In addition,

because the LLC model is syngeneic, tumor microenvironment can be accurately analyzed in the animal model.

LLC cells can be injected subcutaneously (sc), intravenously (iv) and intraperitoneally (ip). In the work presented in Chapter II of this thesis, LLC cells were injected mainly subcutaneously. Tumors are easy to remove, dissect and analyze. With a subcutaneous injection of 1×10^6 cells, LLC tumors are palpable at day 7 after inoculation and have an average weight of 0.3 g at day 11 after inoculation. At this point, micro-metastasis cannot be detected, although the process of metastasis had already begun (Srivastava et al., 2014).

As a limitation, since this is a murine system, findings and evaluations may not be completely transferable to human conditions. Also, subcutaneous injections might not reflect tumor development in a real organ. Nevertheless, this system was successfully used as a preclinical model for Navelbine evaluation *in vivo* (a chemotherapy drug used in the treatment of NSCLC), prior to its implementation in clinical trials (Papageorgiou et al., 2000), showing that this is a valuable model for the research of possible therapies against lung cancer.

4.6 Inflammation and iron: from infection to cancer

It is evident that iron and immune system are intrinsically connected. Evidences from iron overload disorders and infections show us that there might be a loop regulation between iron and immunity: on the one hand, expression of iron related genes and proteins in immune system cells can contribute to iron regulation and homeostasis (reviewed by (Porto and De Sousa, 2007)); on the other hand, inflammation and host-pathogen interaction affect the expression of iron genes and proteins and subsequent regulation of iron homeostasis (reviewed by (Nairz et al., 2014)).

Mutations in HFE, a MHC I molecule, leads to iron overload, a disease known as hereditary hemochromatosis (HH). The majority of HH patients are homozygous for the C282Y mutation in HFE. This mutation impairs the interaction of HFE with $\beta 2$ -microglobulin resulting in the absence of HFE expression at cell surface (Feder et al., 1996). Besides iron overload, HH patients show alterations in the populations of immune cells. HFE defect reduces hepcidin circulation and as consequence, macrophages are iron depleted. HFE expression was shown to be crucial for the iron export in macrophages (Drakesmith et al., 2002; Montosi et al., 2000). Monocytes isolated from HH patients

control better the intracellular replication of *M. tuberculosis* (Olahanmi et al., 2002). In Hfe $-/-$ mice, macrophages control intracellular *Salmonella Typhimurium* better than macrophages from Hfe WT mice (Nairz et al., 2009). In response to LPS, Hfe $-/-$ macrophages produce reduced amounts of TNF and IL-6 which has been attributed to impaired TLR4 dependent signaling (Wang et al., 2009). In a similar way, LPS stimulation of monocytes of HH patients stimulated with LPS also decreased the production of TNF α (Gordeuk et al., 1992).

Patients with β -Thalassemia develop iron overload as a result of blood transfusions and become more susceptible to infections (Wang et al., 2003). Iron overload patients are, in general, more susceptible to infections with pathogens that are iron-sensitive and might benefit from increased circulating or tissue iron levels (Arezes et al., 2015; Valenti et al., 2011). The control of ferroportin/hepcidin axis was shown to be crucial in the process of infections in order to limit the availability of iron to pathogens (see chapter “1.3 The hepcidin/ferroportin axis”).

Several other molecules were implicated in having a dual effect in immunity and iron regulation. **Nitric oxide (NO)** was shown to have both a role in immunity and iron control. NO has a strong affinity for iron and can activate IRP1 RNA-binding activity (Kim and Ponka, 2003; Weiss et al., 1993). **Lipocalin-2 (LCN2)** is produced by several cells in the body including neutrophils and macrophages. It plays an important role in scavenging iron and restricts its availability to pathogens. Besides being an important player in infections and iron metabolism, it is also an important molecule for cancer development. In malignant cells, its proposed functions range from inhibiting apoptosis (in thyroid cancer cells), invasion and angiogenesis (in pancreatic cancer) to increasing proliferation and metastasis (in breast and colon cancer). Further, it stabilizes the proteolytic enzyme matrix metalloprotease-9 (MMP-9) by forming a complex with it, and thereby prevents its autodegradation (Chakraborty et al., 2012). **Lactoferrin**, an iron scavenger produced by macrophages and neutrophils, was shown to stimulate the proliferation and differentiation of T lymphocytes into the Th1 or Th2 phenotypes (reviewed by (Legrand and Mazurier, 2010)). In fact, iron might play an important role in activation and proliferation of immune system cells. Iron and heme complexes were detected in monocyte culture supernatant's after erythrophagocytosis. Culture of activated T-cells with this supernatant cultures was enough to increase T-cell proliferation (Costa et al., 1998).

All this evidences show that here is a strong connection between iron regulation and immunity, especially in case of infections. Nevertheless, iron and immune system might

also be in the interface of other pathologies characterized by sterile inflammation. Cancer is characterized by a strong inflammatory response and alteration in iron levels.

Macrophages play an important role in iron recycling and iron homeostasis, but macrophages are also a big component of the tumor microenvironment. A role for iron recycling in the tumor microenvironment has been suggested, since M2 macrophages were describe as prone to iron release and turn-over. This is especially due to the observation that M2 macrophages express less ferritin and more ferroportin when compared to M1 macrophages: lower iron storage and higher iron export. As mentioned before, this assumption suggests an iron-feed mechanism from macrophages to tumor cells. A better understanding on how iron can affect the tumor microenvironment and macrophage function could be an interesting and important step to explore and provide new therapies for cancer (de Sousa, 2011).

Transferrin bound iron and heme iron, are likely to be the most probable sources of iron found in tumors. Nevertheless, the occurrence of angiogenesis might facilitate the recruitment of inflammatory cells but might also trigger the extravasation of red blood cells into the tumor microenvironment which might break into hemoglobin and heme. Macrophages, as professional iron-recycling cells, are the first candidates that would uptake RBC, hemoglobin and heme, and recycle iron. It is not clear if this process could benefit cancer cells.

The fact that iron can be modulated and modulate inflammation (see chapter “4.3 Iron and the immune system”) strengthens the concept that in the tumor microenvironment might be an active role for iron, not only by supporting cancer cells but also by modulating the immune response.

5. Question and Aims

Different subtypes of macrophages express different subset of genes and proteins related to iron handling (Recalcati et al., 2010), storage and recycling. In addition, heme activates innate immunity by recruiting and activating neutrophils and macrophages (Dutra and Bozza, 2014; Larsen et al., 2012). Macrophages are important for iron recycling and erythropoiesis but are also fundamental players in innate immunity and cancer. Taking all this knowledge in consideration, we asked the question:

What is the effect of heme and iron in macrophage plasticity, activation and function?

To address this question we aimed to:

1. Study the effect of heme and iron in macrophage polarization *in vitro*;
2. Understand how macrophage polarization is modulated in a model of hemolytic disease;
3. Understand how heme, iron and RBC affect the tumor microenvironment and function of tumor-associated macrophages;

We expected to better understand how heme and iron can influence macrophage plasticity in order to promote better therapy for the diseases studied. In order to reply to this question, the research work presented in this thesis is divided between two chapters. The research work presented in “Chapter I” consists of a published research article that shows how heme and iron affect macrophage polarization in the context of hemolytic disorders. The research work presented in “Chapter II” consists of a manuscript (in process of submission) that explores the role of heme and iron in the context of the tumor microenvironment, namely in the plasticity of tumor-associated macrophages.

II – RESEARCH WORK

CHAPTER I:
HEMOPEXIN THERAPY REVERTS HEME-
INDUCED PRO-INFLAMMATORY
PHENOTYPIC SWITCHING OF
MACROPHAGES IN A MOUSE MODEL OF
SICKLE CELL DISEASE

CONTRIBUTIONS

The “Research Work - Chapter I” of this thesis consists in a co-first authorship publication. Here is clarified the contribution of each one of the authors:

Milene Costa da Silva, the candidate to the PhD degree in the University of Porto, contributed to the paper by suggesting and designing the original experiments that led to the publication of this paper. She demonstrated that heme and iron can influence macrophage polarization towards an inflammatory phenotype (M1). She further showed that an already established macrophage polarization can be altered by the addition of heme and/or iron: M1 macrophage polarization is enhanced and M2 macrophage polarization is shifted towards an M1-like phenotype as a consequence of heme/iron treatment. She was further involved in the planning of the *in vivo* experiments presented in the publication. In terms of experimental work, Milene participated in all experiments and figures presented in this publication with the exception of the data presented in Figure 1; Figure 2; Figure S1, Figure S2 and S18, which were performed by Francesca Vinchi at the University of Turin. Milene was the sole responsible investigator for the experiments presented in Figure 3A; Figure S4; Figure S6; Figure S7; Figure S8 and Figure S9. She established *in vitro* polarization assays of bone marrow-derived macrophages (BMDM), as well as the FACS analysis reported in this paper (both, for the *in vitro* and the *in vivo* experiments). She was responsible for histological stainings and all data containing qPCR analyses. Due to collaboration with German Cancer Research Center (DKFZ) she had access to TLR4 knock-out mice for the preparation of BMDM. In collaboration with the University of Turin, Francesca Vinchi had access to the sickle cell mouse model, which was part of the reported study. Both of the authors processed mice for the *in vivo* experiments (removal of spleen and liver; further processing of the samples and analysis of the results) and collaborated for the *in vitro* experiments. The contribution of each author to the publication is clarified in the section “Authorship” with the following text:

“Contribution: Francesca Vinchi and Milene Costa da Silva designed the project, performed the experiments, and wrote the manuscript; Giada Ingoglia and Sara Petrillo contributed to some experiments; Martina U. Muckenthaler, Emanuela Tolosano, and Adelheid Cerwenka designed and supervised the project and wrote the manuscript; and Nathan Bbrinkman and Adrian Zuercher provided Hx and revised the manuscript.”

This is an “Open access” publication. This publication will not be used in any other thesis. The co-authors approve the use of this publication as thesis.

Regular Article

RED CELLS, IRON, AND ERYTHROPOIESIS

Hemopexin therapy reverts heme-induced proinflammatory phenotypic switching of macrophages in a mouse model of sickle cell disease

Francesca Vinchi,^{1,3,*} Milene Costa da Silva,^{1,2,4,5,*} Giada Ingoglia,³ Sara Petrillo,³ Nathan Brinkman,⁶ Adrian Zuercher,⁷ Adelheid Cerwenka,⁵ Emanuela Tolosano,^{3,†} and Martina U. Muckenthaler^{1,2,†}

¹Department of Pediatric Oncology, Hematology and Immunology, University of Heidelberg, Heidelberg, Germany; ²Molecular Medicine Partnership Unit, Heidelberg University & European Molecular Biology Laboratory, Heidelberg, Germany; ³Molecular Biotechnology Center & Department of Molecular Biotechnology and Health Sciences, University of Torino, Torino, Italy; ⁴Graduate Program in Areas of Basic and Applied Biology, Abel Salazar Biomedical Sciences Institute, University of Porto, Porto, Portugal; ⁵Innate Immunity Group, German Cancer Research Center, Heidelberg, Germany; ⁶CSL Behring, Research & Development, Kankakee, IL; and ⁷CSL Behring, Research & Development, Bern, Switzerland

Key Points

- Heme and iron induce macrophage phenotypic switching toward an M1 proinflammatory phenotype.
- By scavenging free heme, hemopexin reverts heme-induced proinflammatory activation of macrophages in a mouse model of sickle cell disease.

Hemolytic diseases, such as sickle cell anemia and thalassemia, are characterized by enhanced release of hemoglobin and heme into the circulation, heme-iron loading of reticulo-endothelial system macrophages, and chronic inflammation. Here we show that in addition to activating the vascular endothelium, hemoglobin and heme excess alters the macrophage phenotype in sickle cell disease. We demonstrate that exposure of cultured macrophages to hemolytic aged red blood cells, heme, or iron causes their functional phenotypic change toward a proinflammatory state. In addition, hemolysis and macrophage heme/iron accumulation in a mouse model of sickle disease trigger similar proinflammatory phenotypic alterations in hepatic macrophages. On the mechanistic level, this critically depends on reactive oxygen species production and activation of the Toll-like receptor 4 signaling pathway. We further demonstrate that the heme scavenger hemopexin protects reticulo-endothelial macrophages from heme overload in heme-loaded Hx-null mice and reduces production of cytokines and reactive oxygen species. Importantly, in sickle mice, the administration of human exogenous hemopexin attenuates the inflammatory phenotype of

macrophages. Taken together, our data suggest that therapeutic administration of hemopexin is beneficial to counteract heme-driven macrophage-mediated inflammation and its pathophysiologic consequences in sickle cell disease. (*Blood*. 2016;127(4):473-486)

Introduction

Several pathologic states are hallmarked by systemic or local release of hemoglobin (Hb) and heme from red blood cells. Sickle cell disease (SCD) and malaria are paradigmatic hemolytic disorders, in which alteration in the structure of red blood cells (RBCs) leads to the release of Hb and heme into the circulation.

Heme is a toxic and pro-oxidant molecule when released in excessive amounts.¹⁻³ To counteract the potentially detrimental effects of Hb and heme, mammals are equipped with extracellular scavenging systems, namely haptoglobin (Hp) and hemopexin (Hx), that bind Hb and heme, respectively.⁴ Hp-Hb and Hx-heme complexes are taken up by receptor-mediated endocytosis into macrophages and hepatocytes, respectively.^{1,5-9} Reticulo-endothelial macrophages located in liver and spleen constitute the major sites for the clearance of aged or damaged RBCs. Following RBC phagocytosis or Hp-mediated Hb internalization, Hb is degraded and heme-iron is recycled for de novo erythropoiesis.³ Within cells, heme is catabolized by the activity of heme oxygenases (inducible HO-1 and constitutive HO-2) into iron, carbon monoxide, and biliverdin. The iron is then either bound by the iron storage protein ferritin, to prevent iron-mediated generation of

radicals, or exported into the bloodstream by the iron exporter ferroportin (Fpn).¹⁰⁻¹² Both RBC clearance and extracellular Hb scavenging are relatively modest events under steady-state conditions, but are drastically enhanced in hemolytic disorders.^{13,14} High levels of extracellular Hb and heme ultimately lead to the saturation and depletion of the Hp/Hx scavenging systems,¹⁵ causing heme-mediated oxidative tissue damage.¹⁶

Increasing evidence demonstrates that heme acts as a proinflammatory molecule that binds and activates Toll-like receptor 4 (TLR4), thus inducing the activation of endothelial cells¹⁷ and the production of inflammatory cytokines, such as tumor necrosis factor (TNF) α in neutrophils and macrophages.¹⁸⁻²² These observations are interesting in the context of SCD,²³⁻²⁸ malaria,^{29,30} and other pathologic conditions associated with hemoglobin/heme release,¹⁵ such as sepsis,³¹⁻³⁴ atherosclerosis,^{35,36} intracerebral hemorrhage,^{37,38} and infections,³⁹ in which levels of proinflammatory cytokines are increased. For example, monocytes from SCD patients show an enhanced state of activation, with increased expression of interleukin (IL)-15 and production of TNF α and IL-1 β .⁴⁰

Submitted August 7, 2015; accepted December 11, 2015. Prepublished online as *Blood* First Edition paper, December 16, 2015; DOI 10.1182/blood-2015-08-663245.

*F.V. and M.C.d.S. contributed equally to this work.

†E.T. and M.U.M. contributed equally to this work.

The online version of this article contains a data supplement.

The publication costs of this article were defrayed in part by page charge payment. Therefore, and solely to indicate this fact, this article is hereby marked "advertisement" in accordance with 18 USC section 1734.

© 2016 by The American Society of Hematology

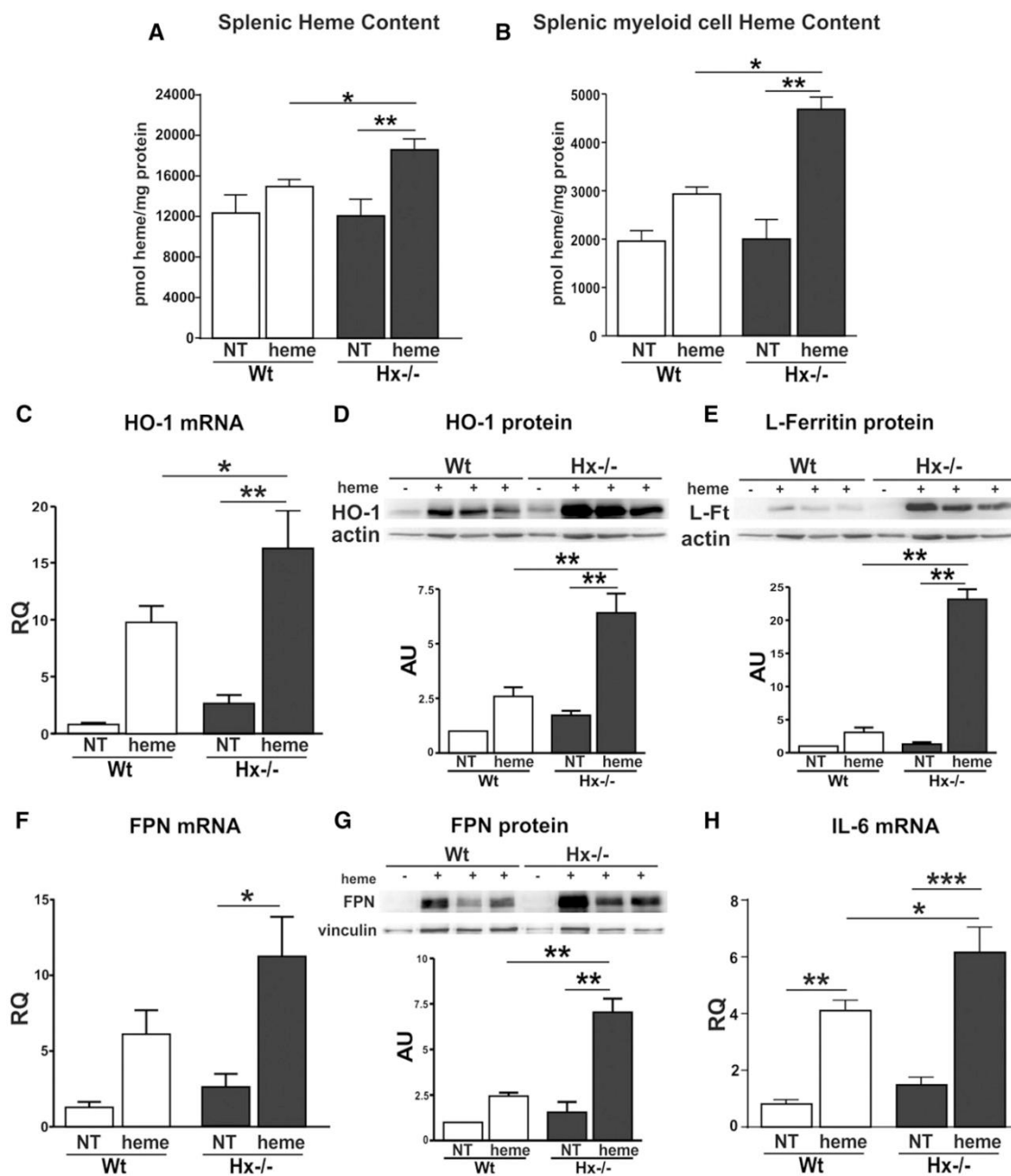


Figure 1. Hx protects macrophages from heme overload. (A-B) Heme content in the spleen and in splenic myeloid cells (CD11b⁺ granulocytes, monocytes, and ferromagnetic macrophages) from untreated (NT) and heme-treated (+heme) (hemin 70 μ mol/kg; 1 hour after injection) wild-type (Wt) and Hx-null (Hx^{-/-}) mice (n = 3). (C-G) HO-1, L-ferritin, and FPN mRNA and protein expression in splenic myeloid cells (granulocytes, monocytes, and macrophages) isolated from the spleen of untreated (NT) or heme-treated (hemin 70 μ mol/kg; 6 hours after injection) wild-type and Hx-null mice. In C and F, HO-1 and FPN mRNA levels were analyzed by qRT-PCR (NT: n = 5; heme: n = 6). Representative western blots of HO-1, L-ferritin, and FPN are shown in D, E, and G (NT: n = 3; heme: n = 6). (H) qRT-PCR analysis of IL-6 mRNA expression in splenic myeloid cells isolated from the spleen of untreated (NT) or heme-treated wild-type and Hx-null mice (hemin 70 μ mol/kg; 6 hours after injection) (untreated, NT: n = 3; heme: n = 6). Values represent mean \pm SEM. * P < .05; ** P < .01; *** P < .001. mRNA levels measured by qRT-PCR are expressed in relative quantity (RQ) to the untreated (NT) sample (RQ = 1); densitometric analysis is reported in arbitrary units (AUs), as the ratio to the untreated (NT) sample (AU = 1).

Reticuloendothelial system macrophages are characterized by marked phenotypical and functional heterogeneity, depending on the microenvironment and the cytokine composition of the niche.⁴¹⁻⁴³ A wide variety of macrophage subtypes has been described both in

vitro and in vivo. The 2 extremes are represented by "classically activated" or M1 macrophages, which are induced by microbial agents and proinflammatory T-helper (Th)1 cytokines (interferon- γ , lipopolysaccharide), and "alternatively activated" or M2 macrophages,

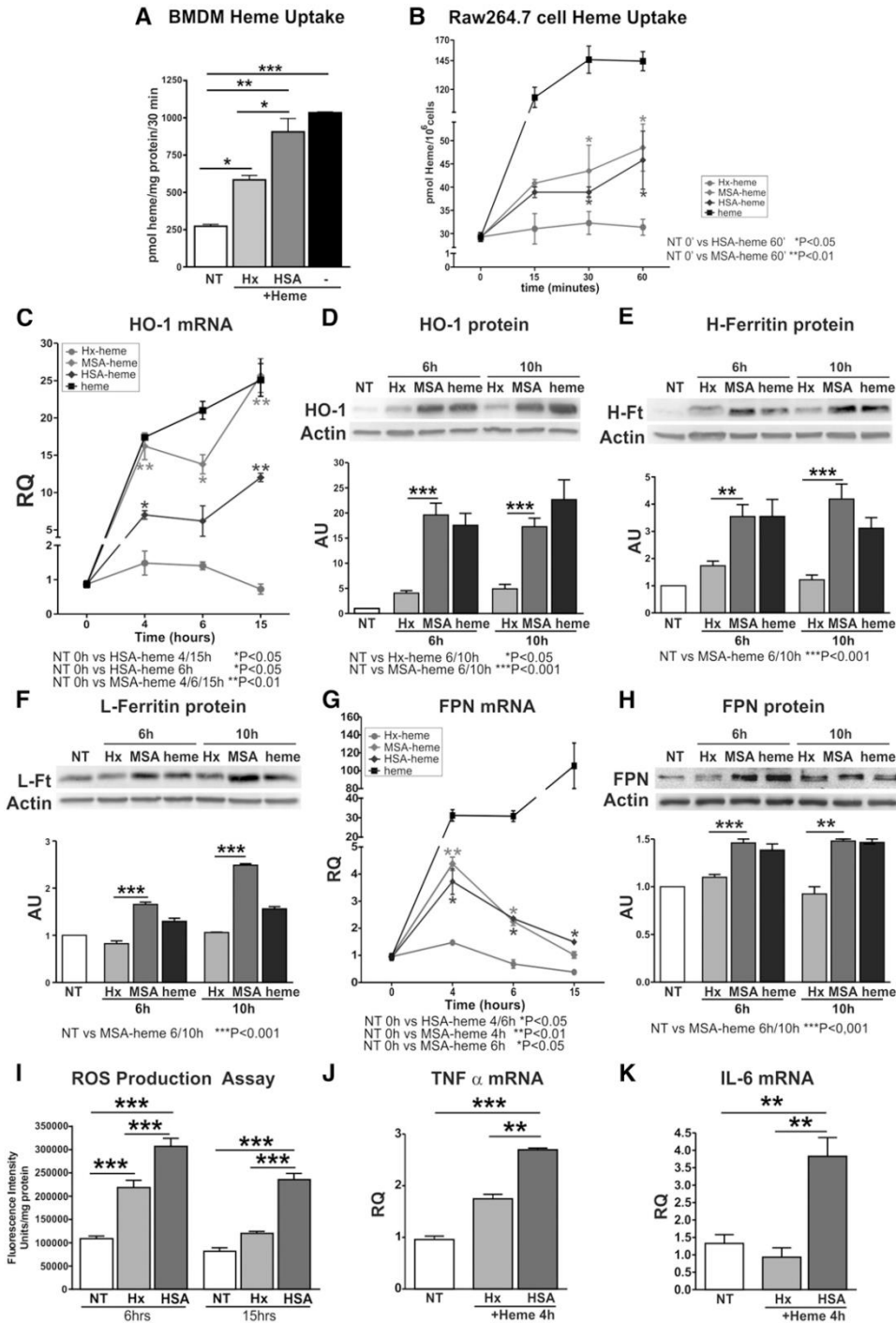


Figure 2. Hx limits heme uptake, iron loading, and the production of ROS and cytokines in BMDM and Raw264.7 cells. (A) Heme levels in BMDMs treated with 5 μ M Hx-heme or HSA-heme for 30 minutes ($n = 3$). (B) Heme levels in Raw264.7 cells treated with Hx-heme, HSA-heme, MSA-heme, or heme alone for 15, 30, or 60 minutes ($n = 3$). (C-H) HO-1, H- and L-ferritin, and FPN expression in Raw264.7 cells incubated with 5 μ M Hx-heme, MSA-heme, or heme alone for the indicated times. In C and G, HO-1 and FPN mRNAs were analyzed by qRT-PCR ($n = 4$). Representative western blots are shown in D, E, F, and H (untreated, NT: $n = 3$; heme: $n = 9$). (I) Measurement of ROS levels in Raw264.7 cells treated with 10 μ M Hx-heme, HSA-heme, or heme alone (6 and 15 hours; $n = 4$). (J-K) qRT-PCR analysis of TNF α and IL-6 mRNA expression in Raw264.7 cells treated with 5 μ M Hx-heme or HSA-heme for 4 hours ($n = 6$). Values represent mean \pm SEM. * $P < .05$; ** $P < .01$; *** $P < .001$. mRNA levels measured by qRT-PCR are expressed in RQ to the untreated (NT) sample (RQ = 1); densitometric analysis is reported in AU, as the ratio to the untreated (NT) sample (AU = 1).

mainly induced by Th2 cytokines (IL-4, IL-10, IL-13).⁴¹⁻⁴⁵ These macrophage populations are functionally different: M1 cells have inflammatory functions and bactericidal activity and produce high levels of proinflammatory cytokines and reactive nitrogen and oxygen radicals; M2 cells have immunoregulatory functions, aid parasite clearance, show increased phagocytic activity, and are involved in cell growth control, matrix remodeling, angiogenesis, and tissue repair.

Recent studies suggest that M1 and M2 macrophages show different expression profiles of iron-related genes.⁴⁶⁻⁴⁹ However, the question whether Hb, heme, or iron could directly affect the phenotype of macrophages and whether heme/iron scavengers could alter or revert this effect has never been investigated. Despite the fact that the dichotomous M1/M2 nomenclature often appears as an oversimplification and does not fully reflect on the complex biology of macrophage subsets, in this study, we took these phenotypes as a reference and analyzed expression of established M1 and M2 markers to define whether heme and iron polarize macrophages toward a pro- or anti-inflammatory phenotype.

We now show that heme, and specifically its iron moiety, promotes pronounced phenotypic changes in macrophages toward an M1-like proinflammatory phenotype, a response mediated by TLR4 signaling and reactive oxygen species (ROS) production. Importantly, the heme scavenger Hx prevents heme-induced proinflammatory phenotypic switching, both in vitro and in vivo. Additionally, administration of exogenous Hx in an experimental model for hemolysis and a mouse model of SCD is beneficial to counteract the heme-driven proinflammatory status of macrophages and its pathophysiologic consequences. These findings have important implication for the control of the inflammatory response in patients showing acute or chronic Hb and heme release.⁵⁰

Materials and methods

Mouse models and treatments

Wild-type, Hx-null,⁵¹ TLR4-null⁵² (on B6J or SV129 genetic background), and knock-in HbA and HbS sickle mice (on mixed genetic background)⁵³ were housed in the animal facility of the Molecular Biotechnology Center (Turin) or Innerbetriebliche Fortbildung (Heidelberg, only for bone marrow-derived macrophage [BMDM] preparation) and maintained on a standard diet containing 200 ppm iron (Teklad 2018S; Harlan). Mouse breeding and experiments were approved by and conducted in compliance with the guidelines of the University of Heidelberg (Germany) and Turin (Italy).

Cell treatment

Raw264.7 cells and BMDMs were treated with 2×10^7 hemolytic aged RBCs, 5 to 15 μ M heme or Zn-mesoporphyrin bound to 5 to 15 μ M albumin or Hx, or with 100 μ M iron-nitilotriacetate (FeNTA) alone or bound to 100 μ M desferrioxamine (DFO).

Preparation of splenic and hepatic macrophages and flow cytometry analysis

Splenic and hepatic macrophage-enriched fractions, obtained by spleen mechanical disruption or liver enzymatic digestion, were analyzed by flow cytometry, as described in supplemental Data available on the *Blood* Web site.

Statistical analysis

Results were expressed as mean \pm standard error of the mean (SEM). Comparisons between 2 groups were performed with 2-sided Welch *t* tests, and among 3 or >3 groups with 1- or 2-way analyses of variance, respectively, followed by the Bonferroni posttest. *P* < .05 was considered significant.

Further details on materials and methods have been included in supplemental Materials and Methods.

Table 1. Raw 264.7 macrophages heme-oxygenase activity assay

Treatment	pmol Bilirubin/mg microsomal protein/hour
NT	181.165 + 20.091
Hx-heme	183.977 + 10.261
HSA-heme	264.141 + 5.582 vs NT; vs Hx-heme ** <i>P</i> < .01
MSA-heme	246.633 + 11.161 vs NT; vs Hx-heme * <i>P</i> < .05
Heme	376.744 + 11.083 vs NT; vs Hx-heme * <i>P</i> < .05

The assay was performed on microsomes purified from Raw 264.7 cells untreated (NT) or treated with 15 μ M Hx-heme, HSA-heme, MSA-heme, or heme alone for 5 hours. Values represent mean + SEM. **P* < .05; ***P* < .01; ****P* < .001. *n* = 4 for each sample.

Results

Lack of hemopexin promotes heme loading of splenic myeloid cells

Recently, we demonstrated that Hx controls hepatic heme uptake and thus limits heme accumulation in extrahepatic tissues, such as the vessel wall and the heart,⁵ preventing heme-induced toxicity and tissue injury.⁵

Here we show that heme-challenged Hx-deficient mice, a model for acute hemolytic event, accumulate more heme in the spleen compared with heme-treated wild-type controls (Figure 1A). Consistently, CD11b⁺ cells (granulocytes and monocytes) and iron-rich cells (macrophages) isolated from heme-treated Hx-null mice show a higher heme content and increased mRNA and protein expression of HO-1, L-ferritin, and Fpn (Figure 1B-G) and elevated mRNA levels of the proinflammatory cytokine IL-6 (Figure 1H). These data suggest that Hx limits heme uptake by white cell populations and that heme accumulation affects the expression of genes involved in iron handling and the inflammatory response.

To directly demonstrate that Hx reduces heme accumulation specifically in macrophages, we measured heme levels in BMDMs incubated with 5 μ M heme bound to albumin (human/murine serum albumin [HSA/MSA]) or Hx (human) in a 1:1 ratio. Consistent with our in vivo findings in Hx-deficient mice, heme levels were significantly increased in BMDMs treated with heme-albumin compared with those treated with heme-Hx (Figure 2A). Furthermore, monocyte/macrophage-like cells (Raw264.7) treated with heme-albumin accumulated higher levels of heme (Figure 2B). Similar results were obtained when cells were exposed to the fluorescent heme analog zinc-mesoporphyrin (ZnMP) bound to albumin or Hx (supplemental Figure 1). Raw 264.7 cells treated with heme-albumin showed increased mRNA and protein expression of HO-1 and FPN, increased protein expression of H- and L-ferritin, and HO activity compared with heme-Hx treated cells (Figure 2C-H; Table 1). In addition, we observed increased ROS production (Figure 2I; supplemental Figure 2), as well as an enhanced expression of IL-6 and TNF α in cells treated with heme-albumin compared with heme-Hx (Figure 2J-K).

Taken together, these data demonstrate that Hx limits macrophage heme overload and prevents the pro-oxidant and proinflammatory effects triggered by heme in cellular assays and in vivo.

Heme and iron polarize macrophages toward an M1-like proinflammatory phenotype

Based on the observation that ROS production and expression of proinflammatory cytokines are elevated in heme-loaded macrophages and that heme triggers sterile inflammation,^{18,54} we hypothesized that heme may induce macrophage polarization toward an inflammatory phenotype.

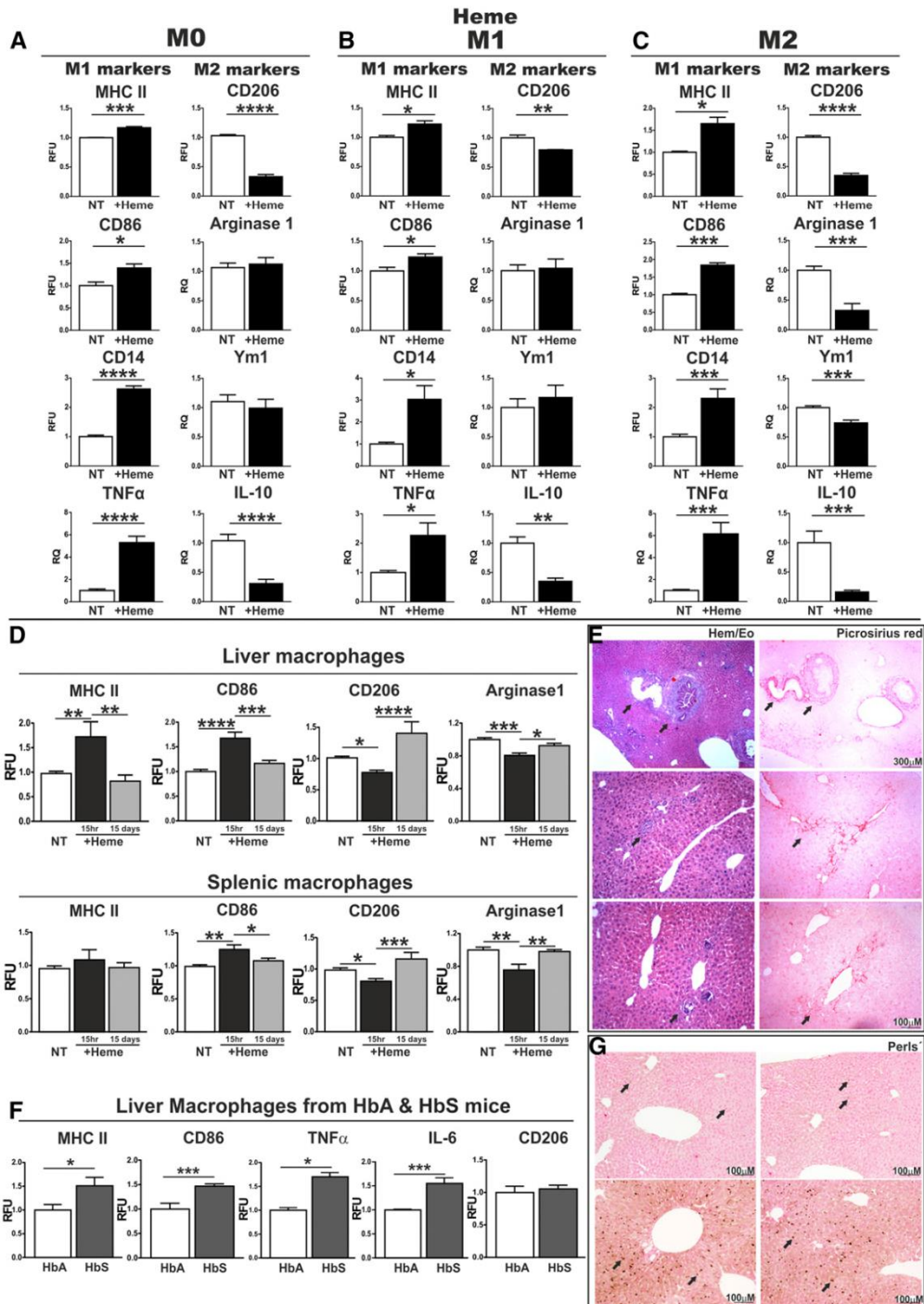


Figure 3. Heme induces macrophage polarization toward an M1-like phenotype, independently of the cell differentiation state. (A) M0, (B) M1, and (C) M2 BMDMs were left untreated (NT) or exposed to 5 μ M heme-BSA (+Heme, 1:1 ratio) for 12 hours. M1 and M2 markers are shown in the left and right column of each panel, respectively. The expression of major histocompatibility complex class II (MHCII), CD86, CD14, and CD206 was analyzed by flow cytometry and is expressed in relative fluorescence units (RFU) as fold change compared with untreated cells (NT). The mRNA levels of TNF α , Arginase-1, Ym1, and IL-10 were analyzed by qRT-PCR and expressed in RQ, as fold change compared with untreated cells (NT). Results shown are the average of ≥ 3 independent experiments. (A direct comparison of expression levels of M1 and M2 markers in M0, M1, and M2 BMDMs is shown in supplemental Figure 7, where fold changes are compared with untreated [NT] M0 cells). (D) Analysis of the M1 markers MHCII and CD86 and the M2 marker CD206 and Arginase-1 in macrophages isolated from liver or spleen of untreated (NT) or heme-treated (hemin 30 μ mol/kg) wild-type mice. Macrophages were analyzed 15 hours or 15 days after intravenous heme injection (n = 6). (E) Hematoxylin/eosin and Picrosirius red staining for collagen on

To test this, we exposed cultured BMDMs (M0; not treated with cytokines) to aged hemolytic RBCs (2×10^7 cells) as a source of Hb, to hemin (5 μ M bound to bovine serum albumin [BSA], 1:1 ratio) or to FeNTA (100 μ M) and analyzed the expression of M1 and M2 macrophage polarization markers by flow cytometry (gating strategy; supplemental Figure 3) and quantitative reverse transcriptase-polymerase chain reaction (qRT-PCR). We show that incubation of M0 BMDMs with aged RBCs increased the expression of M1 polarization markers, in particular MHCII and TNF α , and decreased the expression of the M2 polarization marker CD206 (supplemental Figure 4). Likewise, heme and FeNTA treatment causes the induction of the M1 markers MHCII, CD86, CD14, TNF α , IL-6, and IL1 β and a decrease in the M2 markers CD206, IL-10, and Arginase-1 (the last with FeNTA only) in M0 BMDMs (Figure 3A; supplemental Figures 5, 6A, and 7). We next investigated whether heme and iron could also affect the differentiation of macrophages that were exposed together with cytokines that trigger M1 or M2 polarization. We demonstrate that both hemin and FeNTA treatment enhanced the phenotype of M1 macrophages (Figure 3B; supplemental Figures 6B and 7) and shifted the differentiation of M2 macrophages toward an M1-like phenotype (Figure 3C; supplemental Figures 6C and 7). Importantly, protoporphyrin did not induce TNF α , suggesting a critical proinflammatory role for iron within the heme moiety (supplemental Figure 8). Regulation of iron-related genes in M0, M1, and M2 macrophages was monitored to control for the efficacy of heme and FeNTA treatment (supplemental Figure 9). These results demonstrate that heme induces polarization of macrophages toward a M1-like proinflammatory phenotype and that this effect is independent of the cell differentiation state.

To assess whether heme alters macrophage plasticity in vivo, we injected wild-type mice intravenously with heme (30 μ mol/kg) and analyzed iron levels and the expression of polarization markers by flow cytometry in spleen and liver macrophages, 15 hours or 15 days after heme injection (gating strategy; supplemental Figures 10 and 11). Importantly, 15 hours after heme injection, hepatic macrophages showed iron deposition (data not shown) and an increased expression of the M1 markers MHCII and CD86 and reduced levels of the M2 markers CD206 and Arginase-1 compared with nontreated mice. Likewise, splenic macrophages from heme-treated mice show increased expression of CD86 and reduced levels of CD206 and Arginase-1 (Figure 3D). Modulation of most M1 and M2 markers was reduced 15 days after heme injection, indicating that heme-induced proinflammatory activation of macrophages is a reversible event.

The polarization of macrophages into an M1 proinflammatory phenotype contributes to the perpetuation of inflammation by recruitment of circulating monocytes and leads to hepatocyte apoptosis and fibrosis.⁵⁵ Consistently, we show that repeated heme injections (70 μ mol/kg, 5 injections) cause the recruitment of a massive number of inflammatory cells, deposition of collagen fiber, and liver damage (Figure 3E).

We next assessed whether our findings are of pathophysiologic relevance for a paradigmatic chronic hemolytic disorder such as SCD that is hallmarked by a high amount of circulating Hb/heme, accelerated erythrophagocytosis, and low endogenous levels of Hp and Hx.⁵ Our analysis shows that liver macrophages from HbS sickle mice express significant higher levels of the M1 markers MHCII, CD86, TNF α , and

IL-6 compared with HbA control mice and have enhanced macrophage iron deposition (Figure 3F-G). Taken together, our data demonstrate that heme triggers reversible proinflammatory phenotypic switching of macrophages in vivo that could partially contribute to the inflammatory state associated with chronic hemolytic conditions, such as SCD.

Activation of the TLR4 signaling pathway and ROS production control heme-mediated phenotypic changes of macrophages

To study whether TLR4 activation and/or ROS production are involved in heme-induced M1 polarization of macrophages, BMDMs were treated either with heme alone or together with the TLR4 inhibitor TAK-242 (400 nM) or the antioxidant *N*-acetylcysteine (NAC, 2 mM). Cotreatment of M0 BMDMs with heme and TAK-242 attenuated the increase of the M1 markers MHCII, CD14, TNF α , IL-6, IL-1 β , and CD86 and the decrease of the M2 marker CD206, IL-10, and Ym1 in comparison with heme treatment alone (Figure 4A; supplemental Figures 5 and 12). Similarly, NAC prevented increased expression of MHCII, CD14, TNF α , IL-6, IL-1 β , and CD86 and mildly compensated for the decrease of CD206 and IL-10 following heme treatment (Figure 4D; supplemental Figure 5). In addition, both TAK-242 and NAC attenuated heme-mediated M1 marker induction and M2 marker decrease in M2 BMDMs, whereas a milder effect was observed in M1 BMDMs (Figure 4B-F). Consistent with the data obtained by applying the TLR4 inhibitor, BMDMs from TLR4-null mice show a strongly attenuated increase of the M1 markers CD14, MHCII, IL-1 β , and TNF α on heme treatment. Additional NAC treatment of TLR4-null BMDMs fully rescued the residual heme-mediated induction of these markers (Figure 5A). Likewise, NAC was able to prevent iron-induced M1 polarization in M0, M1, and M2 BMDMs (supplemental Figure 13), indicating that the alteration of macrophage plasticity in response to iron is mostly explained by its pro-oxidant properties.

To test whether ROS production and/or TLR4 activation are crucial for the in vivo response of macrophages to heme, we challenged wild-type mice either with heme alone or together with NAC (500 mg/kg body weight) or TAK-242 (2 mg/kg body weight) and analyzed the expression of macrophage polarization markers in isolated macrophages. In hepatic and splenic macrophages, cotreatment with NAC or TAK-242 reduced the heme-induced upregulation of the M1 markers MHCII and CD86 and attenuated inducible nitric oxide synthase (iNOS) expression. In hepatic macrophages, TAK-242 also diminished heme-driven induction of IL-6 and TNF α and NAC partially recovered CD206 downregulation (Figure 5B-C). The partial rescue observed with both TAK-242 and NAC could be due to the use of suboptimal doses of drugs applied or additional pathways contributing to heme/iron-induced phenotypic switching of macrophages.

These findings suggest that both TLR4 activation and ROS production control heme-mediated programming of macrophages toward the M1 proinflammatory phenotype and that each of the 2 pathways is indicated by a partially overlapping subset of M1 and M2 markers.

The heme scavenger Hx and the iron chelator DFO prevent heme and iron-induced M1 polarization of macrophages

We next tested whether heme and iron scavengers prevent heme and iron-induced macrophage polarization, respectively. M0 BMDMs were exposed to hemolytic aged RBCs, heme, or FeNTA alone or

Figure 3 (continued) liver sections from heme-treated wild-type mice (70 μ mol/kg, 5 injections; scale bar, 300-100 μ m). Arrows indicate infiltrates (hem/eo) and collagen (picrosirius). (F) Analysis of the M1 markers MHCII, CD86, TNF α , and IL-6 and the M2 marker CD206 in hepatic macrophages of control HbA and sickle HbS mice (n = 4). The expression of polarization markers in hepatic and splenic macrophages was analyzed by flow cytometry and is expressed in RFU as fold change compared with untreated wild-type mice (NT) or HbA controls. (G) Perls' staining for iron on liver sections from HbA and HbS mice (scale bar, 100 μ m). Values represent mean \pm SEM. * P < .05; ** P < .01; *** P < .001; **** P < .0001. Regulation of iron-related genes in M0, M1, and M2 macrophages was monitored to control for the efficacy of heme and FeNTA treatment (supplemental Figure 9).

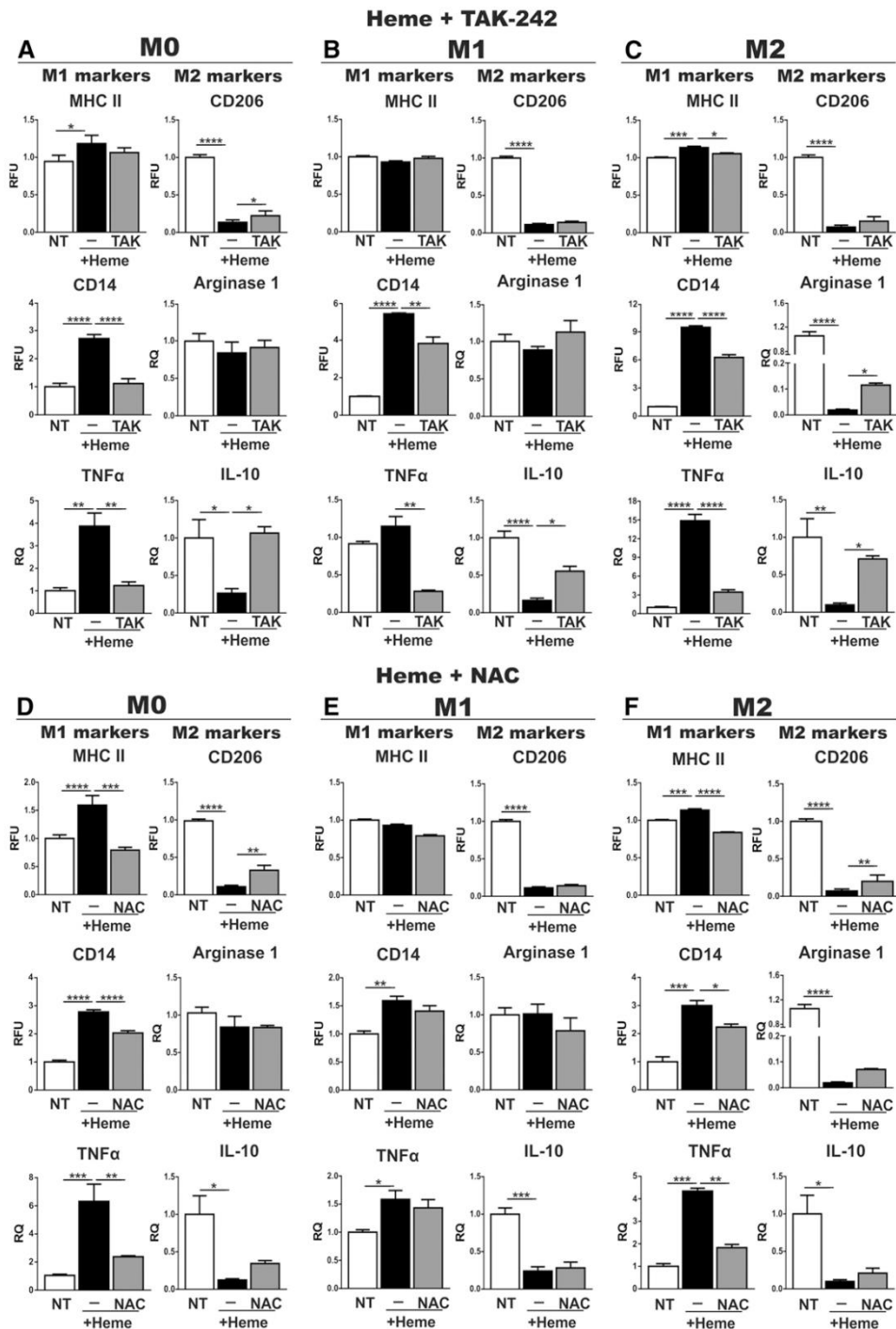


Figure 4. The TLR4 inhibitor TAK-242 and the antioxidant NAC attenuate heme-induced M1 polarization of macrophages. (A, D) M0, (B, E) M1, and (C, F) M2 BMDMs were left untreated (NT) or exposed to 5 μ M heme-BSA (+Heme; heme-BSA 1:1 ratio) with or without (A-C) 400 nM TAK-242 and (D-F) 2 mM NAC for 12 hours. M1 and M2 markers are shown in the left and right column of each panel, respectively. The expression of MHCII, CD14, and CD206 was analyzed by flow cytometry and expressed in RFU as fold change to nontreated (NT) cells. mRNA levels of TNF α , Arginase-1, and IL-10 were analyzed by qRT-PCR and expressed in RQ, as fold change to untreated (NT) cells. Results shown are representative of 3 independent experiments. Values represent mean \pm SEM. * P < .05; ** P < .01; *** P < .001; **** P < .0001.

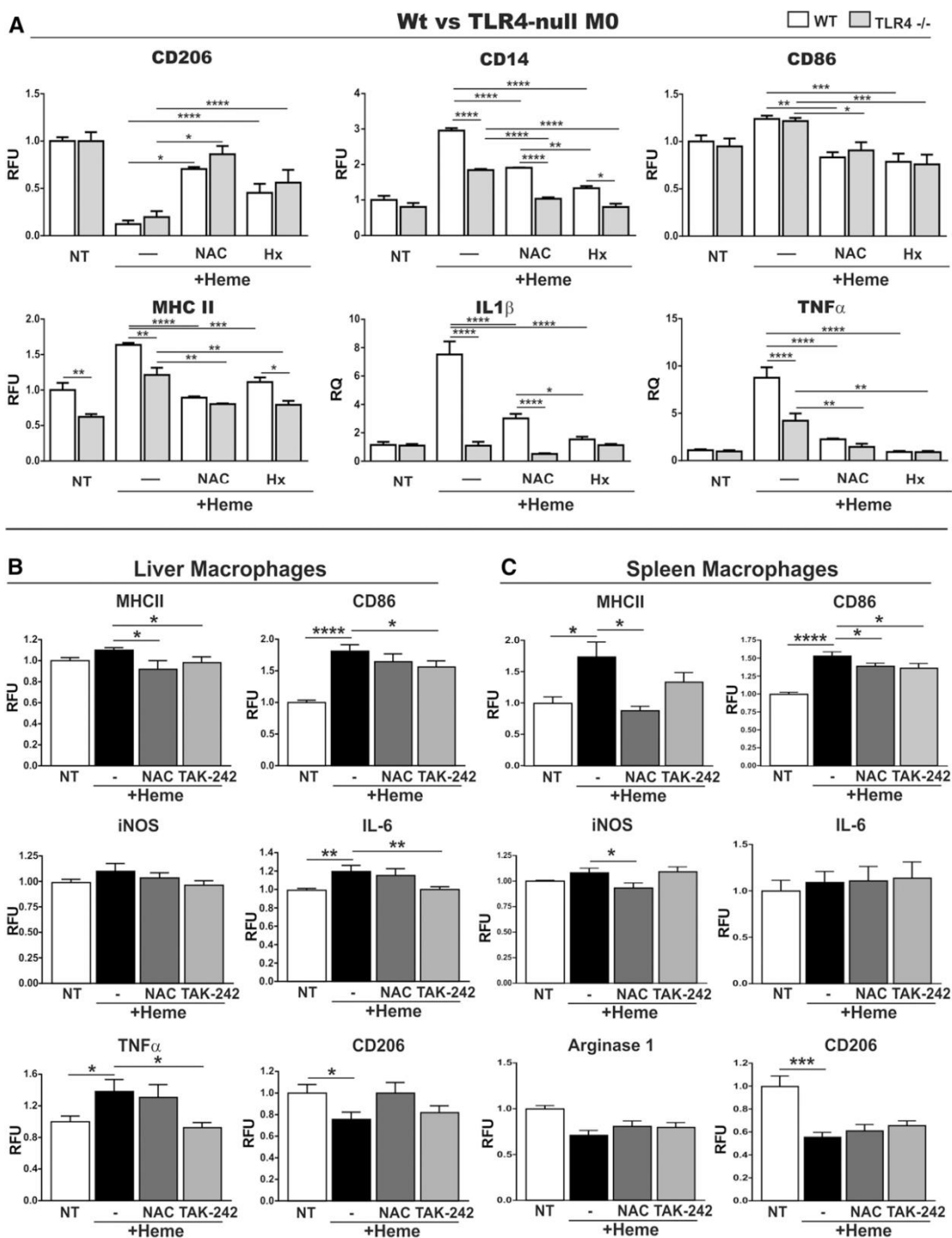


Figure 5. TLR4 signaling and ROS production contribute to heme-induced M1 proinflammatory phenotypic switching of macrophages. (A) M0 BMDMs were prepared from wild-type and TLR4-null mice and left untreated (NT) or exposed to 5 μ M heme-BSA (+Heme; heme-BSA 1:1 ratio) with or without 2 mM NAC or to 5 μ M heme-Hx (Hx; heme-Hx 1:1 ratio) for 12 hours. M1 and M2 markers are shown in the left and right column of each panel, respectively. The expression of CD206, CD14, CD86, and MHCII was analyzed by flow cytometry and expressed in RFU as fold change to untreated cells (NT). mRNA levels of TNF α and IL-1 β were analyzed by qRT-PCR and expressed in RQ, as fold change to untreated cells (NT). Results shown are representative of 3 independent experiments. (B-C) Analysis of the M1 markers MHCII, CD86, iNOS, IL-6, and TNF α and the M2 markers Arginase-1 and CD206 in macrophages isolated from (B) liver or (C) spleen of wild-type mice untreated (NT) or treated with heme (heme-BSA 30 μ mol/kg; 15 hours) with or without TAK-242 (2 mg/kg) or NAC (500 mg/kg) (n = 8). The expression of polarization markers in hepatic and splenic macrophages was analyzed by flow cytometry and is expressed in RFU as fold change compared with untreated wild-type mice (NT). Values represent mean \pm SEM. * P < .05; ** P < .01; *** P < .001; **** P < .0001.

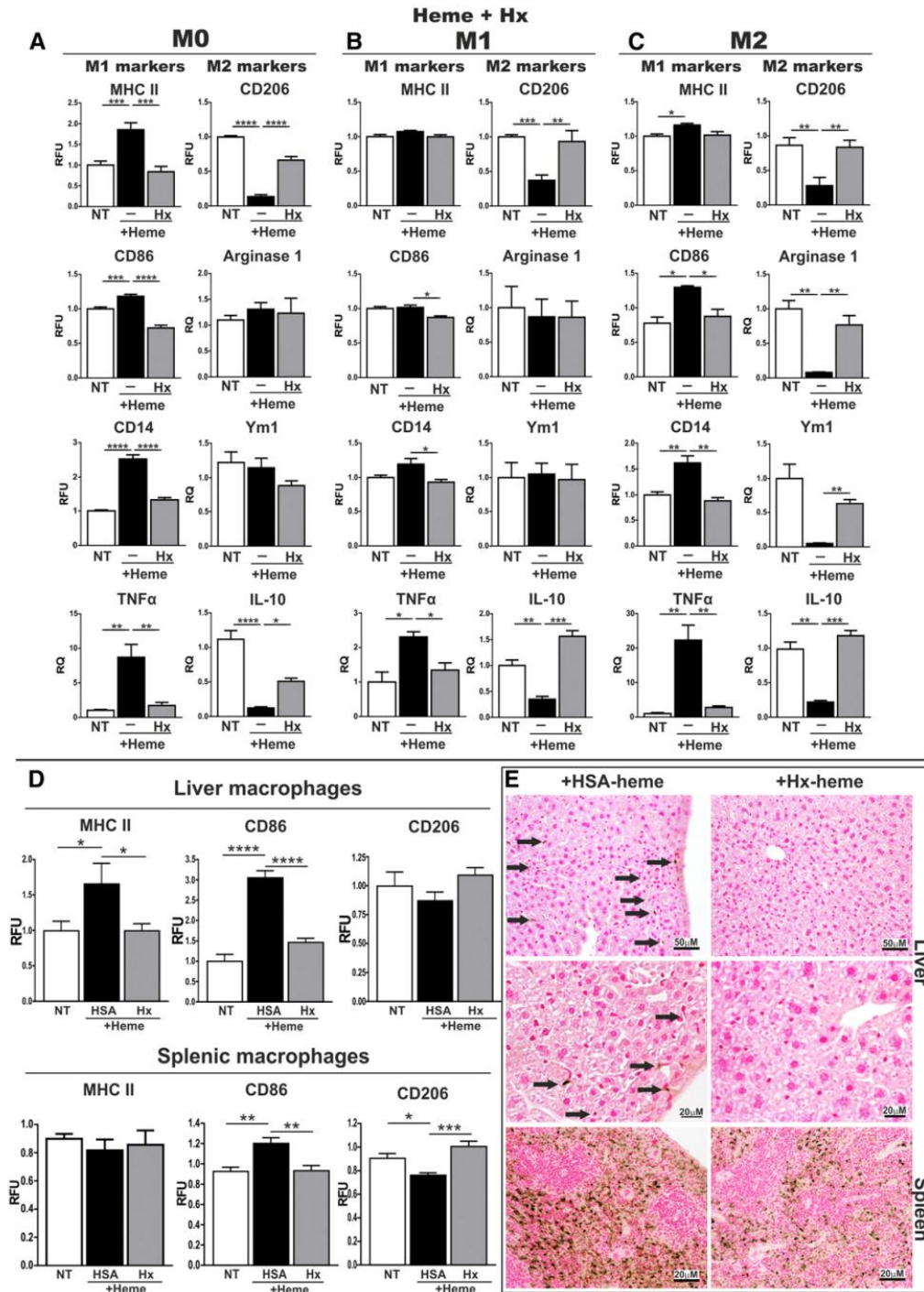


Figure 6. Hx prevents M1 polarization of macrophages in response to heme. (A) M0, (B) M1, and (C) M2 BMDMs were left untreated (NT) or exposed to 5 μ M heme-BSA (+Heme; heme-BSA 1:1 ratio) or 5 μ M heme-Hx (Hx; heme-Hx 1:1 ratio) for 12 hours. M1 and M2 markers are shown in the left and right column of each panel, respectively. Results shown are the average of ≥ 3 independent experiments. (D) Analysis of the M1 markers MHCII and CD86 and the M2 marker CD206 in macrophages from liver and spleen of wild-type mice that remained untreated or were treated with heme-HSA or heme-Hx (complex 15 μ mol/kg; 15 hours) ($n = 5$). The expression of MHCII, CD86, CD14, and CD206 was analyzed by flow cytometry and expressed in RFU as fold change to untreated cells or untreated wild-type animals (NT). mRNA levels of TNF α , Arginase-1, Ym1, and IL-10 were analyzed by qRT-PCR and expressed in RQ, as fold change to untreated cells (NT). (E) Perl's staining for iron on liver and spleen sections from wild-type mice that were treated with heme-HSA or heme-Hx (scale bar, 20-50 μ m). Arrows indicate iron-loaded Kupfer cells. Values represent mean \pm SEM. * $P < .05$; ** $P < .01$; *** $P < .001$; **** $P < .0001$.

Table 2. Viability of BMDMs exposed to heme, FeNTA, and hemolytic RBCs in the presence or absence of Hx and DFO

	NT	+Heme-BSA	+ Heme-Hx
M0	89.07 + 2.443	51.13 + 5.032 vs NT <i>P</i> < .0001	86.25 + 3.036 vs Heme-BSA <i>P</i> < .0001
M1	63.88 + 3.785	46.17 + 2.569 vs NT <i>P</i> < .001	71.95 + 2.737 vs Heme-BSA <i>P</i> < .0001
M2	89.85 + 1.699	52.08 + 2.788 vs NT <i>P</i> < .0001	90.78 + 0.895 vs Heme-BSA <i>P</i> < .00001
		+FeNTA	+ FeNTA-DFO
M0	94.40 + 0.503	72.03 + 5.341 vs NT <i>P</i> < .05	90.23 + 4.670 vs FeNTA <i>P</i> < .05
M1	61.30 + 6.584	45.07 + 5.007 vs NT not significant	55.65 + 6.986 vs FeNTA not significant
M2	93.40 + 1.320	73.13 + 3.464 vs NT <i>P</i> < .01	88.80 + 2.70 vs FeNTA <i>P</i> < .05
		+RBC	+ RBC-Hx
M0	93.98 + 0.349	83.02 + 0.837 vs NT <i>P</i> < .0001	88.75 + 0.150 vs RBC <i>P</i> < .001

Cell viability was assessed by flow cytometry using 7AAD. Viability is reported as percentage viable cells over the total number of analyzed cells.

together with Hx (100 μ M with RBCs; 5 μ M with heme) or DFO (100 μ M with FeNTA). Treatment with Hx or DFO diminished the increase of some M1 polarization markers in BMDMs following treatment with hemolytic RBCs (supplemental Figure 14). In addition, Hx and DFO prevented the heme- and iron-mediated induction of the M1 markers MHCII, CD86, CD14, and TNF α and the decrease of some M2 markers, such as CD206, IL-10, and Arginase-1 (the last for FeNTA only) in M0 BMDMs (Figure 6A; supplemental Figure 15A). Importantly, the expression of polarization markers remained unaltered following treatment with Hx and DFO alone (supplemental Figure 16). Similar data were obtained when M1 or M2 macrophages were exposed to heme or FeNTA in the presence of Hx or DFO (Figure 6B-C; supplemental Figure 15B-C). Interestingly, treatment with Hx and DFO improved the survival of BMDMs exposed to heme and iron, respectively (Table 2).

To assess the potential of heme scavengers for protecting macrophages from heme-triggered polarization *in vivo*, we injected wild-type mice with heme bound to the low-affinity scavenger, HSA, or the high affinity scavenger, Hx, and analyzed macrophage polarization markers. Interestingly, hepatic macrophages derived from mice treated with heme-Hx showed a blunted induction of the M1 markers MHCII and CD86 compared with cells from animals treated with heme-HSA (complex 15 μ mol/kg; 15 hours). Similarly, the heme-mediated induction of the M1 marker CD86 and downregulation of the M2 marker CD206 are rescued in splenic macrophages from heme-Hx-treated mice compared with heme-HSA-challenged animals (Figure 6D). Perl's staining of liver and spleen sections demonstrates that macrophages accumulated more iron following heme-HSA treatment compared with heme-Hx treatment (Figure 6E).

These results suggest that the sequestration of heme and iron by specific scavengers counteracts the proinflammatory state of macrophages associated with M1 differentiation.

Hemopexin therapy ameliorates the proinflammatory status of macrophages in a mouse model of sickle cell disease

We next evaluated whether Hx administration is able to attenuate the proinflammatory status of macrophages in a murine disease model for SCD. The treatment of sickle mice with human Hx (4 mg Hx intraperitoneally once a week, for 3 weeks) decreased the expression of the M1 markers MHCII, CD86, iNOS, and IL-6 in hepatic macrophages compared with HbA control mice, whereas the M2 marker CD206 was not significantly altered. Higher expression of Arginase-1 may be related to the liver fibrotic damage that SCD mice tend to develop, as Arginase-1 contributes to collagen synthesis. Interestingly, the attenuated levels of Arginase-1 following Hx injection may be a consequence of reduced heme-mediated oxidative tissue damage and fibrosis (Figure 7A).

Proinflammatory activation of hepatic resident macrophages is known to induce blood monocyte recruitment, which enhances cytokine production. These cytokines cause hepatocyte apoptosis and

promote fibrosis by inducing activation and transdifferentiation of hepatic stellate cells (HSCs) into myofibroblasts, which is the major collagen-producing cell type. Here we show that Hx treatment decreases expression of the M1 cytokine TNF α , the monocyte chemoattractant protein (MCP)1, and the profibrotic and mitogenic cytokines transforming growth factor (TGF) β and platelet-derived growth factor (PDGF) in the liver of sickle mice. Moreover, Hx administration increases hepatic expression of the matrix metalloproteinases MMP-9, MMP-12, and MMP-13 (mostly expressed by M2 macrophages). It further increases the expression of a marker for resting HSCs, synaptophysin, and reduces the expression of a marker for activated myofibroblast-like HSCs, smooth muscle actin (SMA) (Figure 7B).

Despite these favorable alterations observed in Hx-treated sickle mice, liver damage as measured by collagen deposition and apoptosis of hepatocytes could not be reverted (supplemental Figure 17). In 2- to 3-month-old sickle mice, liver damage is already established, and thus the right timing and dosage of Hx administration may need to be optimized.

We therefore next analyzed heme-Hx-treated wild-type mice that showed decreased hepatic expression of collagens, TGF β , PDGF, SMA, and the tissue inhibitor of MMPs, TIMP2, as well as increased expression of the M2 polarizing colony stimulating factor-1 and MMPs compared with heme-HSA-treated mice (Figure 7C). In addition, wild-type mice treated with heme-Hx showed reduced liver collagen deposition and hepatocyte apoptosis compared with animals treated with heme-HSA (complex 5 μ mol/kg; 7 injections over 2 weeks) (Figure 7D). Consistently, heme-treated Hx-null mice show increased inflammatory cell recruitment and tissue damage in the liver compared with heme-treated wild-type mice (70 μ mol heme/kg; 5 intravenous injections) (supplemental Figure 18).

Taken together, these data suggest that Hx administration decreases heme-driven proinflammatory activation of macrophages. As a consequence, the release of inflammatory cytokines that drive monocyte recruitment and HSC transdifferentiation is reduced, and expression of MMPs that favors scar regression is increased. This results in the resolution of inflammation and decreased hepatic collagen deposition and cell apoptosis. In conclusion, an Hx-based therapy shows beneficial effects, in that it counteracts heme-induced proinflammatory activation of macrophages and attenuates some of its pathophysiologic consequences, such as chronic inflammation, hepatic fibrosis, and apoptosis (Figure 7E).

Discussion

In this study, we show that various sources of heme (hemolytic RBCs, free heme) and iron activate macrophages to differentiate toward an M1-like proinflammatory phenotype, which is hallmarked by the production of inflammatory cytokines and ROS. The underlying mechanisms involve ROS production and TLR4-controlled signaling.

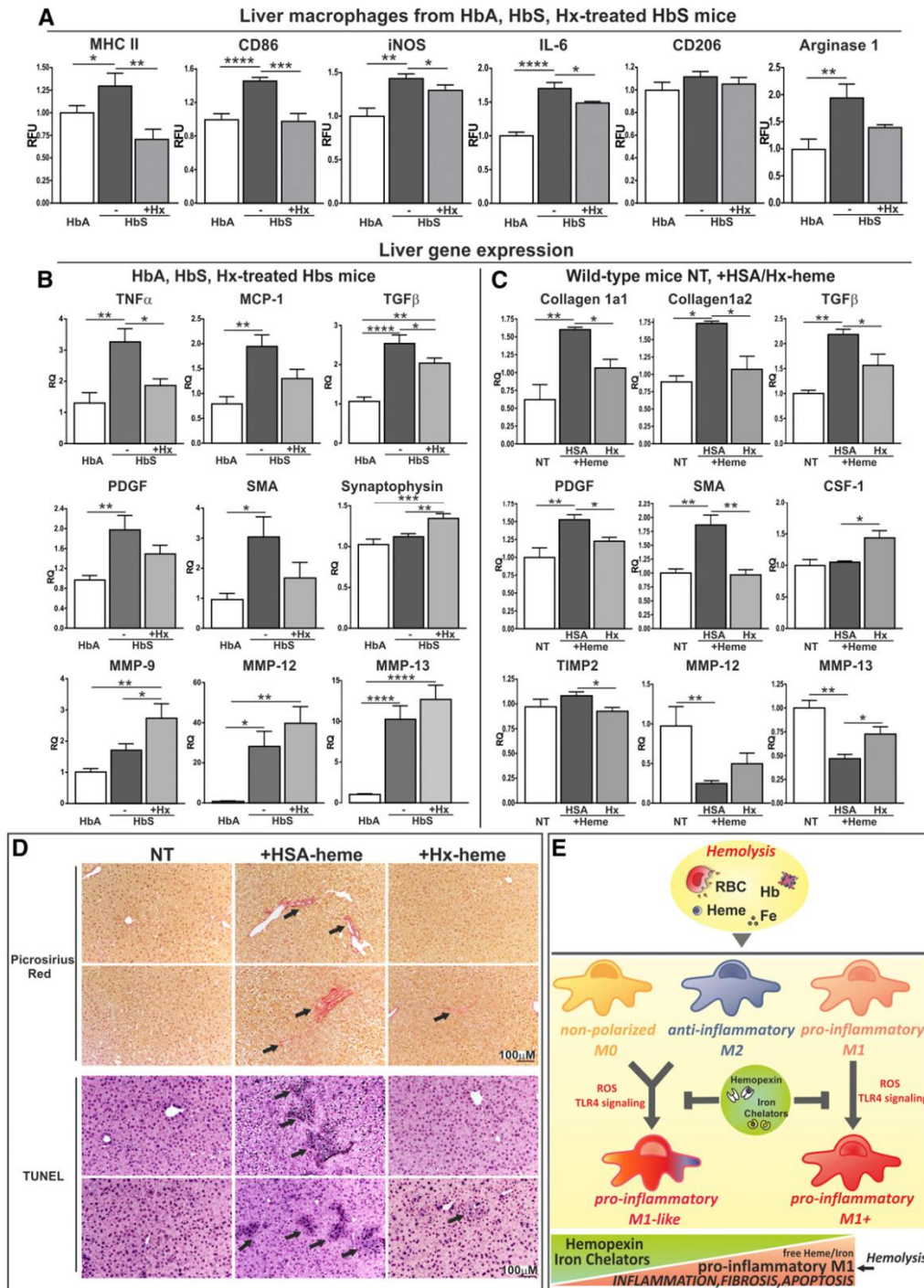


Figure 7. Hx rescues heme-induced M1 polarization of macrophages in a mouse model of sickle cell disease. (A) Analysis of the M1 markers MHCII, CD86, iNOS, and IL-6 and the M2 markers CD206 and Arginase-1 in macrophages from liver of HbA mice and HbS mice that remained untreated or were treated with Hx (4 mg intraperitoneally once a week for 3 weeks) (n = 5). The expression of polarization markers was analyzed by flow cytometry and is expressed in RFU as fold change to HbA animals. (B) qRT-PCR analysis of hepatic mRNA levels of TNF α , MCP-1, TGF β , PDGF, MMP-9, MMP-12, MMP-13, synaptophysin, and SMA in HbA mice and HbS mice that remained untreated or were treated with Hx (4 mg intraperitoneally once a week for 3 weeks) (n = 7). (C) qRT-PCR analysis of hepatic mRNA levels of collagen 1a1, collagen 1a2, TGF β , PDGF, SMA, colony stimulating factor-1, TIMP2, MMP-12, and MMP-13 in wild-type mice that remained untreated or were treated with heme-HSA or heme-Hx (complex 5 μ mol/kg, 7 injections over 2 weeks) (n = 5). (D) Picrosirius red staining for collagen and TUNEL staining for apoptosis in liver sections from wild-type mice that remained untreated or were treated with heme-HSA or heme-Hx (complex 5 μ mol/kg, 7 injections over 2 weeks) (scale bar, 300-100 μ m). Arrows indicate collagen (picrosirius) and

We further demonstrate that heme/iron-controlled macrophage polarization is preventable by heme scavengers or iron chelators. These findings are of relevance for diseases that are characterized by excessive circulating Hb, heme, and/or iron levels and macrophage iron loading.

Macrophages show high plasticity in response to the cytokine composition of the microenvironment. Our data show that Hb, heme, or iron in the microenvironment additionally affect macrophage plasticity. This finding extends previous work that demonstrates that cytokines that drive M1 or M2 polarization determine iron handling.^{46,47,56} In those studies, M1 macrophages show an iron retention phenotype and a gene expression profile with low expression of HO-1, FPN, and CD163 and high expression of ferritin. On the other hand, M2 macrophages show higher expression of HO-1, FPN, and CD163 and low expression of ferritin, likely associated with an iron release phenotype with increased iron uptake, recycling, and export activity. Our data are not entirely consistent with these observations, in that transferrin receptor 1 mRNA levels are higher in M2 compared with M1 macrophages,^{46,47} as reported,^{44,45} whereas HO-1 and FPN mRNA levels do not differ (supplemental Figure 9). These differences may be explained by the protocols applied for monocyte/macrophage differentiation. Despite differences in gene expression patterns, our findings, together with those by Recalcati et al⁴⁶ and Corna et al,⁴⁷ strengthen the concept that macrophage function and iron metabolism are tightly interconnected. Our study further demonstrates that the functional consequences of macrophage exposure to cytokines and iron integrate and eventually potentiate each other, according to their relative amounts available in the microenvironment, rather than having a mutually exclusive effect on macrophage polarization. It is important to note that heme and iron seem to exert a dominant effect on macrophage polarization, inducing a shift toward a proinflammatory phenotype. In particular, the polarization program of macrophages in response to cytokines can be enhanced (M1→M1⁺) or even shifted (M2→M1) by an additional exposure to a heme or an iron source (Figure 7D). Therefore, heme/iron accumulation is expected to modulate the phenotypical differences that macrophages acquire in response to the environmental stimuli.

Recently, a key role for heme in controlling monocyte differentiation into macrophages was demonstrated. This process is increased during pathologic hemolysis.⁵⁷ Here we demonstrate that heme additionally affects the phenotype of differentiated macrophages. An involvement of Hb, heme, and iron in macrophage polarization was postulated in recent studies. In models of chronic venous leg ulcers and wound healing, macrophage iron overload correlates with a proinflammatory M1 phenotype, TNF α , and hydroxyl radical production.⁵⁸ Nieuwenhuizen et al⁵⁹ observed a decrease in M2 and an increase in M1 macrophages in the red pulp of the spleen and in synovial tissue in hemophilic mice. The authors speculated that this results from an increased number of damaged RBCs and a higher level of circulating Hb following hemarthrosis. The data presented here may explain these findings. Macrophage polarization has also been analyzed in atherosclerotic plaques, where erythrophagocytosis in hemorrhagic areas represents an important source of iron for macrophages.⁶⁰⁻⁶⁴ Hemorrhage-associated macrophages (HA or M-hem) in atherosclerotic lesions express high levels of the Hb-Hp scavenger receptor CD163, HO-1, and FPN, accounting for an increased capacity to handle

Hb, facilitated heme catabolism and reduced intracellular free iron. Therefore, in atheroma, the Hb-Hp complex might model macrophages toward a protective HA-macrophage subtype with increased capacity to handle Hb, as well as antioxidative and antiatherogenic properties. In this regard, the saturation of the Hp system is expected to be detrimental, leading to uncontrolled Hb uptake and macrophage activation.

Consistently, we show that the saturation of the Hx system leads to heme accumulation and proinflammatory activation of macrophages. Heme released from cell-free Hb is normally bound to Hx and internalized by hepatocytes, via the LRP1 receptor,⁶⁵ or other thus far unidentified and more specific scavengers. Hx-mediated heme scavenging and hepatic detoxification ensure protection of several extrahepatic tissues against heme toxicity.^{5,6} Here we show that this protective effect extends toward macrophages and is reduced in disorders where the Hx binding capacity is overwhelmed and its synthesis is not appropriate compared with the rate of consumption.^{5,15} This is the case in a mouse model of SCD, which is hallmarked by hemolysis, increased circulating Hb/heme, and low levels of Hp and Hx and shows elevated hepatic macrophage iron levels and M1 polarization.

In our study we further provide mechanistic insight into how heme and iron cause phenotypic changes of macrophages. Here we show that this process depends on the production of ROS and the activation of the TLR4 signaling pathway. This is strengthened by the observation that heme-mediated induction of M1 markers is attenuated in TLR4-null BMDMs and fully abolished when these cells are additionally exposed to NAC. Importantly, by scavenging free heme, Hx prevents heme-induced M1 macrophage polarization and thus avoids both TLR4 activation and ROS formation. These observations are in line with recent studies demonstrating antioxidant and anti-inflammatory properties of Hx,^{5,6,66-68} as well as its ability to prevent heme-triggered TLR4 activation and TNF α production.^{17,54} Thus, Hx treatment provides a clear advantage over pharmacologic approaches in that it combines antioxidant properties together with inhibitory effects on the proinflammatory pathways induced by heme.

Our findings are therefore expected to be relevant for those pathologies in which Hb and heme are released from the RBCs, systemically or locally, and Hp/Hx levels are reduced, thus leading to the activation of innate immune cells and the production of ROS and inflammatory cytokines. We suggest that the extent of inflammation associated with hemolytic disorders may depend on intravascular rather than extravascular hemolysis. In SCD, hemolysis occurs both intra- and extravascular and macrophage exposure to “extracellular” heme triggers inflammation via TLR4 stimulation. In other conditions, such as hereditary spherocytosis, hemolysis is mainly extravascular and RBCs are presented intact to reticuloendothelial system macrophages, thus explaining the milder signs of inflammation in these patients. The extent of inflammation in different hemolytic disorders may therefore depend on how macrophages get in contact with heme, either with heme contained within intact RBCs or in the form of free or bound Hb/heme. Controlled iron accumulation in macrophages, as a consequence of erythrophagocytosis or uptake of iron-bound transferrin, is not expected to represent a stimulus to trigger M1 polarization in vivo.

Figure 7 (continued) apoptotic cells (tunnel). Results shown are representative of 3 independent experiments. Values represent mean \pm SEM. * $P < .05$; ** $P < .01$; *** $P < .001$; **** $P < .0001$. (E) Model for macrophage differentiation in response to Hb, heme, and iron and its protection by heme and iron scavengers. Hb derived from hemolytic RBCs, heme, and iron promotes macrophage differentiation toward an M1-like proinflammatory phenotype, via ROS production and TLR4 signaling activation. This effect is independent of the differentiation state of the macrophages (eg, M0, M1, or M2). Interestingly, M1 macrophages show a potentiated M1 phenotype (M1⁺), and even anti-inflammatory M2 macrophages can be shifted to an M1-like proinflammatory phenotype in response to heme and iron, suggesting that these signals dominate over those triggered by cytokines. Heme or iron scavengers, such as hemopexin (Hx) or desferrioxamine (DFO), protect macrophages from heme or iron-induced M1 polarization, reducing iron loading, cytokine production, and ROS formation.

We propose that the modulation of macrophage polarization toward a less inflammatory phenotype may represent an interesting prophylactic or therapeutic approach in hemolytic disorders. This could be achieved by administration of heme and/or iron scavengers. Recent studies in mouse models of hemolytic disorders demonstrated that the therapeutic administration of Hx increases hepatic heme recovery and detoxification and successfully counteracts heme-induced endothelial activation and dysfunction.⁵ Similarly, in a SCD mouse model, vascular stasis and respiratory failure due to acute chest syndrome were prevented by treatment with purified or recombinant Hx.^{17,69} Here we show that the administration of Hx attenuates the induction of inflammatory cytokines and M1 polarization markers in macrophages triggered by heme. The activation of macrophages toward a proinflammatory phenotype in the liver contributes to the induction of hepatocyte apoptosis, perpetuation of inflammation via leukocyte recruitment, and promotion of fibrosis via cytokine release and HSC activation.⁵⁵ Previously, we showed that Hx therapy attenuates hepatic lipid peroxidation, leukocyte recruitment, and the expression of inflammatory cytokines, such as IL-6 and TNF α , in SCD.^{5,6} Here we additionally show that Hx administration reduces the expression of the chemoattractant MCP-1, the profibrotic TGF β and PDGF, and the activation of HSCs in sickle mice, suggesting that Hx-mediated heme scavenging counteracts heme-driven hepatic fibrosis and tissue injury.

Our data support the idea that heme-induced phenotypic switching of macrophages toward a proinflammatory phenotype can contribute to the exacerbation of inflammation and chronic tissue injury in hemolytic disorders and that Hx therapy could alleviate these pathophysiological consequences by preventing macrophage inflammatory activation.^{3,4,9,40,50,70,71}

Acknowledgments

The authors thank Sonia Levi (University Vita-Salute San Raffaele, Milan, Italy) for the gift of anti-ferritin antibodies, CSL Behring for

hemopexin and albumin purified from human sera, Tim Townes (University of Alabama at Birmingham, Birmingham, AL) for HbA and HbS sickle mice, Marieke Essers (German Cancer Research Center, Heidelberg, Germany) for TLR4-null mice for BMDM preparation, Richard Sparla and Andreas Simmelbauer for helping with some experiments, and Lucia De Franceschi (University of Verona) for critical reading of the manuscript. Microscope images were acquired at the Nikon Imaging Center at the University of Heidelberg, Heidelberg, Germany.

This work was supported by research funding from the Dietmar Hopp-Stiftung and the Deutsche Forschungsgemeinschaft (M.U.M.), Telethon grant GGPI2082 (E.T.), a postdoctoral fellowship granted from the Medical Faculty of the University of Heidelberg (<http://www.medizinische-fakultaet-hd.uni-heidelberg.de>) (F.V.), and a grant by Fundação para a Ciência e Tecnologia, Portugal (M.C.d.S.).

Authorship

Contribution: F.V. and M.C.d.S. designed the project, performed the experiments, and wrote the manuscript; G.I. and S.P. contributed to some experiments; M.U.M., E.T., and A.C. designed and supervised the project and wrote the manuscript; and N.B. and A.Z. provided Hx and revised the manuscript.

Conflict-of-interest disclosure: N.B. and A.Z. are employees of CSL Behring. All other authors declare no competing financial interests.

Correspondence: Martina U. Muckenthaler, Department of Pediatric Oncology, Hematology and Immunology, Otto Meyerhof Zentrum, Im Neuenheimer Feld 350, 69120 Heidelberg, Germany; e-mail: martina.muckenthaler@med.uni-heidelberg.de; or Emanuela Tolosano, Molecular Biotechnology Center, Department of Molecular Biotechnology and Health Sciences, Via Nizza 52, 10126 Torino, Italy; e-mail: emanuela.tolosano@unito.it.

References

- Tolosano E, Fagoonee S, Morello N, Vinchi F, Fiorito V. Heme scavenging and the other facets of hemopexin. *Antioxid Redox Signal*. 2010;12(2):305-320.
- Vinchi F, Ingoglia G, Chiabrando D, et al. Heme exporter FLVCR1a regulates heme synthesis and degradation and controls activity of cytochromes P450. *Gastroenterology*. 2014;146(5):1325-1338.
- Schaer DJ, Buehler PW, Alayash AI, Belcher JD, Vercellotti GM. Hemolysis and free hemoglobin revisited: exploring hemoglobin and heme scavengers as a novel class of therapeutic proteins. *Blood*. 2013;121(8):1276-1284.
- Schaer DJ, Vinchi F, Ingoglia G, Tolosano E, Buehler PW. Haptoglobin, hemopexin, and related defense pathways—basic science, clinical perspectives, and drug development. *Front Physiol*. 2014;5:415.
- Vinchi F, De Franceschi L, Ghigo A, et al. Hemopexin therapy improves cardiovascular function by preventing heme-induced endothelial toxicity in mouse models of hemolytic diseases. *Circulation*. 2013;127(12):1317-1329.
- Vinchi F, Gastaldi S, Silengo L, Altruda F, Tolosano E. Hemopexin prevents endothelial damage and liver congestion in a mouse model of heme overload. *Am J Pathol*. 2008;173(1):289-299.
- Vinchi F, Tolosano E. Therapeutic approaches to limit hemolysis-driven endothelial dysfunction: scavenging free heme to preserve vasculature homeostasis. *Oxid Med Cell Longev*. 2013;2013:396527.
- Chiabrando D, Vinchi F, Fiorito V, Mercurio S, Tolosano E. Heme in pathophysiology: a matter of scavenging, metabolism and trafficking across cell membranes. *Front Pharmacol*. 2014;5:61.
- Schaer DJ, Buehler PW. Cell-free hemoglobin and its scavenger proteins: new disease models leading the way to targeted therapies. *Cold Spring Harb Perspect Med*. 2013;3(6):a013433.
- Gozzelino R, Jeney V, Soares MP. Mechanisms of cell protection by heme oxygenase-1. *Annu Rev Pharmacol Toxicol*. 2010;50:323-354.
- Hentze MW, Muckenthaler MU, Galy B, Camaschella C. Two to tango: regulation of mammalian iron metabolism. *Cell*. 2010;142(1):24-38.
- Marro S, Chiabrando D, Messina E, et al. Heme controls ferroportin1 (FPN1) transcription involving Bach1, Nr2 and a MARE/ARE sequence motif at position -7007 of the FPN1 promoter. *Haematologica*. 2010;95(8):1261-1268.
- De Franceschi L. Pathophysiology of sickle cell disease and new drugs for the treatment. *Mediterr J Hematol Infect Dis*. 2009;1(1):e2009024.
- Walter PB, Harmatz P, Vichinsky E. Iron metabolism and iron chelation in sickle cell disease. *Acta Haematol*. 2009;122(2-3):174-183.
- Muller-Eberhard U, Javid J, Liem HH, Hanstein A, Hanna M. Plasma concentrations of hemopexin, haptoglobin and heme in patients with various hemolytic diseases. *Blood*. 1968;32(5):811-815.
- Boretti FS, Buehler PW, D'Agnillo F, et al. Sequestration of extracellular hemoglobin within a haptoglobin complex decreases its hypertensive and oxidative effects in dogs and guinea pigs. *J Clin Invest*. 2009;119(8):2271-2280.
- Belcher JD, Chen C, Nguyen J, et al. Heme triggers TLR4 signaling leading to endothelial cell activation and vaso-occlusion in murine sickle cell disease. *Blood*. 2014;123(3):377-390.
- Dutra FF, Alves LS, Rodrigues D, et al. Hemolysis-induced lethality involves inflammasome activation by heme. *Proc Natl Acad Sci USA*. 2014;111(39):E4110-E4118.
- Fortes GB, Alves LS, de Oliveira R, et al. Heme induces programmed necrosis on macrophages through autocrine TNF and ROS production. *Blood*. 2012;119(10):2368-2375.
- Figueiredo RT, Fernandez PL, Mourao-Sa DS, et al. Characterization of heme as activator of Toll-like receptor 4. *J Biol Chem*. 2007;282(28):20221-20229.

21. Fernandez PL, Dutra FF, Alves L, et al. Heme amplifies the innate immune response to microbial molecules through spleen tyrosine kinase (Syk)-dependent reactive oxygen species generation. *J Biol Chem*. 2010;285(43):32844-32851.
22. Porto BN, Alves LS, Fernández PL, et al. Heme induces neutrophil migration and reactive oxygen species generation through signaling pathways characteristic of chemotactic receptors. *J Biol Chem*. 2007;282(33):24430-24436.
23. Sakamoto TM, Canalli AA, Traina F, et al. Altered red cell and platelet adhesion in hemolytic diseases: Hereditary spherocytosis, paroxysmal nocturnal hemoglobinuria and sickle cell disease. *Clin Biochem*. 2013;46(18):1798-1803.
24. Jison ML, Munson PJ, Barb JJ, et al. Blood mononuclear cell gene expression profiles characterize the oxidant, hemolytic, and inflammatory stress of sickle cell disease. *Blood*. 2004;104(1):270-280.
25. Francis RB Jr, Haywood LJ. Elevated immunoreactive tumor necrosis factor and interleukin-1 in sickle cell disease. *J Natl Med Assoc*. 1992;84(7):611-615.
26. Malavé I, Perdomo Y, Escalona E, et al. Levels of tumor necrosis factor alpha/cachectin (TNF alpha) in sera from patients with sickle cell disease. *Acta Haematol*. 1993;90(4):172-176.
27. Croizat H. Circulating cytokines in sickle cell patients during steady state. *Br J Haematol*. 1994; 87(3):592-597.
28. Kuvibidila S, Gardner R, Ode D, Yu L, Lane G, Warrior RP. Tumor necrosis factor alpha in children with sickle cell disease in stable condition. *J Natl Med Assoc*. 1997;89(9):609-615.
29. Mohapatra PC, Sarangi A, Sarangi AK, Dalai RK, Sahoo D. Sequential serum cytokine levels of TNF-alpha, IL-4 and IL-12 are associated with prognosis in Plasmodium falciparum malaria. *Indian J Clin Biochem*. 2014;29(3):321-326.
30. Ferreira A, Balla J, Jeney V, Balla G, Soares MP. A central role for free heme in the pathogenesis of severe malaria: the missing link? *J Mol Med (Berl)*. 2008;86(10):1097-1111.
31. Netea MG, van der Meer JW, van Deuren M, Kullberg BJ. Proinflammatory cytokines and sepsis syndrome: not enough, or too much of a good thing? *Trends Immunol*. 2003;24(5): 254-258.
32. Larsen R, Gozzelino R, Jeney V, et al. A central role for free heme in the pathogenesis of severe sepsis. *Sci Transl Med*. 2010;2(51):51ra71.
33. de Jong HK, van der Poll T, Wiersinga WJ. The systemic pro-inflammatory response in sepsis. *J Innate Immun*. 2010;2(5):422-430.
34. Adamzik M, Hamburger T, Petrat F, Peters J, de Groot H, Harimann M. Free hemoglobin concentration in severe sepsis: methods of measurement and prediction of outcome. *Crit Care*. 2012;16(4):R125.
35. Madrid-Miller A, Chávez-Sánchez L, Careaga-Reyna G, et al. Clinical outcome in patients with acute coronary syndrome and outward remodeling is associated with a predominant inflammatory response. *BMC Res Notes*. 2014; 7:669.
36. Battes LC, Cheng JM, Oemrawsingh RM, et al. Circulating cytokines in relation to the extent and composition of coronary atherosclerosis: results from the ATHEROREMO-IVUS study. *Atherosclerosis*. 2014;236(1):18-24.
37. Zhou Y, Wang Y, Wang J, Anne Stetler R, Yang QW. Inflammation in intracerebral hemorrhage: from mechanisms to clinical translation. *Prog Neurobiol*. 2014;115:25-44.
38. Lin S, Yin Q, Zhong Q, et al. Heme activates TLR4-mediated inflammatory injury via MyD88/TRIF signaling pathway in intracerebral hemorrhage. *J Neuroinflammation*. 2012;9:46.
39. Larsen R, Gouveia Z, Soares MP, Gozzelino R. Heme cytotoxicity and the pathogenesis of immune-mediated inflammatory diseases. *Front Pharmacol*. 2012;3:77.
40. Belcher JD, Marker PH, Weber JP, Heibel RP, Vercelotti GM. Activated monocytes in sickle cell disease: potential role in the activation of vascular endothelium and vaso-occlusion. *Blood*. 2000; 96(7):2451-2459.
41. Sica A, Mantovani A. Macrophage plasticity and polarization: in vivo veritas. *J Clin Invest*. 2012; 122(3):787-795.
42. Mantovani A, Biswas SK, Galdiero MR, Sica A, Locati M. Macrophage plasticity and polarization in tissue repair and remodeling. *J Pathol*. 2013; 229(2):176-185.
43. Chinetti-Gbaguidi G, Staels B. Macrophage polarization in metabolic disorders: functions and regulation. *Curr Opin Lipidol*. 2011;22(5):365-372.
44. Butcher MJ, Galkina EV. Phenotypic and functional heterogeneity of macrophages and dendritic cell subsets in the healthy and atherosclerosis-prone aorta. *Front Physiol*. 2012; 3:44.
45. Leitinger N, Schulman IG. Phenotypic polarization of macrophages in atherosclerosis. *Arterioscler Thromb Vasc Biol*. 2013;33(6):1120-1126.
46. Recalcati S, Locati M, Marini A, et al. Differential regulation of iron homeostasis during human macrophage polarized activation. *Eur J Immunol*. 2010;40(3):824-835.
47. Cora G, Campana L, Pignatti E, et al. Polarization dictates iron handling by inflammatory and alternatively activated macrophages. *Haematologica*. 2010;95(11): 1814-1822.
48. Cairo G, Recalcati S, Mantovani A, Locati M. Iron trafficking and metabolism in macrophages: contribution to the polarized phenotype. *Trends Immunol*. 2011;32(6):241-247.
49. Nairz M, Schroll A, Demetz E, Tancevski I, Theurl I, Weiss G. 'Ride on the ferric wheel' - The cycle of iron in macrophages in health and disease. *Immunobiology*. 2014; (Sep):16.
50. Win N, Lee E, Needs M, Chia LW, Stasi R. Measurement of macrophage marker in hyperhaemolytic transfusion reaction: a case report. *Transfus Med*. 2012;22(2):137-141.
51. Tolosano E, Cutuflia MA, Hirsch E, Silengo L, Altruda F. Specific expression in brain and liver driven by the hemopexin promoter in transgenic mice. *Biochem Biophys Res Commun*. 1996; 218(3):694-703.
52. Hoshino K, Takeuchi O, Kawai T, et al. Cutting edge: Toll-like receptor 4 (TLR4)-deficient mice are hyporesponsive to lipopolysaccharide: evidence for TLR4 as the Lps gene product. *J Immunol*. 1999;162(7):3749-3752.
53. Ryan TM, Ciavatta DJ, Townes TM. Knockout-transgenic mouse model of sickle cell disease. *Science*. 1997;278(5339):873-876.
54. Lin T, Kwak YH, Sammy F, et al. Synergistic inflammation is induced by blood degradation products with microbial Toll-like receptor agonists and is blocked by hemopexin. *J Infect Dis*. 2010; 202(4):624-632.
55. Tacke F, Zimmermann HW. Macrophage heterogeneity in liver injury and fibrosis. *J Hepatol*. 2014;60(5):1090-1096.
56. Recalcati S, Locati M, Gammella E, Invernizzi P, Cairo G. Iron levels in polarized macrophages: regulation of immunity and autoimmunity. *Autoimmun Rev*. 2012;11(12):883-889.
57. Haldar M, Kohyama M, So AY, et al. Heme-mediated SPI-C induction promotes monocyte differentiation into iron-recycling macrophages. *Cell*. 2014;156(6):1223-1234.
58. Sindrilaru A, Peters T, Wieschalka S, et al. An unrestrained proinflammatory M1 macrophage population induced by iron impairs wound healing in humans and mice. *J Clin Invest*. 2011;121(3): 985-997.
59. Nieuwenhuizen L, Schutgens RE, Coelevelt K, et al. Hemarthrosis in hemophilic mice results in alterations in M1-M2 monocyte/macrophage polarization. *Thromb Res*. 2014;133(3):390-395.
60. Boyle JJ. Heme and hemoglobin direct macrophage Mhem phenotype and counter foam cell formation in areas of intraplaque haemorrhage. *Curr Opin Lipidol*. 2012;23(5): 453-461.
61. Boyle JJ, Harrington HA, Piper E, et al. Coronary intraplaque hemorrhage evokes a novel atheroprotective macrophage phenotype. *Am J Pathol*. 2009;174(3):1097-1108.
62. Boyle JJ, Johns M, Kamper T, et al. Activating transcription factor 1 directs Mhem atheroprotective macrophages through coordinated iron handling and foam cell protection. *Circ Res*. 2012;110(1):20-33.
63. Yuan XM, Anders WL, Olsson AG, Brunk UT. Iron in human atheroma and LDL oxidation by macrophages following erythrophagocytosis. *Atherosclerosis*. 1996;124(1):61-73.
64. Finn AV, Nakano M, Polavarapu R, et al. Hemoglobin directs macrophage differentiation and prevents foam cell formation in human atherosclerotic plaques. *J Am Coll Cardiol*. 2012; 59(2):166-177.
65. Hvidberg V, Maniecki MB, Jacobsen C, Hejrup P, Møller HJ, Møstrup SK. Identification of the receptor scavenging hemopexin-heme complexes. *Blood*. 2005;106(7):2572-2579.
66. Rolla S, Ingoglia G, Bardina V, et al. Acute-phase protein hemopexin is a negative regulator of Th17 response and experimental autoimmune encephalomyelitis development. *J Immunol*. 2013;191(11):5451-5459.
67. Lin T, Sammy F, Yang H, et al. Identification of hemopexin as an anti-inflammatory factor that inhibits synergy of hemoglobin with HMGB1 in sterile and infectious inflammation. *J Immunol*. 2012;189(4):2017-2022.
68. Liang X, Lin T, Sun G, Beasley-Topcliffe L, Cavallion JM, Warren HS. Hemopexin down-regulates LPS-induced proinflammatory cytokines from macrophages. *J Leukoc Biol*. 2009;86(2):229-235.
69. Ghosh S, Adisa OA, Chappa P, et al. Extracellular heme crisis triggers acute chest syndrome in sickle mice. *J Clin Invest*. 2013;123(11): 4809-4820.
70. Chies JA, Nardi NB. Sickle cell disease: a chronic inflammatory condition. *Med Hypotheses*. 2001; 57(1):46-50.
71. Platt OS. Sickle cell anemia as an inflammatory disease. *J Clin Invest*. 2000;106(3):337-338.

Supplemental Data

CHAPTER I

Supplemental Material and Methods

Mice treatment

All mice analysed were between 2/3 months of age. Mice were treated with heme-albumin (20-30 $\mu\text{mol/kg}$). Pre-treatment with NAC (Sigma, 500mg/kg body weight) or TAK-242 (2mg/kg body weight) was performed 30 min before infusion with heme-albumin. For rescue experiments, heme bound 1:1 to human plasma-derived Hx or albumin (CSL Behring, Switzerland) was injected at a dose of 5-15 $\mu\text{mol/kg}$. HbS sickle mice were treated with 4 mg human Hx ip, once a week for 3 weeks. Mice were sacrificed 1h, 6h, 15h or 15 days after heme injection, tissue samples were collected and either directly analysed or snap frozen until further analysis.

Heme (hemin chloride, Frontier Scientific, Logan, Utah) was dissolved in 0.1 N NaOH and diluted in PBS at a final concentration of 10 mmol/L. pH was adjusted at 7.4 with 0.1 N HCl. Freshly prepared heme was injected into the tail vein of mice at a dose of 30-70 $\mu\text{mol/kg}$.

Heme and ZnMP Content Quantification

Heme content in spleen, splenic macrophages, BMDMs and Raw 264.7 cells was quantified fluorometrically by the method of Sassa (Sassa et al). Briefly, tissues were homogenized in phosphate buffered saline (PBS) and the protein content was determined by using the Bio-Rad protein assay system (Bio-Rad, Munchen, Germany). 10 μg of protein samples were incubated with 0.5 ml of 2 M Oxalic Acid (Sigma-Aldrich) at 95°C for 30 min. Samples were subsequently centrifuged at 14000 rpm for 5 min. Fluorescence emission in the supernatant was determined spectrofluorimetrically (Glomax, Promega). Excitation and emission wavelengths were set at 405 and 662 nm, respectively. The background was evaluated by measuring fluorescence in non-

boiled samples. ZnMP was quantified in BMDM extract by fluorescence, with an excitation wavelength of 407 nm and an emission wavelength of 578 nm (Glomax, Promega).

BMDM Preparation

The murine monocyte/macrophage Raw264.7 cell line (ATCC TIB-71) cultured in DMEM medium supplemented with 10% FBS and 1% Penicillin/Streptomycin (Gibco). BMDMs were differentiated in vitro from bone marrow stem cell progenitors for one week using RPMI medium supplemented with 10 ng/ml M-CSF (M9170, Sigma-Aldrich), 10% FBS and 1% Penicillin/Streptomycin (Gibco). BMDMs were co-treated with 100 ng/ml LPS plus 20 ng/ml IFN γ , to obtain M1 macrophages, and 20 ng/ml IL-4 plus 20 ng/ml IL-10, to obtain M2 macrophages, together with heme or iron for 12 and 18 hours, respectively. For each independent experiment, BMDMs were prepared from three different mice.

Quantitative Real-Time Polymerase Chain Reaction Analysis

Total RNA was extracted from cells using the RNeasy Mini Kit (Qiagen) and from liver using Trizol (Qiagen). 0.5 to 1 μ g of total RNA was reverse transcribed by using RevertAid H Minus reverse transcriptase (Thermo Scientific), random primers (Invitrogen) and dNTPs (Thermo Scientific). qRT-PCR was performed on a Step One Plus Real Time PCR System (Applied Biosystems, California, USA). Primers and probes were designed using the ProbeFinder software (www.roche-applied-science.com) (See TableS1). Differences in Relative Quantity (RQ) are shown as fold-change compared to the control condition (untreated wild-type mice or cells, NT).

Protein Extraction and Western Blotting

Protein extracts were prepared as previously reported and protein concentration was determined using the Bio-Rad protein assay system (Bio-Rad, Munchen, Germany). 50 µg of total protein extracts were separated by 8-12% SDS-PAGE and analyzed by Western blotting using antibodies against HO-1 (Stressgen, Victoria, Canada), L-/H-Ferritin (kindly provided by Sonia Levi), FPN (Alpha Diagnostic Intl. Inc., San Antonio, TX), vinculin (produced in the laboratory at the Molecular Biotechnology Center in Turin) and actin (Santa Cruz). Densitometric analysis is reported in Arbitrary Unit (AU), as ratio to the untreated (NT) sample (AU=1).

Measurement of intracellular ROS accumulation

Accumulation of ROS in Raw 264.7 cells was assessed by using the oxidant-sensitive fluorescent dye 29,79-dichlorodihydrofluorescein diacetate (H₂DCFDA; Molecular Probes, Inc., Eugene, OR). H₂DCFDA penetrates easily into the cells. Upon crossing the cellular membrane, H₂DCFDA undergoes deacetylation by intracellular esterases producing a non-fluorescent compound that becomes highly green fluorescent following oxidation by intracellular ROS. Within the cell the probe reacts with ROS to form fluorescent 28,78 dichlorofluorescein (DCF), which is detected with spectrofluorometry. Raw 264.7 cells untreated or treated for 6/15/20 hrs with 10/15 µM Hx-heme, HSA-heme or heme alone were incubated with 5µM H₂DCFDA in Hanks' balanced salt solution (HBSS) for 30 min at 37 °C under 5% CO₂ atmosphere. Then cells were washed twice with HBSS, trypsinized and analyzed by flow cytometry using a FACS flow cytometer or a fluorimeter plate reader (Promega). Fluorescence was recorded in the fluorimeter reader at excitation and emission wavelengths of 485 and 530 respectively. The background fluorescence caused by buffer and DCF was subtracted from the total fluorescence in each well

generated by cell extract in presence of DCF. Fluorescence intensity units were normalized by mg of cell proteins and expressed as arbitrary fluorescence units/mg protein.

Heme Oxygenase activity assay

Heme-Oxygenase activity was measured by spectrophotometric determination of bilirubin produced from hemin added as the substrate. Raw 264.7 cells were lysed with a hypotonic buffer (0.1 M potassium phosphate, 2mM MgCl₂, Complete Protease Inhibitor Cocktail, Roche Diagnostics Corp., Milano, Italy, pH 7.4) for 15' on ice. After brief sonication. 0.6 M sucrose was added to cell lysates in order to obtain an hysotonic solution (final 0.25 M sucrose). Lysates were centrifuged at 1000 x g for 10 min at 4 °C to pellet nuclei, and supernatants centrifuged at 12000 g for 15 min at 4 °C to pellet mitochondria. Finally, supernatants were ultracentrifuged at 105000 g for 1 hour at 4 °C. Microsomal fractions were resuspended in 100 mM potassium phosphate buffer pH 7.4, containing 2 mM MgCl₂ and Complete protease inhibitor. Protein concentration was determined using a small aliquot of these suspensions (Bio-Rad). The microsomal supernatant fraction (cytosol) from the liver of a normal rat served as source of biliverdin reductase. Liver supernatant was prepared fresh from rat liver by homogenization in 0.1 M sodium citrate buffer, pH 5, containing 10% glycerol. HO-1 activity assay was carried out by incubating 600 µg microsome proteins with a reaction mixture containing 1 mM NADPH, 2 mM glucose-6-phosphate, 1U glucose-6-phosphate dehydrogenase (Sigma-Aldrich), 25 µM hemin, 2 mg of rat-liver cytosol and 100 mM potassium phosphate buffer, pH 7.4 (400 µl final volume). The reaction was conducted in the dark for 1h at 37 °C and terminated by placing tubes on ice for 2 min. The amount of bilirubin was determined by the difference in absorption between 464 and 530 nm (extinction coefficient, 40 mM⁻¹ cm⁻¹ for bilirubin). HO activity was expressed in picomoles of bilirubin formed per milligram microsomal protein per hour.

Cell heme treatment

Heme or ZnMP was dissolved in DMSO to obtain a 4 mM stock solution. Heme was mixed 1:1 with human albumin (HSA, CSL Behring), murine or bovine albumin (Sigma-Aldrich) or Hx (CSL Behring, Switzerland), in order to obtain 25 μ M complex solutions, and incubated for 30 minutes at 37°C. These solutions were diluted to 5 μ M in culture medium for cell treatments. FeNTA was prepared by mixing a 10mM solution of FeCl₃ with a 40mM solution of NTA. DFO was dissolved in water and then added to FeNTA at a 1:1 ratio for 30 minutes at 37°C. These solutions were diluted to 100 μ M in culture medium for cell treatments. N-acetylcysteine (NAC, Sigma-Aldrich) was dissolved in water to prepare a 100 mM stock solution and used at a final concentration of 2.5 mM in cell medium. TAK-242 was dissolved in DMSO and further diluted to a stock solution of 300 μ M and used at a final concentration of 400 nM on cells.

Hemolytic RBC preparation

Mice blood was collected on ethylenediaminetetraacetic acid (EDTA). After 3 washes with phosphate buffer saline (PBS), mouse red blood cells (RBC) were resuspended in Hepes buffer (10 mM Hepes, 140 mM NaCl, BSA 0.1%, pH 7.4). For in vitro RBC ageing, cells (2×10^8 cells/ml in Hepes buffer) were incubated overnight at 30°C with 2,5 mM calcium and 0,5 mM of the ionophore A23187 (Calbiochem, CA, USA). Treated RBC were then centrifuged (1500 rpm 5 min), washed twice with PBS and resuspended in RPMI medium (2×10^7 cells/ml). After 6h of incubation, macrophages were washed 3 times with HBSS to remove free RBCs and lysed for RNA extraction or harvested for flow cytometry analysis. The extent of hemolysis of aged RBCs was evaluated measuring heme levels in the medium used to treat cells.

Isolation of splenic myeloid cells

Granulocytes, monocytes and macrophages were isolated from a cell suspension of the spleen by using anti-CD11b microbeads and applying a magnetic field (MACS), following manufacturer's instructions (Miltenyi Biotech, Bergisch Gladbach, Germany). With this approach, CD11b⁺ granulocytes and monocytes (selected by immunomagnetic isolation with CD11b antibody) and CD11b^{low} iron-rich ferromagnetic macrophages (selected by a magnetic field only) were isolated.

Macrophage isolation from spleen and liver

Macrophages were isolated from spleen or single hepatic lobules. One third of the spleen was passed through a 100 µm Cell Strainer (BD). A single liver lobe was perfused with PBS and then Hepatocyte Liver Digest Medium (Gibco). Perfusion with the Digest Medium was kept until the liver lobe felt very soft. Subsequently, the lobe was disrupted and the cell suspension forced through a 100 µm Cell Strainer. Liver cells were centrifuged at 60 g for 2 minutes and then at 100g for 2 additional minutes, to separate hepatocytes (pellet) from non-hepatocytic cells (supernatant). Both the liver supernatant and spleen cell suspension were then added to a RBC lysis solution to remove RBCs. Afterwards, spleen and liver suspension was centrifuged at 1700 rpm 5 min 4°C. Spleen and hepatic macrophage enriched fractions were then stained for flow cytometry analysis or kept frozen for mRNA analysis.

Flow cytometry

BMDMs and *ex vivo* macrophages were incubated with Fc- γ receptor blocking solution (CD16/32) and next stained with anti-mouse CD206-FITC, CD86-PE, MHC II-PacificBlue, CD14-APC-Cy7, F4/80-APC, CD45.2-Pacific Blue or GR1-APC-Cy7, 7AAD (BioLegend, California, USA) and CD11b-Horizon V500 (BD Biosciences). For the intracellular staining, cells were washed and then subjected to surface antigen staining using the antibodies described for flow cytometry (after blocking in Fc- γ receptor blocking solution). Cells were fixed and permeabilized in Perm/wash solution (eBioscience) according to manufacturers instruction and then stained in Permeabilization Buffer (eBioscience). Intracellular cytokine staining was performed using an anti-mouse TNF α -FITC (Becton Dickinson), IL-6-PE (Biolegend), iNOS-FITC (Becton Dickinson) and Arginase-1-PE (R&D systems). Data were acquired by a FACS Aria flow cytometer (BD, Biosciences) and analysis was performed using the FlowJo Software (Tree Star Inc). The expression of surface markers is shown as Relative Fluorescence Units (RFU), whereby the geometric mean fluorescence intensity (MFI) of the cells stained with the isotype-matched antibody was subtracted from the MFI of those stained with the specific antibody. Differences in RFU are expressed as fold-change to the control condition (untreated cells or mice, NT).

DAB-enhanced Perls' staining

Liver and spleen obtained from adult mice were fixed for 24 hr in 10% neutral buffered formalin (Sigma), dehydrated, and paraffin embedded. Tissue sections (5 μ m) were mounted on Polysine slides (Thermo Scientific) and stained with Accustain Iron Stain No. HT20 (Sigma-Aldrich) following manufacturer's instructions. The Perls' blue staining was further enhanced using the DAB peroxidase substrate kit SK-4100 (Vector Laboratories, Burlingame, CA).

Picrosirius Red staining for collagen

Liver sections were stained in Weigert's haematoxylin (Sigma, HT1079), followed by Sirius red solution for one hour (Direct Red 80", Sigma, 365548). Slides were washed in two changes of saturated aqueous solution of picric acid (1.3% in water; Sigma, P6744-1GA), dehydrated and mounted.

TUNEL staining for apoptosis

For the terminal deoxynucleotidyl transferase-mediated dUTP nick-end labeling (TUNEL) assay, liver sections were stained using the In Situ Cell Death Detection kit (Roche Molecular Biochemicals, Indianapolis, IN), according to the manufacturer's instructions. Slides were counterstained with Nuclear Fast Red (Dako) and mounted.

Supplementary Text

Raw 264.7 cells were incubated with the heme fluorescent analog ZnMP complexed with Hx or Albumin (of different origin, human serum albumin-HSA or murine serum albumin-MSA) or alone. ZnMP uptake was higher in cells treated with ZnMP-Albumin or ZnMP alone than in cells incubated with ZnMP-Hx (Figure S1A,B). ZnMP is an heme analog able to inhibit HO activity, therefore its amount in the cell represents the fraction of molecule that is taken up and accumulated, without being degraded. Comparing the heme and the ZnMP uptake experiments, it is worth noting that Hx allows heme uptake in the cell (ZnMP-Hx uptake line, Figure S1A) to an amount that could be rapidly degraded by HO, keeping constant the total intracellular heme levels (heme-Hx uptake line, Figure 2B)

Supplementary Figures:

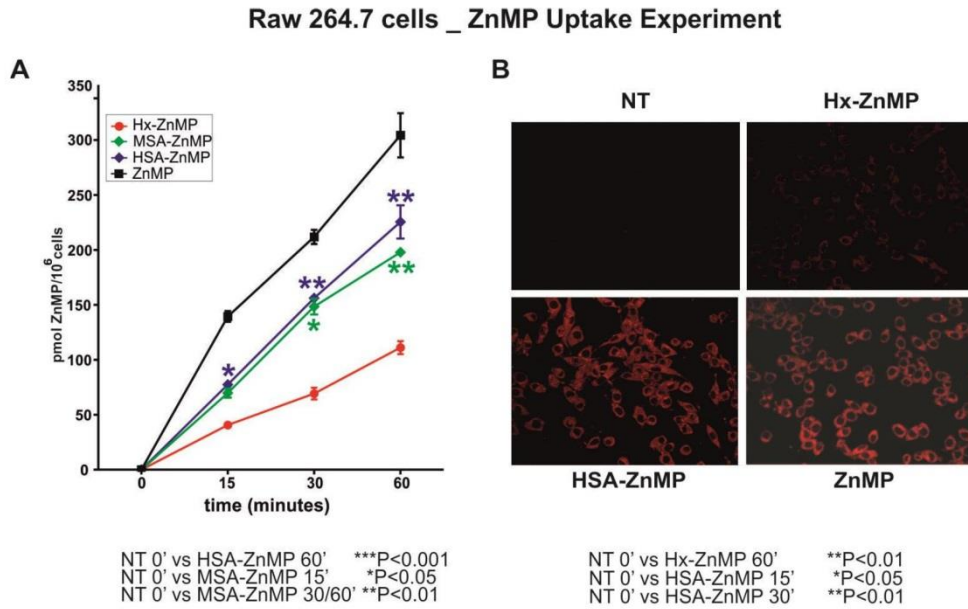


Figure S1. Hx limits ZnMP uptake in Raw 264.7 cells. (A) ZnMP uptake in Raw264.7 cells untreated (0 min) or incubated with 5 μ M Hx-ZnMP, HSA-ZnMP, MSA-ZnMP or ZnMP alone for 15, 30, or 60 min. Results shown are representative of three independent experiments. Values represent mean \pm SEM. ***P<0.001; ****P <0.0001. (B) Representative images of Raw264.7 cells incubated with 5 μ M Hx-ZnMP, HSA-ZnMP or ZnMP alone for 30 min.

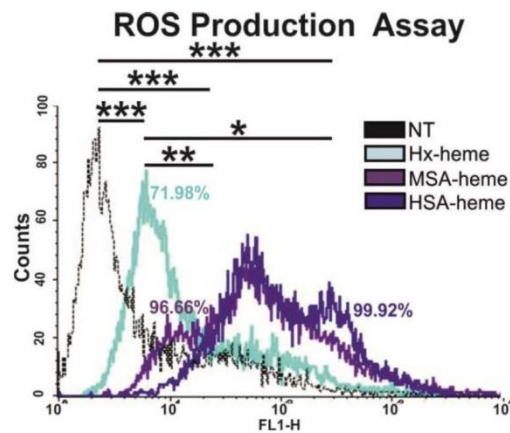


Figure S2. Hx limits heme-induced ROS production in Raw 264.7 cells. Representative FACS analysis of H₂DCFDA fluorescence in Raw264.7 cells untreated (NT) or treated with 15 μ M Hx-heme, HSA-heme or MSA-heme for 20 hours. Results shown are representative of three independent experiments. Values represent mean \pm SEM. *P<0.05; **P<0.01; ***P<0.001.

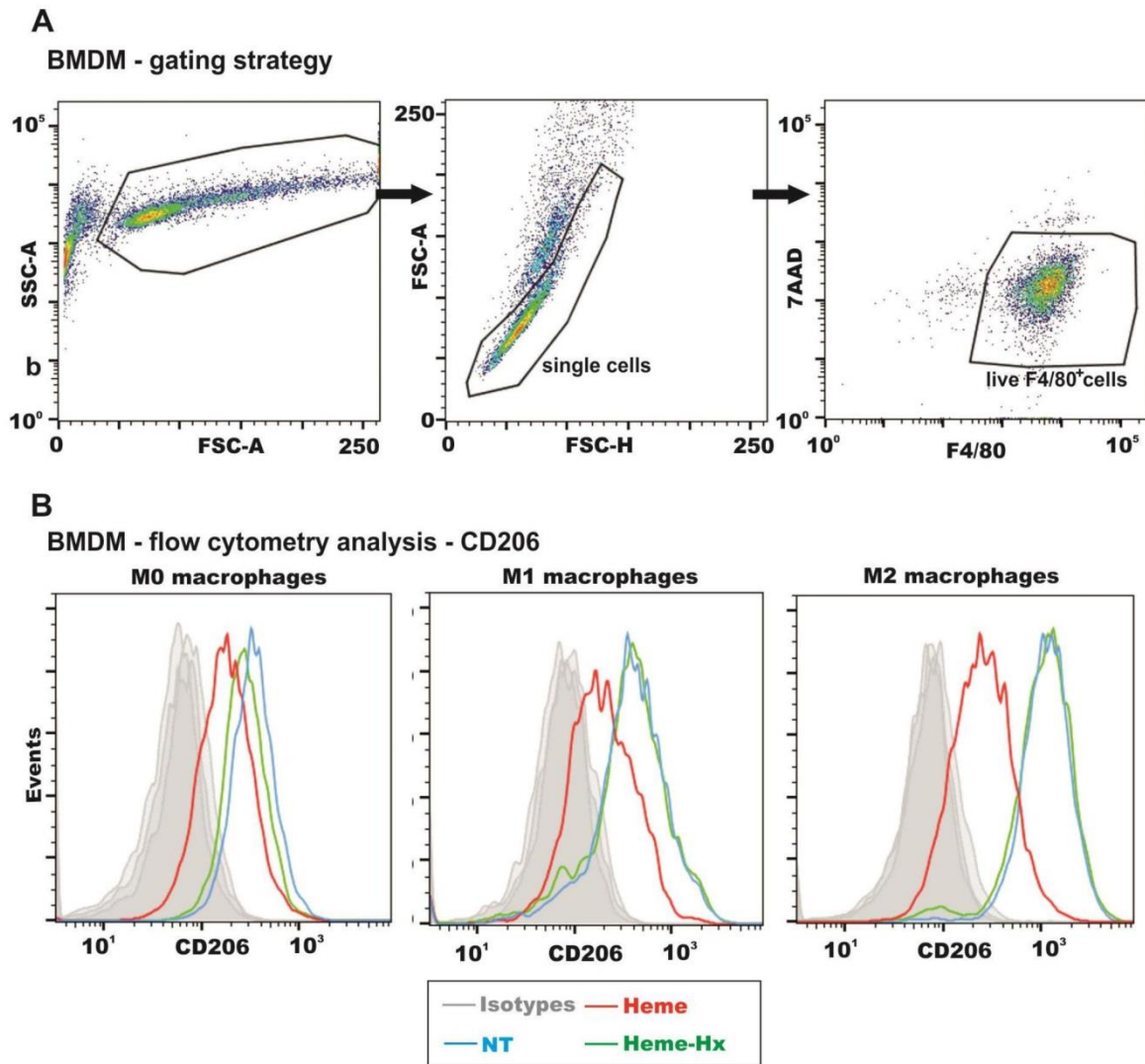


Figure S3. Gating strategy and an example for heme-induced M1 polarization in BMDMs. (A) Gating strategy used to select BMDMs: after the selection of single live cells, the analysis of polarization markers was performed on the F4/80⁺ cells. (B) Representative flow cytometry analysis of the M2 marker CD206 in BMDM untreated (NT), treated with heme-bound to Hx or to BSA, as control. Heme-BSA induces a shift in the expression of CD206 that is rescued by the addition of the heme scavenger Hx.

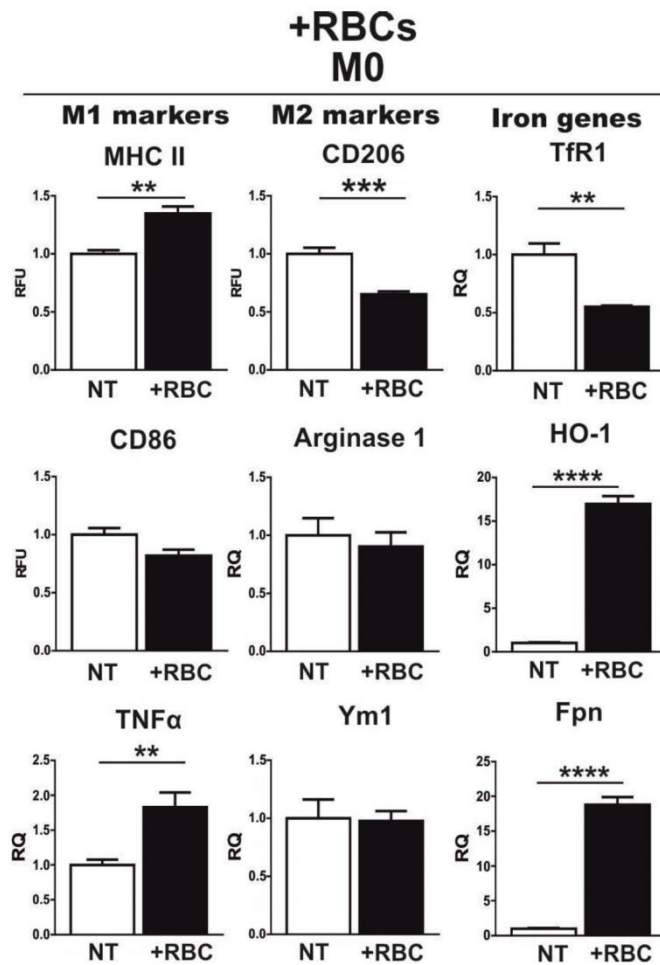


Figure S4. Aged RBCs induce macrophage polarization towards a M1-like phenotype. BMDMs were left untreated (NT) or exposed to 2×10^7 aged RBCs (+RBC) for 6 hours. M1 markers are shown in the left column, M2 markers in the central column and iron genes in the right column of the panel. The expression of MHCII, CD86 and CD206 was analysed by flow cytometry and is expressed in Relative Fluorescence Units (RFU) as fold change compared to untreated cells (NT). The mRNA levels of Arginase1, TNF α , Ym1, TfR1, HO-1 and Fpn were analysed by qRT-PCR and expressed in Relative Quantity (RQ), as fold change compared to untreated cells (NT). Results shown are the average of three independent experiments. Values represent mean \pm SEM. **P<0.01; ***P<0.001; ****P <0.0001.

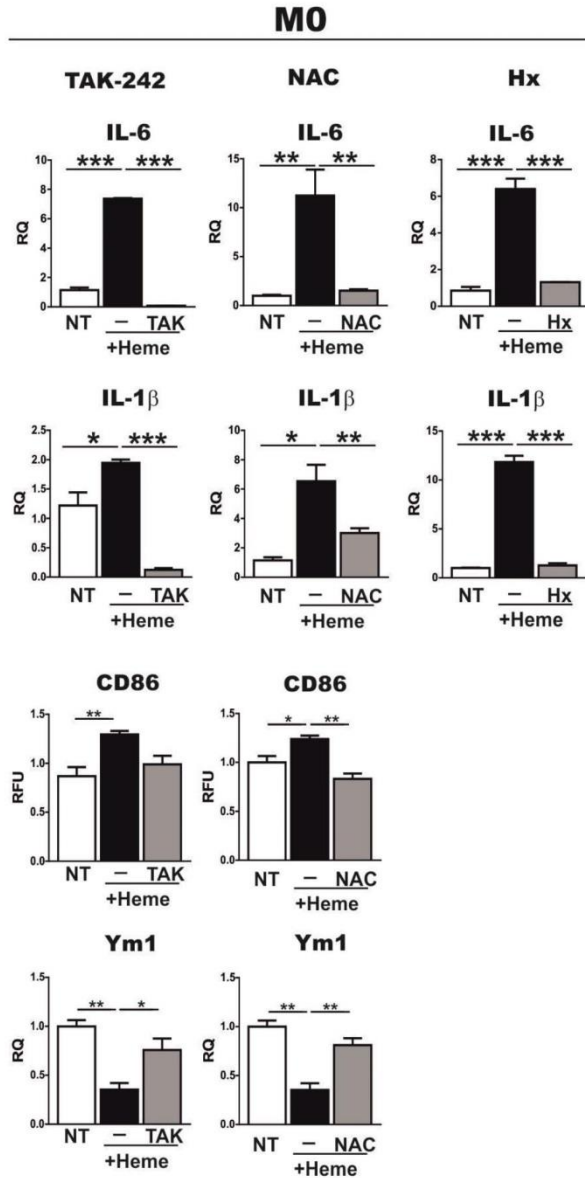


Figure S5. Heme induces the expression of pro-inflammatory cytokines. M0 BMDMs were left untreated (NT) or exposed to 5 μ M BSA-heme (+Heme) without (black bar) or with 400nM TAK-242, 2mM NAC or with 5 μ M heme-Hx (grey bar) for 12 hours. The mRNA levels of IL-6, IL-1 β and Ym1 were analysed by qRT-PCR and expressed in Relative Quantity (RQ), as fold change compared to untreated cells (NT). The expression of CD86 was analysed by flow cytometry and expressed in Relative Fluorescence Units (RFU) as fold change compared to M0 untreated cells (NT). Results shown are the average of at least three independent experiments. Values represent mean \pm SEM. *P<0.05; **P<0.01; ***P<0.001.

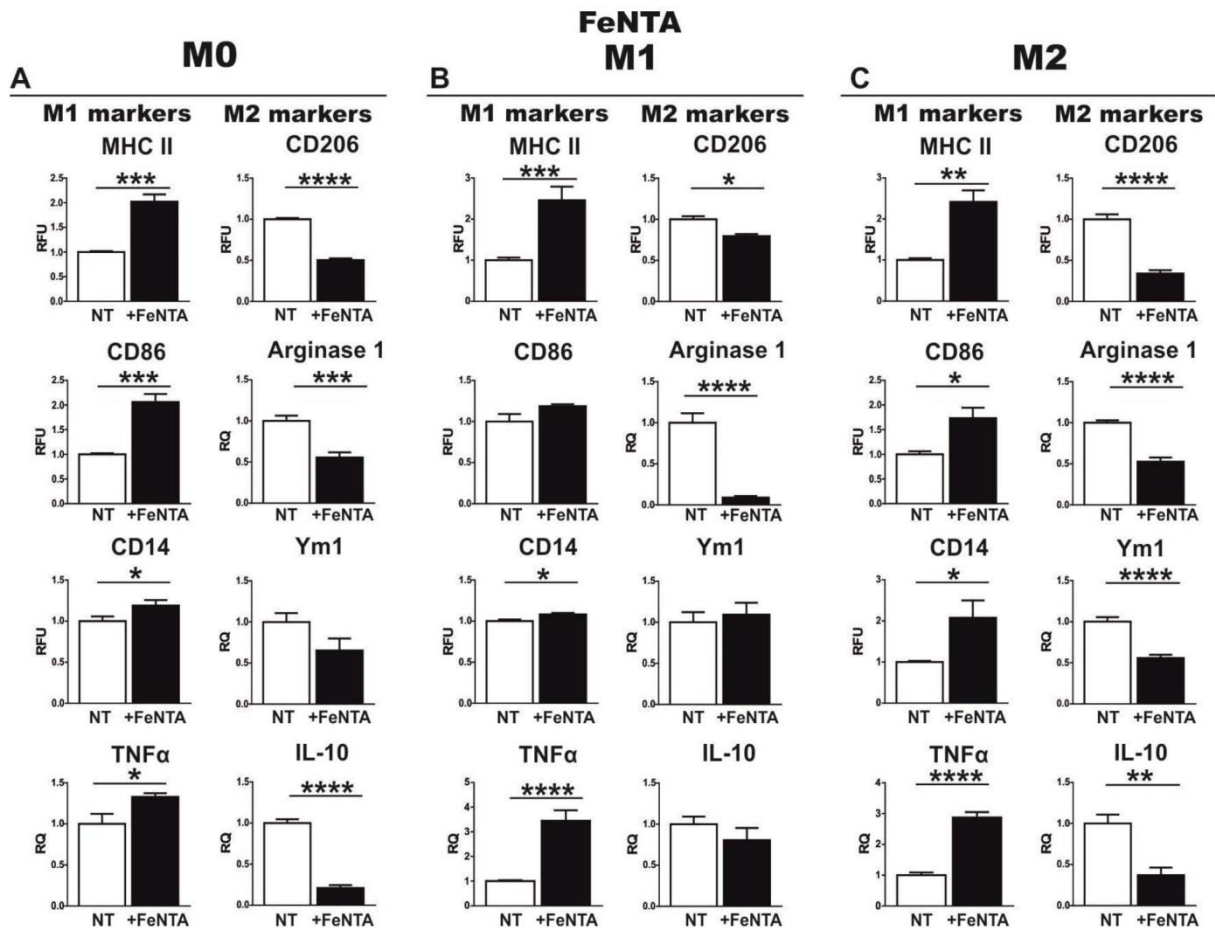


Figure S6. FeNTA induces macrophage polarization towards a M1-like phenotype, independently of the initial cell differentiation state. M0 (A), M1 (B) and M2 (C) BMDMs were left untreated (NT) or exposed to 100 μ M FeNTA (+FeNTA) for 18 hours. M1 and M2 markers are shown in the left and right column of each panel, respectively. The expression of MHCII, CD86, CD14 and CD206 was analysed by flow cytometry and is expressed in Relative Fluorescence Units (RFU) as fold change compared to untreated cells (NT). The mRNA levels of TNF α , Arginase-1, Ym1 and IL-10 were analysed by qRT-PCR and expressed in Relative Quantity (RQ), as fold change compared to untreated cells (NT). Results shown are the average of at least three independent experiments. Values represent mean \pm SEM. *P<0.05; **P<0.01; ***P<0.001; ****P <0.0001.

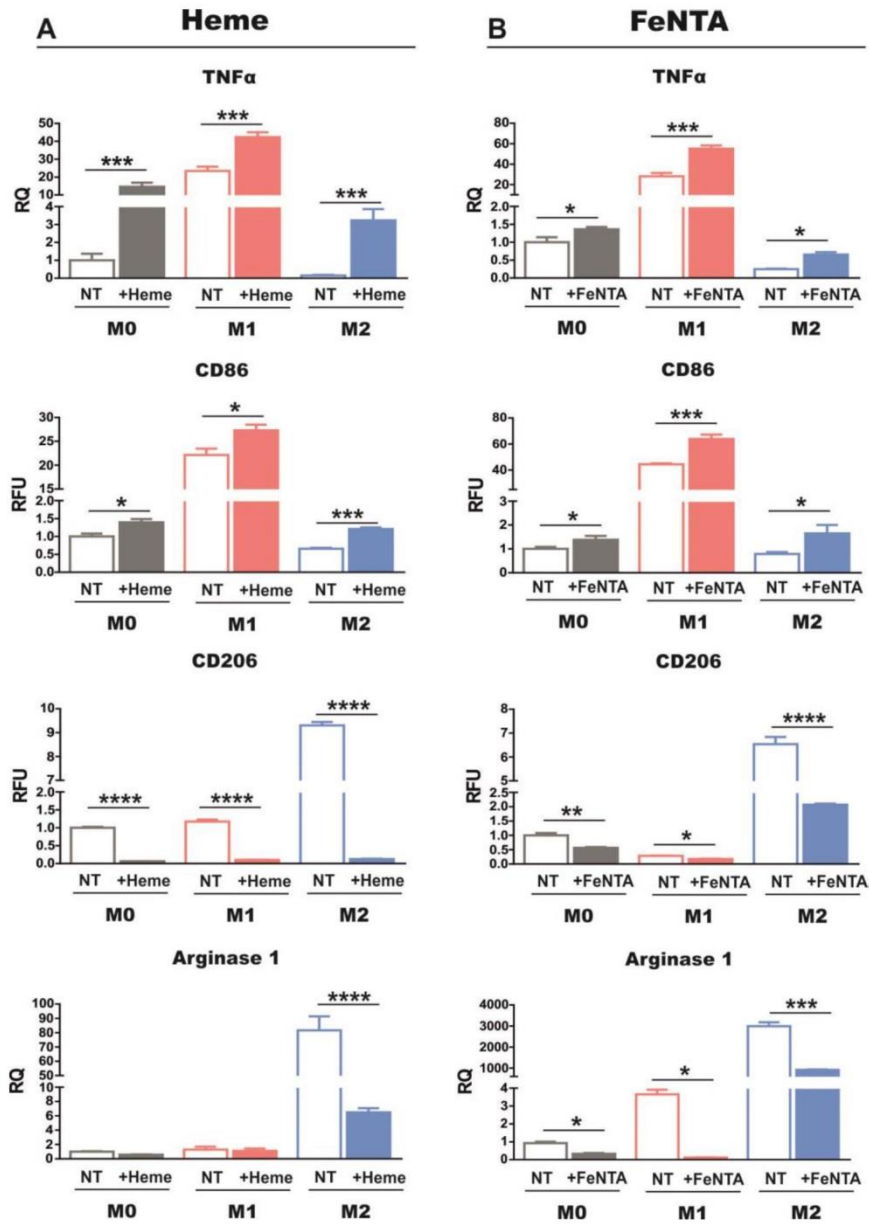


Figure S7. Expression of M1 and M2 markers in M0, M1 and M2 BMDMs. M0, M1 and M2 BMDMs were left untreated (NT) or exposed to 5 μ M BSA-heme (+Heme) for 12 hours (A) or 100 μ M FeNTA (+FeNTA) for 18 hours (B). The expression of CD86 and CD206 was analysed by flow cytometry and expressed in Relative Fluorescence Units (RFU) as fold change compared to M0 untreated cells (black empty bar, NT). The mRNA levels of TNF α and Arginase1 were analysed by qRT-PCR and expressed in Relative Quantity (RQ), as fold change compared to M0 untreated cells (grey empty bar, NT). Results shown are the average of at least three independent experiments. Values represent mean \pm SEM. *P<0.05; ***P<0.001; ****P <0.0001.

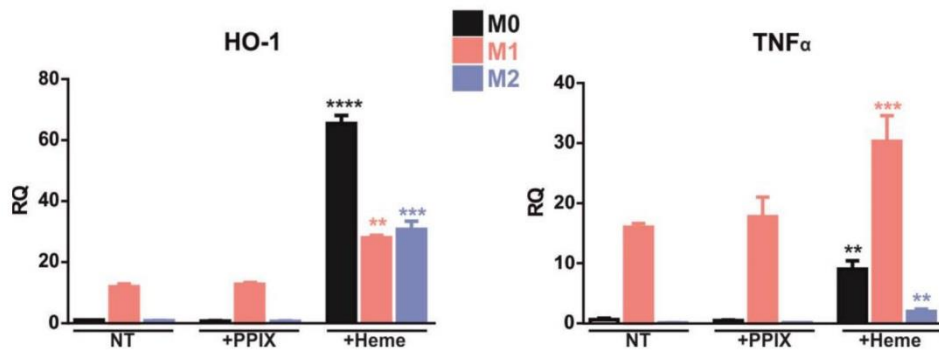


Figure S8. Protoporphyrin IX does not affect the expression of iron genes and polarization markers. M0, M1 and M2 BMDMs were left untreated (NT) or exposed to 5 μ M Protoporphyrin IX (+PPIX) or to 5 μ M BSA-heme (+Heme) for 12 hours. The mRNA levels of HO-1 and TNF α were analysed by qRT-PCR and expressed in Relative Quantity (RQ), as fold change compared to M0 untreated cells (NT). Values represent mean \pm SEM. **P<0.01; ***P<0.001.

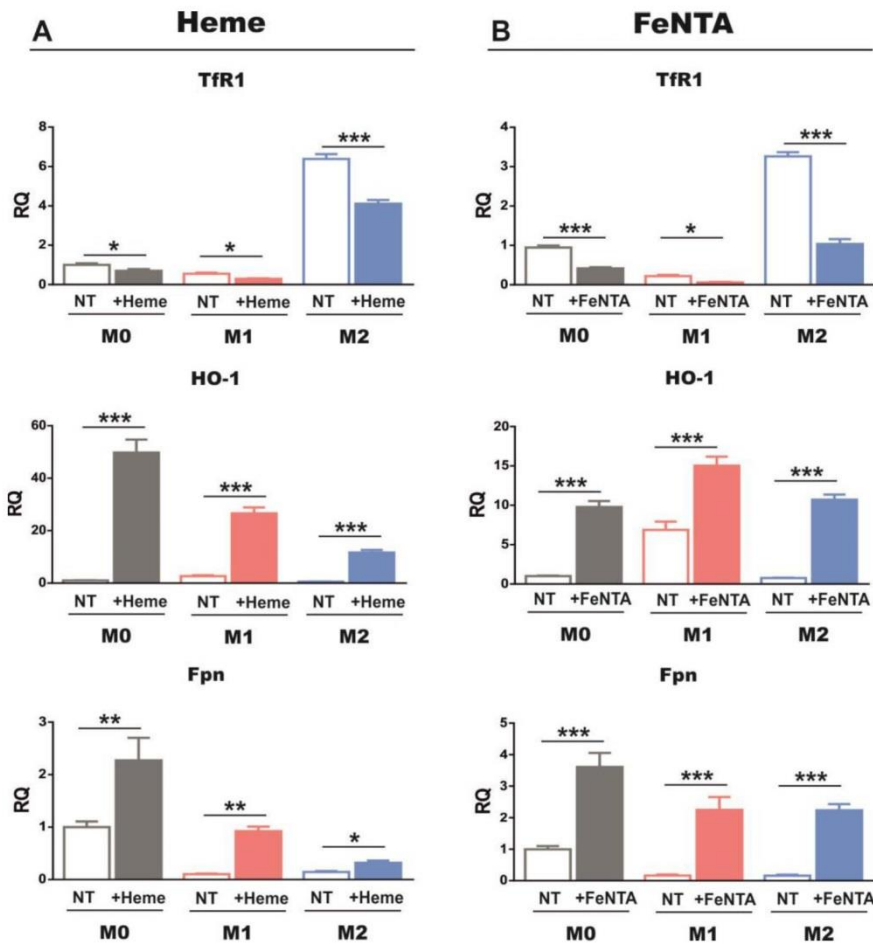


Figure S9. Expression of iron-related genes in M0, M1 and M2 BMDM untreated or treated with heme or iron. M0, M1 and M2 BMDMs were left untreated (NT) or exposed to 5 μ M BSA-heme (+Heme) for 12 hours (A) or 100 μ M FeNTA (+FeNTA) for 18 hours (B). The mRNA levels of TfR1, HO-1 and Fpn were analysed by qRT-PCR and expressed in Relative Quantity (RQ), as fold change compared to M0 untreated cells (grey empty bar, NT). Results shown are the average of at least three independent experiments. Values represent mean \pm SEM. *P<0.05; **P<0.01; ***P<0.001.

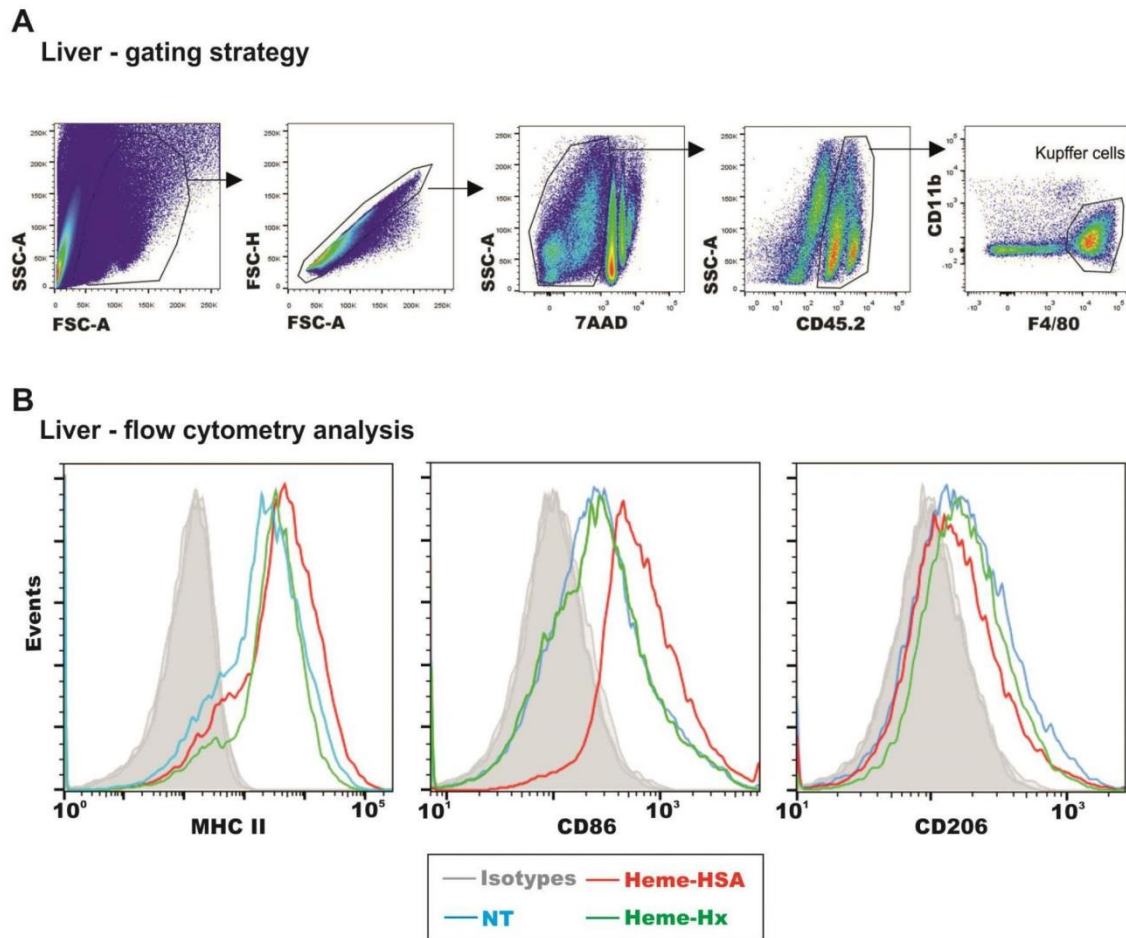


Figure S10. Gating strategy and example of heme-induced M1 polarization in ex vivo hepatic macrophages. (A) Gating strategy used to select liver macrophages: after the selection of single live cells, the analysis of polarization markers was performed on the Gr1⁻ F4/80⁺ CD11b^{low} liver cells. (B) Representative flow cytometry analysis of MHCII, CD86 and CD206 in macrophages isolated from the liver of mice challenged with Hx-heme or HSA-heme. HSA-heme induces a shift in the expression of polarization markers that is prevented in cells from animals challenged with Hx-heme.

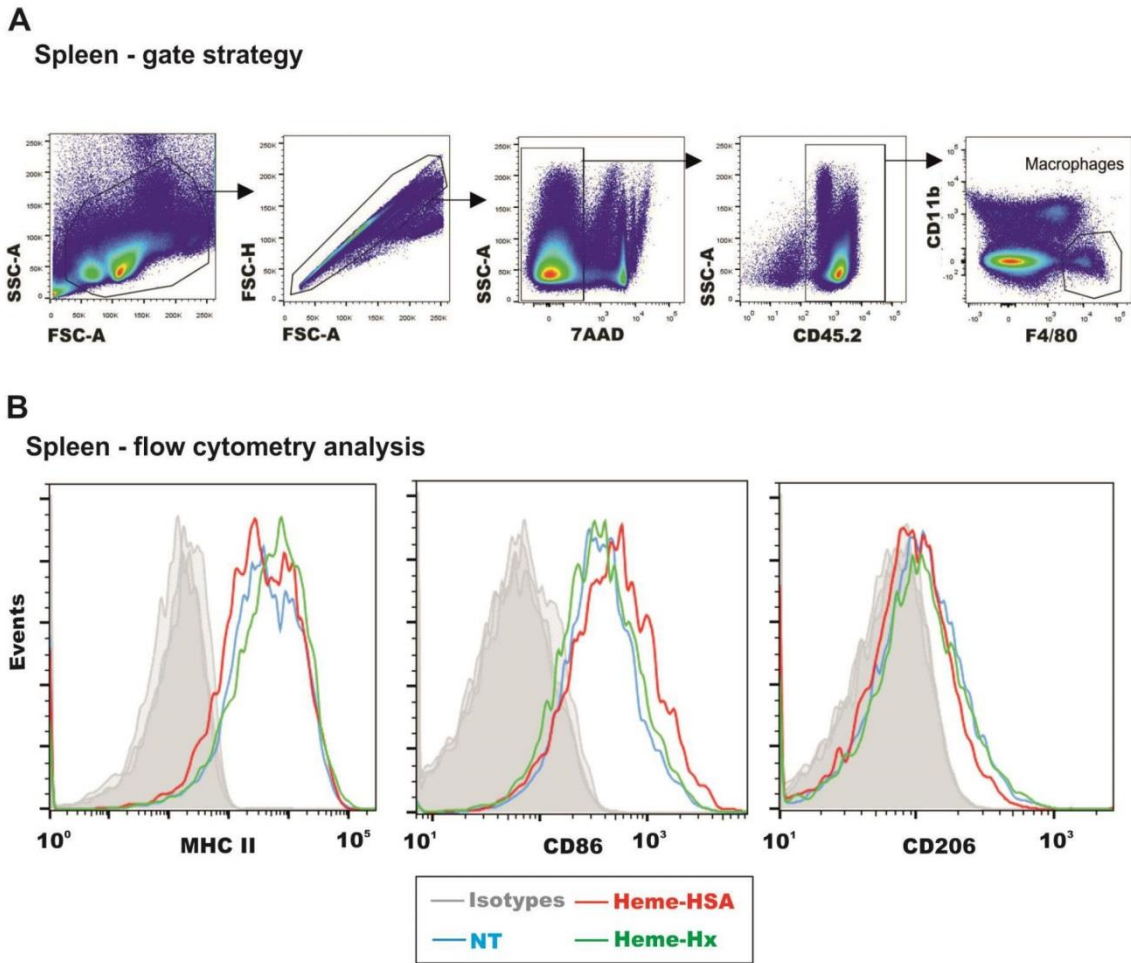


Figure S11. Gating strategy and example of heme-induced M1 polarization in ex vivo splenic macrophages. (A) Gating strategy used to select spleen macrophages: after the selection of single live cells, the analysis of polarization markers was performed on Gr1⁻ F4/80⁺ CD11b^{low} spleen cells. (B) Representative flow cytometry analysis of MHCII, CD86 and CD206 in macrophages isolated from the spleen of mice challenged with Hx-heme or HSA-heme. HSA-heme induces a shift in the expression of polarization markers that is prevented in cells from animals challenged with Hx-heme.

M0

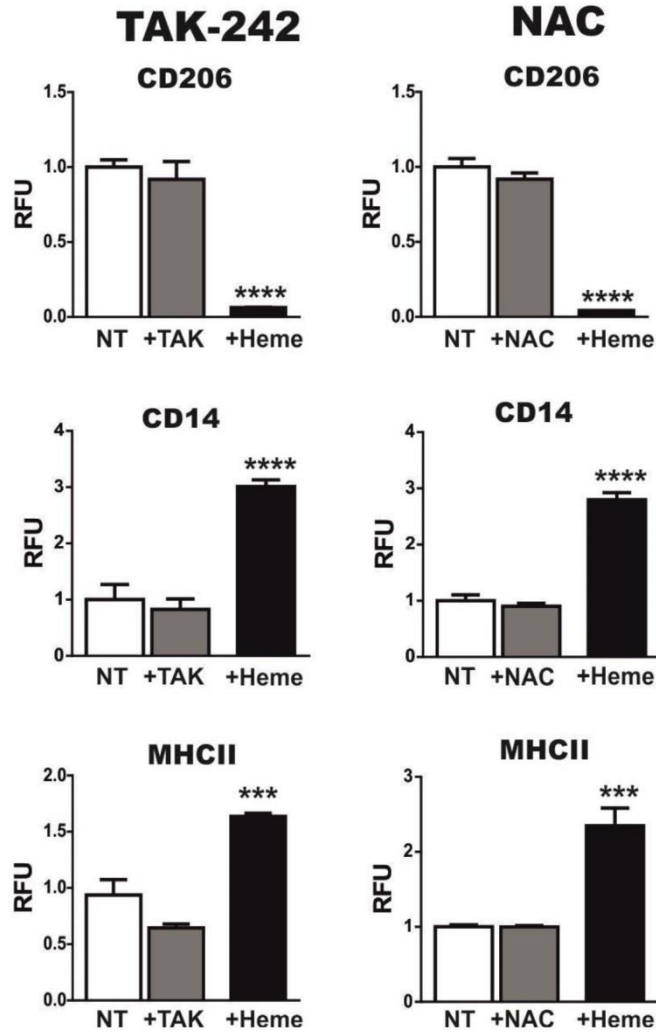


Figure S12. TAK-242 and NAC do not affect the expression of polarization markers per se. M0 BMDMs were left untreated (NT) or treated with 400nM TAK-242 or 2mM NAC for 12 hours. The expression of CD206, CD14 and MHCII was analysed by flow cytometry and expressed in Relative Fluorescence Units (RFU) as fold change compared to untreated cells (NT). Values represent mean \pm SEM. ***P<0.001; ****P<0.0001.

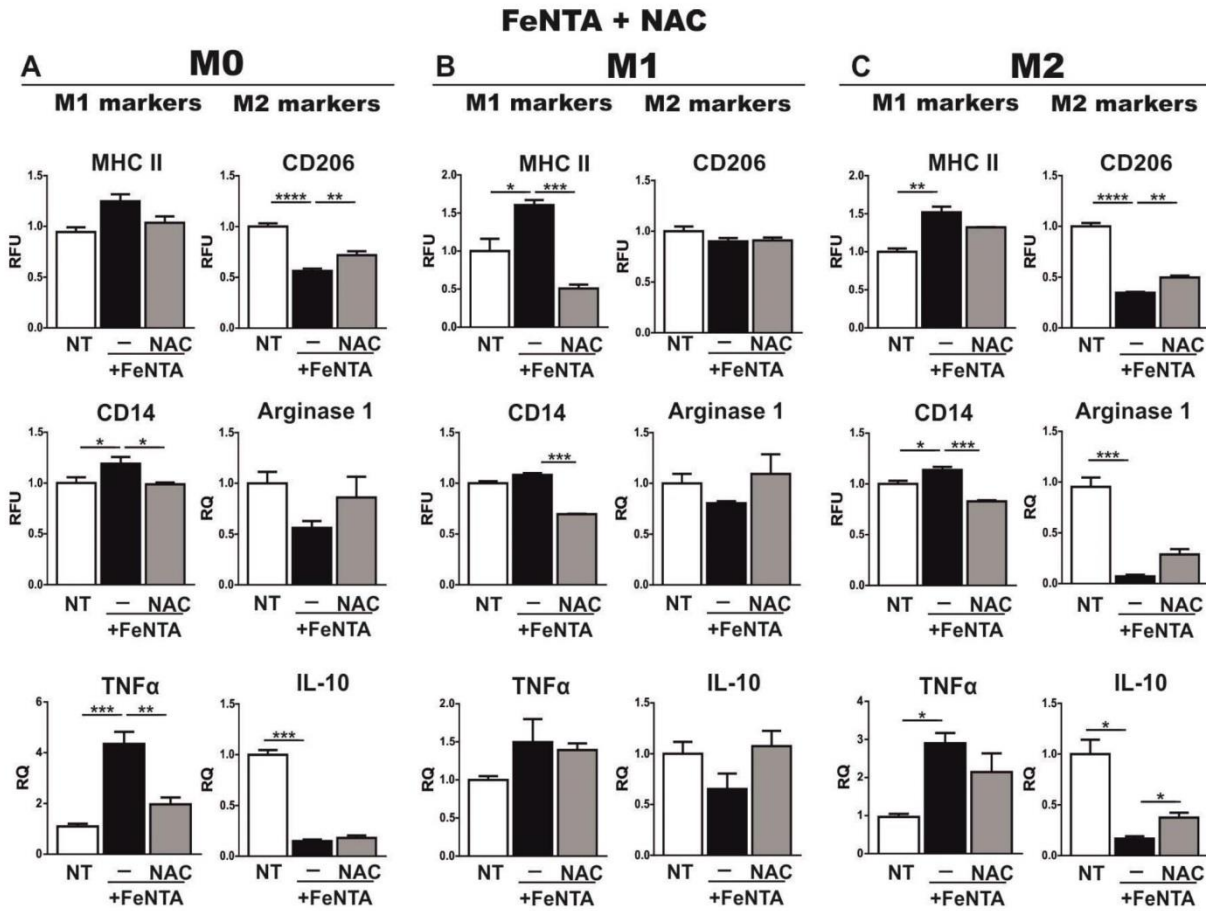


Figure S13. The anti-oxidant NAC rescue iron-induced M1 polarization of macrophages. M0 (A), M1 (B) and M2 (C) BMDMs were left untreated (NT) or exposed to 100 μ M FeNTA (+FeNTA) with or without 2mM NAC for 18 hours. M1 and M2 markers are shown in the left and right column of each panel, respectively. The expression of MHCII, CD14 and CD206 was analysed by flow cytometry and expressed in RFU as fold change to untreated cells (NT). mRNA levels of TNF α , Arginase-1 and IL-10 were analysed by qRT-PCR and expressed in RQ, as fold change to untreated cells (NT). Results shown are representative of three independent experiments. Values represent mean \pm SEM. *P<0.05; **P<0.01; ***P<0.001; ****P<0.0001.

+RBCs + Hx/DFO
M0

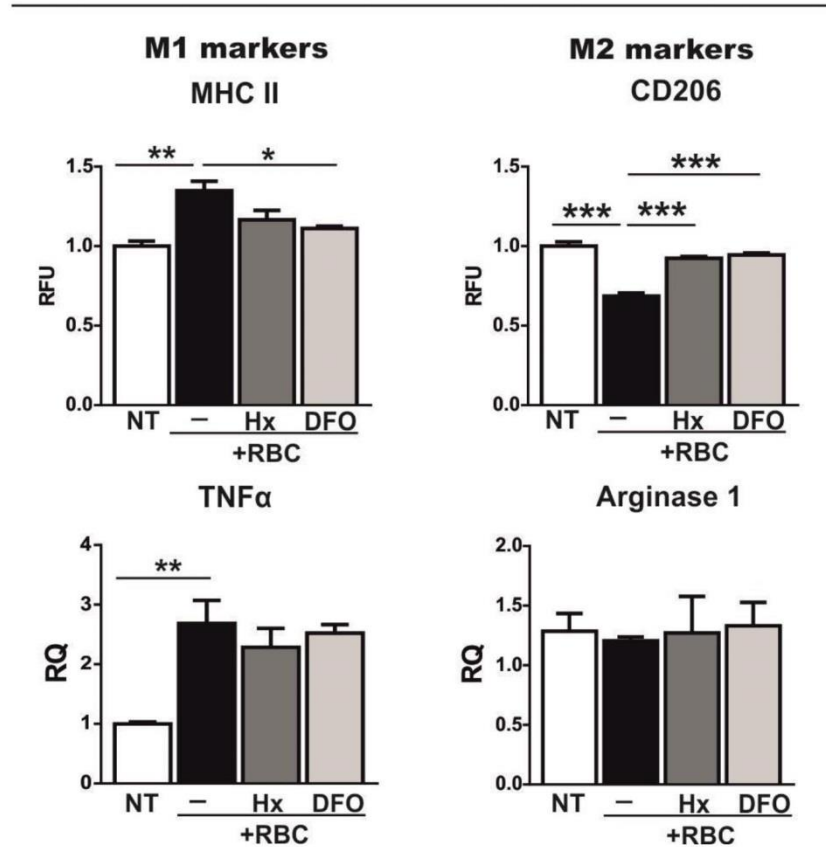


Figure S14. Hx and DFO prevent M1 polarization of macrophages following hemolytic aged RBC treatment. M0 BMDMs were left untreated (NT) or exposed to 2×10^7 aged RBCs (+RBC) with or without 100μM Hx or 100μM DFO for 6 hours. M1 and M2 markers are shown in the left and right column of the panel, respectively. The expression of MHCII and CD206 was analysed by flow cytometry and expressed in RFU as fold change to untreated cells (NT). mRNA levels of TNFα and Arginase1 were analysed by qRT-PCR and expressed in RQ, as fold change to untreated cells (NT). Results shown are representative of three independent experiments. Values represent mean \pm SEM. *P<0.05; **P<0.01; ***P<0.001.

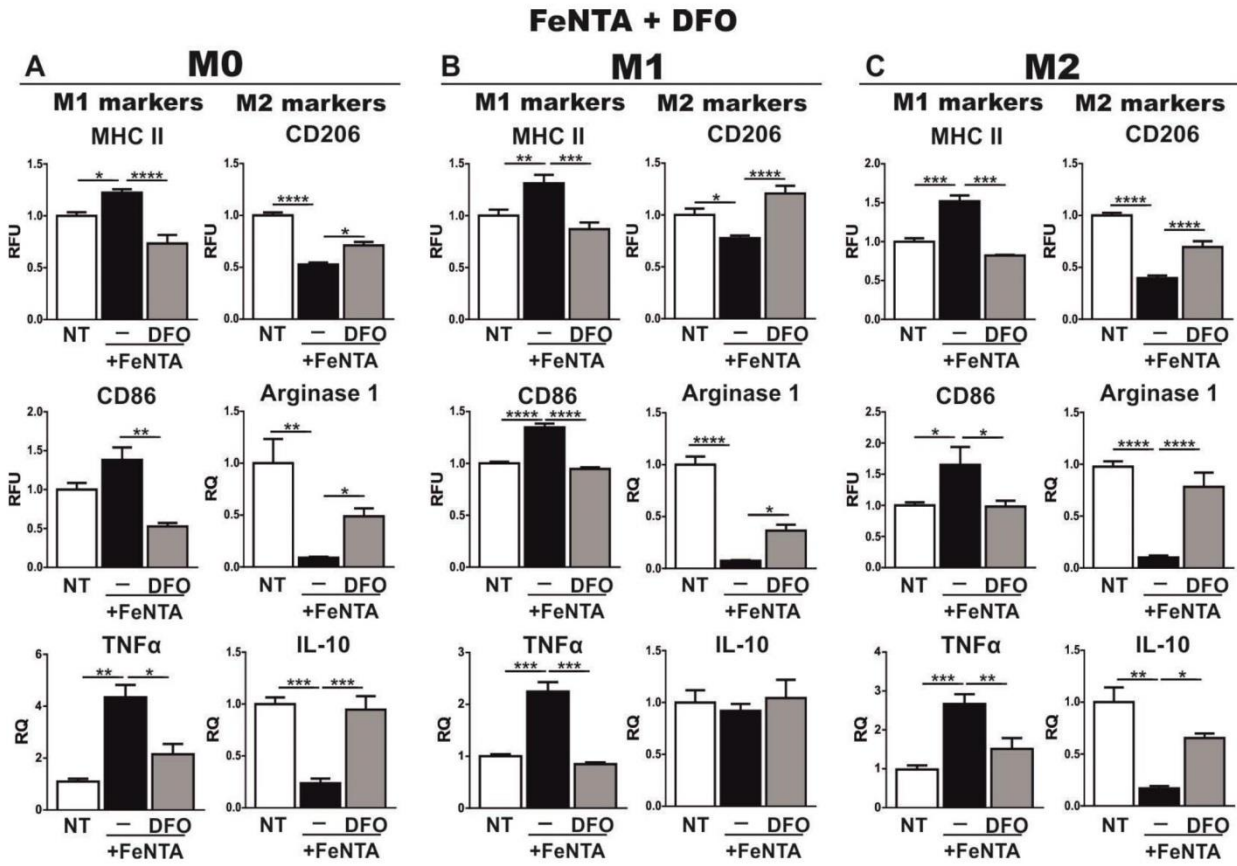


Figure S15. DFO prevent M1 polarization of macrophages in response to iron. M0 (A), M1 (B) and M2 (C) BMDMs were left untreated (NT) or exposed to 100µM FeNTA (+FeNTA), with or without 100µM DFO for 18 hours. M1 and M2 markers are shown in the left and right column of each panel, respectively. The expression of MHCII, CD86 and CD206 was analysed by flow cytometry and expressed in RFU as fold change to untreated cells (NT). mRNA levels of TNFα, Arginase-1 and IL-10 were analysed by qRT-PCR and expressed in RQ, as fold change to untreated cells (NT). Results shown are representative of three independent experiments. Values represent mean ± SEM. *P<0.05; **P<0.01; ***P<0.001; ****P<0.0001.

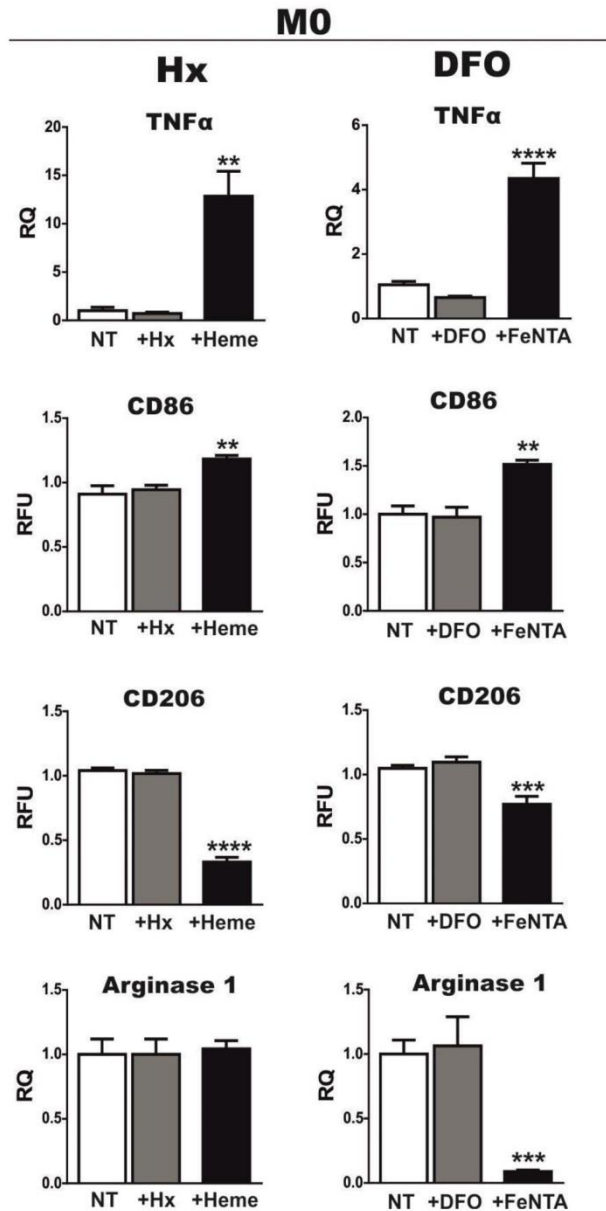


Figure S16. Hx and DFO do not affect the expression of polarization markers per se. qRT-M0 BMDMs were left untreated (NT) or treated with 100 μ M DFO for 18 hours or 5 μ M Hx for 12 hours. The expression of CD86 and CD206 was analysed by flow cytometry and expressed in Relative Fluorescence Units (RFU) as fold change compared to untreated cells (NT). The mRNA levels of TNF α and Arginase1 were analysed by qRT-PCR and expressed in Relative Quantity (RQ), as fold change compared to untreated cells (NT). Values represent mean \pm SEM. **P<0.01; ***P<0.001; ****P<0.0001.

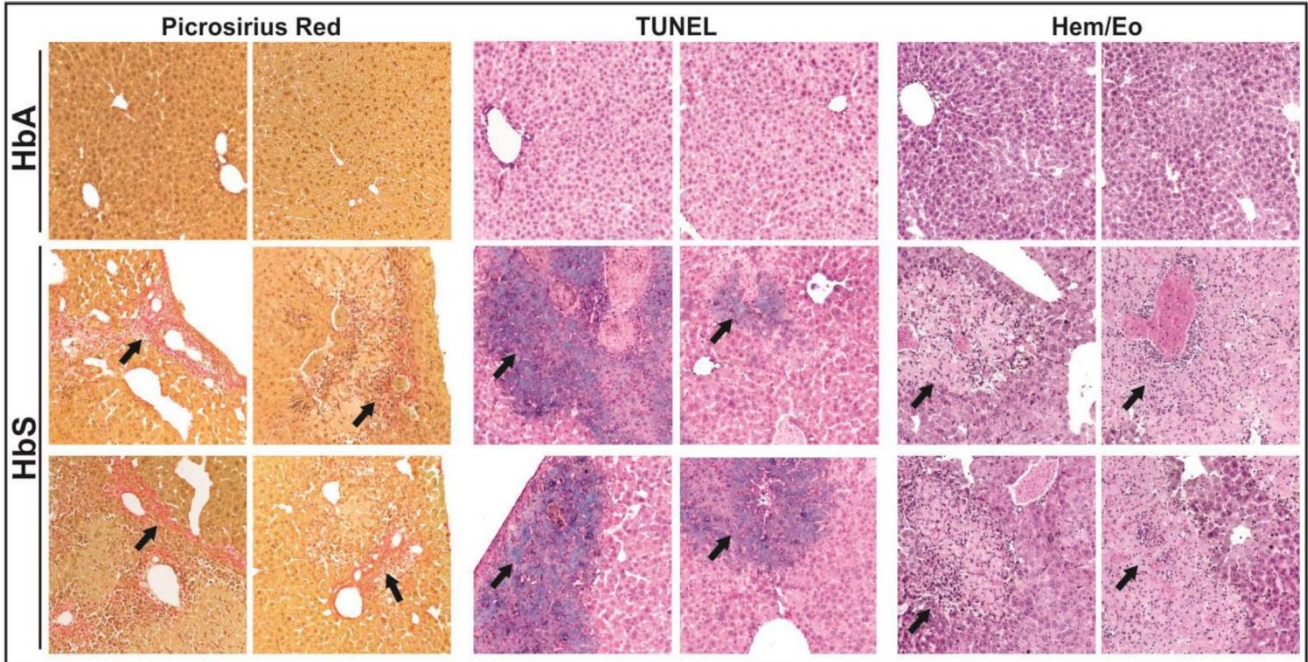


Figure S17. Sickle mice show increased hepatic collagen deposition and parenchymal cell apoptosis. Picrosirius red staining for collagen (left panel), TUNEL staining for apoptosis (central panel) and hematoxylin/eosin staining (right panel) on liver sections from control HbA and sickle HbS mice. Arrows indicate collagen (picrosirius), apoptotic cells (tunel), damaged areas and infiltrating cells (Heme/eo).

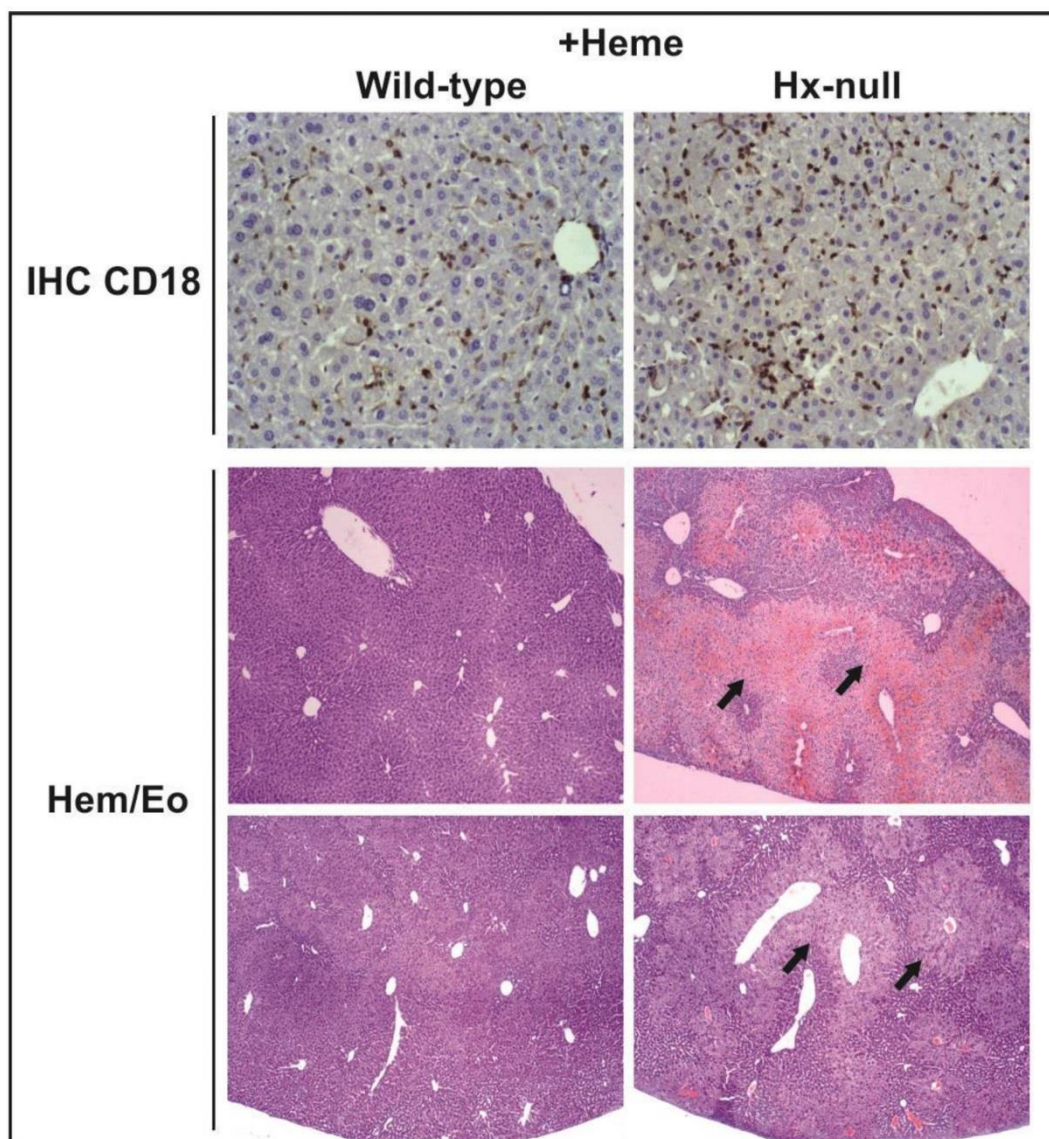


Figure S18. Increased leukocyte recruitment and liver damage in heme-treated Hx-null mice. Immunohistochemistry for CD18 (IHC, upper panel) and hematoxylin/eosin staining (Hem/Eo, bottom panels) was performed on sections of liver from heme-treated wild-type (left column) and Hx-null mice (right column) (heme treatment: 70 μmol heme/kg body weight, 6 hours). The IHC for CD18 reveals an increased number of CD18⁺ cells in heme-treated Hx-null compared to wild-type mice. Areas of necrosis/apoptosis (light violet areas, heme/eo staining) are almost exclusively visible in heme-treated Hx-null mice.

Table S1. Sequence of primers used for qRT-PCR.

TNF α	Forward 5' TGCCTATGTCTCAGCCTCTTC 3' Reverse 5' GAGGCCATTGGGAACCTCT 3'
IL-6	Forward 5' GCTACCAAAGTGGATATAATCAGGA 3' Reverse 5' CCAGGTAGCTATGGTACTCCAGAA 3'
HO-1	Forward 5' AGGCTAAGACCGCCTTCCT 3' Reverse 5' TGTGTTCTCTGTCAGCATCA 3'
Fpn	Forward 5' TGTCAGCCTGCTGTTTGAGGA 3' Reverse 5' TCTTGACAGCAACTGTGTCACCG 3'
TfR1	Forward 5' CCCATGACGTTGAATTGAACCT 3' Reverse 5' GTAGTCTCCACGAGCGGAATA 3'
Arg-1	Forward 5' AATCTGCATGGGCAACCTGT 3' Reverse 5' GTCTACGTCTCGCAAGCCAA 3'
Ym1	Forward 5' CCAGCAGAAGCTCTCCAGAAGCA 3' Reverse 5' GGCCTGTCCTTAGCCCAACTGGT 3'
eCAD	Forward 5' AACGCTCCTGTCTTCAACCC 3' Reverse 5'GGTCACTTTGAGTGTGGCGA 3'
RPL19	Forward 5' AGGCATATGGGCATAGGGAAGAG 3' Reverse 5' TTGACCTTCAGGTACAGGCTGTG 3'
IL-1 β	Forward 5' GCAACTGTTCTGAACTCAACT 3' Reverse 5' ATCTTTGGGGTCCGTCAACT 3'
IL-10	Forward 5' ACTGCACCCACTCCAGT 3' Reverse 5' GTCCAGCTGGTCTTTGTT 3'
Col1a1	Forward 5' CATGTTACGCTTTGTGGACCT 3' Reverse 5' GCAGCTGACTTCAGGGATGT 3'
Col1a2	Forward 5' GCAGGTTACCTACTCTGTCTCT 3' Reverse 5' CTTGCCCCATTCATTTGTCT 3'
MMP9	Forward 5' GCCGACTTTTGTGGTCTTCC 3' Reverse 5' GGTACAAGTATGCCTCTGCCA 3'
MMP12	Forward 5' GAACTTGCAAGTCGGAGGGAA 3' Reverse 5' TCTTGACAAGTACCATTGAGCA 3'
MMP13	Forward 5' GCCAGAAGTCCCAACCAT 3' Reverse 5' TCAGAGCCAGAAATTTCTCC 3'
MCP-1	Forward 5' CATCCACGTGTTGGCTCA 3' Reverse 5' GATCATCTTGCTGGTGAATGAGT 3'
CSF-1	Forward 5' GGTGGACTGCCAGTATAGAAAG 3' Reverse 5' TCCCATATGTCTCTTCCATAAA 3'
PDGF	Forward 5' AGGAGGAGACAGATGTGAGGT 3' Reverse 5' TTCAGGAATGTCACACGCCA 3'
SMA	Forward 5' CTCTCTCCAGCCATCTTCAT 3' Reverse 5' TATAGGTGGTTTCGTGGATGC 3'
Synaptophysin	Forward 5' CAAGGCTACGGCCAACAG 3' Reverse 5' GTCTTCGTGGGCTTCACTG 3'
TIMP2	Forward 5' CGTTTTGCAATGCAGACGTA 3' Reverse 5' GGAATCCACCTCCTTCTCG 3'

CHAPTER II:
A ROLE FOR HEME AND IRON IN THE TUMOR
MICROENVIRONMENT

CONTRIBUTIONS

The “Research Work - Chapter II” of this thesis consists in a manuscript that will soon be submitted for publication. Here is clarified the contribution of each one of the authors:

Manuscript:

Milene Costa da Silva, Margareta P. Correia, Ana Stojanovic, Michael Meister, Thomas Muley, Adelheid Cerwenka, Martina U. Muckenthaler. A role for heme and iron in the tumor microenvironment. *Manuscript in preparation.*

Milene Costa da Silva, the candidate for the PhD degree at the University of Porto, contributed the original idea to this project, and was responsible for the design and performance of all experiments as well as for the analysis and presentation of the results, following intensive discussions with her supervisor, Professor Martina Muckenthaler. In addition, she wrote the final version of the manuscript as an integral part of her future paper (in preparation for submission) and of the thesis. She was helped for some experiments by Margareta P. Correia and Ana Stojanovic.

The contribution of each author to the manuscript is clarified in the section “Authorship” with the following text:

“Author contributions: Milene Costa da Silva designed the project, performed the experiments, and wrote the manuscript; Margareta P. Correia and Ana Stojanovic helped with some experiments; Michael Meister and Thomas Muley provided human histology slides and patient data; Adelheid Cerwenka and Martina U. Muckenthaler supervised the project.”

A role for heme and iron in the tumor microenvironment

Milene Costa da Silva^{1,2,3,4}, Margareta P. Correia⁴, Ana Stojanovic⁴, Michael Meister^{5,6,7},
Thomas Muley^{5,6,7}, Adelheid Cerwenka⁴, Martina U. Muckenthaler^{1,2,6,7}

¹Department of Pediatric Oncology, Hematology and Immunology, University of Heidelberg, Heidelberg, Germany. ²Molecular Medicine Partnership Unit (MMPU), Heidelberg University & EMBL, Heidelberg, Germany. ³Graduate Program in Areas of Basic and Applied Biology (GABBA), Abel Salazar Biomedical Sciences Institute (ICBAS), University of Porto, Porto, Portugal. ⁴Innate Immunity Group, German Cancer Research Center (DKFZ), Heidelberg, Germany ⁵Translational Research Unit, Thoraxklinik at University Hospital Heidelberg, Heidelberg, Germany ⁶Translational Lung Research Center Heidelberg (TLRCH) ⁷German Center for Lung Research (DZL), Germany

ABSTRACT

Macrophages play a critical role in the tumor microenvironment. Here, we investigate whether leakage of red blood cells from the vasculature, and/or consequent release of heme and iron due to hemolysis, affect the inflammatory response of tumor-associated macrophages (TAMs) and tumor growth. We show that iron accumulates preferentially in TAMs in tumor samples from patients with non-small cell lung cancer and in samples of experimental murine lung tumors, whereas cancer cells are relatively iron spared. Iron loaded macrophages are located close to red blood cell extravasation sites in the tumor microenvironment and are enriched at the periphery of the tumor. Hemorrhagic areas in tumors do not only show increased numbers of iron loaded TAMs but also enhanced infiltration of myeloid cells. We observed an enhanced inflammatory response, with increased expression of cytokines and chemokines responsible for macrophage and neutrophil recruitment, namely Cxcl1, Cxcl2, Csf1 and Csf2. Co-culturing of macrophages with tumor cells or with conditioned media (CM) from tumor cells polarizes macrophages towards an M2-like phenotype. This phenotype can be shifted to a M1-like inflammatory phenotype by applying different sources of iron (Ferric Nitriolotriacetate (FeNTA), heme or hemolytic RBC). Taken together, we have identified a novel subpopulation of TAMs, whose phenotype is characterized by iron loading. We propose that iron and heme in addition to being important for tumor growth, also modulate the immune response, macrophage plasticity and cytokine production in the tumor microenvironment.

INTRODUCTION

The tumor microenvironment is characterized by high cellular complexity that alters tumor progression (1). It includes fibroblasts, stroma, blood vessels and infiltrates of immune cells. Tumor-associated macrophages (TAMs) are a major component of the tumor microenvironment since they can represent up to 50% of the mass of infiltrated cells (2). Macrophages show high plasticity, reflected on their capacity to integrate diverse signals from the microenvironment and to acquire distinct phenotypes (3). Macrophage functions and phenotype depend mainly on their origin and the diversity of stimuli they encounter in different niches (4, 5).

According to their responses to Th1 and Th2 cell derived cytokines, macrophages were subdivided in two classes: M1 macrophages (classical activation) and M2 macrophages (alternative activation) (6-9). M1 macrophages are polarized in the presence of pro-inflammatory stimuli such as Interferon-gamma (IFN γ), tumor necrosis factor alpha (TNF α) and Toll-like Receptor 4 (TLR4) adjuvants such as lipopolysaccharide (LPS). M2

macrophages are polarized in the presence of interleukin (IL)-4, IL-13 and IL-10. This dichotomy suggests that TAMs could be either tumor killing (M1) or tumor promoting (M2) (10). Several studies classified TAMs as M2-like macrophages due to their ability to sustain tumor cell proliferation and invasion (11, 12). Regarding iron related functions, M2 macrophages are linked to iron recycling and high iron turn-over when compared to M1 macrophages. M2 macrophages express high levels of cluster of differentiation (CD)163, Heme Oxygenase-1 (HO-1) and Ferroportin and low expression levels of Ferritin (13), suggesting that M2 macrophages might function as iron donors to cancer cells.

Iron is important for tumor cell proliferation; in fact, clinical and population-based studies collectively support a model in which increased iron levels in the human body are associated with an increased cancer risk and increased tumor growth (14). Tumors take up iron via transferrin-bound iron, which supports cellular functions such as DNA synthesis (15).

Occurrence of angiogenesis may facilitate the recruitment of inflammatory cells but will also trigger the extravasation of red blood cells (RBC) into the tumor microenvironment. These in turn may release hemoglobin and heme upon hemolysis. Each RBC contains around 1.2×10^9 molecules of heme, and each heme moiety has one ferrous ion within the center of the porphyrin ring (16). Thus RBC may serve as a significant iron source for tumors.

An important function of macrophages is the recycling of iron. Thus, it is possible that macrophages in the tumor microenvironment would exercise such a function locally.

Recently we demonstrated that various sources of heme (hemolytic RBC, free heme) and iron activate macrophages to differentiate towards an M1-like proinflammatory phenotype, which is hallmarked by the production of inflammatory cytokines (TNF α , IL-1 β and IL-6) and reactive oxygen species (ROS). We further demonstrated that already polarized M2 macrophages can shift towards a pro-inflammatory M1-like phenotype in the presence of heme and iron (17). Additional studies also linked iron accumulation and macrophage plasticity, supporting the idea that iron drives macrophages towards a pro-inflammatory phenotype (18, 19).

Inflammation regulates the expression of iron-related genes and proteins and thus affects iron homeostasis. As a result of cancer-related inflammation, cancer patients show impairment of systemic iron homeostasis and develop a form of anemia (20). Anemia of cancer may result from the stimulation of hepatic transcription of hepcidin by circulating cytokines, such as IL-6, IL-1 α and IL-1 β (21-23). Hepcidin binds and degrades the iron exporter ferroportin in macrophages, causing intracellular iron sequestration, decreased plasma iron levels and anemia due to decreased iron availability.

So far, the consequences of iron availability for the composition of the tumor microenvironment and for TAMs polarization have not been studied. Based on the findings that inflammation disturbs iron homeostasis and heme and iron sources can influence macrophage polarization and function (17), we now explored whether RBC extravasation as well as heme and iron release from RBC can affect the composition of the tumor microenvironment. We focused our analysis on how heme and iron can affect the plasticity of tumor-associated macrophages, and how tumor related-inflammation affects systemic iron homeostasis in a mouse model of Lewis Lung Carcinoma (LLC).

RESULTS

Iron accumulates in a subset of tumor-associated macrophages, but not in cancer cells in human non-small cell lung cancer

To explore the distribution of iron in the tumor microenvironment, Perls' staining was performed on 19 sections from human non-small cell lung cancer (NSCLC). Table 1 summarizes the clinical information available from this cohort of patients (age, gender, survival, histology, tumor grade, smoking history and presence of RBC) grouped by iron staining. Histology slides positive for Perls' staining (=blue) were considered as "iron positive" (n=11) while the slides negative for Perls' staining were considered as "iron negative" (n=8). We observed that, when iron is detected, it is localized mainly in the periphery of tumors. Iron positive cells accumulate near areas where RBC are visible (10 patients out of 11). RBC were identified according to their morphology and light pink/orange coloration after Perls' staining (Figure 1A). In general, cancer cells appear to be negative for iron staining, while some infiltrating cells are clearly positive. Since macrophages are the prime candidates to phagocytose RBC and sequester iron in the tumor microenvironment, we performed immunostaining for the macrophage/monocyte marker, CD68. Iron staining strongly correlates with positive immune staining for CD68, suggesting that macrophages accumulate iron in the tumor microenvironment (Figure 1B). To better understand if iron accumulates in tumor-associated macrophages, we isolated lymphocytes from fresh tumors tissue (lung adenocarcinoma) and separated them according their iron content using magnetic isolation (see "Material and Methods"). Table 2 summarizes the information regarding the fresh lung adenocarcinoma samples. Cells obtained within the "magnetic" fraction (cells that respond to a magnetic field due to their high iron content) stain for iron accumulation and are additionally positive for CD68 staining. This clearly demonstrates that iron accumulates in macrophages associated with adenocarcinoma. Cells in the flow through (cells that don't respond to the magnetic field), are negative for iron staining but some cells are positive for CD68, showing that in

addition to iron containing macrophages, an iron negative population of macrophages co-exists (Figure 1C). To explore whether iron accumulation in macrophages might be associated with specific areas in the tumor (e.g. the tumor center or the invasive front) we performed iron staining on tissue micro-arrays (TMAs) from 116 patients with lung cancer. From each patient, three areas of the original histology block were represented: normal lung, tumor center or the invasive front (Figure 1D). From the 116 patients analyzed, 38 stained positively for iron at least in the tumor center and/or the invasive front. Table 3 summarizes the information about this cohort of patients, separated in two groups: iron positive and iron negative. Quantification of iron staining revealed that signals are significantly higher in the invasive areas of the tumor, compared with normal lung and tumor center (Fig. 1E). Although these findings suggest that iron accumulation in TAMs might be connected to angiogenesis and RBC leakage, we cannot exclude that environmental factors contribute to iron loading in macrophages. For example, it was demonstrated that alveolar macrophages can accumulate iron due to cigarette smoking (24, 25). Since 100% of the patients analyzed have a smoking history, it is not clear whether iron loading in macrophages is only due to micro-bleedings and RBC extravasation in the tumor microenvironment. Rather it may be a mixture of smoking and hemorrhage. Nevertheless, some patients do not show iron deposition in macrophages in spite of their smoking history.

Table 1. Patient characteristics: histology slides

Variable	Iron positive (n=11)	Iron negative (n=8)
Age (years, mean \pm SEM)	64,00 \pm 2,676	55,13 \pm 3,777
Gender (male:female)	9:2	7:1
Survival (live:dead (%))	4:7(57)	1:7(14)
Histology: number (%)		
Adenocarcinoma	4 (36)	4 (50)
Squamous	6 (55)	4 (50)
Large cell	1 (9)	0
Tumor grade: number (%)		
1	1 (9)	0
2	4 (36)	4 (50)
3	6 (55)	4 (50)
Smoker: number (%)	11 (100)	8 (100)
Presence of RBC		
near iron positive cells	10:1	-----
(yes:no)		

Table 2. Patient characteristics: fresh lung tumors

Variable	Patient			
	1*	2	3	4
Age	73	54	74	69
Gender	Female	Female	male	male
Histology	Adenocarcinoma	Adenocarcinoma	Adenocarcinoma	Adenocarcinoma
Tumor grade	2	3	2	2
Smoker	yes	yes	yes	yes

*cytospin slides from this patient are represented in Figure 1C

Table 3. Clinicopathological characterization of patients (n=116) from TMAs of non-small cell lung carcinoma

Variable	Iron positive (n=38)	Iron negative (n=78)	P-value
Age (years, mean \pm SEM)	61,65 \pm 1,364	64,82 \pm 0,8501	0,0453 (*)
Gender (male:female)	28:10	61:17	
Tumor size (cm, mean \pm SEM)	3,712 \pm 0,3292	4,230 \pm 0,2146	0,1823 (ns)
Histology: number (%)			
Adenocarcinoma	18 (47)	28 (36)	
Squamous	20 (53)	45 (58)	
Large cell	0	5(6)	
Tumor grade: number (%)			
1	0	1 (1)	
2	10 (26)	30 (38)	
3	28 (74)	47 (66)	
Survival (live:dead, (%))	17:21(80)	29:49(60)	

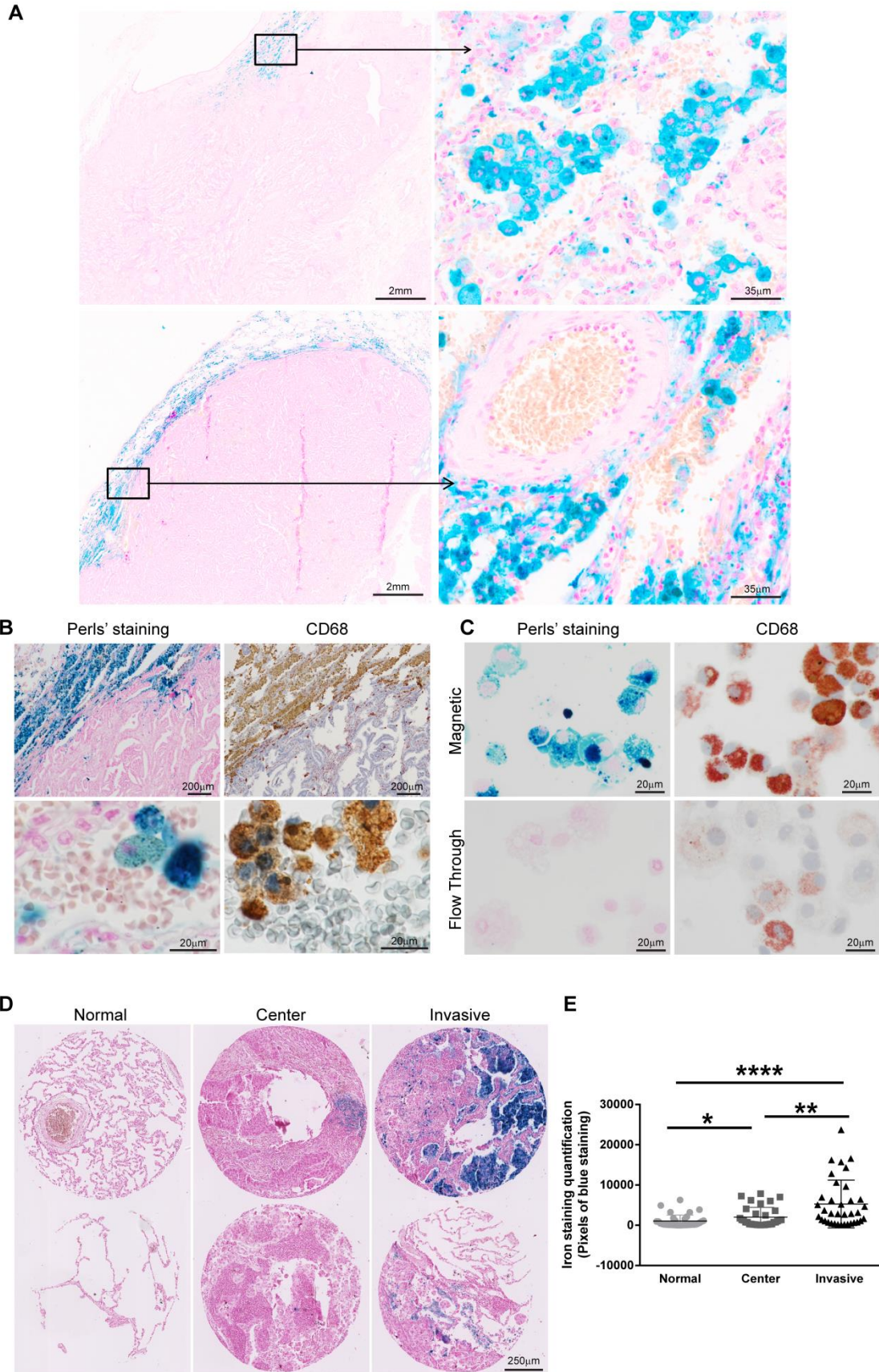


Figure 1. Tumor-associated macrophages are positive for iron staining and accumulate near RBC. (A) Representative examples of Perls' staining of two different patients with lung adenocarcinoma. Blue staining represents iron. Red blood cells show an orange coloration. (B) Representative examples of Perls' staining and anti-CD68 immunostaining in lung adenocarcinoma. Blue staining represents iron and brown staining represents CD68 positive cells. (C) Perls' staining and anti-CD68 immunostaining after magnetic isolation. Blue staining represents iron staining and red staining anti-CD68 staining. Results are representative of 4 patients. (D) Example of Perls' staining of TMAs of non-small cell lung carcinoma. The upper panel corresponds to normal lung, tumor center and invasive front of a patient with squamous cell carcinoma. The lower panel corresponds to normal lung, tumor center and invasive front of a patient with adenocarcinoma (E) Quantification of TMAs' Perls' staining in normal, center and invasive areas. Quantification of iron staining was performed using the Image Pro-Premier 3D software. The software calculated the area of pixels corresponding to blue staining (iron staining) (n=38 patients). Data are shown as mean \pm SEM. *p < 0.05, **p < 0.01, ***p < 0.001, and ****p < 0.0001.

Iron loaded macrophages are present in the Lewis Lung Carcinoma mouse model

To better define the source of iron in TAMs (e.g. RBC or environmental factors) we next analyzed a mouse model of Lewis Lung Carcinoma (LLC).

LLC is a widely used syngeneic mouse model for NSCLC (26). The fact that LLC can be injected in an immunocompetent murine background, such as C57BL, makes this mouse model an important tool to study tumor-related inflammation. 15 days after LLC injection (1×10^6 tumor cells were injected subcutaneously (sc) in the flanks of mice), mice were sacrificed and tumors and organs were removed for further analysis. Consistent with findings in human non-small cell lung carcinomas, tumor cells were negative for iron staining. Cells that stained positive for Perls' staining with DAB enhancement were localized within infiltrating cells near the periphery of LLC tumors. Hematoxylin and eosin (H&E) staining in consecutive slides revealed that RBC in the proximity of iron loaded cells (RBC stain bright pink in H&E staining), suggesting that iron loaded TAMs are localized in areas where RBC extravasation occurs (Figure 2A). We also injected 1×10^5 LLC cells intravenously (iv) in the tail vein. In intravenous injections, LLC cells colonize the lungs. Mice were sacrificed 15 days after injection and lungs were removed and stained for iron. As observed in subcutaneous tumors, when iron loaded macrophages were detected, they were also associated with areas of RBC extravasation. Tumor cells of lung colonies are negative for iron staining (Figure 2A). To better understand the growth dynamics of LLC sc tumors, we followed tumor growth by measuring tumor weight and the number of infiltrated cells in a time dependent manner. Tumors were analyzed at day 7, 11 and 15. We observed an exponential tumor growth after day 7 that also correlated with

an increase in the number of infiltrated cells in the tumors (Figure 2B). Iron loaded macrophages were detected in the tumor at day 11 and day 15 after LLC injection (Figure 2C). These data show that iron loaded TAMs not present since the beginning of tumor development, but rather appear with increase in tumor growth and probably with angiogenesis.

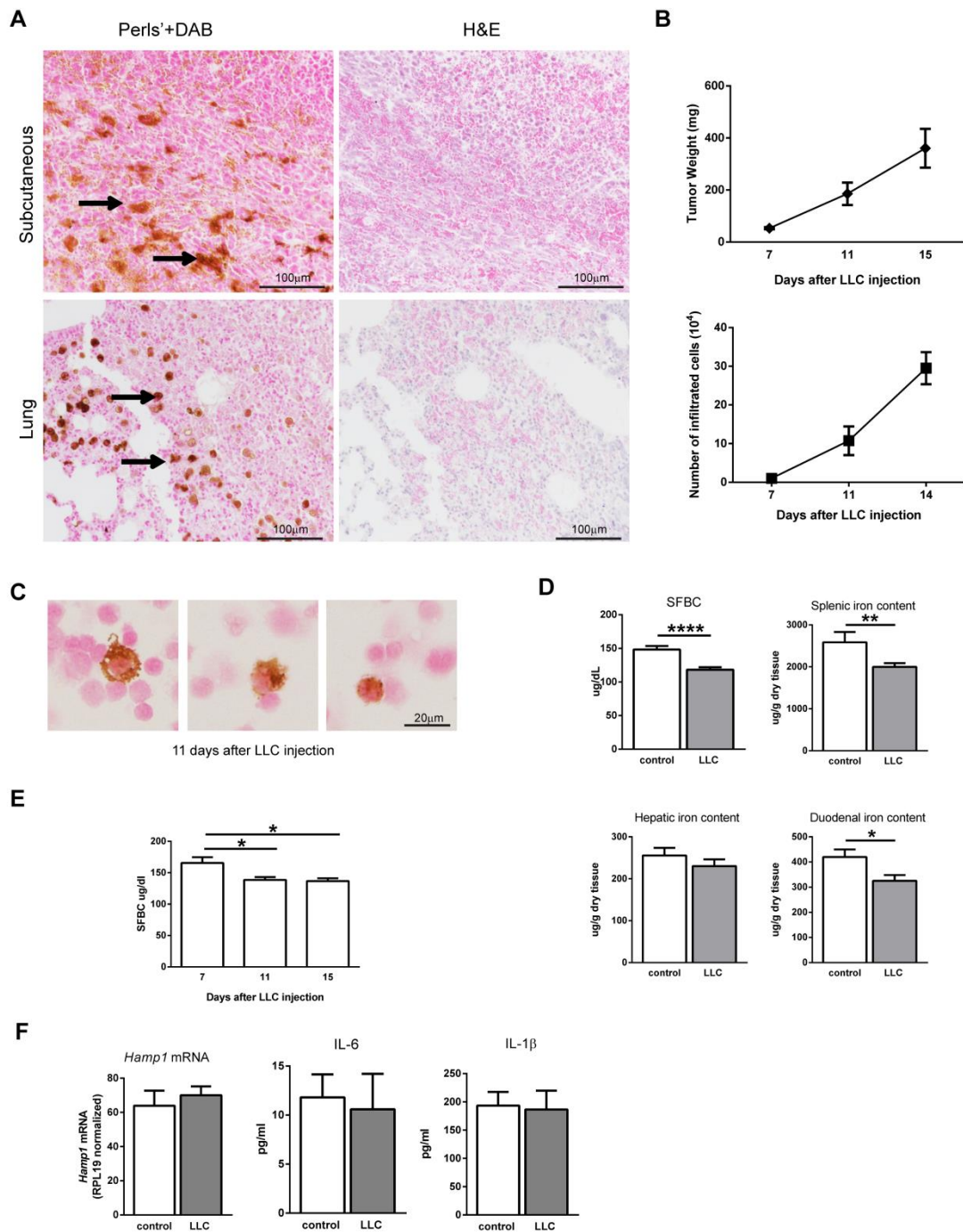


Figure 2. Iron parameters are altered in tumor bearing mice. (A) Representative examples of Perls' staining with DAB enhancement in LLC tumors. Tumors were removed 15 days after subcutaneous (sc) (representative of 10 tumors) or intravenous (iv) injection (LLC cells colonize the lung after iv injection, n=3 mice). Brown staining represents iron accumulation in macrophages (black arrows show examples of iron loaded macrophages). Consecutive slides were stained with Hematoxylin & Eosin (H&E) demonstrating a co-localization of RBC with iron loaded macrophages. RBC appear as bright pink dots after Eosin staining. **(B)** Tumor weight (mg) and number of infiltrated cells (10^4) of LLC tumors injected subcutaneously (n=3 per time point). The total count of live cells was performed after lymphocyte purification. Mice were sacrificed and tumors removed at the indicated days after injection (day 7, 11 and 15). **(C)** Representative examples of Perls' staining with DAB enhancement in cytopsin preparations of lymphocytes purified from LLC tumors. Tumors were collected at day 11 after LLC injection. Brown staining represents iron. **(D)** Iron measurements in the serum (SFBC), spleen, liver and duodenum of non-injected mice (control, n=16) and LLC-bearing mice (LLC, n=32). Serum and tissues were collected 15 days after subcutaneous injection. **(E)** Iron measurements in the serum (SFBC) of LLC tumor-bearing mice injected subcutaneously (n=3 per time point). Serum was collected at the indicated days after LLC injection (day 7, 11 and 15). **(F)** *Hamp1* messenger RNA (mRNA) expression in liver from control (n=8 mice) and LLC mice (n=14 mice) determined by quantitative RT-PCR. mRNA levels were normalized to *Rpl19* mRNA levels. IL-6 and IL-1 β levels in serum of control mice (n=5 mice) and LLC-bearing mice (n=8 mice). Liver tissue and serum were collected 15 days after subcutaneous injection. Data are shown as mean \pm SEM. *p < 0.05, **p < 0.01, ***p < 0.001, and ****p < 0.0001.

Mice injected with Lewis Lung Carcinoma (LLC) show altered systemic iron parameters

Inflammation causes the redistribution of iron to macrophages (27-29). Since inflammation is a consequence of cancer, we further characterized iron regulation in LLC-bearing mice. We compared iron levels in serum, spleen, liver and duodenum of control mice (non-injected) with LLC-bearing mice, 15 days after LLC sc injection. The tumor-bearing mice showed a reduction in serum iron levels (SFBC) as well as a reduction in splenic and duodenal iron content (Figure 2D). The reduction of iron levels can be observed already at day 11 after LLC injection (Figure 2E). The hepcidin/ferroportin regulatory axis is crucial for the regulation of systemic iron levels (30, 31). Hepcidin, the major systemic regulator of ferroportin was shown to be increased in some cancers (32-34). Hepcidin targets ferroportin for degradation promoting iron retention in macrophages. We evaluated the expression of hepatic hepcidin in LLC-bearing mice, compared to control mice. We also quantified the levels of IL-6 and IL-1 β in the serum, since these cytokines were shown to induce hepcidin expression. At day 15 after LLC injection, hepcidin mRNA levels in the liver were not altered, suggesting that iron retention in TAMs and the decreased in serum iron levels are independent of systemic hepcidin. Consistent

with this finding, serum IL-6 and IL-1 β levels were not increased in tumor bearing mice (Figure 2F). Thus, the reduction in serum iron levels and duodenum iron content may be explained by high iron requirements for tumor growth. The decrease in splenic iron content is unexpected and may be due to the infiltration of CD11b⁺/Gr1⁺ cells (myeloid cells) which are iron spared (Figure 3A-C). The population of iron recycling macrophages (Gr-1^{neg}/CD11b^{low}/F4/80^{high}), however, was not altered (Figure 3C). Possibly the decrease in iron levels may be caused by a shift in the ratio between iron spared and iron loaded cells. In fact, Perls' staining with DAB enhancement shows a dispersion of iron loaded cells in the red pulp of the spleen in LLC-bearing mice when compared to control mice (Figure 3B). The expression of ferroportin was detected both in WT as well as in LLC-bearing mice, suggesting that the iron recycling and export capacity of splenic macrophages is not affected by LLC-derived inflammation (Figure 3B). We also observed that the infiltration of myeloid cells in the spleen causes an increase in splenic weight (Figure 3D). The analysis of splenic macrophages (Gr-1^{neg}/CD11b^{low}/F4/80^{high}) revealed an increase in the expression of CD206 and a decrease the expression of major histocompatibility complex (MHC) II, suggesting that tumor-derived factors can also affect the polarization of distant tumor-site macrophages (Figure 3E). We conclude that the alteration in iron parameters is likely due to tumor cells growth and expansion of myeloid cells, rather than a consequence of increased hepcidin expression.

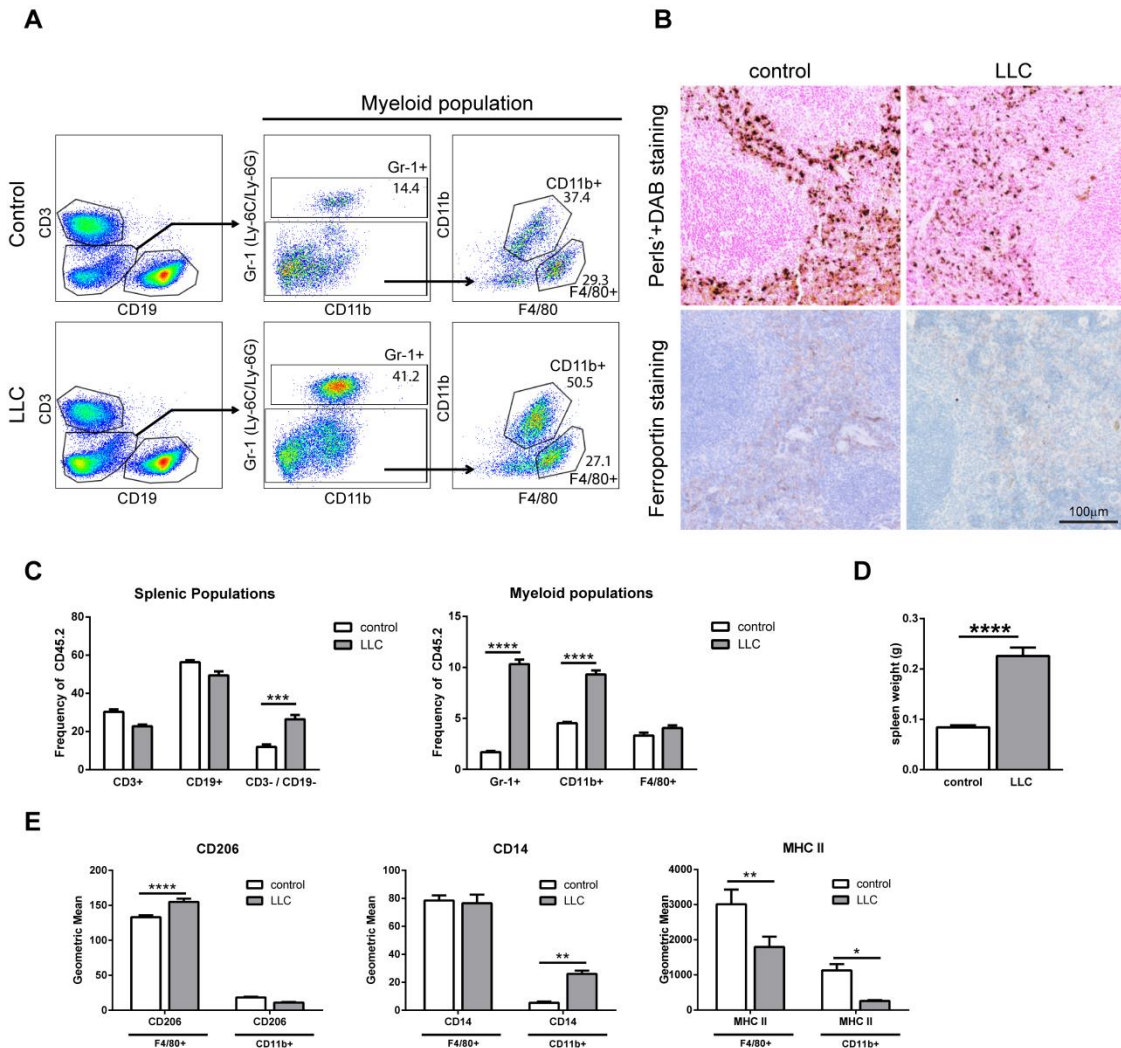


Figure 3. Analysis of spleens of control mice and LLC-bearing mice. (A) Gating strategy used to analyze the splenic populations from control mice (non-injected) and LLC-bearing mice (LLC). Analysis was performed at day 15 after injection. **(B)** Perls' staining with DAB enhancement and anti-ferroportin staining in spleen from control and LLC-bearing mice. Brown staining in "Perls'+ DAB staining" represents iron staining. Red staining represents ferroportin expression. Samples are representative of 4 different mice in each group. **(C)** Frequency of CD3⁺, CD19⁺ and CD3⁻/CD19⁻ (double negative cells) relative to CD45.2 cells (total number of leukocytes) in control and LLC-bearing mice (n=8 mice per group). Frequency of Gr-1⁺ cells (gated as CD11b⁺/Gr-1⁺); CD11b⁺ cells (gated as CD11b⁺/Gr-1⁻) and F4/80⁺ cells (gated as Gr-1^{neg}/Cd11b^{low}/F4/80^{high}) relative to CD45.2 cells (total number of leukocytes) in control and LLC-bearing mice (n=8 mice per group). **(D)** Spleen weight in control mice and LLC-bearing mice (n=8 mice per group). **(E)** Analysis of the expression of CD206, CD14 and MHC II in CD11b⁺ cells (gated as CD11b⁺/Gr-1⁻) and F4/80⁺ cells (gated as Gr-1^{neg}/Cd11b^{low}/F4/80^{high}) in the spleen (n=8 mice per group), expression is shown as geometric mean. Data are shown as mean \pm SEM. *p < 0.05, **p < 0.01, ***p < 0.001, and ****p < 0.0001.

Tumor-associated macrophages of LLC lack the expression of ferroportin

We next focused our attention on the iron-loaded macrophages within the tumor microenvironment by sorting CD11b⁺/Gr-1⁻/F4/80⁺ cells from tumors (gating strategy is shown in Figure 4). Iron loaded cells were contained within this fraction and not present in the remaining cells (data not shown). Magnetic isolation separated TAMs into two populations: iron negative macrophages (“Fe neg”) and iron positive macrophages (“Fe pos”) (Figure 5A). The comparison of these two populations by quantitative RT-PCR showed that “Fe pos” TAMs express increased mRNA levels of *Cd163* and *Hmox1* (Figure 5B). CD163 is mainly expressed in macrophages and is the scavenger receptor for haptoglobin-hemoglobin complexes and for hemoglobin alone (35). HO-1 is an enzyme responsible for heme catabolism. This reinforces the idea that “Fe pos” macrophages obtain their iron by phagocytosing RBC or their products. We next analyzed the expression of ferroportin (*Fpn*). *Fpn* mRNA expression in TAMs is almost undetectable and not different between “Fe pos” and “Fe neg” TAMs (Figure 5C). To understand if iron retention in TAMs may be caused by the absence of ferroportin expression we cultured M-CSF-differentiated BMDM for 24h with 50% conditioned media (CM) from LLC cells (DMEM was used as NT control). Interestingly, addition of CM polarized bone marrow-derived macrophages (BMDM) towards an M2 phenotype with increased expression of *Cd163*, *Arginase-1*, *Ccl2* (Figure 5D) and CD206 (data not shown), while the expression of *Fpn* was decreased (Figure 5D). We performed anti-ferroportin immuno-staining in sorted TAMs to analyze the expression of Ferroportin at the protein level. Cell suspensions from spleen of control mice were used as positive control and we used rabbit IgG isotype as negative control for background unspecific staining. Splenic macrophages clearly express ferroportin at the protein level, while TAMs are negative for ferroportin expression (Figure 5E). These data demonstrate for the first time that, although TAMs are M2-like, in this tumor model they don't express ferroportin and therefore may retain iron. Since CM increased the expression of *Cd163* we wondered if macrophages polarized by LLC cells would have an increased ability to take up RBC. We compared the uptake of RBC in BMDM either treated with CM from LLC or with DMEM (NT). BMDM polarized with CM were able to take up more RBC, as quantified by intracellular heme measurements (Figure 5F). In BMDM treated with LLC conditioned media (CM), *Cd163* mRNA expression is further increased in the presence of RBC, when compared to CM alone (Figure 5G), suggesting that the upregulation of *Cd163* is a consequence of iron loading or RBC ingestion. Treatment of BMDM in co-culture with LLC cells with aged RBC, heme or FeNTA, for 24h, was able to decrease CD206 (M2 marker) and increase CD14 (M1 marker) (Figure 5H and 5I), suggesting that products of RBC degradation and subsequent

iron loading of TAMs drive the polarization of TAMs towards a pro-inflammatory phenotype.

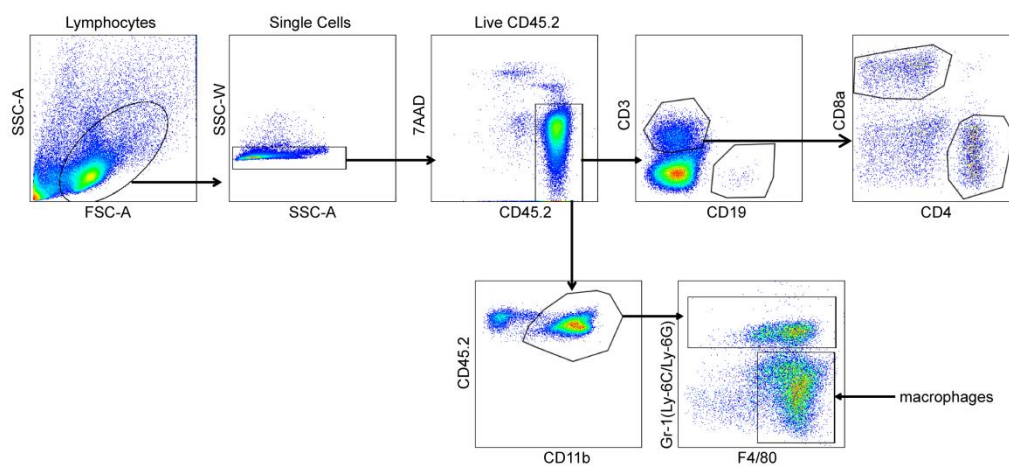


Figure 4. Gating strategy to select macrophages from LLC cell suspensions. Gating strategy used to select macrophages: after the selection of single live CD45.2 cells, the analysis of polarization markers was performed on CD11b⁺/Gr-1⁻/F4/80⁺ cells.

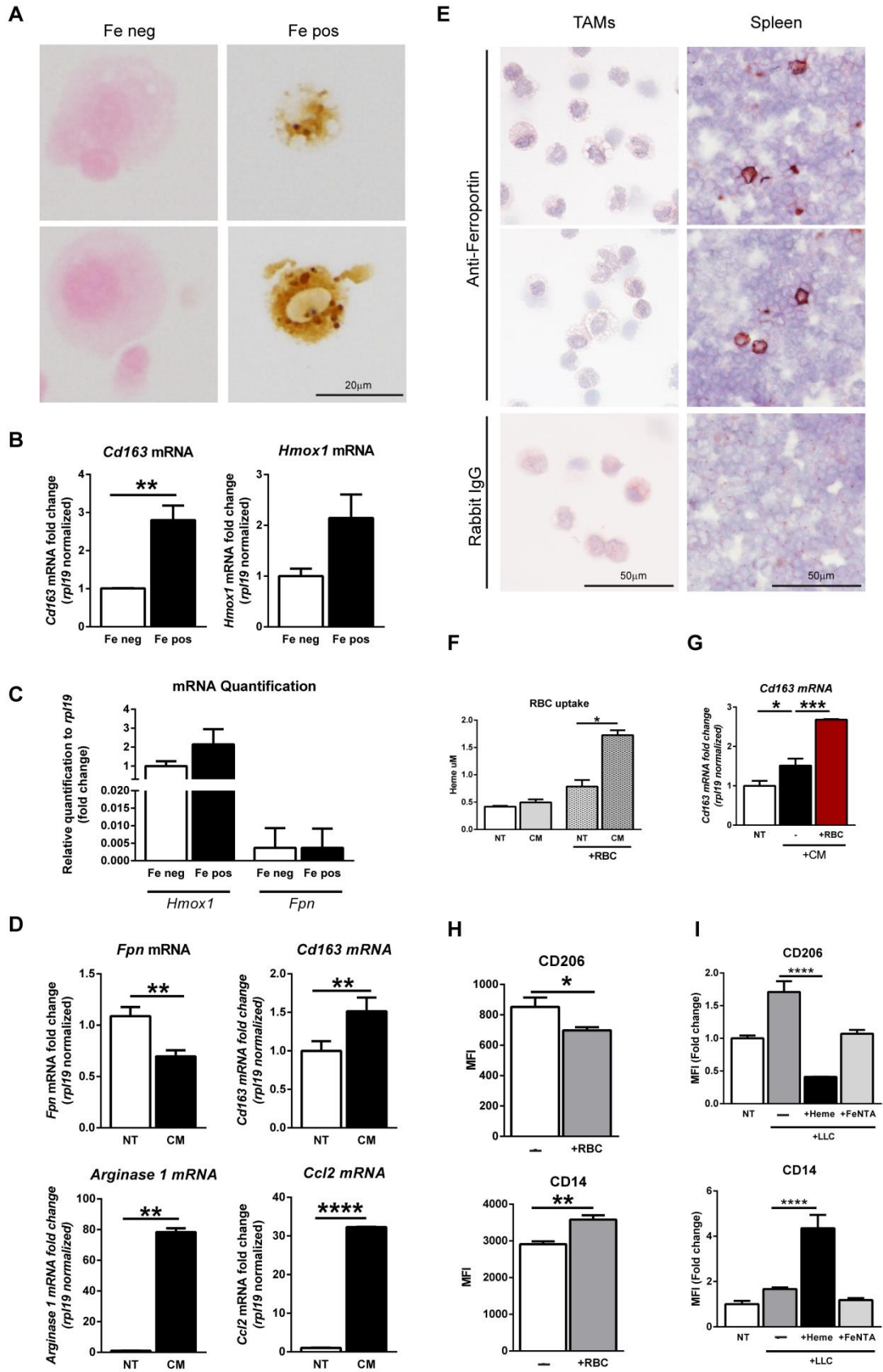
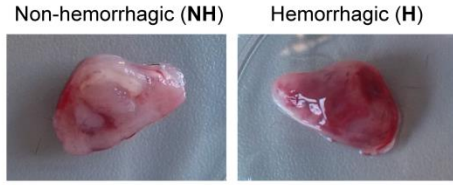


Figure 5. TAMs lack the expression of ferroportin. (A) Perls' staining with DAB enhancement of sorted TAMs ($CD11b^+/Gr1^-/F4/80^+$) after magnetic isolation. Two different populations were isolated: iron negative TAMs (Fe neg) and iron positive TAMs (Fe pos). TAMs were isolated from tumors 15 days after LLC injection. **(B)** *Cd163* and *Hmox1* mRNA expression in “Fe pos” and “Fe neg” TAMs determined by quantitative RT-PCR (n=3 independent experiments, each experiment with pooled TAMs from 8 mice sacrificed 15 days after LLC injection). *Cd163* and *Hmox1* mRNA levels were normalized to *Rpl19* mRNA levels. **(C)** Comparison of relative expression of *Hmox1* and *Fpn* in “Fe pos” and “Fe neg” TAMs determined by quantitative RT-PCR (n=3 independent experiments, each experiment with pooled TAMs from 8 mice sacrificed 15 days after LLC injection). *Hmox1* and *Fpn* mRNA levels were normalized to *Rpl19* mRNA levels. **(D)** mRNA expression of *Fpn*, *Cd163*, *Arginase 1* and *Ccl2* by quantitative RT-PCR of BMDM treated with control DMEM (NT) or treated with conditioned media from LLC cells (CM) for 24h. Results are expressed as fold change relative to control (NT). (n=9; results represent at least 3 independent experiments). *Fpn*, *Cd163*, *Arginase 1* and *Ccl2* mRNA levels were normalized to *Rpl19* mRNA levels. **(E)** Anti-ferroportin staining in cytopsin slides from sorted TAMs ($CD11b^+/Gr1^-/F4/80^+$) and cell suspension from spleen of WT mice without LLC injection (used as positive control). Bright red staining represents ferroportin expression. Rabbit IgG was used as isotype control. Stainings are representative of samples from 4 different mice. Tumors were removed 15 days after LLC injection. **(F)** Heme measurements in BMDM treated with control DMEM treated (NT) and treated with conditioned media from LLC cells after incubation with RBC for 12h (n=3). **(G)** *Cd163* mRNA expression by quantitative RT-PCR of BMDM treated with control DMEM (NT) or treated with conditioned media from LLC cells (CM), without (-) or with RBC (+RBC) for 24h. Results are expressed as fold change relative to control (NT). (n=9; results represent at least 3 independent experiments). *Cd163* mRNA levels were normalized to *Rpl19* mRNA levels. **(H)** Expression of CD206 and CD14 measured by flow cytometry in BMDM co-cultured with LLC cells, non-treated (-) or treated (+RBC) with aged RBC for 24h. Results are show as Mean Fluorescence Intensity (MFI) (n=6). **(I)** Expression of CD206 and CD14 measured by flow cytometry in BMDM alone (NT) or co-cultured with LLC cells, non-treated (-) or treated with 5 μ M heme (+Heme) or 100 μ M FeNTA (+FeNTA) for 12h (n=6). Results are shown as MFI fold change to NT control. Data are shown as mean \pm SEM. *p < 0.05, **p < 0.01, ***p < 0.001, and ****p < 0.0001.

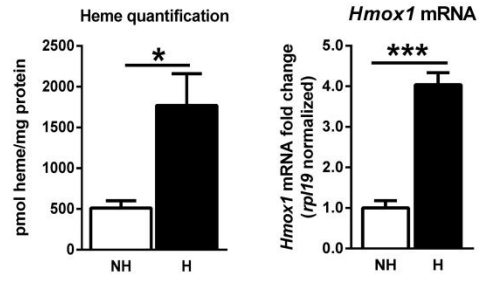
Hemorrhagic areas in LLC tumors show an increased inflammatory response and recruitment of myeloid cells

Iron loaded macrophages are located in hemorrhagic areas of the tumor. Thus, iron loading is likely to be a consequence of RBC uptake in the tumor microenvironment rather than of uptake of circulating iron. Heme is known to promote inflammation by activating macrophages, neutrophils and endothelial cells (36). We therefore dissected hemorrhagic areas (H) and non-hemorrhagic areas (NH) from the same tumor (Figure 6A) and quantified heme and *Hmox1* mRNA expression as a validation for the dissection. As expected heme and *Hmox1* levels are increased in hemorrhagic areas (Figure 6B). In terms of infiltrates, H and NH areas differed in the percentage of Gr-1⁺ cells (gated as CD11b⁺/Gr-1⁺) cells, while the percentage of TAMs (CD11b⁺/ Gr-1⁻/F4/80⁺) is not changed (Figure 6C). Gr-1 (Ly-6C/Ly-6G) is expressed in neutrophils and granulocytes and myeloid-derived suppressor cells (MDSCs). Since heme was shown to promote neutrophil recruitment by increasing *Cxcl1* (37, 38), we further analyze the expression of *Cxcl1* and *Cxcl2*, which are chemokines known for their neutrophil and myeloid cells chemoattractant activity. Both of these chemokines were increased in H areas when compared to NH areas (Figure 6D). *Csf1* and *Csf2* are macrophage differentiation factors and were also increased in H areas (Figure 6D). Since iron positive macrophages accumulate in areas of RBC extravasation we checked for the expression of *Cd163* and other macrophage markers. As expected, *Cd163* was increased in hemorrhagic areas. *Mmp9* which is produced by macrophages was also increased in hemorrhagic areas (Figure 6E). Next we evaluated the polarization of TAMs (CD11b⁺/ Gr-1⁻/F4/80⁺) (gating strategy represented in Figure 4) located in hemorrhagic areas. CD206 is mildly decreased whereas CD14 expression is increased. The mRNA expression of *Nos2* and the pro-fibrotic *Tgfβ* were also increased in hemorrhagic areas as well as *Il-1β* and *Il-6*. Altogether this data supports the evidence that RBC extravasation and breakage, as well as iron loading in macrophages, stimulate pro-inflammatory activity of macrophages and modulate inflammation in the tumor microenvironment.

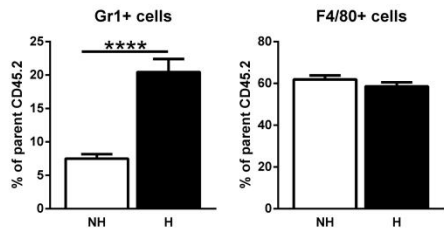
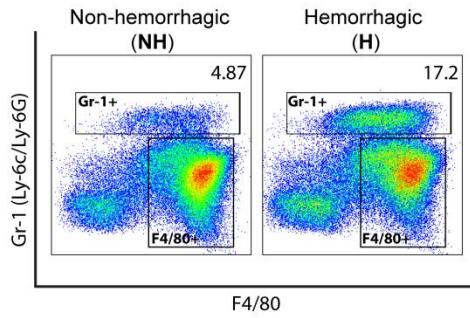
A



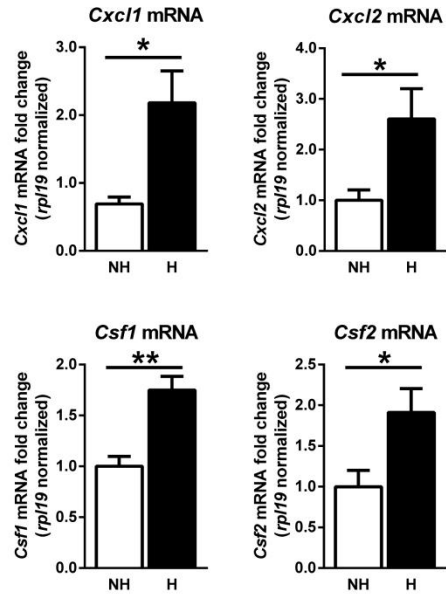
B



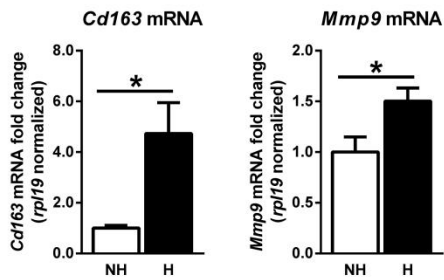
C



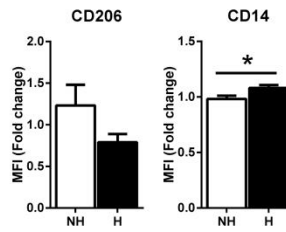
D



E



F



G

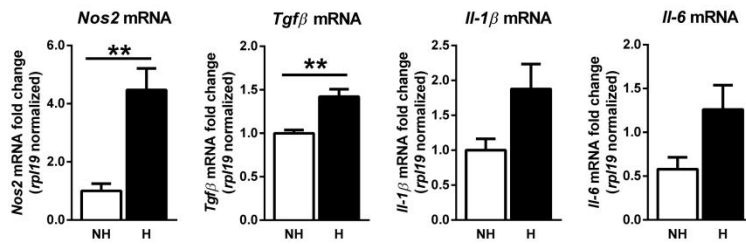


Figure 6. Hemorrhagic areas from LLC tumors show significantly increased inflammation markers. (A) Photograph of a LLC tumor removed from flank at day 15 after injection of LLC demonstrating the co-existence of non-hemorrhagic area (NH) and hemorrhagic area (H). (B) Heme quantification and *Hmox1* mRNA expression determined by quantitative RT-PCR in non-hemorrhagic (NH) and hemorrhagic areas (H) (n=6 tumors with respective NH and H areas, removed 15 days after injection). *Hmox1* mRNA levels were normalized to *Rpl19* mRNA levels. (C) Representative plots and quantification of Gr-1⁺ cells (gated as CD11b⁺/Gr1⁺) and F4/80⁺ cells (gated as CD11b⁺/Gr1⁻/F4/80⁺) in non-hemorrhagic (NH) and hemorrhagic areas (H) of LLC (n=6 tumors with respective NH and H areas, removed 15 days after injection). Results are expressed as percentage of cells inside CD45.2⁺ population. (D) mRNA expression of *Cxcl1*, *Cxcl2*, *Csf1* and *Csf2* determined by quantitative RT-PCR of total tumor mass of non-hemorrhagic (NH) and hemorrhagic areas (H) (n=6 tumors with respective NH and H areas, removed 15 days after injection). All mRNA levels were normalized to *Rpl19* mRNA levels. (E) mRNA expression of *Cd163* and *Mmp9* determined by quantitative RT-PCR of total tumor mass of non-hemorrhagic (NH) and hemorrhagic areas (H) (n=6 tumors with respective NH and H areas, removed 15 days after injection). All mRNA levels were normalized to *Rpl19* mRNA levels. (F) Expression of CD206 and CD14 measured by flow cytometry in F4/80⁺ cells from non-hemorrhagic (NH) and hemorrhagic areas (H). MFI is shown as fold change to NH. (n=6 tumors with respective NH and H areas, removed 15 days after injection). (G) mRNA expression of *Nos2*, *Tgfb*, *IL-1β* and *IL-6* determined by quantitative RT-PCR of total tumor mass of non-hemorrhagic (NH) and hemorrhagic areas (H) (n=6 tumors with respective NH and H areas, removed 15 days after injection). All mRNA levels were normalized to *Rpl19* mRNA levels. Data are shown as mean ± SEM. *p < 0.05, **p < 0.01, ***p < 0.001, and ****p < 0.0001.

Iron increases the inflammatory response in LLC tumor bearing mice

To better understand the impact of iron and iron-loaded macrophages in tumor progression we analyzed a mouse model with a point mutation (C236S) in ferroportin. This mutation causes ferroportin resistance to hepcidin-mediated degradation. As consequence serum iron levels are increased and splenic macrophages and Kupffer cells are iron depleted (31). Contrary to our expectations, we didn't observe a more pronounced tumor growth or a proliferative advantage of LLC injected in C326S mice when compared to WT mice (Figure 7A). Injected LLC cells respond to iron overload by downregulating *Tfr1* and upregulating *Fpn* and *HO-1* (Figure 7B), suggesting that iron supplies for tumor growth are not limiting in WT mice. We next explored the iron content and ferroportin expression in TAMs. Unexpectedly, TAMs from both WT and C326S mice can be iron loaded. As observed previously, iron loaded macrophages are surrounding areas of RBC extravasation (Figure 7C). We further observed a difference in macrophage

numbers, when we normalize the total number of macrophages per gram of tumor. We observed that C326S mice show a mildly increased number of TAMs compared to WT mice (Figure 7D). This is expected to be a consequence of increased CCL2 levels, a chemokine responsible for monocyte recruitment. CCL2 protein levels were increased in the serum of C326S mice, and at mRNA level in tumor lysates (Figure 7E). GM-CSF promotes the differentiation of monocytes. This cytokine was also increased in the serum and at mRNA level in tumor lysates (Figure 7F). We next sorted TAMs from WT and C326S mice ($CD11b^+/Gr1^-/F4/80^+$) and we showed that both are negative for anti-ferroportin immuno-staining, with the exception of few macrophages in the C326S mice (Figure 7G). Because in C326S mice ferroportin is resistant to hepcidin binding, this result demonstrates that the absence of ferroportin expression in TAMs is independent of hepcidin activity. This finding is consistent with the fact that hepatic hepcidin is unchanged in LLC-injected mice (Fig. 2F). In terms of polarization we observed a decrease in the expression of the mannose receptor CD206 (M2 marker) while, MHC II and CD86 (M1 markers) expression was not altered (Figure 7H). When compared to WT LLC-bearing mice, C326S LLC-bearing mice had increased circulating levels of IL-6, IL-1 β , TNF α and IL-10 (Figure 7I). Altogether this data points in the direction that excess of iron might have a pro-inflammatory effect in the tumor microenvironment, rather than promoting tumor growth.

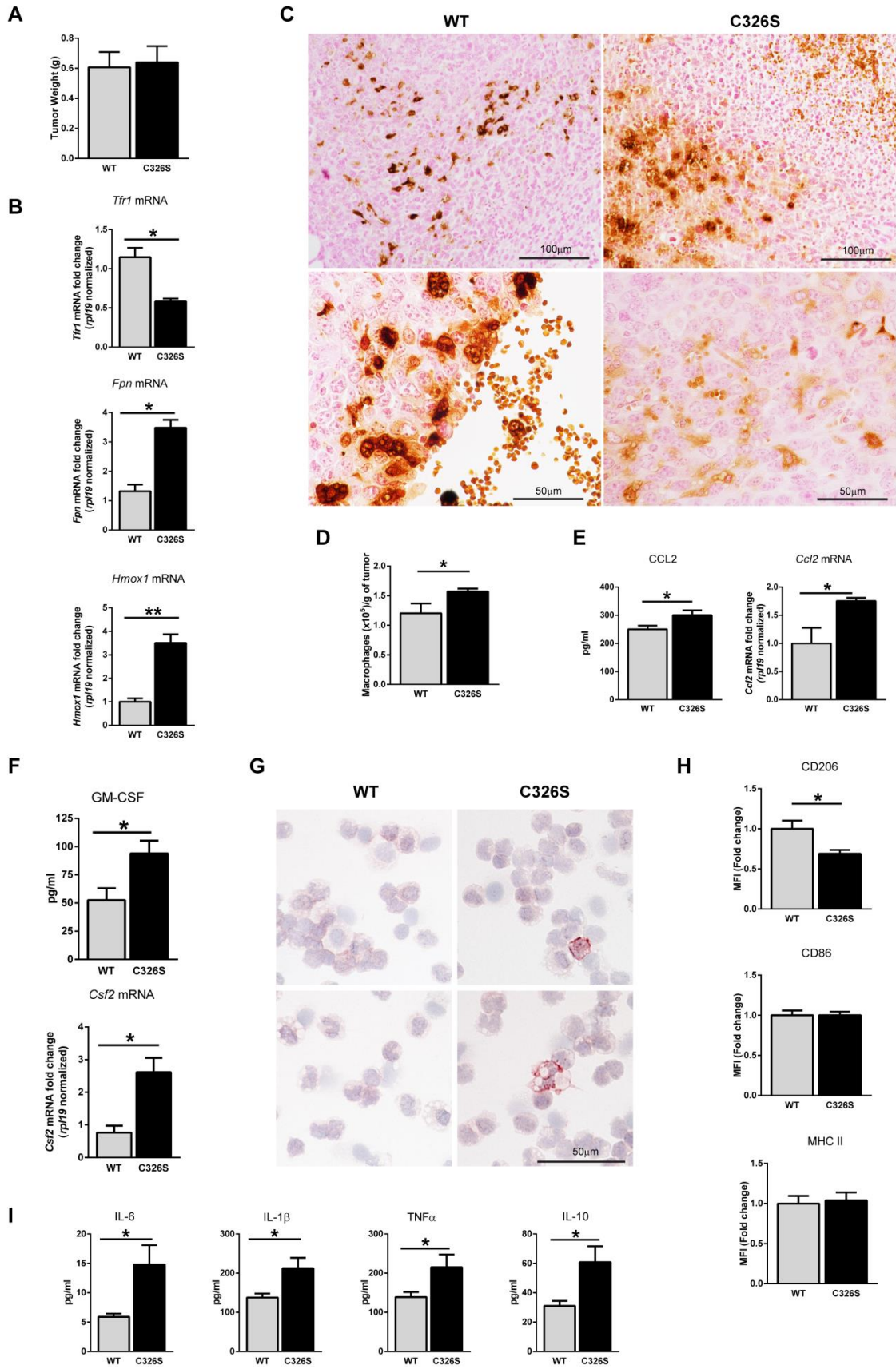


Figure 7. Iron overload increases CCL2 and macrophage numbers in LLC tumors. (A) Tumor weight analyzed in WT mice and C326S mice 15 days after subcutaneous injection of LLC (n=9 tumors per group). **(B)** *Tfr1*, *Fpn* and *Hmox1* mRNA expression in LLC tumors from WT mice and C326S mice 15 days after LLC injection (n=6 tumors per group) All mRNA levels were normalized to *Rpl19* mRNA levels. **(C)** Representative Perls' staining with DAB enhancement of subcutaneous LLC in WT mice and C326S mice (images are representative of n=6 tumors per group). Brown staining represents iron. **(D)** Number of macrophages per g of tumor in subcutaneous LLC in WT and C326S mice. The percentage of F4/80+ cells (gated CD11b⁺/Gr-1⁻/F4/80⁺) was normalized to total counts of CD45.2 cells and divided by tumor weight (g) (n=6 tumors per group). **(E)** Serum quantification of CCL2 and mRNA expression of *Ccl2* determined by quantitative RT-PCR of total tumor mass of WT and C326S mice (n=6 mice per group). *Ccl2* mRNA levels were normalized to *Rpl19* mRNA levels. **(F)** Serum quantification of GM-CSF and mRNA expression of *Csf2* determined by quantitative RT-PCR of total tumor mass of WT and C326S mice after 15 days of LLC injection (n=6). *Csf2* mRNA levels were normalized to *Rpl19* mRNA levels. **(G)** Anti-ferroportin staining in sorted TAMs (CD11b⁺/Gr-1⁻/F4/80⁺) from LLC tumors of WT and C326S mice. Red staining represents ferroportin expression. Images are representative of 4 different mice. **(H)** Expression of CD206, CD86 and MHC II measured by flow cytometry in F4/80+ cells (F4/80⁺: CD11b⁺/Gr-1⁻/F4/80⁺). Results are shown as MFI fold change to WT (n=9 tumors analyzed). **(I)** Serum quantification of IL-6, IL-1 β , TNF α and IL-10 in WT and C326S LLC-bearing mice after 15 days of LLC injection (n=6 mice per group). All samples were analyzed after 15 days of LLC injection. Data are shown as mean \pm SEM. *p < 0.05, **p < 0.01, ***p < 0.001, and ****p < 0.0001.

DISCUSSION

During the last decade, the role of the tumor microenvironment in cancer progression and therapy has been widely explored. Several studies unraveled the important role of immune cells in tumor progression (39-41). Macrophages were shown to be key players in the tumor microenvironment and in tumor-related inflammation (2, 42, 43).

The tumor microenvironment (TME) is hallmarked by a high complexity of different cell types, soluble factors and micronutrients. Macrophages and iron (in the form of transferrin bound iron, RBC and its degradation products, hemoglobin and heme) are part of the TME. Here, we dissected the role of iron in the tumor microenvironment. We hypothesized that iron in the tumor microenvironment may play an important role either for tumor cell proliferation or in the inflammatory response, especially by altering TAMs plasticity. Cancer related inflammation may further impact on systemic iron regulation, interconnecting iron and cancer (44). Here we show that TAMs of human non-small cell lung carcinoma (NSCLC) and experimental Lung Lewis Carcinoma (LLC) in mice can be separated into two different populations according to their iron content: iron loaded and

iron spared macrophages. Iron loaded TAMs are predominantly located in invasive areas of the tumor and near RBC leakage, suggesting that the most probable source of iron is derived from RBC that leak from fragile vessels into the tumor microenvironment. We show that iron loaded macrophages are hallmarked by the expression of CD163 and HO-1 (*Hmox1*), which are associated with hemoglobin uptake and iron recycling, respectively. In BMDM treated with LLC conditioned media (CM), *Cd163* mRNA expression is additionally increased in the presence of RBC, when compared to CM alone (Fig. S5), suggesting that the upregulation of *Cd163* is a consequence of iron loading or RBC ingestion. In hemorrhagic areas of the tumors where RBC and iron loaded TAMs accumulate, both *Hmox1* and *Cd163* mRNA levels are increased (Figure 5B and 5F).

TAMs from LLC are characterized by the absence or very low expression of ferroportin. We demonstrate that low ferroportin levels are not due to hepcidin mediated regulation (Figure 2F). We propose that downregulation of ferroportin may be a consequence of the differentiation of precursor cells (monocytes and myeloid-derived suppressor cells-MDSCs) into macrophages. Monocytes and myeloid cells recruited to the TME encounter in the tumor microenvironment cytokines and chemokines that trigger their differentiation. These cytokines may induce a macrophage phenotype that inhibits ferroportin expression. M-CSF (*Csf1*) and GM-CSF (*Csf2*) are factors that contribute to monocyte differentiation into macrophages and were also implicated in controlling ferroportin expression (45). Human monocytes differentiated with M-CSF expressed higher levels of ferroportin when compared with monocytes stimulated with GM-CSF (45). M-CSF and GM-CSF are both present in the microenvironment of LLC. In fact these cytokines are increased within hemorrhagic areas. In the case of GM-CSF, it is also increased in tumors and in the circulation of iron overloaded mice, when compared to WT mice. The expression of GM-CSF may explain the absence of ferroportin in macrophages, but further studies are required to understand the mechanism by which TAMs from LLC prevent ferroportin expression. LLC cells are able to polarize macrophages towards an M2 phenotype (46). In a different study, M2 macrophages were shown to express more ferroportin when compared to M1 macrophages (13). Our data provide evidence that LLC macrophages shown several features of the M2 phenotype, however, ferroportin is absent which is expected to cause an iron retention phenotype.

A recent study in breast cancer demonstrated that TAMs from breast cancer show an iron “donor” phenotype with increased expression of ferroportin, showing that the expression of proteins involved in iron metabolism in TAMs might be tissue-specific and strictly dependent on the niche (47).

Taken together, our data suggests that TAMs ingest and recycle RBC in the tumor microenvironment but they are unable to export recycled iron. Iron retention in

macrophages results in a shift in the polarization profile towards a more pro-inflammatory phenotype. TAMs from hemorrhagic areas decrease CD206 (M2 marker) and increase CD14 (M1 marker). IL-6 and IL-1 β are markers for the M1 polarization phenotype and are also increased in hemorrhagic areas. This is consistent with our previous finding that iron and heme stimulation of BMDM (M0, M1 and M2 polarized) triggers an M1-like polarization phenotype (17). Whether or not iron-controlled changes in TAMs affect tumor growth or metastasis is not yet clear.

Hemorrhagic areas show an enrichment of myeloid cells characterized as CD11b⁺/Gr-1⁺ cells. Myeloid cells can act as precursor for macrophages, and may be further differentiated in the tumor microenvironment (48). CD11b⁺/Gr-1⁺ cells are very abundant in the LLC tumor model. Previous studies demonstrated that LLC tumor bearing mice show increased hematopoiesis and an increase in the proportion of monocytes in the peripheral blood, spleen, and bone marrow (49). The increase CD11b⁺/Gr-1⁺ cells in hemorrhagic areas may be just a consequence of extravasation of circulating cells into the tumor microenvironment due to vessel damage. Elevated CD11b⁺/Gr-1⁺ myeloid cells are associated with impaired immune reactivity and increased tumor progression (50-52). CD11b⁺/Gr-1⁺ cells secrete pro-angiogenic factors such as matrix metalloproteinases 9 (MMP9) and iNOS. They are able to differentiate into endothelium-like cells or other vascular cells (53-55). Consistent with these findings we observe an increase in MMP9 and iNOS (*Nos2*) mRNA expression in hemorrhagic areas. We also observed an increased expression of Cxcl1 and Cxcl2, which might be produced by these cells and act as chemoattractant factors to myeloid cells, neutrophils and macrophages. Vessel damage and accumulation of CD11b⁺/Gr-1⁺ cells and RBC alter the tumor microenvironment composition and may have consequences in the immune response.

Here we show that serum iron levels in WT LLC-bearing mice are decreased, probably due to tumor cell proliferation. LLC tumors that develop in iron overload conditions (C326S mice) didn't show an increased or faster proliferation and tumor size. In fact, mRNA expression of total tumor mass suggests that LLC cells downregulate TfR1 to decrease iron uptake and upregulate Ferroportin to increase iron export. Cancer cells are negative for iron staining, suggesting these cells do not accumulate excessive amounts of iron. This may be explained by iron toxicity. Iron dependent -ROS generation can be toxic to cancer cells (56) which explains why cancer cells control cellular iron levels. We conclude that iron in the TME may be more important for the modulation of the inflammatory response, rather than for tumor growth. Since macrophages are key players in iron homeostasis, the increase in CCL2 levels and consequent increase in macrophage numbers in response to iron overload, may be explained as an attempt to prevent iron toxicity.

Although the concept M1/M2 has been used to classify macrophages (57), it seems that the picture is far more complex than this. *In vivo*, macrophages can be exposed to several and diverse stimuli and express both M1 and M2 markers. Several studies have revised the concept of macrophage polarization introducing new nomenclatures and categories (58-61). Here we identified a subpopulation of TAMs, of which the phenotype is directly related to iron loading and that may have functional implication in the modulation of the immune response in tumors. We propose a model in which hemorrhagic areas in the tumor microenvironment are characterized by an increase in CD11b⁺/Gr-1⁺ cells, iron loaded macrophages and myeloid-cell attractant chemokines. Iron loading in macrophages, due to RBC and heme uptake, alters macrophage polarization and may contribute to changes in cancer related inflammation (Figure 8). We show for the first time that RBC, due to their iron component may play a role in sterile inflammation in the tumor microenvironment.

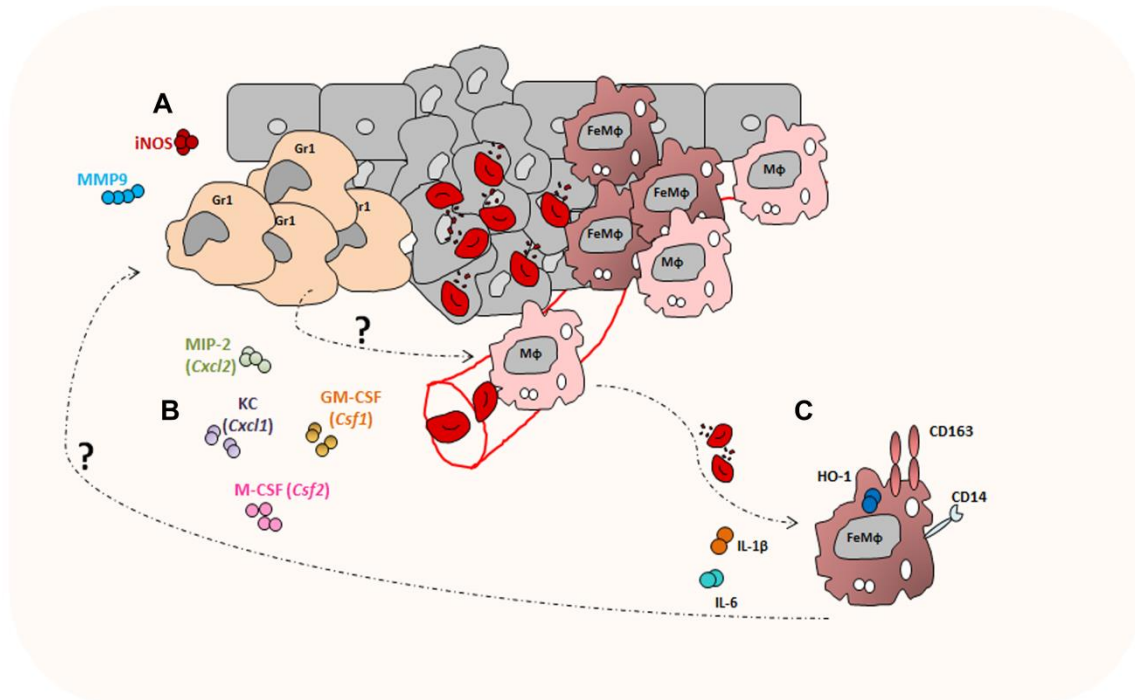


Figure 8. Hemorrhagic areas as a “new niche” within the tumor microenvironment (A) RBC and CD11b⁺/Gr-1⁺ cells extravasate from vessels into the tumor microenvironment. CD11b⁺/Gr-1⁺ cells secrete pro-angiogenic factors such as MMP9 and iNOS. **(B)** Hemorrhagic areas are hallmarked by increased chemokine levels that facilitate recruitment and differentiation of myeloid cells. **(C)** Macrophages (MΦ) take up RBC and respective degradation products (hemoglobin and heme), present in the tumor microenvironment and retain the iron (FeMΦ). Iron retention changes the phenotype of macrophages and induces the expression of CD163, HO-1, CD14 and possibly IL-6 and IL-1β. The consequences of the phenotypic changes in TAMs in response to iron accumulation for the tumor microenvironment require further investigations.

MATERIAL AND METHODS

Human samples for histology

Tissue samples (slides for histology staining) from 19 different patients were provided by Lung Biobank Heidelberg a member of the Biomaterial bank Heidelberg (BMBH) and the Biobank platform of the German Center for Lung Research (DZL) with ethics approval number of 270/2001. Table 1 summarizes the information of this cohort of patients grouped by iron content. Histology slides positive for Perls' staining (=blue) were considered as "iron positive" while the slides negative for Perls' staining were considered as "iron negative".

Tissue-micro arrays (TMAs) were provided by the tissue bank of the National Center for Tumor Diseases (NCT, Heidelberg, Germany) in accordance with the regulations of the tissue bank and the approval of the ethics committee of Heidelberg University. A total of 116 patients of non-small lung carcinoma were analyzed regarding iron content. From each patient, three areas of the original histology block were represented: normal lung, tumor center and invasive front. The classification of the TMA was performed according to the 6th edition of the Tumor Node Metastasis (TMN) staging system for non-small cell lung carcinoma. From the 122 patients, 38 stained positively for iron at least in tumor center and/or invasive front. Table 3 summarizes the information about this cohort of patients, separated in two groups: iron positive and iron negative. Quantification of iron staining was performed using the Image Pro-Premier 3D software. The software calculated the area of pixels corresponding to blue staining (iron staining).

Preparation of single cell suspensions from fresh human lung adenocarcinoma

Tumors were obtained in collaboration with Thoraxklinik Heidelberg. Table 2 summarizes the patient data. Fresh tumors were mechanically dissociated with tweezers and scalpel and digested with 5mg/tumor of DNase (SIGMA) and Hyaluronidase (SIGMA) in 10ml PBS/tumor for 30 min in a 37°C shaking water-bath. After enzymatic digestion, tumor suspension was strained using a 70µm cell strainer (Becton Dickinson) and washed with PBS. For the isolation of lymphocytes cell suspensions were layered over a density gradient solution (Biocoll Separating Solution, 1.077g/ml, Biochrom AG, Germany) in a 1:1 volume ratio and centrifuged at 450g for 30 min without brake, at room temperature. Afterwards, leukocyte layers were carefully collected and washed twice with PBS at 1500 rpm for 10min at 4°C and further resuspended in 5mls of cold PBS. Cells were further processed for magnetic isolation (see "Magnetic isolation" description in Material and Methods).

Cell culture

LLC cells were grown at 37 °C in a humidified atmosphere of 5% CO₂/95% air in DMEM medium supplemented with 10% heat-inactivated fetal bovine serum and 1% penicillin/streptomycin (Sigma) under sterile tissue culture conditions.

Mice and tumor model

Females and males, 8- to 10- weeks, C57BL/6N and C326S.Fpn mice were used. All mice experiments were performed under the guidelines of IBF/DKFZ with the project number G-267/12, all experiments were approved by “Regierungspräsidium Karlsruhe”. LLC cells were detached with trypsin-EDTA (Sigma) washed twice in PBS at room temperature, passed through a 40µm cell strainer, counted and injected (1×10^6 in 100µl PBS) subcutaneously into the flanks of mice or intravenously (1×10^5 in 100µl PBS). Mice were sacrificed after 15 days of injection to obtain maximum tumor growth within the ethical guidelines. Mice that developed ulcers or necrotic tumors were sacrificed and not considered for the experiments. Blood was removed directly from the heart by cardiac puncture. Lung tumor that formed as a result of iv injection of LLC cells were only analyzed for histology. Subcutaneous tumors were resected and dissected very carefully to avoid tissue damage and micro-bleedings induced during animal preparation. Tumors were transferred to 5 ml PBS on ice and tumor weight (g) was measured on a scale by transferring the specimen to a sterile Petri dish after removal the excess of PBS with paper towel. When indicated, hemorrhagic areas (H) were separated from non-hemorrhagic areas (NH) according to the color exhibited in the tumor mass (H-red, NH-white), otherwise, total tumors were processed. Resected tumors were then processed for cytospin, FACS analysis and FACS sorting, snap frozen until further analysis or fixed in formalin for immunohistochemistry and histological analysis.

Preparation of single cell suspensions from mouse tumors

After resection, tumors were mechanically dissociated with tweezers and scalpel and digested with 5mg/tumor of DNase (SIGMA) and Hyaluronidase (SIGMA) in 10ml PBS/tumor for 30 min in a 37°C shaking water-bath. After enzymatic digestion, tumor suspension was strained using a 70µm cell strainer (Becton Dickinson), washed with cold PBS and centrifuged at 1500 r.p.m. at 4 °C. Red blood cells, dead cells and tumor cells were removed by gradient purification using a Lympholyte solution (Cederlane). Briefly, 7mls of tumor suspension were added on top of 7mls of Lympholyte solution and centrifuged at 1500xG at 20°C for 25 minutes without break. The ring of live cells (CD45+ cells) was removed together with the upper part and washed again in cold PBS. Cell pellet

was resuspended in FACS buffer (1% FBS, 0.01% sodium azide in PBS) and kept on ice for the respective procedures.

Magnetic isolation

Cell suspensions were resuspended in 5mls of PBS and pass through a LS column (Miltenyi Biotech) attached to a magnetic board. Columns were washed 3 times with 5mls of PBS. Cells that were adherent to the column (iron positive – magnetic fraction) were flushed with 5mls PBS. Both magnetic fraction and flow through were washed with cold PBS (1500r.p.m. 10min 4°C), resuspended in PBS and centrifuged for cytopsin preparations.

Flow cytometry

Cells were resuspended in 100µl of supernatant from 2.42G cells and placed at 4°C for 15 min to block non-specific FC receptor binding. Cells were then washed with FACS buffer and afterwards incubated with fluorescently labeled antibodies (antibodies used are listed in Table 4) at 4°C in the dark for 30 min and then washed with FACS buffer, resuspended in 200µl FACS buffer, and evaluated on a FACSAria II (Becton Dickinson) flow cytometer. Cell death was determined using 7AAD (BioLegend). Data were further analyzed using FlowJo software (Tree Star).

Table 4. Antibodies used for Flow cytometry (anti-mouse)

Antibody	Fluorophore	Clone	Isotype	Manufacturer
F4/80	APC	BM8	Rat IgG2a, κ	BioLegend
CD11b	APC-Cy7	M1/70	Rat IgG2b, κ	BD Pharmingen
	FITC	M1/70		BDPHarmingen
	Horizon V500	M1/70		BD Horizon
GR1	AlexaFluor 700	RB6-8C5	Rat IgG2b, κ	BioLegend
CD3	FITC	17A2	Rat IgG2b, κ	BioLegend
CD19	PE	6D5	Rat IgG2a, κ	BioLegend
CD4	PE-Cy7	RM4-5	Rat IgG2a, κ	BioLegend
CD8a	APC	53-6.7	Rat IgG2a, κ	BioLegend
CD206	FITC	MR5D3	Rat IgG2a, κ	BioLegend
CD86	PE	GL-1	Rat IgG2a, κ	BioLegend
MHC II	PE-Cy7	M5/114.15.2	Rat IgG2b, κ	BioLegend
CD14	APC-Cy7	Sa14-2	Rat IgG2a, κ	BioLegend
CD45.2	Pacific Blue	104	Mouse (SJL) IgG2a, κ	BioLegend

Tissue iron measurements

Serum iron concentration was assessed using the SFBC kit (Biolabo). Tissue non-heme iron content was measured using the bathophenanthroline method and calculated against dry weight tissue (62).

Histological characterization of cytopsin slides

Single cell suspension (200µl) was transferred to Cytospin funnels and centrifuged in a Cytospin Cyto centrifuge (Thermo Scientific) at 500 r.p.m. for 5 min. Iron staining was performed using Accustain Iron Stain No. HT20 (Sigma-Aldrich) following manufacturer's instructions. When indicated, Perls' blue staining was further enhanced using the DAB peroxidase substrate kit SK-4100 (Vector Labs). For immunostaining, cytopsin samples were fixed and permeabilized in ice cold acetone for 5 minutes, washed in PBS and treated with H₂O₂ to block endogenous peroxidase. Immunostaining was performed according to the instructions of the Vectastain ABC mouse, rat and rabbit kits (Vector Labs). Anti-mouse ferroportin staining was performed using MTP11-A rabbit polyclonal antibody (Anti-Mouse Metal Transporter Protein1/Ferroportin (MTP1/IREG1/Fpn) from Alpha Diagnostics); rabbit IgG was used as isotype control for the ferroportin staining. Anti-human CD68 staining was performed using Monoclonal Mouse Anti-Human PG-M1 clone (DAKO). Tissue slides were developed using the Vector AEC substrate (Vector Labs), rinsed with distilled water, counterstained with hematoxylin, washed in PBS, and mounted using the VectaMount AQ mounting medium (Vector Labs). Images were acquired with a Ni-E Nikon microscope.

Histology and Immunohistochemistry analysis

Tissues obtained from mice (tumors and other organs) were fixed for 24h in 10% neutral buffered formalin (Sigma-Aldrich), dehydrated, and paraffin embedded. Tissue sections (5µm) were attached to Polysine slides (Thermo Scientific), dewaxed and rehydrated. Iron staining was performed using Accustain Iron Stain No. HT20 (Sigma-Aldrich) following manufacturer's instructions. When indicated, the Perls' blue staining was further enhanced using the DAB peroxidase substrate kit SK-4100 (Vector Labs). For Hematoxylin & Eosin staining, sections were stained in Weigert's hematoxylin (Sigma-Aldrich), followed by Eosin (Sigma-Aldrich), dehydrated and mounted. For immunohistochemistry, sections were treated for 10 min with 3% H₂O₂ (Sigma-Aldrich) to block the endogenous peroxidases. Tissue slides were subjected to microwave-mediated antigen retrieval using the Citraplus reagent (Biogenex). Immunostaining was performed using the Vectastain ABC mouse, rat and rabbit kits (Vector Labs) following

manufacturer's instructions. Anti-mouse ferroportin staining was performed using MTP11-A rabbit polyclonal antibody (Anti-Mouse Metal Transporter Protein1/Ferroportin (MTP1/IREG1/Fpn) from Alpha Diagnostics) and anti-human CD68 staining was performed using Monoclonal Mouse Anti-Human PG-M1 clone (DAKO). Tissue slides were developed using the Vector AEC substrate (Vector Labs), rinsed with distilled water, counterstained with Weigert's hematoxylin (Sigma-Aldrich), washed in PBS, and mounted using the VectaMount AQ mounting medium (Vector Labs).

Preparation of BMDM

Bone marrow cells were flushed from tibia and femur using ice-cold HBSS and filtered through a 70 μ m cell strainer. Cells were seeded at a density of 350,000 cells/cm² in RPMI1640-Glutamax medium (Life Technologies) supplemented with 10% of heat-inactivated FBS (Thermo Scientific), 1% penicillin/streptomycin (Sigma-Aldrich), and 10 ng/ml M-CSF (Sigma-Aldrich). After 4 days, non-adherent cells were removed by HBSS washing, and the medium was replaced daily until cell harvesting (typically 6–7 days after seeding). For each independent experiment, BMDM were prepared from three different mice.

Red Blood Cell preparation

Red Blood Cell aging was performed as described (63). Mice blood was collected on ethylenediaminetetraacetic acid (EDTA). After 3 washes with phosphate buffer saline (PBS), mouse red blood cells (RBC) were resuspended in Hepes buffer (10 mM Hepes, 140 mM NaCl, BSA 0.1%, pH 7.4). For *in vitro* RBC ageing, cells (1x10⁸ cells/ml in Hepes buffer) were incubated overnight at 30°C with 2,5 mM calcium and 0,5 mM of the ionophore A23187 (Calbiochem). Treated RBC were then centrifuged (1500 rpm 5 min), washed twice with PBS and resuspended in RPMI medium (2x10⁷cells/ml).

BMDM treatment and co-cultures

LLC cells were plated at 1x10⁴/ml of complete DMEM (10%FBS, 1%PenStrep) and conditioned media (CM) was collected when LLC cells were about 80% confluent. CM was passed through a 0.22 μ m filter and stored at -20°C until further use. BMDM were treated with 50% RPMI with 10ng/ml M-CSF (SIGMA) and either 50% complete DMEM (NT, control) or 50% CM of LLC for 24h. For co-culture experiments, LLC cells were seeded in a transwell filter of 0.4 μ m (BD Falcon) and placed in co-culture with BMDM for 48h. After 48h incubation, BMDM were treated with heme bound to BSA (5 μ M), FeNTA (100 μ M) for 12h or aged RBC. RBC were seeded at 2x10⁷/ml (3mls in a 6 well plate and 1ml in 24 well plates) for 12h or 24h.

RNA isolation and qRT-PCR analysis

Total tissue RNA was isolated using TRIzol (Life Technologies), RNA from cells was extracted using the RNeasy Mini Kit (Qiagen) or Arcturus Picopure RNA Isolation Kit, (Applied Biosystems). 0.5µg to 1µg of total RNA was reverse transcribed by using RevertAid H Minus reverse transcriptase (Thermo Scientific), random primers (Invitrogen) and dNTPs (Thermo Scientific). Quantitative RT-PCR was performed using SYBR green on a Step One Plus Real Time PCR System (Applied Biosystems, California, USA). The primers used are listed in Table 5. Differences in relative quantification are shown as fold-change compared to the control condition. Ribosomal protein L19 (RPL19) was used to normalize cDNA levels.

Table 5. Primers for quantitative RT-PCR (*mus musculus*)

Gene	Sequence
<i>Rpl19</i>	Forward 5' AGGCATATGGGCATAGGGAAGAG 3' Reverse 5' TTGACCTTCAGGTACAGGCTGTG 3'
<i>Hamp1</i>	Forward 5'CCTATCTCCATCAACAGAT 3' Reverse 5'TGCAACAGATAACCACACTG 3'
<i>Cd163</i>	Forward 5' TCTCAGTGCCTCTGCTGTCA 3' Reverse 5' CGCCAGTCTCAGTTCCTTCT 3'
<i>Hmox1</i>	Forward 5' AGGCTAAGACCGCCTTCCT 3' Reverse 5' TGTGTTCTCTGTCAGCATCA 3'
<i>Fpn</i>	Forward 5' TGTCAGCCTGCTGTTTGCAGGA 3' Reverse 5' TCTTGCAGCAACTGTGTCACCG 3'
<i>Arginase 1</i>	Forward 5' AATCTGCATGGGCAACCTGT 3' Reverse 5' GTCTACGTCTCGCAAGCCAA 3'
<i>Ccl2</i>	Forward 5' CATCCACGTGTTGGCTCA 3' Reverse 5' GATCATCTTGCTGGTGAATGAGT 3'
<i>Cxcl1</i>	Forward 5'AGACTCCAGCCACACTCCAA 3' Reverse 5' TGACAGCGCAGCTCATTG 3'
<i>Cxcl2</i>	Forward 5'AAAATCATCCAAAAGATACTGAACAA 3' Reverse 5'CTTTGGTTCTTCCGTTGAGG 3'
<i>Csf1</i>	Forward 5' GGTGGAAGTCCAGTATAGAAAG 3' Reverse 5' TCCCATATGTCTCCTTCCATAAA 3'
<i>Csf2</i>	Forward 5' GCATGTAGAGGCCATCAAAGA 3' Reverse 5' CGGGTCTGCACACATGTTA 3'
<i>Mmp9</i>	Forward 5' GCCGACTTTTGTGGTCTTCC 3' Reverse 5' GGTACAAGTATGCCTCTGCCA 3'
<i>Nos2</i>	Forward 5' TGGAGACTGTCCAGCAATG 3' Reverse 5' CAAGGCCAAACACAGCATACC 3'

<i>Tgfβ</i>	Forward 5' TGGAGCAACATGTGGA ACTC 3' Reverse 5' CAGCAGCCGGTTACCAAG 3'
<i>Il-1β</i>	Forward 5' GCAACTGTTCTGAACTCAACT 3' Reverse 5' ATCTTTTGGGGTCCGTCAACT 3'
<i>Il-6</i>	Forward 5' GCTACCAA ACTGGATATAATCAGGA 3' Reverse 5' CCAGGTAGCTATGGTACTCCAGAA3'
<i>Tfr1</i>	Forward 5' CCCATGACGTTGAATTGAACCT 3' Reverse 5' GTAGTCTCCACGAGCGGAATA 3'

Heme measurements in BMDM

BMDM incubated with aged RBC were washed 3x with HBSS, detach with StemPro® Accutase® (Gibco), counted, centrifuged and the pellet was then solubilized by adding 500µl of concentrated formic acid. The heme concentration of the formic acid solution was determined spectrophotometrically (SpectraMax, Molecular Devices) at 400 nm and normalized to the number of cells.

Protein quantification and Tissue heme measurements

Protein lysates were obtained by homogenizing snap-frozen tissues or cell suspension in RIPA buffer supplemented with protease inhibitors (Roche). Protein concentration was determined using the DC protein assay ((Bio-Rad). Protein samples (10µg) were incubated with 0.5 ml of 2 M Oxalic Acid (Sigma-Aldrich) at 95°C for 30 min. Samples were subsequently centrifuged at 14000 rpm for 5 min. Fluorescence emission in the supernatant was determined in a spectrofluorimeter (SpectraMax, Molecular Devices). Excitation and emission wavelengths were set at 405 and 662 nm, respectively. The background was evaluated by measuring fluorescence in non-boiled samples.

Measurement of cytokines

Cytokine protein levels were determined in the serum of mice applying Multiplex bead-array based technology. Measurements were performed on a BioPlex200 System using the Bio-Plex Pro Cytokine Reagent Kit and Bio-Plex Pro Mouse Cytokine sets (Bio-Rad) according to manufacturer's instructions. Cytokine protein levels are given as picogram/ml of serum.

Statistical analysis

Data are shown as mean ± SEM, and the number of mice (n) is indicated. Statistical analyses were performed using Prism v.6 (GraphPad). Comparisons between two groups were performed with two-sided Welch t-tests, and among three or more than three groups

with one- or two-way ANOVA, respectively, followed by Bonferroni post-test. * $p < 0.05$, ** $p < 0.01$, *** $p < 0.001$, and **** $p < 0.0001$ are indicated.

Acknowledgments: We thank NCT Nationales Centrum für Tumorerkrankungen Heidelberg (NCT) and Dr. Arne Warth (NCT-Heidelberg) for providing Tissue Micro-Arrays (TMAs) from lung cancer patients; Liz Meister (Thoraxklinik at University Hospital Heidelberg) for helping with the procedures to isolate cells from human tumors; Dr. Margareta Müller and Dr. Sabine Hensler (Furtwangen University, Furtwangen) for sharing the knowledge with co-culture experiments. We specially thank Maria de Sousa for critical reading and advice. **Funding:** This work was supported by Fundação para a Ciência e Tecnologia by means of a PhD fellowship SFRH/BD/51290/2010 awarded to M.C.d.S.; “Stiftungen und Preise 2012” awarded by faculty of Medicine, Heidelberg and Deutsches Zentrum für Lungenforschung (DZL) with the reference TP CF-1.1. **Author contributions:** M.C.d.S. designed the project, performed the experiments, and wrote the manuscript; M.P.C. and A.S. helped with some experiments; M.M. and T.M. provided human histology slides and patient data; A.C. and M.U.M. supervised the project. **Competing interests:** The authors declare that they have no competing interests.

REFERENCES

1. D. Hanahan, R. A. Weinberg, Hallmarks of cancer: the next generation. *Cell* **144**, 646-674 (2011).
2. G. Solinas, G. Germano, A. Mantovani, P. Allavena, Tumor-associated macrophages (TAM) as major players of the cancer-related inflammation. *J Leukoc Biol* **86**, 1065-1073 (2009).
3. A. Sica, A. Mantovani, Macrophage plasticity and polarization: in vivo veritas. *The Journal of clinical investigation* **122**, 787-795 (2012).
4. M. P. Soares, I. Hamza, Macrophages and Iron Metabolism. *Immunity* **44**, 492-504 (2016).
5. T. A. Wynn, A. Chawla, J. W. Pollard, Macrophage biology in development, homeostasis and disease. *Nature* **496**, 445-455 (2013).
6. C. D. Mills, Anatomy of a discovery: m1 and m2 macrophages. *Frontiers in immunology* **6**, 212 (2015).
7. C. D. Mills, K. Kincaid, J. M. Alt, M. J. Heilman, A. M. Hill, M-1/M-2 macrophages and the Th1/Th2 paradigm. *J Immunol* **164**, 6166-6173 (2000).
8. S. Gordon, Alternative activation of macrophages. *Nat Rev Immunol* **3**, 23-35 (2003).
9. G. B. Mackaness, Cellular resistance to infection. *J Exp Med* **116**, 381-406 (1962).
10. A. Sica, P. Larghi, A. Mancino, L. Rubino, C. Porta, M. G. Totaro, M. Rimoldi, S. K. Biswas, P. Allavena, A. Mantovani, Macrophage polarization in tumour progression. *Seminars in cancer biology* **18**, 349-355 (2008).
11. A. Mantovani, S. Sozzani, M. Locati, P. Allavena, A. Sica, Macrophage polarization: tumor-associated macrophages as a paradigm for polarized M2 mononuclear phagocytes. *Trends Immunol* **23**, 549-555 (2002).

12. J. W. Pollard, Tumour-educated macrophages promote tumour progression and metastasis. *Nat Rev Cancer* **4**, 71-78 (2004).
13. S. Recalcati, M. Locati, A. Marini, P. Santambrogio, F. Zaninotto, M. De Pizzol, L. Zammataro, D. Girelli, G. Cairo, Differential regulation of iron homeostasis during human macrophage polarized activation. *Eur J Immunol* **40**, 824-835 (2010).
14. S. V. Torti, F. M. Torti, Iron and cancer: more ore to be mined. *Nat Rev Cancer* **13**, 342-355 (2013).
15. M. F. Macedo, M. de Sousa, Transferrin and the transferrin receptor: of magic bullets and other concerns. *Inflammation & allergy drug targets* **7**, 41-52 (2008).
16. T. Korolnek, I. Hamza, Macrophages and iron trafficking at the birth and death of red cells. *Blood* **125**, 2893-2897 (2015).
17. F. Vinchi, M. Costa da Silva, G. Ingoglia, S. Petrillo, N. Brinkman, A. Zuercher, A. Cerwenka, E. Tolosano, M. U. Muckenthaler, Hemopexin therapy reverts heme-induced proinflammatory phenotypic switching of macrophages in a mouse model of sickle cell disease. *Blood* **127**, 473-486 (2016).
18. A. Sindrilaru, T. Peters, S. Wieschalka, C. Baican, A. Baican, H. Peter, A. Hainzl, S. Schatz, Y. Qi, A. Schlecht, J. M. Weiss, M. Wlaschek, C. Sunderkotter, K. Scharffetter-Kochanek, An unrestrained proinflammatory M1 macrophage population induced by iron impairs wound healing in humans and mice. *The Journal of clinical investigation* **121**, 985-997 (2011).
19. A. Kroner, A. D. Greenhalgh, J. G. Zarruk, R. Passos Dos Santos, M. Gaestel, S. David, TNF and increased intracellular iron alter macrophage polarization to a detrimental M1 phenotype in the injured spinal cord. *Neuron* **83**, 1098-1116 (2014).
20. H. Ludwig, S. Van Belle, P. Barrett-Lee, G. Birgegard, C. Bokemeyer, P. Gascon, P. Kosmidis, M. Krzakowski, J. Nortier, P. Olmi, M. Schneider, D. Schrijvers, The European Cancer Anaemia Survey (ECAS): a large, multinational, prospective survey defining the prevalence, incidence, and treatment of anaemia in cancer patients. *Eur J Cancer* **40**, 2293-2306 (2004).
21. E. Nemeth, S. Rivera, V. Gabayan, C. Keller, S. Taudorf, B. K. Pedersen, T. Ganz, IL-6 mediates hypoferremia of inflammation by inducing the synthesis of the iron regulatory hormone hepcidin. *The Journal of clinical investigation* **113**, 1271-1276 (2004).
22. P. Lee, H. Peng, T. Gelbart, L. Wang, E. Beutler, Regulation of hepcidin transcription by interleukin-1 and interleukin-6. *Proceedings of the National Academy of Sciences of the United States of America* **102**, 1906-1910 (2005).
23. S. Rivera, L. Liu, E. Nemeth, V. Gabayan, O. E. Sorensen, T. Ganz, Hepcidin excess induces the sequestration of iron and exacerbates tumor-associated anemia. *Blood* **105**, 1797-1802 (2005).
24. A. B. Thompson, T. Bohling, A. Heires, J. Linder, S. I. Rennard, Lower respiratory tract iron burden is increased in association with cigarette smoking. *The Journal of laboratory and clinical medicine* **117**, 493-499 (1991).
25. L. J. Wesselius, M. E. Nelson, B. S. Skikne, Increased release of ferritin and iron by iron-loaded alveolar macrophages in cigarette smokers. *American journal of respiratory and critical care medicine* **150**, 690-695 (1994).
26. A. Kellar, C. Egan, D. Morris, Preclinical Murine Models for Lung Cancer: Clinical Trial Applications. *BioMed research international* **2015**, 621324 (2015).
27. X. B. Liu, N. B. Nguyen, K. D. Marquess, F. Yang, D. J. Haile, Regulation of hepcidin and ferroportin expression by lipopolysaccharide in splenic macrophages. *Blood cells, molecules & diseases* **35**, 47-56 (2005).
28. F. Yang, X. B. Liu, M. Quinones, P. C. Melby, A. Ghio, D. J. Haile, Regulation of reticuloendothelial iron transporter MTP1 (Slc11a3) by inflammation. *The Journal of biological chemistry* **277**, 39786-39791 (2002).

29. C. Guida, S. Altamura, F. A. Klein, B. Galy, M. Boutros, A. J. Ulmer, M. W. Hentze, M. U. Muckenthaler, A novel inflammatory pathway mediating rapid hepcidin-independent hypoferremia. *Blood* **125**, 2265-2275 (2015).
30. E. Nemeth, M. S. Tuttle, J. Powelson, M. B. Vaughn, A. Donovan, D. M. Ward, T. Ganz, J. Kaplan, Hepcidin regulates cellular iron efflux by binding to ferroportin and inducing its internalization. *Science* **306**, 2090-2093 (2004).
31. S. Altamura, R. Kessler, H. J. Grone, N. Gretz, M. W. Hentze, B. Galy, M. U. Muckenthaler, Resistance of ferroportin to hepcidin binding causes exocrine pancreatic failure and fatal iron overload. *Cell metabolism* **20**, 359-367 (2014).
32. S. Zhang, Y. Chen, W. Guo, L. Yuan, D. Zhang, Y. Xu, E. Nemeth, T. Ganz, S. Liu, Disordered hepcidin-ferroportin signaling promotes breast cancer growth. *Cellular signalling* **26**, 2539-2550 (2014).
33. Z. K. Pinnix, L. D. Miller, W. Wang, R. D'Agostino, Jr., T. Kute, M. C. Willingham, H. Hatcher, L. Tesfay, G. Sui, X. Di, S. V. Torti, F. M. Torti, Ferroportin and iron regulation in breast cancer progression and prognosis. *Sci Transl Med* **2**, 43ra56 (2010).
34. L. Tesfay, K. A. Clausen, J. W. Kim, P. Hegde, X. Wang, L. D. Miller, Z. Deng, N. Blanchette, T. Arvedson, C. K. Miranti, J. L. Babitt, H. Y. Lin, D. M. Peehl, F. M. Torti, S. V. Torti, Hepcidin regulation in prostate and its disruption in prostate cancer. *Cancer Res* **75**, 2254-2263 (2015).
35. D. J. Schaer, C. A. Schaer, P. W. Buehler, R. A. Boykins, G. Schoedon, A. I. Alayash, A. Schaffner, CD163 is the macrophage scavenger receptor for native and chemically modified hemoglobins in the absence of haptoglobin. *Blood* **107**, 373-380 (2006).
36. F. F. Dutra, M. T. Bozza, Heme on innate immunity and inflammation. *Frontiers in pharmacology* **5**, 115 (2014).
37. R. T. Figueiredo, P. L. Fernandez, D. S. Mourao-Sa, B. N. Porto, F. F. Dutra, L. S. Alves, M. F. Oliveira, P. L. Oliveira, A. V. Graca-Souza, M. T. Bozza, Characterization of heme as activator of Toll-like receptor 4. *The Journal of biological chemistry* **282**, 20221-20229 (2007).
38. B. N. Porto, L. S. Alves, P. L. Fernandez, T. P. Dutra, R. T. Figueiredo, A. V. Graca-Souza, M. T. Bozza, Heme induces neutrophil migration and reactive oxygen species generation through signaling pathways characteristic of chemotactic receptors. *The Journal of biological chemistry* **282**, 24430-24436 (2007).
39. S. I. Grivennikov, F. R. Greten, M. Karin, Immunity, inflammation, and cancer. *Cell* **140**, 883-899 (2010).
40. S. Ostrand-Rosenberg, P. Sinha, Myeloid-derived suppressor cells: linking inflammation and cancer. *J Immunol* **182**, 4499-4506 (2009).
41. A. Mantovani, P. Allavena, A. Sica, F. Balkwill, Cancer-related inflammation. *Nature* **454**, 436-444 (2008).
42. J. Condeelis, J. W. Pollard, Macrophages: obligate partners for tumor cell migration, invasion, and metastasis. *Cell* **124**, 263-266 (2006).
43. P. Allavena, A. Sica, G. Solinas, C. Porta, A. Mantovani, The inflammatory micro-environment in tumor progression: the role of tumor-associated macrophages. *Critical reviews in oncology/hematology* **66**, 1-9 (2008).
44. M. de Sousa, An outsider's perspective--ecotaxis revisited: an integrative review of cancer environment, iron and immune system cells. *Integr Biol (Camb)* **3**, 343-349 (2010).
45. E. Sierra-Filardi, M. A. Vega, P. Sanchez-Mateos, A. L. Corbi, A. Puig-Kroger, Heme Oxygenase-1 expression in M-CSF-polarized M2 macrophages contributes to LPS-induced IL-10 release. *Immunobiology* **215**, 788-795 (2010).
46. O. R. Colegio, N. Q. Chu, A. L. Szabo, T. Chu, A. M. Rhebergen, V. Jairam, N. Cyrus, C. E. Brokowski, S. C. Eisenbarth, G. M. Phillips, G. W. Cline, A. J. Phillips,

- R. Medzhitov, Functional polarization of tumour-associated macrophages by tumour-derived lactic acid. *Nature* **513**, 559-563 (2014).
47. O. Marques, G. Porto, A. Rema, F. Faria, A. Cruz Paula, M. Gomez-Lazaro, P. Silva, B. Martins da Silva, C. Lopes, Local iron homeostasis in the breast ductal carcinoma microenvironment. *BMC cancer* **16**, 187 (2016).
 48. D. I. Gabrilovich, S. Nagaraj, Myeloid-derived suppressor cells as regulators of the immune system. *Nat Rev Immunol* **9**, 162-174 (2009).
 49. M. R. Young, M. Newby, H. T. Wepsic, Hematopoiesis and suppressor bone marrow cells in mice bearing large metastatic Lewis lung carcinoma tumors. *Cancer Res* **47**, 100-105 (1987).
 50. J. Marx, Cancer immunology. Cancer's bulwark against immune attack: MDS cells. *Science* **319**, 154-156 (2008).
 51. H. H. Yan, M. Pickup, Y. Pang, A. E. Gorska, Z. Li, A. Chytil, Y. Geng, J. W. Gray, H. L. Moses, L. Yang, Gr-1+CD11b+ myeloid cells tip the balance of immune protection to tumor promotion in the premetastatic lung. *Cancer Res* **70**, 6139-6149 (2010).
 52. P. Sinha, V. K. Clements, S. Ostrand-Rosenberg, Reduction of myeloid-derived suppressor cells and induction of M1 macrophages facilitate the rejection of established metastatic disease. *J Immunol* **174**, 636-645 (2005).
 53. L. Yang, L. M. DeBusk, K. Fukuda, B. Fingleton, B. Green-Jarvis, Y. Shyr, L. M. Matrisian, D. P. Carbone, P. C. Lin, Expansion of myeloid immune suppressor Gr+CD11b+ cells in tumor-bearing host directly promotes tumor angiogenesis. *Cancer Cell* **6**, 409-421 (2004).
 54. E. Suzuki, V. Kapoor, A. S. Jassar, L. R. Kaiser, S. M. Albelda, Gemcitabine selectively eliminates splenic Gr-1+/CD11b+ myeloid suppressor cells in tumor-bearing animals and enhances antitumor immune activity. *Clin Cancer Res* **11**, 6713-6721 (2005).
 55. C. Murdoch, M. Muthana, S. B. Coffelt, C. E. Lewis, The role of myeloid cells in the promotion of tumour angiogenesis. *Nat Rev Cancer* **8**, 618-631 (2008).
 56. S. J. Dixon, K. M. Lemberg, M. R. Lamprecht, R. Skouta, E. M. Zaitsev, C. E. Gleason, D. N. Patel, A. J. Bauer, A. M. Cantley, W. S. Yang, B. Morrison, 3rd, B. R. Stockwell, Ferroptosis: an iron-dependent form of nonapoptotic cell death. *Cell* **149**, 1060-1072 (2012).
 57. F. O. Martinez, S. Gordon, The M1 and M2 paradigm of macrophage activation: time for reassessment. *F1000prime reports* **6**, 13 (2014).
 58. B. Z. Qian, J. W. Pollard, Macrophage diversity enhances tumor progression and metastasis. *Cell* **141**, 39-51 (2010).
 59. D. M. Mosser, J. P. Edwards, Exploring the full spectrum of macrophage activation. *Nat Rev Immunol* **8**, 958-969 (2008).
 60. P. J. Murray, J. E. Allen, S. K. Biswas, E. A. Fisher, D. W. Gilroy, S. Goerdts, S. Gordon, J. A. Hamilton, L. B. Ivashkiv, T. Lawrence, M. Locati, A. Mantovani, F. O. Martinez, J. L. Mege, D. M. Mosser, G. Natoli, J. P. Saeij, J. L. Schultze, K. A. Shirey, A. Sica, J. Suttles, I. Udalova, J. A. van Ginderachter, S. N. Vogel, T. A. Wynn, Macrophage activation and polarization: nomenclature and experimental guidelines. *Immunity* **41**, 14-20 (2014).
 61. J. Xue, S. V. Schmidt, J. Sander, A. Draffehn, W. Krebs, I. Quester, D. De Nardo, T. D. Gohel, M. Emde, L. Schmidleithner, H. Ganesan, A. Nino-Castro, M. R. Mallmann, L. Labzin, H. Theis, M. Kraut, M. Beyer, E. Latz, T. C. Freeman, T. Ulas, J. L. Schultze, Transcriptome-based network analysis reveals a spectrum model of human macrophage activation. *Immunity* **40**, 274-288 (2014).
 62. J. D. Torrance, T. H. Bothwell, A simple technique for measuring storage iron concentrations in formalinised liver samples. *The South African journal of medical sciences* **33**, 9-11 (1968).

63. C. Delaby, C. Rondeau, C. Pouzet, A. Willemetz, N. Pilard, M. Desjardins, F. Canonne-Hergaux, Subcellular localization of iron and heme metabolism related proteins at early stages of erythrophagocytosis. *PloS one* **7**, e42199 (2012).

III – GENERAL DISCUSSION

1. Main findings

The main findings of this thesis are summarized as the following:

- Heme and iron can induce the differentiation of macrophages towards a M1-like phenotype.
- Heme and iron also reprogram already differentiated M1 and M2 macrophages. The M1 macrophage phenotype is potentiated, while the M2 phenotype is shifted towards a M1-like phenotype.
- This differentiation program is controlled by signaling pathways under TLR4 activation and ROS formation.
- Macrophages from the RES of mouse models with acute hemolysis and sickle cells disease show an M1-like phenotype.
- Hemopexin administration, in complex with heme, prevents the pro-inflammatory phenotype observed in macrophages after exposure to heme;
- Hemopexin administration as a therapeutical approach, rescues the M1-like phenotype of macrophages and attenuated liver damage in a mouse model of sickle cell disease;

- In the context of the tumor microenvironment, we observed that in human non-small cell lung cancer and in a mouse model for Lewis Lung Carcinoma, tumor-associated macrophages retain iron while cancer cells are negative for iron staining;
- Iron retention in macrophages correlates with their location in invasive areas of the tumor;
- Iron loaded macrophages are localized in hemorrhagic areas of the tumor;
- TAMs do not express ferroportin and the lack of ferroportin is not mediated by hepcidin;
- Iron accumulation in TAMs may be a result of the uptake of RBC;
- In the model used, iron seems to be more important for the modulation of the inflammatory response, than for tumor growth.

2. Discussion

Macrophages are characterized by a chameleonic behavior in response to the stimuli of the environment. These cells are not only crucial for iron recycling and homeostasis, they also participate in immune responses. The concept of polarization is based on the expression of markers (for example cytokines or surface receptors) that are associated either with the M1 or with the M2 phenotype. Although *in vivo* the scenario is far more complex than this, in this thesis the simplified concept of M1/M2 polarization was used to understand if macrophages are closer to a proinflammatory phenotype (M1) or to an anti-inflammatory phenotype (M2), and as consequence, if macrophages contribute to enhanced inflammation and tissue damage or improve tissue repair and anti-inflammatory responses, respectively. In this research work, I aimed to understand how heme and iron can affect RES macrophage polarization in the context of hemolytic disorders and also how RBC extravasation in the tumor microenvironment, as well as heme and iron release might contribute to TAMs function and phenotype.

HEME AND IRON SHAPE MACROPHAGE PLASTICITY: A ROLE IN HEMOLYTIC DISORDERS

Heme and iron shape macrophage plasticity towards a pro-inflammatory phenotype

Several studies associated iron accumulation in macrophage with an effect on polarization. In human chronic venous leg ulcers and in a mouse model for wound healing, a population of macrophages characterized by high expression of the iron scavenger receptor CD163, is responsible for the perpetuation of inflammation, tissue breakdown, and impaired wound healing, via release of TNF α , ONOO \cdot , and OH \cdot (Sindrilaru et al., 2011). These findings associate iron with a pro-inflammatory phenotype of macrophages. Recently, a study in spinal cord injury showed that macrophages/microglia in spinal cord injuries can accumulate iron which results in the increase of TNF α expression and the appearance of a macrophage population with a proinflammatory mixed M1/M2 phenotype. They also reported that increased loading of M2 macrophages with iron induces a rapid switch from M2 to M1 phenotype (Kroner et al., 2014). In both of these cases, a predominant M1 state is detrimental to recovery since it prevents healing and repair. A study of joint bleedings demonstrated that hemarthrosis alters monocyte/macrophage polarization, resulting in a blood monocyte M1 phenotype and a combined M1-M2 monocyte/macrophage phenotype in the joint. (Nieuwenhuizen et al., 2014). All these reports support the idea that heme and iron affect macrophage

plasticity and polarization, and that this phenotypic changes have a functional impact in the respective diseases studied.

Here I show that unstimulated macrophages (M0) can develop a M1-like phenotype in response to heme treatment, with increased expression of markers such as TNF α , IL1 β , IL-6 and CD14 and decreased expression of M2 markers such as CD206, IL-10 and Arginase-1. In a similar way, treatment with a source of iron (FeNTA) also induces M1-like polarization (although the effect of heme is stronger). Not only heme and iron can predispose macrophages towards an M1-like phenotype, they can also enhance the phenotype of already polarized M1 macrophages (LPS and IFN γ) by increasing the expression of M1 markers. Co-stimulation of macrophages with cytokines that promote M2 polarization (IL-4 and IL-10) with heme or iron shifted macrophage polarization towards a M1 pro-inflammatory phenotype, when compared to cytokine treatment alone. Heme and iron thus show a dominant effect over cytokines.

Macrophages localized in lesions probably originate from monocyte recruitment and the observed iron loading in macrophages occurs due to extravascular hemolysis. In hemolytic disorders, intravascular hemolysis is a dominant feature due to RBC breakage. We wondered if macrophages from the RES (specifically splenic macrophages and Kupffer cells) could be affected in terms of polarization and inflammatory response due to excessive exposure to heme. Using a mimic disease model for SCD and an acute model for hemolysis (intravenous injection of heme) we were able to extend our *in vitro* findings to the *in vivo* situation and show that macrophages from the RES, when exposed to heme, are polarized towards a M1-like phenotype.

Macrophage polarization by heme and iron is dependent on TLR4 activation and ROS formation

Regarding the mechanism by which heme activates macrophages, it was previously reported that heme could act through TLR4, as an activator of sterile inflammation (Figueiredo et al., 2007; Lin et al., 2012). TLR4 activation by heme triggers the activation of MyD88 and the secretion of pro-inflammatory cytokines. Heme can also induce ROS generation independently of TLR4. Both TLR4-dependent MyD88 activation and ROS generation contribute to the activation of the MAPKs signaling pathway that activates NF- κ B and induces the production of TNF α and other inflammatory cytokines (reviewed by (Dutra and Bozza, 2014)). Our data additionally demonstrate that TLR4 activation and ROS formation are responsible for the induction of M1 polarization by heme. Heme was unable to activate BMDMs from TLR4 KO mice to the same extent as WT mice. Also the use of TAK-242, a TLR4 inhibitor, prevented most of the effect of heme *in vitro* and *in vivo*. Although the effect was attenuated, the expression of some markers was still

induced to a milder extent. These results can be explained by the formation of ROS that is independent from TLR4 activation. Co-treatment of TLR4 KO BMDMs with heme and N-acetyl-cysteine (NAC), an antioxidant, was able to fully prevent the expression of M1 markers and downregulation of M2 markers. In case of FeNTA, the activation of macrophages may be mainly due to iron-dependent ROS formation. Also in this setting, NAC was able to at least partially rescue the effect of FeNTA in inducing M1 polarization. The incomplete prevention might be due to suboptimal doses applied or activation of unknown signaling pathways.

Hemopexin prevents the pro-inflammatory induction and switching of macrophages

We observed that Kupffer cells from a mouse model of SCD and Kupffer cells and splenic macrophages from a mouse model of acute hemolysis (injection of heme-albumin complex) display a M1-like phenotype, when compared to the respective controls. Not always mouse models resemble the human pathology, nevertheless, inflammation and increased levels of inflammatory cytokines were observed in hemolytic disorders. Sickle cell disease is well recognized as a chronic inflammatory disease (Belcher et al., 2003; Belcher et al., 2000; Jison et al., 2004). Elevated blood levels of inflammatory cytokines such as IL-1 β , IL-6, TNF α and increased inflammatory biomarkers such as C-reactive protein have been described in patients with SCD (Croizat, 1994; Kuvibidila et al., 1997; Lanaro et al., 2009; Malave et al., 1993). Also, monocytes from patients with SCD show an activation state with production of IL-15, TNF α and IL-1 β (Belcher et al., 2000). Our findings might explain in part the inflammation observed in these patients, since activation of macrophages towards a M1 pro-inflammatory phenotype might contribute to the production of inflammatory cytokines observed in patients with hemolytic disorders.

In hemolytic disorders, Hp and Hx become saturated and are not sufficient to detoxify circulating heme; therefore heme toxicity is not prevented (Muller-Eberhard et al., 1968). The exogenous administration of heme scavengers might thus be used as a therapeutic approach to clear heme and prevent its deleterious effect. Our data show that, incubation of macrophages with heme-Hx prevents their pro-inflammatory induction and switching of macrophages, when compared to heme-albumin. Since hemopexin keeps heme “out” from macrophages or it mediates its uptake, it prevents TLR4 activation and ROS formation, and subsequent macrophage inflammatory response. Actually, treatment of macrophages with Hx turned out to be more efficient in preventing M1 polarization when compared to TLR4 inhibition and NAC treatment. Long-term treatment of SCD mice with exogenous Hx was able to rescue the M1-like inflammatory profile of macrophages,

suggesting that Hx is a great candidate to be used as a therapeutic approach to reduce inflammation in SCD and other hemolytic disorders.

Hemopexin as a therapeutic approach for hemolytic disorders

M1 activation of macrophages is associated with liver injury and fibrosis (Tacke and Zimmermann, 2014). M1 macrophages produce IL-1 β , TNF α and MCP-1 that contributes to liver injury and recruitment of inflammatory monocytes. M1-like Kupffer cells also activate hepatic stellate cells (HSC) to promote fibrosis via paracrine mechanisms, involving the expression of the pro-fibrotic and mitogenic cytokines TGF- β and PDGF (Pradere et al., 2013). The effect of Hx treatment in SCD mice, not only rescued the M1-like Kupffer cell polarization, but also decreased markers of macrophage-mediated liver injury such as TNF α , MCP-1, TGF- β and PDGF. Hx treatment also decreased the expression of smooth muscle actin (SMA) a marker of HSC activation and increased the expression of synaptophysin, a marker for resting HSC. Hepatic macrophages produce several matrix metalloproteinases, including MMP-9, MMP-12 and MMP-13 that contribute to matrix degradation and resolution of liver injury and fibrosis (Fallowfield et al., 2007; Pellicoro et al., 2012). SCD mice treated with hemopexin show an increased expression of these MMPs, suggesting that Hx administration helps to prevent fibrosis and tissue injury. Altogether these results support the idea that Hx treatment has great potential to reduce liver injury and inflammation in SCD patients.

To complement these results we used a mouse model that mimics chronic hemolysis by repetitive injections of heme-albumin. We observed significantly increased collagen deposition and hepatocyte apoptosis in mice with repetitive injections of heme-albumin (mimicking chronic hemolysis) when compared to heme-Hx injected mice. Also, heme-albumin injected mice show a significant increase in collagens, TGF- β , PDGF and SMA, once more supporting the evidence that macrophage activation by heme contributes to liver injury and fibrosis. In addition heme toxicity may directly impact on hepatocytes. Injection of heme-Hx prevented collagen deposition, apoptosis of hepatocytes and signs of liver fibrosis. Administration of Hx was further shown to prevent the lethal outcome in severe sepsis in mice (Larsen et al., 2010). These authors suggested that Hx administration could be a viable therapeutic intervention also for pathologies associated with hemolysis. Here we conclude that administration of hemopexin reduces macrophage activation and tissue damage promoted by heme in hemolytic disorders, confirming Hx as a promising therapy.

HEME AND IRON SHAPE MACROPHAGE PLASTICITY: A ROLE IN CANCER

Is iron an essential nutrient for cancer cells?

One of the major questions concerning the field of iron and cancer is: what is precisely the role of iron in cancer? Several studies support the idea that excess of iron or iron administration, are contributing factors for the onset and development of cancer (Knekt et al., 1994; Stevens et al., 1988). The excess of iron triggers the formation of ROS that promote DNA damage and mutagenesis, which are events involved in cancer initiation (Dizdaroglu and Jaruga, 2012).

The majority of studies point to the direction that iron is an essential nutrient for cancer cells. As a co-factor of many enzymes, iron is involved in several cellular processes, namely cell division. The lack of ferroportin in cancer cells, the only known iron exporter, was associated with worse prognosis in breast cancer and with increased proliferation of lung cancer cell lines, supporting a model where iron retention in cancer cells increases cell survival and proliferation (Babu and Muckenthaler, 2016; Pinnix et al., 2010). Iron chelation therapies, aimed to deprive cancer cells from iron and promote cancer cell death, have been investigated (Corce et al., 2016; Yu et al., 2012) but so far have not been established as cancer treatment.

A different perspective relies on the fact that iron-derived ROS might lead to cancer cell death. When the antioxidant defenses of the cell are compromised, the excess of iron leads to iron-dependent, oxidative death named ferroptosis (Dixon et al., 2012).

When we address cancer, one of the most important features to consider is the role of the tumor microenvironment (TME) (Hanahan and Weinberg, 2011; Mantovani et al., 2008; Mantovani and Sica, 2010). Although iron seems to have an impact in the cancer cell itself, the role of iron in the tumor microenvironment may be of great importance and should not be neglected (de Sousa, 2011). In this thesis I explored how iron can affect the tumor microenvironment. I aimed to address the following questions: where is iron located in the tumor microenvironment? What is the consequence of iron accumulation in the tumor microenvironment? Is tumor growth affecting iron homeostasis? Is iron affecting tumor growth? The results presented in this thesis contribute to extending the knowledge about the role of heme and iron in the TME, namely the importance of iron in the context of “sterile inflammation” and in the polarization of TAMs.

Iron accumulates in tumor-associated macrophages

Possible sources of iron reaching the tumor microenvironment are transferrin bound iron (that can be taken up by cancer cells via TfR1) and heme iron present in RBC (Macedo and de Sousa, 2008). The occurrence of angiogenesis may facilitate the transport of

nutrients to cancer cells but it also allows for the infiltration of immune cells and extravasation of RBC.

In Chapter II we show that in human non-small cell lung carcinoma and mouse Lung Lewis Carcinoma (LLC), iron (detected by Perls' staining) is found in TAMs while cancer cells are negative for Perls' staining. The presence of iron loaded macrophages coincides with the presence of RBC in the tumor microenvironment.

The localization of iron loaded TAMs in invasive areas and near sites of RBC leakage, suggests that the most probable source of iron is derived from RBC that leak from fragile vessels in the tumor microenvironment. In fact, due to the high extent of angiogenesis, cancer tissue is a privileged site for leaking of RBC and subsequent extravascular hemolysis.

Microbleedings and intratumoral hemorrhage are likely to occur in later stages of tumor growth (de Vries et al., 2012; Li et al., 2012; Sun et al., 2016; Zimmerman and Bilaniuk, 1980). Each RBC contains around 1.2×10^9 molecules of heme, and each heme moiety has one ferrous ion within the center of the porphyrin ring (Korolnek and Hamza, 2015). Thus, RBC may serve as a significant iron source for tumors. It is possible that macrophages in the tumor microenvironment are also involved in RBC clearance, in order to protect the cancer tissue against iron toxicity.

Heme and iron released during intravascular hemolysis, have an impact on the polarization and activation of RES macrophages, as shown in Chapter I. As mentioned earlier in this thesis, M1 macrophages can be characterized as "tumor-killing" and M2 macrophages as "tumor-helping". Taking this knowledge in consideration I explored whether iron accumulation in TAMs (in this case due to extravascular hemolysis) might also have a possible effect on macrophage polarization and function.

Iron content defines a subpopulation of TAMs

In the LLC model, iron loaded TAMs are characterized by the expression of heme degrading enzyme HO-1 (*Hmox1*) and by the expression of hemoglobin (Hb) scavenger receptor CD163, capable of endocytosing pro-oxidant free Hb complexed to acute phase protein haptoglobin (Hp) or hemoglobin alone (Schaer et al., 2006b). Other studies, in different models and diseases, have identified macrophages characterized by the expression of CD163 and HO-1. In atherosclerosis, Boyle and colleagues defined a subtype of macrophages in atherosclerotic plaques that is directly correlated with hemorrhage inside the lesions (Boyle, 2012; Boyle et al., 2009; Boyle et al., 2012). This subtype of macrophages, called Mhem macrophages, also express elevated levels of CD163, HO-1 and IL-10. Mhem macrophages are beneficial for atherosclerosis since they are capable of mediating efficient cholesterol efflux (Boyle, 2012). Other studies examined

the transcriptional response of blood derived human macrophages to Hb by gene array analysis. They observed a non-inflammatory macrophage response, characterized by the induction of an anti-oxidative and anti-inflammatory gene expression pattern with most prominent induction of HO-1 (Schaer et al., 2006a).

In another study, human macrophages that were derived from blood monocytes stimulated with M-CSF were shown to express increased levels of CD163 and HO-1 when compared to GM-CSF derived macrophages. In the presence of LPS, M-CSF differentiated macrophages produced IL-10, a process dependent on HO-1 expression. HO-1 expression in metastatic melanoma was primarily detected in CD163-positive TAMs, which are known to exhibit an M2-skewed polarization phenotype (Sierra-Filardi et al., 2010). These authors suggested that the CD163/HO-1/IL-10 axis contributes to the generation of an immunosuppressive environment within the tumor stroma. Our data show that the expression of CD163 and HO-1 in TAMs is connected to iron uptake. However, it is not clear yet whether this population of macrophages would have an immunosuppressive or immune-stimulating function in the tumor microenvironment. So far, published studies point to the direction that CD163 and HO-1 expression is associated with immune regulation and suppression.

Nevertheless, the presence of iron within macrophages may change their behavior and phenotype. The circumstances in which iron is presented to macrophages is very important. Erythrophagocytosis is a physiological process and should not activate macrophages towards a pro-inflammatory phenotype. RBC were shown to block NO-mediated suppressor activity, since NO binds avidly to hemoglobin (Mills, 2001). CD163 on macrophages was shown to work as an adhesion receptor for erythroblasts (Fabriek et al., 2007). In the context of the tumor microenvironment, iron can be presented to macrophages either in the form of intact RBC or along with its degradation components: hemoglobin and heme. It is not known if TAMs have the same recycling capacity as of RES macrophages. BMDM treated with conditioned media of LLC cancer cells increased the uptake of aged RBC and/or RBC products, when compared to non-stimulated macrophages. This evidence suggests that cancer-related inflammation might also increase the phagocytic capacity of macrophages (Richards et al., 2016).

In the Chapter I of this thesis I have shown that heme and iron, can shift the polarization of M2-polarized macrophages towards an M1-like, pro-inflammatory phenotype. To support this evidence, we show that co-culture of macrophages with LLC cells triggers their polarization towards an M2 phenotype, but, further incubation with iron sources (aged/hemolytic RBC, Heme and FeNTA) was able to shift this polarization by decreasing the M2 marker CD206 and increasing the M1 marker CD14.

In vivo, hemorrhagic areas (where leaked RBC and iron loaded macrophages accumulate) show an increase in inflammatory cytokines such as IL-6, IL-1 β and also high levels of iNOS (*Nos2*) which are all markers for M1 polarization. In contrast, markers of M2 polarization such as Arginase 1 and Ym1 are not changed (data not shown). Nevertheless, although these cytokines are associated with M1 activity, the impact of these cytokines in tumor growth and proliferation might not have the expected “tumor killing” effect. As an example, in LLC tumors, IL-1 β was shown to induce VEGF, CXCL2, and hepatocyte growth factor (HGF). The induction of these angiogenic factors, produced by tumor and stromal cells, promoted an increase in tumor vasculature (Saijo et al., 2002). Further experiments are necessary to understand the functional consequences of RBC extravasation and iron accumulation in TAMs towards tumor progression.

The expression of Ferroportin is absent in TAMs from LLC tumors

The absence of ferroportin expression in TAMs is also an intriguing observation. TAMs from LLC were shown to be negative for ferroportin expression at mRNA and protein level. This downregulation or absence of ferroportin is independent of hepcidin, suggesting that it rather occurs at the transcriptional level than post-translational level.

Not all macrophages from the human body express ferroportin. Macrophages from the RES, such as Kupffer cells and splenic macrophages are known to express ferroportin. The expression of ferroportin in these cells is regulated on several levels (see chapter 1.3). Hepcidin is the systemic regulator of ferroportin expression (Altamura et al., 2014). By contrast, peritoneal macrophages and alveolar macrophages don't express ferroportin and retain iron in conditions of iron overload (unpublished data). The expression of ferroportin in different subtypes of macrophages is probably dependent on the differentiation process during the establishment of embryonic-origin populations or in the case of TAMs, the cytokines encountered in the niche by recruited monocytes.

Macrophage precursor cells (monocytes and myeloid-derived suppressor cells- MDSCs) encounter cytokines and chemokines in the tumor microenvironment that trigger their differentiation. These cytokines might lead to a macrophage phenotype that does not allow for ferroportin expression. As an example, splenic macrophages, known to export iron and to express ferroportin, are dependent on the transcription factor SPI-C to differentiate into iron recycling macrophages. The niche of the tumor microenvironment is different from the splenic niche and probably, TAMs are not differentiated to display an iron recycling phenotype, but rather support tissue remodeling and angiogenesis. TAMs (CD11b^{high} /F4/80^{high}) are rather similar to peritoneal macrophages (CD11b^{high} /F4/80^{high}) than to splenic macrophages (CD11b^{low}/F4/80^{high}).

We and others showed that LLC cells are able to polarize macrophages towards an M2 phenotype (Colegio et al., 2014). M2 macrophages were shown to express more ferroportin when compared to M1 macrophages (Recalcati et al., 2010). In contrast to this study we even observed a slight downregulation of ferroportin when we use CM from LLC cells or cytokines that polarize macrophages towards an M2 phenotype. Here we show that although macrophages associated with LLC tumors show several features of M2 macrophages, ferroportin is absent and leads to an iron retention phenotype. This might be explained by the complexity of stimuli that macrophages encounter *in vivo*, within the tumor microenvironment that are not seen *in vitro*, and as well, by the differences in the protocols used to differentiate the cells *in vitro*. A recent study in breast cancer demonstrated that TAMs from breast cancer show an iron “donor” phenotype with increased expression of ferroportin, supporting the idea that the expression of proteins involved in iron metabolism in TAMs might be tissue-specific and strictly dependent on the niche (Marques et al., 2016).

M-CSF (*Csf1*) and GM-CSF (*Csf2*) are factors that contribute to monocyte differentiation into macrophages and were also implicated in controlling ferroportin expression (Sierra-Filardi et al., 2010). Human monocytes differentiated with M-CSF expressed higher levels of ferroportin when compared with monocytes stimulated with GM-CSF (Sierra-Filardi et al., 2010). M-CSF and GM-CSF are both present in the microenvironment of LLC. In fact these cytokines are even increased in hemorrhagic areas (See Research work, Chapter II, Figure 6D). In the case of GM-CSF, it is also increased in tumors and in the circulation of iron overloaded mice, when compared to WT mice. The expression of GM-CSF in the tumor tissue might explain the absence of ferroportin in macrophages, but nevertheless the mechanism by which TAMs from LLC downregulate ferroportin expression requires further investigation.

The fact that TAMs don't express ferroportin might contribute to iron retention and subsequently to the iron-derived inflammatory phenotype. Our data suggest that a subset of TAMs ingest and recycle RBC from the tumor microenvironment but they are unable to export recycled iron. We propose a model where, iron uptake by TAMs, increases the expression of iron-recycling related proteins such as CD163 and HO-1 and further iron retention induces a pro-inflammatory behavior. HO-1 and CD163 are markers of M2 macrophages and immune suppression but are also important players in iron metabolism. In the context of the tumor microenvironment macrophages express M1 and M2 markers (Qian and Pollard, 2010), showing that the process of macrophage polarization and plasticity in the tumor microenvironment is far more complex than the M1/M2 dichotomy (Mosser and Edwards, 2008; Murray et al., 2014; Qian and Pollard, 2010; Xue et al., 2014). Here we show that iron accumulation in TAMs contributes to the definition of al

subpopulation of tumor-associated macrophages, whose function might be dependent on (or might be a consequence of) iron loading.

Hemorrhagic areas as a “new niche” within the TME

During the last decade, the role of the tumor microenvironment in cancer progression and therapy has been widely explored. Several studies unraveled the important role of immune cells in tumor progression (Grivennikov et al., 2010; Mantovani et al., 2008; Ostrand-Rosenberg and Sinha, 2009). Macrophages were shown to be key players in the tumor microenvironment and tumor-related inflammation (Allavena et al., 2008; Condeelis and Pollard, 2006; Solinas et al., 2009).

The fact that macrophages can support angiogenesis and invasion makes them of extreme importance (Condeelis and Pollard, 2006). In the model studied, macrophages represent around 60% of the infiltrated leukocytes. Here we show that hemorrhagic areas are characterized by iron loaded macrophages but also by an enrichment of CD11b⁺/Gr-1⁺ cells. CD11b⁺/Gr-1⁺ myeloid-derived suppressor cells (MDSCs) cells are important component of the tumor microenvironment (Gabrilovich and Nagaraj, 2009).

CD11b⁺/Gr-1⁺ cells are very abundant in the LLC tumor model. Previous studies demonstrated that LLC tumor bearing mice have increased hematopoiesis and an increase in the proportion of monocytes in the peripheral blood, spleen, and bone marrow (Young et al., 1987). The increase in this population in hemorrhagic areas might be just a consequence of extravasation of circulating cells into the tumor microenvironment due to vessel damage. Elevated CD11b⁺/Gr-1⁺ myeloid cells are associated with impaired immune reactivity and increased tumor progression (Marx, 2008; Sinha et al., 2005; Yan et al., 2010). CD11b⁺/Gr-1⁺ myeloid cells are involved in the tumor vasculature and secrete pro-angiogenic factors such as matrix metalloproteinases 9 (MMP9) and iNOS or differentiating into endothelium-like cells or other vascular cells (Murdoch et al., 2008; Suzuki et al., 2005; Yang et al., 2004).

Consistent with these findings we observe an increase in MMP9 and iNOS (*Nos2*) mRNA in hemorrhagic areas. We also observed an increased expression of Cxcl1 and Cxcl2, which might be produced by these cells and act as pro-angiogenic factors and chemoattractant factors to myeloid cells, neutrophils and macrophages. Vessel damage and accumulation of CD11b⁺/Gr-1⁺ cells and RBC alter the tumor microenvironment and may have consequences in the immune response. CD11b⁺/Gr-1⁺ myeloid cells can further differentiate into macrophages (Gabrilovich and Nagaraj, 2009). The increase in the expression of Csf1 and Csf2 may indicate that there is a further differentiation of these cells into macrophages, but this has not yet been proven. It is not known if the expansion

of CD11b⁺/Gr-1⁺ cells is somehow involved in iron homeostasis, but the fact that there is an expansion of this population in bone marrow and spleen might affect erythropoiesis and iron recycling.

Does cancer related-inflammation affect iron or does iron affect inflammation in cancer?

Inflammation, cancer and iron are interconnected and can mutually affect each other. On the one hand, iron/heme/RBC in the tumor microenvironment might have an important role not only in tumor cell proliferation but also in the inflammatory response, especially in the modulation of TAMs plasticity. On the other hand, cancer related inflammation was shown to have an impact on systemic iron regulation (Kim et al., 2014; Maccio et al., 2015).

The decrease observed in serum iron levels can be explained by tumor growth, suggesting that LLC cancer cells can obtain the necessary iron from circulation. LLC tumors in iron overload conditions didn't show increased proliferation and tumor size, when compared to WT mice. In fact, mRNA expression of total tumor mass suggests that LLC cells injected in iron overload mice (C326S mice) downregulate TfR1 to decrease iron uptake and upregulate Ferroportin to increase iron export.

Cancer cells are negative for iron staining, supporting the evidence that cancer cells do not accumulate excessive amounts of iron. This can be explained by iron toxicity. Iron dependent -ROS generation can be toxic to cancer cells (Dixon et al., 2012) which explains why cancer cells control iron levels. Iron seems to be more important for the modulation of the inflammatory response, than for tumor growth. We observed an increase in cytokines in the circulation of LLC-bearing iron overloaded mice (IL-1 β , IL-6, TNF α , IL-10, GM-CSF, CCL2) when we compare to WT LLC-bearing mice. In terms of macrophage counts, tumors from iron overloaded mice had an increase number of macrophages, probably a result of CCL2 increased expression. Once more, CCL2 expression is increased by iron levels (Valenti et al., 2011; Zager, 2005) but the mechanism by which iron affects CCL2 expression is not known.

LLC-bearing mice develop alterations in iron homeostasis. Serum iron levels are decreased, probably due to tumor growth and leakage of RBC in to the tumor microenvironment. Also, infiltration of CD11b⁺/Gr-1⁺ cells in the bone marrow might affect erythropoiesis. The infiltration of the same cell type in the spleen changes the architecture of the spleen and possibly causes a decrease in RBC recycling. Expression of hepcidin is not affected in this tumor model.

As mentioned previously, cancer patients frequently develop anemia of cancer. Since anemia of cancer might have a negative impact in the quality of life of cancer patients,

treatments have been introduced in order to fight anemia. The treatment options for anemia of cancer include blood transfusion, iron administration and erythropoiesis-stimulating agents (ESAs). Since I observed a modulatory role of iron and RBC in the tumor microenvironment, it will be of interest to explore the effects of RBC transfusion in cancer patients.

Around 15% of anemic cancer patients are treated with RBC transfusions (Cremieux et al., 2000). Each unit of RBC with a volume of 300 mL contains approximately 200 mL RBC, and after administration to an adult patient Hb levels rise 1 g/dL. One unit of RBC contains 200 mg of iron, which is released when hemoglobin from the transfused RBC is metabolized after RBC death. The mean life span of transfused RBC is 100–110 days, although in the first 24 hours 10%–15% are lost (Luten et al., 2008). This implicates that in the first 24h of transfusion, hemolysis of transfused RBC might occur and the release of heme might have an implication on inflammation and immune system activation as described before. In fact, one of the major complications of RBC transfusion is iron overload. After transfusing 10–15 RBC units, excess of iron is typically present in the liver, heart, skin, and endocrine organs.

Several retrospective studies looked at the impact of RBC transfusions on treatment outcome in patients with cancer. In patients with head and neck cancer, RBC transfusion was associated with decreased survival time and higher local recurrence (Bhide et al., 2009). Administering RBC transfusions in patients with thoracic malignancies translated into a higher perioperative mortality rate whereas there was no impact on overall survival in patients with non-small cell lung cancer (Thomas et al., 2007). Studies in patients with cervical cancer showed no important effect of transfusion in patients who were treated with surgery in relation to survival. In one study evaluating its impact in patients treated with radiotherapy, there was a shorter survival rate (Santin et al., 2003). In colorectal cancer, a meta-analysis showed a higher recurrence rate in patients receiving RBC transfusions at the time of surgery and also a higher infection rate (Amato and Pescatori, 2006; Houbiers et al., 1997). An overall increased mortality was observed after RBC transfusions in patients with colorectal, head and neck, breast, gastric, and prostate cancer (Vamvakas and Blajchman, 2001).

In summary, it is uncertain whether RBC transfusion is a good strategy to ameliorate anemia of cancer. Also the effect of iron in tumor growth and recurrence has not been entirely elucidated. Additional studies and analysis of cancer patients are required to dissect how RBC transfusion and iron supplementation might contribute to changes not only in the tumor cells, but also in the tumor microenvironment.

3. Future Perspectives

Several open questions remain.

Regarding heme-induced activation of macrophages in hemolytic disorders, it is still unknown if this would be considered an advantage or disadvantage in the case of infections. Patients with hemolytic disorders receive frequent blood transfusions. The frequency of blood transfusions is associated with an increased risk for infections. On the one hand, the fact that macrophages are activated towards a M1-like phenotype may predispose them to a faster response against pathogens. Nevertheless, we also showed that treatment with heme and iron decrease the viability of M1 macrophages (See Research work, Chapter I, Table2). As consequence, macrophages may no longer be able to respond accordingly to infections. Besides this, iron overload might be an advantage for several pathogens that are dependent on iron to proliferate. Hemopexin therapy and iron chelation therapies might be a promising therapeutic approach, also in case of infections. It might increase macrophage fitness and decrease the availability of iron for pathogens. Current projects in the lab are addressing this question.

Regarding iron and the tumor microenvironment, the main question “are these iron loaded macrophages “tumor helping” or “tumor killing”?” has so far not been entirely addressed.

According to Mills (Mills, 2015), the classification of macrophages in M1 or M2 macrophages only defines if macrophages can kill tumor cells, or help tumor cells to proliferate. I am currently doing experiments addressing this question. As an experimental set-up, I am using co-culture of macrophages with cancer cells, iron treatments and live imaging to understand the relationship of iron-loaded macrophages with cancer cells or other immune cells. The regulation of ferroportin in TAMs is also an important issue to be resolved. It is not known why TAMs from certain tumors don't express ferroportin. Experiments are ongoing to understand the mechanism underlying the absence of ferroportin in TAMs associated with LLC.

Another important aspect is the implication of iron loaded macrophages in the prognosis of cancer. Since they are associated with RBC extravasation and angiogenesis, the presence of these macrophages might be correlated with metastatic tumors and aggressive phenotypes. Iron staining and correlation with macrophage infiltrates might be a useful prognosis tool and needs to be performed in a large patient cohort. Analysis of tissue microarrays from cancer patients is being performed in order to address this question.

IV – REFERENCES

REFERENCES

- Adeegbe, D.O., and Nishikawa, H. (2013). Natural and induced T regulatory cells in cancer. *Frontiers in immunology* 4, 190.
- Allavena, P., Sica, A., Solinas, G., Porta, C., and Mantovani, A. (2008). The inflammatory micro-environment in tumor progression: the role of tumor-associated macrophages. *Critical reviews in oncology/hematology* 66, 1-9.
- Altamura, S., Kessler, R., Grone, H.J., Gretz, N., Hentze, M.W., Galy, B., and Muckenthaler, M.U. (2014). Resistance of ferroportin to hepcidin binding causes exocrine pancreatic failure and fatal iron overload. *Cell metabolism* 20, 359-367.
- Amato, A., and Pescatori, M. (2006). Perioperative blood transfusions for the recurrence of colorectal cancer. *The Cochrane database of systematic reviews*, CD005033.
- Arezes, J., Jung, G., Gabayan, V., Valore, E., Ruchala, P., Gulig, P.A., Ganz, T., Nemeth, E., and Bulut, Y. (2015). Hepcidin-induced hypoferremia is a critical host defense mechanism against the siderophilic bacterium *Vibrio vulnificus*. *Cell host & microbe* 17, 47-57.
- Babu, K.R., and Muckenthaler, M.U. (2016). miR-20a regulates expression of the iron exporter ferroportin in lung cancer. *J Mol Med (Berl)* 94, 347-359.
- Balla, G., Vercellotti, G.M., Muller-Eberhard, U., Eaton, J., and Jacob, H.S. (1991). Exposure of endothelial cells to free heme potentiates damage mediated by granulocytes and toxic oxygen species. *Laboratory investigation; a journal of technical methods and pathology* 64, 648-655.
- Belcher, J.D., Bryant, C.J., Nguyen, J., Bowlin, P.R., Kielbik, M.C., Bischof, J.C., Hebbel, R.P., and Vercellotti, G.M. (2003). Transgenic sickle mice have vascular inflammation. *Blood* 101, 3953-3959.
- Belcher, J.D., Chen, C., Nguyen, J., Milbauer, L., Abdulla, F., Alayash, A.I., Smith, A., Nath, K.A., Hebbel, R.P., and Vercellotti, G.M. (2014). Heme triggers TLR4 signaling leading to endothelial cell activation and vaso-occlusion in murine sickle cell disease. *Blood* 123, 377-390.
- Belcher, J.D., Marker, P.H., Weber, J.P., Hebbel, R.P., and Vercellotti, G.M. (2000). Activated monocytes in sickle cell disease: potential role in the activation of vascular endothelium and vaso-occlusion. *Blood* 96, 2451-2459.
- Besson-Fournier, C., Latour, C., Kautz, L., Bertrand, J., Ganz, T., Roth, M.P., and Coppin, H. (2012). Induction of activin B by inflammatory stimuli up-regulates expression of the iron-regulatory peptide hepcidin through Smad1/5/8 signaling. *Blood* 120, 431-439.
- Bhide, S.A., Ahmed, M., Rengarajan, V., Powell, C., Miah, A., Newbold, K., Nutting, C.M., and Harrington, K.J. (2009). Anemia during sequential induction chemotherapy and chemoradiation for head and neck cancer: the impact of blood transfusion on treatment outcome. *International journal of radiation oncology, biology, physics* 73, 391-398.
- Biswas, S.K., Allavena, P., and Mantovani, A. (2013). Tumor-associated macrophages: functional diversity, clinical significance, and open questions. *Seminars in immunopathology* 35, 585-600.
- Biswas, S.K., and Mantovani, A. (2010). Macrophage plasticity and interaction with lymphocyte subsets: cancer as a paradigm. *Nature immunology* 11, 889-896.

REFERENCES

- Bonde, A.K., Tischler, V., Kumar, S., Soltermann, A., and Schwendener, R.A. (2012). Intratumoral macrophages contribute to epithelial-mesenchymal transition in solid tumors. *BMC cancer* 12, 35.
- Borrego, F., Ulbrecht, M., Weiss, E.H., Coligan, J.E., and Brooks, A.G. (1998). Recognition of human histocompatibility leukocyte antigen (HLA)-E complexed with HLA class I signal sequence-derived peptides by CD94/NKG2 confers protection from natural killer cell-mediated lysis. *J Exp Med* 187, 813-818.
- Boyle, J.J. (2012). Heme and haemoglobin direct macrophage Mhem phenotype and counter foam cell formation in areas of intraplaque haemorrhage. *Current opinion in lipidology* 23, 453-461.
- Boyle, J.J., Harrington, H.A., Piper, E., Elderfield, K., Stark, J., Landis, R.C., and Haskard, D.O. (2009). Coronary intraplaque hemorrhage evokes a novel atheroprotective macrophage phenotype. *The American journal of pathology* 174, 1097-1108.
- Boyle, J.J., Johns, M., Kampfer, T., Nguyen, A.T., Game, L., Schaer, D.J., Mason, J.C., and Haskard, D.O. (2012). Activating transcription factor 1 directs Mhem atheroprotective macrophages through coordinated iron handling and foam cell protection. *Circulation research* 110, 20-33.
- Boyle, J.J., Johns, M., Lo, J., Chiodini, A., Ambrose, N., Evans, P.C., Mason, J.C., and Haskard, D.O. (2011). Heme induces heme oxygenase 1 via Nrf2: role in the homeostatic macrophage response to intraplaque hemorrhage. *Arteriosclerosis, thrombosis, and vascular biology* 31, 2685-2691.
- Bronte, V., Wang, M., Overwijk, W.W., Surman, D.R., Pericle, F., Rosenberg, S.A., and Restifo, N.P. (1998). Apoptotic death of CD8+ T lymphocytes after immunization: induction of a suppressive population of Mac-1+/Gr-1+ cells. *J Immunol* 161, 5313-5320.
- Campbell, J.A. (1940). Effects of Precipitated Silica and of Iron Oxide on the Incidence of Primary Lung Tumours in Mice. *British medical journal* 2, 275-280.
- Chakraborty, S., Kaur, S., Guha, S., and Batra, S.K. (2012). The multifaceted roles of neutrophil gelatinase associated lipocalin (NGAL) in inflammation and cancer. *Biochimica et biophysica acta* 1826, 129-169.
- Chanvorachote, P., and Luanpitpong, S. (2016). Iron Induces Cancer Stem Cells and Aggressive Phenotypes in Human Lung Cancer Cells. *American journal of physiology. Cell physiology*, ajpcell 00322 02015.
- Chen, G., Fillebeen, C., Wang, J., and Pantopoulos, K. (2007). Overexpression of iron regulatory protein 1 suppresses growth of tumor xenografts. *Carcinogenesis* 28, 785-791.
- Chen, H.L., Gabrilovich, D., Tampe, R., Girgis, K.R., Nadaf, S., and Carbone, D.P. (1996). A functionally defective allele of TAP1 results in loss of MHC class I antigen presentation in a human lung cancer. *Nature genetics* 13, 210-213.
- Cheng, Y., Zak, O., Aisen, P., Harrison, S.C., and Walz, T. (2004). Structure of the human transferrin receptor-transferrin complex. *Cell* 116, 565-576.
- Chitu, V., and Stanley, E.R. (2006). Colony-stimulating factor-1 in immunity and inflammation. *Curr Opin Immunol* 18, 39-48.

- Chiu, D., and Lubin, B. (1989). Oxidative hemoglobin denaturation and RBC destruction: the effect of heme on red cell membranes. *Seminars in hematology* 26, 128-135.
- Colegio, O.R., Chu, N.Q., Szabo, A.L., Chu, T., Rhebergen, A.M., Jairam, V., Cyrus, N., Brokowski, C.E., Eisenbarth, S.C., Phillips, G.M., Cline, G.W., Phillips, A.J., and Medzhitov, R. (2014). Functional polarization of tumour-associated macrophages by tumour-derived lactic acid. *Nature* 513, 559-563.
- Condeelis, J., and Pollard, J.W. (2006). Macrophages: obligate partners for tumor cell migration, invasion, and metastasis. *Cell* 124, 263-266.
- Corce, V., Gouin, S.G., Renaud, S., Gaboriau, F., and Deniaud, D. (2016). Recent advances in cancer treatment by iron chelators. *Bioorganic & medicinal chemistry letters* 26, 251-256.
- Corhay, J.L., Weber, G., Bury, T., Mariz, S., Roelandts, I., and Radermecker, M.F. (1992). Iron content in human alveolar macrophages. *The European respiratory journal* 5, 804-809.
- Corna, G., Campana, L., Pignatti, E., Castiglioni, A., Tagliafico, E., Bosurgi, L., Campanella, A., Brunelli, S., Manfredi, A.A., Apostoli, P., Silvestri, L., Camaschella, C., and Rovere-Querini, P. (2010). Polarization dictates iron handling by inflammatory and alternatively activated macrophages. *Haematologica* 95, 1814-1822.
- Cortez-Retamozo, V., Etzrodt, M., Newton, A., Rauch, P.J., Chudnovskiy, A., Berger, C., Ryan, R.J., Iwamoto, Y., Marinelli, B., Gorbатов, R., Forghani, R., Novobrantseva, T.I., Kotliansky, V., Figueiredo, J.L., Chen, J.W., Anderson, D.G., Nahrendorf, M., Swirski, F.K., Weissleder, R., and Pittet, M.J. (2012). Origins of tumor-associated macrophages and neutrophils. *Proceedings of the National Academy of Sciences of the United States of America* 109, 2491-2496.
- Costa, L.M.G., Moura, E.M.F., Moura, J.J.G., and de Sousa, M. (1998). Iron Compounds after Erythrophagocytosis: Chemical Characterization and Immunomodulatory Effects. *Biochemical and biophysical research communications* 247, 159-165.
- Cremieux, P.Y., Barrett, B., Anderson, K., and Slavin, M.B. (2000). Cost of outpatient blood transfusion in cancer patients. *Journal of clinical oncology : official journal of the American Society of Clinical Oncology* 18, 2755-2761.
- Croizat, H. (1994). Circulating cytokines in sickle cell patients during steady state. *British journal of haematology* 87, 592-597.
- De Palma, M., Venneri, M.A., Galli, R., Sergi Sergi, L., Politi, L.S., Sampaolesi, M., and Naldini, L. (2005). Tie2 identifies a hematopoietic lineage of proangiogenic monocytes required for tumor vessel formation and a mesenchymal population of pericyte progenitors. *Cancer Cell* 8, 211-226.
- de Sousa, M. (2011). An outsider's perspective--ecotaxis revisited: an integrative review of cancer environment, iron and immune system cells. *Integr Biol (Camb)* 3, 343-349.
- de Vries, M., Hogendoorn, P.C., Briaire-de Bruyn, I., Malessy, M.J., and van der Mey, A.G. (2012). Intratumoral hemorrhage, vessel density, and the inflammatory reaction contribute to volume increase of sporadic vestibular schwannomas. *Virchows Archiv : an international journal of pathology* 460, 629-636.

REFERENCES

- Dhodapkar, M.V., Steinman, R.M., Krasovsky, J., Munz, C., and Bhardwaj, N. (2001). Antigen-specific inhibition of effector T cell function in humans after injection of immature dendritic cells. *J Exp Med* 193, 233-238.
- Dixon, L.J., Barnes, M., Tang, H., Pritchard, M.T., and Nagy, L.E. (2013). Kupffer cells in the liver. *Comprehensive Physiology* 3, 785-797.
- Dixon, S.J., Lemberg, K.M., Lamprecht, M.R., Skouta, R., Zaitsev, E.M., Gleason, C.E., Patel, D.N., Bauer, A.J., Cantley, A.M., Yang, W.S., Morrison, B., 3rd, and Stockwell, B.R. (2012). Ferroptosis: an iron-dependent form of nonapoptotic cell death. *Cell* 149, 1060-1072.
- Dizdaroglu, M., and Jaruga, P. (2012). Mechanisms of free radical-induced damage to DNA. *Free radical research* 46, 382-419.
- Donovan, A., Lima, C.A., Pinkus, J.L., Pinkus, G.S., Zon, L.I., Robine, S., and Andrews, N.C. (2005). The iron exporter ferroportin/Slc40a1 is essential for iron homeostasis. *Cell metabolism* 1, 191-200.
- Doyle, A.G., Herbein, G., Montaner, L.J., Minty, A.J., Caput, D., Ferrara, P., and Gordon, S. (1994). Interleukin-13 alters the activation state of murine macrophages in vitro: comparison with interleukin-4 and interferon-gamma. *Eur J Immunol* 24, 1441-1445.
- Drakesmith, H., Sweetland, E., Schimanski, L., Edwards, J., Cowley, D., Ashraf, M., Bastin, J., and Townsend, A.R. (2002). The hemochromatosis protein HFE inhibits iron export from macrophages. *Proceedings of the National Academy of Sciences of the United States of America* 99, 15602-15607.
- Dutra, F.F., and Bozza, M.T. (2014). Heme on innate immunity and inflammation. *Frontiers in pharmacology* 5, 115.
- Epelman, S., Lavine, K.J., and Randolph, G.J. (2014). Origin and functions of tissue macrophages. *Immunity* 41, 21-35.
- Fabrick, B.O., Polfliet, M.M., Vloet, R.P., van der Schors, R.C., Ligtenberg, A.J., Weaver, L.K., Geest, C., Matsuno, K., Moestrup, S.K., Dijkstra, C.D., and van den Berg, T.K. (2007). The macrophage CD163 surface glycoprotein is an erythroblast adhesion receptor. *Blood* 109, 5223-5229.
- Fallowfield, J.A., Mizuno, M., Kendall, T.J., Constandinou, C.M., Benyon, R.C., Duffield, J.S., and Iredale, J.P. (2007). Scar-associated macrophages are a major source of hepatic matrix metalloproteinase-13 and facilitate the resolution of murine hepatic fibrosis. *J Immunol* 178, 5288-5295.
- Feder, J.N., Gnirke, A., Thomas, W., Tsuchihashi, Z., Ruddy, D.A., Basava, A., Dormishian, F., Domingo, R., Jr., Ellis, M.C., Fullan, A., Hinton, L.M., Jones, N.L., Kimmel, B.E., Kronmal, G.S., Lauer, P., Lee, V.K., Loeb, D.B., Mapa, F.A., McClelland, E., Meyer, N.C., Mintier, G.A., Moeller, N., Moore, T., Morikang, E., Prass, C.E., Quintana, L., Starnes, S.M., Schatzman, R.C., Brunke, K.J., Drayna, D.T., Risch, N.J., Bacon, B.R., and Wolff, R.K. (1996). A novel MHC class I-like gene is mutated in patients with hereditary haemochromatosis. *Nature genetics* 13, 399-408.
- Ferris, C.D., Jaffrey, S.R., Sawa, A., Takahashi, M., Brady, S.D., Barrow, R.K., Tysoe, S.A., Wolosker, H., Baranano, D.E., Dore, S., Poss, K.D., and Snyder, S.H. (1999). Haem oxygenase-1 prevents cell death by regulating cellular iron. *Nature cell biology* 1, 152-157.

REFERENCES

- Fidler, I.J. (1988). Macrophage therapy of cancer metastasis. Ciba Foundation symposium 141, 211-222.
- Figueiredo, R.T., Fernandez, P.L., Mourao-Sa, D.S., Porto, B.N., Dutra, F.F., Alves, L.S., Oliveira, M.F., Oliveira, P.L., Graca-Souza, A.V., and Bozza, M.T. (2007). Characterization of heme as activator of Toll-like receptor 4. *The Journal of biological chemistry* 282, 20221-20229.
- Fontenot, J.D., Gavin, M.A., and Rudensky, A.Y. (2003). Foxp3 programs the development and function of CD4⁺CD25⁺ regulatory T cells. *Nature immunology* 4, 330-336.
- Fortes, G.B., Alves, L.S., de Oliveira, R., Dutra, F.F., Rodrigues, D., Fernandez, P.L., Souto-Padron, T., De Rosa, M.J., Kelliher, M., Golenbock, D., Chan, F.K., and Bozza, M.T. (2012). Heme induces programmed necrosis on macrophages through autocrine TNF and ROS production. *Blood* 119, 2368-2375.
- Fridlender, Z.G., Sun, J., Kim, S., Kapoor, V., Cheng, G., Ling, L., Worthen, G.S., and Albelda, S.M. (2009). Polarization of tumor-associated neutrophil phenotype by TGF-beta: "N1" versus "N2" TAN. *Cancer Cell* 16, 183-194.
- Gabrilovich, D. (2004). Mechanisms and functional significance of tumour-induced dendritic-cell defects. *Nat Rev Immunol* 4, 941-952.
- Gabrilovich, D.I., and Nagaraj, S. (2009). Myeloid-derived suppressor cells as regulators of the immune system. *Nat Rev Immunol* 9, 162-174.
- Ganz, T. (2012). Macrophages and systemic iron homeostasis. *Journal of innate immunity* 4, 446-453.
- Gautier, E.L., Shay, T., Miller, J., Greter, M., Jakubzick, C., Ivanov, S., Helft, J., Chow, A., Elpek, K.G., Gordonov, S., Mazloom, A.R., Ma'ayan, A., Chua, W.J., Hansen, T.H., Turley, S.J., Merad, M., and Randolph, G.J. (2012). Gene-expression profiles and transcriptional regulatory pathways that underlie the identity and diversity of mouse tissue macrophages. *Nature immunology* 13, 1118-1128.
- Goldstraw, P., Ball, D., Jett, J.R., Le Chevalier, T., Lim, E., Nicholson, A.G., and Shepherd, F.A. (2011). Non-small-cell lung cancer. *Lancet* 378, 1727-1740.
- Gordeuk, V.R., Ballou, S., Lozanski, G., and Brittenham, G.M. (1992). Decreased concentrations of tumor necrosis factor-alpha in supernatants of monocytes from homozygotes for hereditary hemochromatosis. *Blood* 79, 1855-1860.
- Gordon, S. (2003). Alternative activation of macrophages. *Nat Rev Immunol* 3, 23-35.
- Goswami, T., and Andrews, N.C. (2006). Hereditary hemochromatosis protein, HFE, interaction with transferrin receptor 2 suggests a molecular mechanism for mammalian iron sensing. *The Journal of biological chemistry* 281, 28494-28498.
- Graca-Souza, A.V., Arruda, M.A., de Freitas, M.S., Barja-Fidalgo, C., and Oliveira, P.L. (2002). Neutrophil activation by heme: implications for inflammatory processes. *Blood* 99, 4160-4165.
- Grivennikov, S.I., Greten, F.R., and Karin, M. (2010). Immunity, inflammation, and cancer. *Cell* 140, 883-899.

REFERENCES

- Guida, C., Altamura, S., Klein, F.A., Galy, B., Boutros, M., Ulmer, A.J., Hentze, M.W., and Muckenthaler, M.U. (2015). A novel inflammatory pathway mediating rapid hepcidin-independent hypoferraemia. *Blood* 125, 2265-2275.
- Gunshin, H., Mackenzie, B., Berger, U.V., Gunshin, Y., Romero, M.F., Boron, W.F., Nussberger, S., Gollan, J.L., and Hediger, M.A. (1997). Cloning and characterization of a mammalian proton-coupled metal-ion transporter. *Nature* 388, 482-488.
- Hanahan, D., and Weinberg, R.A. (2000). The hallmarks of cancer. *Cell* 100, 57-70.
- Hanahan, D., and Weinberg, R.A. (2011). Hallmarks of cancer: the next generation. *Cell* 144, 646-674.
- Hashimoto, D., Chow, A., Noizat, C., Teo, P., Beasley, M.B., Leboeuf, M., Becker, C.D., See, P., Price, J., Lucas, D., Greter, M., Mortha, A., Boyer, S.W., Forsberg, E.C., Tanaka, M., van Rooijen, N., Garcia-Sastre, A., Stanley, E.R., Ginhoux, F., Frenette, P.S., and Merad, M. (2013). Tissue-resident macrophages self-maintain locally throughout adult life with minimal contribution from circulating monocytes. *Immunity* 38, 792-804.
- Hebbel, R.P., Morgan, W.T., Eaton, J.W., and Hedlund, B.E. (1988). Accelerated autoxidation and heme loss due to instability of sickle hemoglobin. *Proceedings of the National Academy of Sciences of the United States of America* 85, 237-241.
- Hentze, M.W., Muckenthaler, M.U., and Andrews, N.C. (2004). Balancing acts: molecular control of mammalian iron metabolism. *Cell* 117, 285-297.
- Hentze, M.W., Muckenthaler, M.U., Galy, B., and Camaschella, C. (2010). Two to tango: regulation of Mammalian iron metabolism. *Cell* 142, 24-38.
- Houbiers, J.G., van de Velde, C.J., van de Wattering, L.M., Hermans, J., Schreuder, S., Bijnen, A.B., Pahlplatz, P., Schattenkerk, M.E., Wobbes, T., de Vries, J.E., Klementschi, P., van de Maas, A.H., and Brand, A. (1997). Transfusion of red cells is associated with increased incidence of bacterial infection after colorectal surgery: a prospective study. *Transfusion* 37, 126-134.
- Huang, B., Pan, P.Y., Li, Q., Sato, A.I., Levy, D.E., Bromberg, J., Divino, C.M., and Chen, S.H. (2006). Gr-1+CD115+ immature myeloid suppressor cells mediate the development of tumor-induced T regulatory cells and T-cell anergy in tumor-bearing host. *Cancer Res* 66, 1123-1131.
- Hvidberg, V., Maniecki, M.B., Jacobsen, C., Hojrup, P., Moller, H.J., and Moestrup, S.K. (2005). Identification of the receptor scavenging hemopexin-heme complexes. *Blood* 106, 2572-2579.
- Jeney, V., Balla, J., Yachie, A., Varga, Z., Vercellotti, G.M., Eaton, J.W., and Balla, G. (2002). Pro-oxidant and cytotoxic effects of circulating heme. *Blood* 100, 879-887.
- Jison, M.L., Munson, P.J., Barb, J.J., Suffredini, A.F., Talwar, S., Logun, C., Raghavachari, N., Beigel, J.H., Shelhamer, J.H., Danner, R.L., and Gladwin, M.T. (2004). Blood mononuclear cell gene expression profiles characterize the oxidant, hemolytic, and inflammatory stress of sickle cell disease. *Blood* 104, 270-280.
- Kaplan, D.H., Shankaran, V., Dighe, A.S., Stockert, E., Aguet, M., Old, L.J., and Schreiber, R.D. (1998). Demonstration of an interferon gamma-dependent tumor surveillance system in immunocompetent mice. *Proceedings of the National Academy of Sciences of the United States of America* 95, 7556-7561.

REFERENCES

- Kautz, L., Jung, G., Valore, E.V., Rivella, S., Nemeth, E., and Ganz, T. (2014). Identification of erythroferrone as an erythroid regulator of iron metabolism. *Nature genetics* 46, 678-684.
- Kautz, L., Meynard, D., Monnier, A., Darnaud, V., Bouvet, R., Wang, R.H., Deng, C., Vaulont, S., Mosser, J., Coppin, H., and Roth, M.P. (2008). Iron regulates phosphorylation of Smad1/5/8 and gene expression of Bmp6, Smad7, Id1, and Atoh8 in the mouse liver. *Blood* 112, 1503-1509.
- Kellar, A., Egan, C., and Morris, D. (2015). Preclinical Murine Models for Lung Cancer: Clinical Trial Applications. *BioMed research international* 2015, 621324.
- Kelly, J.M., Darcy, P.K., Markby, J.L., Godfrey, D.I., Takeda, K., Yagita, H., and Smyth, M.J. (2002). Induction of tumor-specific T cell memory by NK cell-mediated tumor rejection. *Nature immunology* 3, 83-90.
- Kemna, E., Pickkers, P., Nemeth, E., van der Hoeven, H., and Swinkels, D. (2005). Time-course analysis of hepcidin, serum iron, and plasma cytokine levels in humans injected with LPS. *Blood* 106, 1864-1866.
- Kim, A., Rivera, S., Shprung, D., Limbrick, D., Gabayan, V., Nemeth, E., and Ganz, T. (2014). Mouse models of anemia of cancer. *PloS one* 9, e93283.
- Kim, S., and Ponka, P. (2003). Role of nitric oxide in cellular iron metabolism. *Biometals : an international journal on the role of metal ions in biology, biochemistry, and medicine* 16, 125-135.
- Knekt, P., Reunanen, A., Takkunen, H., Aromaa, A., Heliövaara, M., and Hakulinen, T. (1994). Body iron stores and risk of cancer. *Int J Cancer* 56, 379-382.
- Knutson, K.L., and Disis, M.L. (2005). Tumor antigen-specific T helper cells in cancer immunity and immunotherapy. *Cancer immunology, immunotherapy : CII* 54, 721-728.
- Kohyama, M., Ise, W., Edelson, B.T., Wilker, P.R., Hildner, K., Mejia, C., Frazier, W.A., Murphy, T.L., and Murphy, K.M. (2009). Role for Spi-C in the development of red pulp macrophages and splenic iron homeostasis. *Nature* 457, 318-321.
- Korolnek, T., and Hamza, I. (2015). Macrophages and iron trafficking at the birth and death of red cells. *Blood* 125, 2893-2897.
- Kroner, A., Greenhalgh, A.D., Zarruk, J.G., Passos Dos Santos, R., Gaestel, M., and David, S. (2014). TNF and increased intracellular iron alter macrophage polarization to a detrimental M1 phenotype in the injured spinal cord. *Neuron* 83, 1098-1116.
- Kukulj, S., Jaganjac, M., Boranic, M., Krizanac, S., Santic, Z., and Poljak-Blazi, M. (2010). Altered iron metabolism, inflammation, transferrin receptors, and ferritin expression in non-small-cell lung cancer. *Med Oncol* 27, 268-277.
- Kumar, S., and Bandyopadhyay, U. (2005). Free heme toxicity and its detoxification systems in human. *Toxicology letters* 157, 175-188.
- Kuvibidila, S., Gardner, R., Ode, D., Yu, L., Lane, G., and Warriar, R.P. (1997). Tumor necrosis factor alpha in children with sickle cell disease in stable condition. *Journal of the National Medical Association* 89, 609-615.

- Lanaro, C., Franco-Penteado, C.F., Albuquerque, D.M., Saad, S.T., Conran, N., and Costa, F.F. (2009). Altered levels of cytokines and inflammatory mediators in plasma and leukocytes of sickle cell anemia patients and effects of hydroxyurea therapy. *J Leukoc Biol* 85, 235-242.
- Laoui, D., Movahedi, K., Van Overmeire, E., Van den Bossche, J., Schoupe, E., Mommer, C., Nikolaou, A., Morias, Y., De Baetselier, P., and Van Ginderachter, J.A. (2011). Tumor-associated macrophages in breast cancer: distinct subsets, distinct functions. *The International journal of developmental biology* 55, 861-867.
- Larsen, R., Gouveia, Z., Soares, M.P., and Gozzelino, R. (2012). Heme cytotoxicity and the pathogenesis of immune-mediated inflammatory diseases. *Frontiers in pharmacology* 3, 77.
- Larsen, R., Gozzelino, R., Jeney, V., Tokaji, L., Bozza, F.A., Japiassu, A.M., Bonaparte, D., Cavalcante, M.M., Chora, A., Ferreira, A., Marguti, I., Cardoso, S., Sepulveda, N., Smith, A., and Soares, M.P. (2010). A central role for free heme in the pathogenesis of severe sepsis. *Sci Transl Med* 2, 51ra71.
- Lee, P., Peng, H., Gelbart, T., Wang, L., and Beutler, E. (2005). Regulation of hepcidin transcription by interleukin-1 and interleukin-6. *Proceedings of the National Academy of Sciences of the United States of America* 102, 1906-1910.
- Legrand, D., and Mazurier, J. (2010). A critical review of the roles of host lactoferrin in immunity. *Biometals : an international journal on the role of metal ions in biology, biochemistry, and medicine* 23, 365-376.
- Lewis, C.E., and Pollard, J.W. (2006). Distinct role of macrophages in different tumor microenvironments. *Cancer Res* 66, 605-612.
- Li, R.K., Zeng, M.S., Rao, S.X., Qiang, J.W., Dai, Y.M., Ji, Y., Chen, C.Z., and Renate, J. (2012). Using a 2D multibreath-hold susceptibility-weighted imaging to visualize intratumoral hemorrhage of hepatocellular carcinoma at 3T MRI: correlation with pathology. *Journal of magnetic resonance imaging : JMRI* 36, 900-906.
- Lin, E.Y., and Pollard, J.W. (2007). Tumor-associated macrophages press the angiogenic switch in breast cancer. *Cancer Res* 67, 5064-5066.
- Lin, S., Yin, Q., Zhong, Q., Lv, F.L., Zhou, Y., Li, J.Q., Wang, J.Z., Su, B.Y., and Yang, Q.W. (2012). Heme activates TLR4-mediated inflammatory injury via MyD88/TRIF signaling pathway in intracerebral hemorrhage. *Journal of neuroinflammation* 9, 46.
- Linde, N., Lederle, W., Depner, S., van Rooijen, N., Gutschalk, C.M., and Mueller, M.M. (2012). Vascular endothelial growth factor-induced skin carcinogenesis depends on recruitment and alternative activation of macrophages. *The Journal of pathology* 227, 17-28.
- Liu, X.B., Nguyen, N.B., Marquess, K.D., Yang, F., and Haile, D.J. (2005). Regulation of hepcidin and ferroportin expression by lipopolysaccharide in splenic macrophages. *Blood cells, molecules & diseases* 35, 47-56.
- Ludwig, H., Van Belle, S., Barrett-Lee, P., Birgegard, G., Bokemeyer, C., Gascon, P., Kosmidis, P., Krzakowski, M., Nortier, J., Olmi, P., Schneider, M., and Schrijvers, D. (2004). The European Cancer Anaemia Survey (ECAS): a large, multinational,

REFERENCES

prospective survey defining the prevalence, incidence, and treatment of anaemia in cancer patients. *Eur J Cancer* 40, 2293-2306.

Luten, M., Roerdinkholder-Stoelwinder, B., Schaap, N.P., de Grip, W.J., Bos, H.J., and Bosman, G.J. (2008). Survival of red blood cells after transfusion: a comparison between red cells concentrates of different storage periods. *Transfusion* 48, 1478-1485.

Lyoumi, S., Puy, H., Tamion, F., Bogard, C., Leplingard, A., Scotte, M., Vranckx, R., Gauthier, F., Hiron, M., Daveau, M., Nordmann, Y., Deybach, J.C., and Lebreton, J.P. (1999). Heme and acute inflammation role in vivo of heme in the hepatic expression of positive acute-phase reactants in rats. *European journal of biochemistry / FEBS* 261, 190-196.

Ma, J., Liu, L., Che, G., Yu, N., Dai, F., and You, Z. (2010). The M1 form of tumor-associated macrophages in non-small cell lung cancer is positively associated with survival time. *BMC cancer* 10, 112.

Maccio, A., Madeddu, C., Gramignano, G., Mulas, C., Tanca, L., Cherchi, M.C., Floris, C., Omoto, I., Barracca, A., and Ganz, T. (2015). The role of inflammation, iron, and nutritional status in cancer-related anemia: results of a large, prospective, observational study. *Haematologica* 100, 124-132.

Macedo, M.F., and de Sousa, M. (2008). Transferrin and the transferrin receptor: of magic bullets and other concerns. *Inflammation & allergy drug targets* 7, 41-52.

Mackness, G.B. (1962). Cellular resistance to infection. *J Exp Med* 116, 381-406.

Maffettone, C., Chen, G., Drozdov, I., Ouzounis, C., and Pantopoulos, K. (2010). Tumorigenic properties of iron regulatory protein 2 (IRP2) mediated by its specific 73-amino acids insert. *PloS one* 5, e10163.

Malave, I., Perdomo, Y., Escalona, E., Rodriguez, E., Anchustegui, M., Malave, H., and Arends, T. (1993). Levels of tumor necrosis factor alpha/cachectin (TNF alpha) in sera from patients with sickle cell disease. *Acta haematologica* 90, 172-176.

Mantovani, A., Allavena, P., Sica, A., and Balkwill, F. (2008). Cancer-related inflammation. *Nature* 454, 436-444.

Mantovani, A., Biswas, S.K., Galdiero, M.R., Sica, A., and Locati, M. (2013). Macrophage plasticity and polarization in tissue repair and remodelling. *The Journal of pathology* 229, 176-185.

Mantovani, A., and Sica, A. (2010). Macrophages, innate immunity and cancer: balance, tolerance, and diversity. *Curr Opin Immunol* 22, 231-237.

Marques, O., Porto, G., Rema, A., Faria, F., Cruz Paula, A., Gomez-Lazaro, M., Silva, P., Martins da Silva, B., and Lopes, C. (2016). Local iron homeostasis in the breast ductal carcinoma microenvironment. *BMC cancer* 16, 187.

Marro, S., Chiabrando, D., Messana, E., Stolte, J., Turco, E., Tolosano, E., and Muckenthaler, M.U. (2010). Heme controls ferroportin1 (FPN1) transcription involving Bach1, Nrf2 and a MARE/ARE sequence motif at position -7007 of the FPN1 promoter. *Haematologica* 95, 1261-1268.

Martinez, F.O., and Gordon, S. (2014). The M1 and M2 paradigm of macrophage activation: time for reassessment. *F1000prime reports* 6, 13.

REFERENCES

- Martinez, F.O., Gordon, S., Locati, M., and Mantovani, A. (2006). Transcriptional profiling of the human monocyte-to-macrophage differentiation and polarization: new molecules and patterns of gene expression. *J Immunol* 177, 7303-7311.
- Martinez, F.O., Helming, L., and Gordon, S. (2009). Alternative activation of macrophages: an immunologic functional perspective. *Annu Rev Immunol* 27, 451-483.
- Martinez, F.O., Sica, A., Mantovani, A., and Locati, M. (2008). Macrophage activation and polarization. *Frontiers in bioscience : a journal and virtual library* 13, 453-461.
- Marx, J. (2008). Cancer immunology. Cancer's bulwark against immune attack: MDS cells. *Science* 319, 154-156.
- Mazzieri, R., Pucci, F., Moi, D., Zonari, E., Ranghetti, A., Berti, A., Politi, L.S., Gentner, B., Brown, J.L., Naldini, L., and De Palma, M. (2011). Targeting the ANG2/TIE2 axis inhibits tumor growth and metastasis by impairing angiogenesis and disabling rebounds of proangiogenic myeloid cells. *Cancer Cell* 19, 512-526.
- McKie, A.T., Marciani, P., Rolfs, A., Brennan, K., Wehr, K., Barrow, D., Miret, S., Bomford, A., Peters, T.J., Farzaneh, F., Hediger, M.A., Hentze, M.W., and Simpson, R.J. (2000). A novel duodenal iron-regulated transporter, IREG1, implicated in the basolateral transfer of iron to the circulation. *Molecular cell* 5, 299-309.
- Mills, C.D. (2001). Macrophage arginine metabolism to ornithine/urea or nitric oxide/citrulline: a life or death issue. *Critical reviews in immunology* 21, 399-425.
- Mills, C.D. (2015). Anatomy of a discovery: m1 and m2 macrophages. *Frontiers in immunology* 6, 212.
- Mills, C.D., Kincaid, K., Alt, J.M., Heilman, M.J., and Hill, A.M. (2000). M-1/M-2 macrophages and the Th1/Th2 paradigm. *J Immunol* 164, 6166-6173.
- Mirsadraee, S., Oswal, D., Alizadeh, Y., Caulo, A., and van Beek, E., Jr. (2012). The 7th lung cancer TNM classification and staging system: Review of the changes and implications. *World journal of radiology* 4, 128-134.
- Mocsai, A. (2013). Diverse novel functions of neutrophils in immunity, inflammation, and beyond. *J Exp Med* 210, 1283-1299.
- Monteiro, A.P., Pinheiro, C.S., Luna-Gomes, T., Alves, L.R., Maya-Monteiro, C.M., Porto, B.N., Barja-Fidalgo, C., Benjamim, C.F., Peters-Golden, M., Bandeira-Melo, C., Bozza, M.T., and Canetti, C. (2011). Leukotriene B4 mediates neutrophil migration induced by heme. *J Immunol* 186, 6562-6567.
- Montosi, G., Paglia, P., Garuti, C., Guzman, C.A., Bastin, J.M., Colombo, M.P., and Pietrangelo, A. (2000). Wild-type HFE protein normalizes transferrin iron accumulation in macrophages from subjects with hereditary hemochromatosis. *Blood* 96, 1125-1129.
- Mosser, D.M., and Edwards, J.P. (2008). Exploring the full spectrum of macrophage activation. *Nat Rev Immunol* 8, 958-969.
- Movahedi, K., Laoui, D., Gysemans, C., Baeten, M., Stange, G., Van den Bossche, J., Mack, M., Pipeleers, D., In't Veld, P., De Baetselier, P., and Van Ginderachter, J.A. (2010). Different tumor microenvironments contain functionally distinct subsets of macrophages derived from Ly6C(high) monocytes. *Cancer Res* 70, 5728-5739.

REFERENCES

- Muckenthaler, M.U., Galy, B., and Hentze, M.W. (2008). Systemic iron homeostasis and the iron-responsive element/iron-regulatory protein (IRE/IRP) regulatory network. *Annual review of nutrition* 28, 197-213.
- Muller-Eberhard, U., Javid, J., Liem, H.H., Hanstein, A., and Hanna, M. (1968). Plasma concentrations of hemopexin, haptoglobin and heme in patients with various hemolytic diseases. *Blood* 32, 811-815.
- Munn, D.H., Sharma, M.D., Lee, J.R., Jhaver, K.G., Johnson, T.S., Keskin, D.B., Marshall, B., Chandler, P., Antonia, S.J., Burgess, R., Slingluff, C.L., Jr., and Mellor, A.L. (2002). Potential regulatory function of human dendritic cells expressing indoleamine 2,3-dioxygenase. *Science* 297, 1867-1870.
- Murdoch, C., Muthana, M., Coffelt, S.B., and Lewis, C.E. (2008). The role of myeloid cells in the promotion of tumour angiogenesis. *Nat Rev Cancer* 8, 618-631.
- Murray, P.J., Allen, J.E., Biswas, S.K., Fisher, E.A., Gilroy, D.W., Goerdt, S., Gordon, S., Hamilton, J.A., Ivashkiv, L.B., Lawrence, T., Locati, M., Mantovani, A., Martinez, F.O., Mege, J.L., Mosser, D.M., Natoli, G., Saeij, J.P., Schultze, J.L., Shirey, K.A., Sica, A., Suttles, J., Udalova, I., van Ginderachter, J.A., Vogel, S.N., and Wynn, T.A. (2014). Macrophage activation and polarization: nomenclature and experimental guidelines. *Immunity* 41, 14-20.
- Nairz, M., Haschka, D., Demetz, E., and Weiss, G. (2014). Iron at the interface of immunity and infection. *Frontiers in pharmacology* 5, 152.
- Nairz, M., Schleicher, U., Schroll, A., Sonnweber, T., Theurl, I., Ludwiczek, S., Talasz, H., Brandacher, G., Moser, P.L., Muckenthaler, M.U., Fang, F.C., Bogdan, C., and Weiss, G. (2013). Nitric oxide-mediated regulation of ferroportin-1 controls macrophage iron homeostasis and immune function in *Salmonella* infection. *J Exp Med* 210, 855-873.
- Nairz, M., Theurl, I., Schroll, A., Theurl, M., Fritsche, G., Lindner, E., Seifert, M., Crouch, M.L., Hantke, K., Akira, S., Fang, F.C., and Weiss, G. (2009). Absence of functional Hfe protects mice from invasive *Salmonella enterica* serovar Typhimurium infection via induction of lipocalin-2. *Blood* 114, 3642-3651.
- Nathan, C.F., Murray, H.W., Wiebe, M.E., and Rubin, B.Y. (1983). Identification of interferon-gamma as the lymphokine that activates human macrophage oxidative metabolism and antimicrobial activity. *J Exp Med* 158, 670-689.
- Nau, G.J., Richmond, J.F., Schlesinger, A., Jennings, E.G., Lander, E.S., and Young, R.A. (2002). Human macrophage activation programs induced by bacterial pathogens. *Proceedings of the National Academy of Sciences of the United States of America* 99, 1503-1508.
- Nausch, N., and Cerwenka, A. (2008). NKG2D ligands in tumor immunity. *Oncogene* 27, 5944-5958.
- Nelson, M.E., O'Brien-Ladner, A.R., and Wesselius, L.J. (1996). Regional variation in iron and iron-binding proteins within the lungs of smokers. *American journal of respiratory and critical care medicine* 153, 1353-1358.
- Nemeth, E., Rivera, S., Gabayan, V., Keller, C., Taudorf, S., Pedersen, B.K., and Ganz, T. (2004a). IL-6 mediates hypoferrremia of inflammation by inducing the synthesis of the iron regulatory hormone hepcidin. *The Journal of clinical investigation* 113, 1271-1276.

REFERENCES

- Nemeth, E., Tuttle, M.S., Powelson, J., Vaughn, M.B., Donovan, A., Ward, D.M., Ganz, T., and Kaplan, J. (2004b). Heparin regulates cellular iron efflux by binding to ferroportin and inducing its internalization. *Science* 306, 2090-2093.
- Nemeth, E., Valore, E.V., Territo, M., Schiller, G., Lichtenstein, A., and Ganz, T. (2003). Heparin, a putative mediator of anemia of inflammation, is a type II acute-phase protein. *Blood* 101, 2461-2463.
- Nieuwenhuizen, L., Schutgens, R.E., Coeleveld, K., Mastbergen, S.C., Roosendaal, G., Biesma, D.H., and Lafeber, F.P. (2014). Hemarthrosis in hemophilic mice results in alterations in M1-M2 monocyte/macrophage polarization. *Thrombosis research* 133, 390-395.
- Ohri, C.M., Shikotra, A., Green, R.H., Waller, D.A., and Bradding, P. (2009). Macrophages within NSCLC tumour islets are predominantly of a cytotoxic M1 phenotype associated with extended survival. *The European respiratory journal* 33, 118-126.
- Olakanmi, O., Schlesinger, L.S., Ahmed, A., and Britigan, B.E. (2002). Intraphagosomal *Mycobacterium tuberculosis* acquires iron from both extracellular transferrin and intracellular iron pools. Impact of interferon-gamma and hemochromatosis. *The Journal of biological chemistry* 277, 49727-49734.
- Orlandi, R., De Bortoli, M., Ciniselli, C.M., Vaghi, E., Caccia, D., Garrisi, V., Pizzamiglio, S., Veneroni, S., Bonini, C., Agresti, R., Daidone, M.G., Morelli, D., Camaschella, C., Verderio, P., and Bongarzone, I. (2014). Heparin and ferritin blood level as noninvasive tools for predicting breast cancer. *Annals of oncology : official journal of the European Society for Medical Oncology / ESMO* 25, 352-357.
- Ostrand-Rosenberg, S., and Sinha, P. (2009). Myeloid-derived suppressor cells: linking inflammation and cancer. *J Immunol* 182, 4499-4506.
- Papageorgiou, A., Stravoravdi, P., Sahpazidou, D., Natsis, K., Chrysogelou, E., and Toliou, T. (2000). Effect of navelbine on inhibition of tumor growth, cellular differentiation and estrogen receptor status on Lewis lung carcinoma. *Chemotherapy* 46, 188-194.
- Papanikolaou, G., and Pantopoulos, K. (2005). Iron metabolism and toxicity. *Toxicology and applied pharmacology* 202, 199-211.
- Pauling, L., Itano, H.A., and et al. (1949). Sickle cell anemia a molecular disease. *Science* 110, 543-548.
- Pellicoro, A., Aucott, R.L., Ramachandran, P., Robson, A.J., Fallowfield, J.A., Snowdon, V.K., Hartland, S.N., Vernon, M., Duffield, J.S., Benyon, R.C., Forbes, S.J., and Iredale, J.P. (2012). Elastin accumulation is regulated at the level of degradation by macrophage metalloelastase (MMP-12) during experimental liver fibrosis. *Hepatology* 55, 1965-1975.
- Peyssonnaud, C., Zinkernagel, A.S., Datta, V., Lauth, X., Johnson, R.S., and Nizet, V. (2006). TLR4-dependent heparin expression by myeloid cells in response to bacterial pathogens. *Blood* 107, 3727-3732.
- Pinnix, Z.K., Miller, L.D., Wang, W., D'Agostino, R., Jr., Kute, T., Willingham, M.C., Hatcher, H., Tesfay, L., Sui, G., Di, X., Torti, S.V., and Torti, F.M. (2010). Ferroportin and iron regulation in breast cancer progression and prognosis. *Sci Transl Med* 2, 43ra56.
- Porto, B.N., Alves, L.S., Fernandez, P.L., Dutra, T.P., Figueiredo, R.T., Graca-Souza, A.V., and Bozza, M.T. (2007). Heme induces neutrophil migration and reactive oxygen

species generation through signaling pathways characteristic of chemotactic receptors. *The Journal of biological chemistry* 282, 24430-24436.

Porto, G., and De Sousa, M. (2007). Iron overload and immunity. *World journal of gastroenterology : WJG* 13, 4707-4715.

Poss, K.D., and Tonegawa, S. (1997). Heme oxygenase 1 is required for mammalian iron reutilization. *Proceedings of the National Academy of Sciences of the United States of America* 94, 10919-10924.

Pradere, J.P., Kluwe, J., De Minicis, S., Jiao, J.J., Gwak, G.Y., Dapito, D.H., Jang, M.K., Guenther, N.D., Mederacke, I., Friedman, R., Dragomir, A.C., Aloman, C., and Schwabe, R.F. (2013). Hepatic macrophages but not dendritic cells contribute to liver fibrosis by promoting the survival of activated hepatic stellate cells in mice. *Hepatology* 58, 1461-1473.

Qian, B.Z., and Pollard, J.W. (2010). Macrophage diversity enhances tumor progression and metastasis. *Cell* 141, 39-51.

Recalcati, S., Locati, M., Marini, A., Santambrogio, P., Zaninotto, F., De Pizzol, M., Zammataro, L., Girelli, D., and Cairo, G. (2010). Differential regulation of iron homeostasis during human macrophage polarized activation. *Eur J Immunol* 40, 824-835.

Reiter, C.D., Wang, X., Tanus-Santos, J.E., Hogg, N., Cannon, R.O., 3rd, Schechter, A.N., and Gladwin, M.T. (2002). Cell-free hemoglobin limits nitric oxide bioavailability in sickle-cell disease. *Nat Med* 8, 1383-1389.

Richards, A.L., Hendrickson, J.E., Zimring, J.C., and Hudson, K.E. (2016). Erythrophagocytosis by plasmacytoid dendritic cells and monocytes is enhanced during inflammation. *Transfusion* 56, 905-916.

Rivera, S., Liu, L., Nemeth, E., Gabayan, V., Sorensen, O.E., and Ganz, T. (2005). Hepcidin excess induces the sequestration of iron and exacerbates tumor-associated anemia. *Blood* 105, 1797-1802.

Rodriguez, P.C., Zea, A.H., DeSalvo, J., Culotta, K.S., Zabaleta, J., Quiceno, D.G., Ochoa, J.B., and Ochoa, A.C. (2003). L-arginine consumption by macrophages modulates the expression of CD3 zeta chain in T lymphocytes. *J Immunol* 171, 1232-1239.

Ryter, S.W., and Tyrrell, R.M. (2000). The heme synthesis and degradation pathways: role in oxidant sensitivity. Heme oxygenase has both pro- and antioxidant properties. *Free radical biology & medicine* 28, 289-309.

Saijo, Y., Tanaka, M., Miki, M., Usui, K., Suzuki, T., Maemondo, M., Hong, X., Tazawa, R., Kikuchi, T., Matsushima, K., and Nukiwa, T. (2002). Proinflammatory cytokine IL-1 beta promotes tumor growth of Lewis lung carcinoma by induction of angiogenic factors: in vivo analysis of tumor-stromal interaction. *J Immunol* 169, 469-475.

Sangaletti, S., Di Carlo, E., Gariboldi, S., Miotti, S., Cappetti, B., Parenza, M., Rumio, C., Brekken, R.A., Chiodoni, C., and Colombo, M.P. (2008). Macrophage-derived SPARC bridges tumor cell-extracellular matrix interactions toward metastasis. *Cancer Res* 68, 9050-9059.

Santin, A.D., Bellone, S., Parrish, R.S., Coke, C., Dunn, D., Roman, J., Theus, J.W., Cannon, M.J., Parham, G.P., and Pecorelli, S. (2003). Influence of allogeneic blood

transfusion on clinical outcome during radiotherapy for cancer of the uterine cervix. *Gynecologic and obstetric investigation* 56, 28-34.

Schaer, C.A., Schoedon, G., Imhof, A., Kurrer, M.O., and Schaer, D.J. (2006a). Constitutive endocytosis of CD163 mediates hemoglobin-heme uptake and determines the noninflammatory and protective transcriptional response of macrophages to hemoglobin. *Circulation research* 99, 943-950.

Schaer, D.J., Schaer, C.A., Buehler, P.W., Boykins, R.A., Schoedon, G., Alayash, A.I., and Schaffner, A. (2006b). CD163 is the macrophage scavenger receptor for native and chemically modified hemoglobins in the absence of haptoglobin. *Blood* 107, 373-380.

Schrijvers, D. (2011). Management of anemia in cancer patients: transfusions. *The oncologist* 16 Suppl 3, 12-18.

Shand, F.H., Ueha, S., Otsuji, M., Koid, S.S., Shichino, S., Tsukui, T., Kosugi-Kanaya, M., Abe, J., Tomura, M., Ziogas, J., and Matsushima, K. (2014). Tracking of intertissue migration reveals the origins of tumor-infiltrating monocytes. *Proceedings of the National Academy of Sciences of the United States of America* 111, 7771-7776.

Sica, A., Erreni, M., Allavena, P., and Porta, C. (2015). Macrophage polarization in pathology. *Cellular and molecular life sciences : CMLS* 72, 4111-4126.

Sica, A., Larghi, P., Mancino, A., Rubino, L., Porta, C., Totaro, M.G., Rimoldi, M., Biswas, S.K., Allavena, P., and Mantovani, A. (2008). Macrophage polarization in tumour progression. *Seminars in cancer biology* 18, 349-355.

Sica, A., and Mantovani, A. (2012). Macrophage plasticity and polarization: in vivo veritas. *The Journal of clinical investigation* 122, 787-795.

Sierra-Filardi, E., Vega, M.A., Sanchez-Mateos, P., Corbi, A.L., and Puig-Kroger, A. (2010). Heme Oxygenase-1 expression in M-CSF-polarized M2 macrophages contributes to LPS-induced IL-10 release. *Immunobiology* 215, 788-795.

Sindrilaru, A., Peters, T., Wieschalka, S., Baican, C., Baican, A., Peter, H., Hainzl, A., Schatz, S., Qi, Y., Schlecht, A., Weiss, J.M., Wlaschek, M., Sunderkotter, C., and Scharffetter-Kochanek, K. (2011). An unrestrained proinflammatory M1 macrophage population induced by iron impairs wound healing in humans and mice. *The Journal of clinical investigation* 121, 985-997.

Sinha, P., Clements, V.K., and Ostrand-Rosenberg, S. (2005). Reduction of myeloid-derived suppressor cells and induction of M1 macrophages facilitate the rejection of established metastatic disease. *J Immunol* 174, 636-645.

Smith, A., and Morgan, W.T. (1978). Transport of heme by hemopexin to the liver: evidence for receptor-mediated uptake. *Biochemical and biophysical research communications* 84, 151-157.

Soe-Lin, S., Apte, S.S., Andriopoulos, B., Jr., Andrews, M.C., Schranzhofer, M., Kahawita, T., Garcia-Santos, D., and Ponka, P. (2009). Nramp1 promotes efficient macrophage recycling of iron following erythrophagocytosis in vivo. *Proceedings of the National Academy of Sciences of the United States of America* 106, 5960-5965.

Solinas, G., Germano, G., Mantovani, A., and Allavena, P. (2009). Tumor-associated macrophages (TAM) as major players of the cancer-related inflammation. *J Leukoc Biol* 86, 1065-1073.

REFERENCES

- Srivastava, K., Hu, J., Korn, C., Savant, S., Teichert, M., Kapel, S.S., Jugold, M., Besemfelder, E., Thomas, M., Pasparakis, M., and Augustin, H.G. (2014). Postsurgical adjuvant tumor therapy by combining anti-angiopoietin-2 and metronomic chemotherapy limits metastatic growth. *Cancer Cell* 26, 880-895.
- Srivastava, M.K., Sinha, P., Clements, V.K., Rodriguez, P., and Ostrand-Rosenberg, S. (2010). Myeloid-derived suppressor cells inhibit T-cell activation by depleting cystine and cysteine. *Cancer Res* 70, 68-77.
- Stevens, R.G., Jones, D.Y., Micozzi, M.S., and Taylor, P.R. (1988). Body iron stores and the risk of cancer. *The New England journal of medicine* 319, 1047-1052.
- Stojanovic, A., and Cerwenka, A. (2011). Natural killer cells and solid tumors. *Journal of innate immunity* 3, 355-364.
- Stojanovic, A., Correia, M.P., and Cerwenka, A. (2013). Shaping of NK cell responses by the tumor microenvironment. *Cancer Microenviron* 6, 135-146.
- Sun, J., Xing, Z., Xing, W., Zheng, L., Chen, J., Fan, M., Chen, T., and Zhang, Z. (2016). Intratumoral Macroscopic Fat and Hemorrhage Combination Useful in the Differentiation of Benign and Malignant Solid Renal Masses. *Medicine* 95, e2960.
- Sun, S., Schiller, J.H., and Gazdar, A.F. (2007). Lung cancer in never smokers--a different disease. *Nat Rev Cancer* 7, 778-790.
- Suzuki, E., Kapoor, V., Jassar, A.S., Kaiser, L.R., and Albelda, S.M. (2005). Gemcitabine selectively eliminates splenic Gr-1+/CD11b+ myeloid suppressor cells in tumor-bearing animals and enhances antitumor immune activity. *Clin Cancer Res* 11, 6713-6721.
- Swirski, F.K., Nahrendorf, M., Etzrodt, M., Wildgruber, M., Cortez-Retamozo, V., Panizzi, P., Figueiredo, J.L., Kohler, R.H., Chudnovskiy, A., Waterman, P., Aikawa, E., Mempel, T.R., Libby, P., Weissleder, R., and Pittet, M.J. (2009). Identification of splenic reservoir monocytes and their deployment to inflammatory sites. *Science* 325, 612-616.
- Tacke, F., and Zimmermann, H.W. (2014). Macrophage heterogeneity in liver injury and fibrosis. *Journal of hepatology* 60, 1090-1096.
- Tanno, T., Bhanu, N.V., Oneal, P.A., Goh, S.H., Staker, P., Lee, Y.T., Moroney, J.W., Reed, C.H., Luban, N.L., Wang, R.H., Eling, T.E., Childs, R., Ganz, T., Leitman, S.F., Fucharoen, S., and Miller, J.L. (2007). High levels of GDF15 in thalassemia suppress expression of the iron regulatory protein hepcidin. *Nat Med* 13, 1096-1101.
- Tanno, T., Porayette, P., Sripichai, O., Noh, S.J., Byrnes, C., Bhupatiraju, A., Lee, Y.T., Goodnough, J.B., Harandi, O., Ganz, T., Paulson, R.F., and Miller, J.L. (2009). Identification of TWSG1 as a second novel erythroid regulator of hepcidin expression in murine and human cells. *Blood* 114, 181-186.
- Taylor, M., Qu, A., Anderson, E.R., Matsubara, T., Martin, A., Gonzalez, F.J., and Shah, Y.M. (2011). Hypoxia-inducible factor-2alpha mediates the adaptive increase of intestinal ferroportin during iron deficiency in mice. *Gastroenterology* 140, 2044-2055.
- Theurl, I., Aigner, E., Theurl, M., Nairz, M., Seifert, M., Schroll, A., Sonnweber, T., Eberwein, L., Witcher, D.R., Murphy, A.T., Wroblewski, V.J., Wurz, E., Datz, C., and Weiss, G. (2009). Regulation of iron homeostasis in anemia of chronic disease and iron deficiency anemia: diagnostic and therapeutic implications. *Blood* 113, 5277-5286.

REFERENCES

- Thomas, P., Michelet, P., Barlesi, F., Thirion, X., Doddoli, C., Giudicelli, R., and Fuentes, P. (2007). Impact of blood transfusions on outcome after pneumonectomy for thoracic malignancies. *The European respiratory journal* 29, 565-570.
- Torti, S.V., and Torti, F.M. (2013). Iron and cancer: more ore to be mined. *Nat Rev Cancer* 13, 342-355.
- Trapani, J.A., and Smyth, M.J. (2002). Functional significance of the perforin/granzyme cell death pathway. *Nat Rev Immunol* 2, 735-747.
- Tsiftoglou, A.S., Tsamadou, A.I., and Papadopoulou, L.C. (2006). Heme as key regulator of major mammalian cellular functions: molecular, cellular, and pharmacological aspects. *Pharmacology & therapeutics* 111, 327-345.
- Valenti, L., Dongiovanni, P., Motta, B.M., Swinkels, D.W., Bonara, P., Rametta, R., Burdick, L., Frugoni, C., Fracanzani, A.L., and Fargion, S. (2011). Serum hepcidin and macrophage iron correlate with MCP-1 release and vascular damage in patients with metabolic syndrome alterations. *Arteriosclerosis, thrombosis, and vascular biology* 31, 683-690.
- Vamvakas, E.C., and Blajchman, M.A. (2001). Deleterious clinical effects of transfusion-associated immunomodulation: fact or fiction? *Blood* 97, 1180-1195.
- van Kempen, L.C., Ruiter, D.J., van Muijen, G.N., and Coussens, L.M. (2003). The tumor microenvironment: a critical determinant of neoplastic evolution. *European journal of cell biology* 82, 539-548.
- Varol, C., Mildner, A., and Jung, S. (2015). Macrophages: development and tissue specialization. *Annu Rev Immunol* 33, 643-675.
- Vercellotti, G.M., Balla, G., Balla, J., Nath, K., Eaton, J.W., and Jacob, H.S. (1994). Heme and the vasculature: an oxidative hazard that induces antioxidant defenses in the endothelium. *Artificial cells, blood substitutes, and immobilization biotechnology* 22, 207-213.
- Vesely, M.D., Kershaw, M.H., Schreiber, R.D., and Smyth, M.J. (2011). Natural innate and adaptive immunity to cancer. *Annu Rev Immunol* 29, 235-271.
- Vinchi, F., Gastaldi, S., Silengo, L., Altruda, F., and Tolosano, E. (2008). Hemopexin prevents endothelial damage and liver congestion in a mouse model of heme overload. *The American journal of pathology* 173, 289-299.
- Vinchi, F., Muckenthaler, M.U., Da Silva, M.C., Balla, G., Balla, J., and Jeney, V. (2014). Atherogenesis and iron: from epidemiology to cellular level. *Frontiers in pharmacology* 5, 94.
- Vivier, E., Raulet, D.H., Moretta, A., Caligiuri, M.A., Zitvogel, L., Lanier, L.L., Yokoyama, W.M., and Ugolini, S. (2011). Innate or adaptive immunity? The example of natural killer cells. *Science* 331, 44-49.
- Wagener, F.A., Eggert, A., Boerman, O.C., Oyen, W.J., Verhofstad, A., Abraham, N.G., Adema, G., van Kooyk, Y., de Witte, T., and Figdor, C.G. (2001). Heme is a potent inducer of inflammation in mice and is counteracted by heme oxygenase. *Blood* 98, 1802-1811.

REFERENCES

- Wagener, F.A., Feldman, E., de Witte, T., and Abraham, N.G. (1997). Heme induces the expression of adhesion molecules ICAM-1, VCAM-1, and E selectin in vascular endothelial cells. *Proc Soc Exp Biol Med* 216, 456-463.
- Wang, L., Harrington, L., Trebicka, E., Shi, H.N., Kagan, J.C., Hong, C.C., Lin, H.Y., Babitt, J.L., and Cherayil, B.J. (2009). Selective modulation of TLR4-activated inflammatory responses by altered iron homeostasis in mice. *The Journal of clinical investigation* 119, 3322-3328.
- Wang, S.C., Lin, K.H., Chern, J.P., Lu, M.Y., Jou, S.T., Lin, D.T., and Lin, K.S. (2003). Severe bacterial infection in transfusion-dependent patients with thalassemia major. *Clinical infectious diseases : an official publication of the Infectious Diseases Society of America* 37, 984-988.
- Weiss, G., and Goodnough, L.T. (2005). Anemia of chronic disease. *The New England journal of medicine* 352, 1011-1023.
- Weiss, G., Goossen, B., Doppler, W., Fuchs, D., Pantopoulos, K., Werner-Felmayer, G., Wachter, H., and Hentze, M.W. (1993). Translational regulation via iron-responsive elements by the nitric oxide/NO-synthase pathway. *The EMBO journal* 12, 3651-3657.
- White, C., Yuan, X., Schmidt, P.J., Bresciani, E., Samuel, T.K., Campagna, D., Hall, C., Bishop, K., Calicchio, M.L., Lapierre, A., Ward, D.M., Liu, P., Fleming, M.D., and Hamza, I. (2013). HRG1 is essential for heme transport from the phagolysosome of macrophages during erythrophagocytosis. *Cell metabolism* 17, 261-270.
- Willekens, F.L., Werre, J.M., Kruijt, J.K., Roerdinkholder-Stoelwinder, B., Groenen-Dopp, Y.A., van den Bos, A.G., Bosman, G.J., and van Berkel, T.J. (2005). Liver Kupffer cells rapidly remove red blood cell-derived vesicles from the circulation by scavenger receptors. *Blood* 105, 2141-2145.
- Wu, T., Sempos, C.T., Freudenheim, J.L., Muti, P., and Smit, E. (2004). Serum iron, copper and zinc concentrations and risk of cancer mortality in US adults. *Annals of epidemiology* 14, 195-201.
- Wynn, T.A., Chawla, A., and Pollard, J.W. (2013). Macrophage biology in development, homeostasis and disease. *Nature* 496, 445-455.
- Xiong, W., Wang, L., and Yu, F. (2014). Regulation of cellular iron metabolism and its implications in lung cancer progression. *Med Oncol* 31, 28.
- Xue, J., Schmidt, S.V., Sander, J., Draffehn, A., Krebs, W., Quester, I., De Nardo, D., Gohel, T.D., Emde, M., Schmidleithner, L., Ganesan, H., Nino-Castro, A., Mallmann, M.R., Labzin, L., Theis, H., Kraut, M., Beyer, M., Latz, E., Freeman, T.C., Ulas, T., and Schultze, J.L. (2014). Transcriptome-based network analysis reveals a spectrum model of human macrophage activation. *Immunity* 40, 274-288.
- Yan, H.H., Pickup, M., Pang, Y., Gorska, A.E., Li, Z., Chytil, A., Geng, Y., Gray, J.W., Moses, H.L., and Yang, L. (2010). Gr-1+CD11b+ myeloid cells tip the balance of immune protection to tumor promotion in the premetastatic lung. *Cancer Res* 70, 6139-6149.
- Yang, F., Liu, X.B., Quinones, M., Melby, P.C., Ghio, A., and Haile, D.J. (2002). Regulation of reticuloendothelial iron transporter MTP1 (Slc11a3) by inflammation. *The Journal of biological chemistry* 277, 39786-39791.

REFERENCES

- Yang, L., DeBusk, L.M., Fukuda, K., Fingleton, B., Green-Jarvis, B., Shyr, Y., Matrisian, L.M., Carbone, D.P., and Lin, P.C. (2004). Expansion of myeloid immune suppressor Gr⁺CD11b⁺ cells in tumor-bearing host directly promotes tumor angiogenesis. *Cancer Cell* 6, 409-421.
- Young, M.R., Newby, M., and Wepsic, H.T. (1987). Hematopoiesis and suppressor bone marrow cells in mice bearing large metastatic Lewis lung carcinoma tumors. *Cancer Res* 47, 100-105.
- Yu, Y., Gutierrez, E., Kovacevic, Z., Saletta, F., Obeidy, P., Suryo Rahmanto, Y., and Richardson, D.R. (2012). Iron chelators for the treatment of cancer. *Current medicinal chemistry* 19, 2689-2702.
- Zager, R.A. (2005). Parenteral iron treatment induces MCP-1 accumulation in plasma, normal kidneys, and in experimental nephropathy. *Kidney international* 68, 1533-1542.
- Zhang, C., and Zhang, F. (2015). Iron homeostasis and tumorigenesis: molecular mechanisms and therapeutic opportunities. *Protein & cell* 6, 88-100.
- Zhang, S., Chen, Y., Guo, W., Yuan, L., Zhang, D., Xu, Y., Nemeth, E., Ganz, T., and Liu, S. (2014). Disordered hepcidin-ferroportin signaling promotes breast cancer growth. *Cellular signalling* 26, 2539-2550.
- Zimmerman, R.A., and Bilaniuk, L.T. (1980). Computed tomography of acute intratumoral hemorrhage. *Radiology* 135, 355-359.